ADAPTIVE SPATIALLY-DISTRIBUTED WATER-QUALITY MODELING: AN APPLICATION TO MECHANISTICALLY SIMULATE PHOSPHORUS CONDITIONS IN THE VARIABLE-DENSITY SURFACE-WATERS OF COASTAL EVERGLADES WETLANDS

By

STUART JOHN MULLER

A DISSERTATION PRESENTED TO THE GRADUATE SCHOOL
OF THE UNIVERSITY OF FLORIDA IN PARTIAL FULFILLMENT
OF THE REQUIREMENTS FOR THE DEGREE OF
DOCTOR OF PHILOSOPHY

UNIVERSITY OF FLORIDA

2010

Dedicated to everyone, for everything, truly. But most of all, it must be said, for Julie.
Elen sila lumenn' omentielvo.

ACKNOWLEDGMENTS

I thank the USGS, SFWMD, and UF for fiscal support throughout this journey. I thank my committee: Dr. Greg Kiker, for being the original spark that has lead to so much light; Dr. Andrew James, for his vision for TaRSE; Dr. Mark Brown, for his example and his conversation; Dr. Jim Jawitz, for his support, both personal and professional; and dear Dr. Rafael Muñoz-Carpena, for the commitment of his generosity and the conviction of his faith, which have given me more than any Ph.D. is really supposed to. I thank my incredible family for persistent genes, boundless opportunity, an enquiring mind, and an open heart; my cats for the peace of their innocence when I had to let mine go; my friends for making life what it is, even when it isn't; and my Love for being so patient, and so kind, and so adorable.

TABLE OF CONTENTS

page

LIST OF TABLES

LIST OF FIGURES

LIST OF ABBREVIATIONS

aRSE	a Reaction Simulation Engine
CERP	Comprehensive Everglades Restoration Plan
eFAST	extended Fourier Amplitude Sensitivity Test
ENP	Everglades National Park
FAST	Fourier Amplitude Sensitivity Test
FDEP	Florida Department of Environmental Protection
FTaRSELOADDS	Flow, Transport and Reaction Simulation Engine in a Linked Overland-Aquifer Density Dependent System
FTLOADDS	Flow and Transport in a Linked Overland-Aquifer Density Dependent System
GSA	Global sensitivity analysis
P	Phosphorus
PDF	Probability Distribution Function
SFRSM	South Florida Regional Simulation Model
SFWMD	South Florida Water Management District
SFWMM	South Florida Water Management Model
SICS	Southern Inland and Coastal Systems
SRP	Soluble Reactive Phosphorus
SWIFT2D	Surface-water Integrated Flow and Transport in 2 Dimensions
TaRSE	Transport and Reaction Simulation Engine
TIME	Tides and Inflows in the Mangroves of the Everglades
TP	Total phosphorus
UA	Uncertainty Analysis
USGS	United States Geological Survey

Abstract of Dissertation Presented to the Graduate School
of the University of Florida in Partial Fulfillment of the
Requirements for the Degree of Doctor of Philosophy

ADAPTIVE SPATIALLY-DISTRIBUTED WATER-QUALITY MODELING: AN APPLICATION TO MECHANISTICALLY SIMULATE PHOSPHORUS CONDITIONS IN THE VARIABLE-DENSITY SURFACE-WATERS OF COASTAL EVERGLADES WETLANDS

By

Stuart John Muller

August 2010

Chair: Rafael Muñoz-Carpena
Major: Agricultural and Biological Engineering

The Everglades region known as the Southern Inland and Coastal Systems is an important area that supports numerous endangered species and plays a crucial role in regulating water-quality conditions in Florida Bay. Taylor Slough is a major feature of this region and represents the primary surface-water pathway for freshwater inputs to Florida Bay. The slough is also subject to intensive flow management under the Comprehensive Everglades Restoration Plan, yet the consequences of such management for water-quality in these oligotrophic and sensitive wetlands are not well understood. A flexible phosphorus water-quality model was therefore developed and tested as an exploratory management tool for the region. Complex local hydrodynamics required that a spatially-distributed hydrodynamic model be used to simulate flow and transport and the USGS model FTLOADDS was selected for this. A user-definable biogeochemical reactive component (aRSE) was then coupled with the hydrodynamic model and the resulting FTaRSELOADDS model was tested against analytical solutions and field data.

Hydrodynamic field testing showed that depth-varying Manning's resistance was important for accurately capturing wet and dry conditions during the experimental period. Conceptual water-quality models of increasing complexity were tested against experimental phosphorus field data. Results revealed that a simple daily averaging method was the best approach for atmospheric deposition of phosphorus, which is a crucial but very uncertain water-quality input. A simple conservative transport model provided the best fit between modeled and total phosphorus concentration data. Similar results were also obtained with a more complex and mechanistically justifiable water-quality model. The adaptability of the biogeochemical component was used to study how additional model complexity affects model uncertainty, sensitivity and relevance by evaluating progressively more complex conceptual models using global sensitivity and uncertainty analyses. The framework applying these methods is suggested as a useful way of evaluating models in general, and deciding upon a relevant model structure when the freedom to dictate complexity exists.

CHAPTER 1
INTRODUCTION

The Southern Inland and Coastal Systems of the Everglades: A Region at Risk

The Southern Inland and Coastal Systems (SICS) region of the southern Everglades (Figure 1-1) connects Taylor Slough and the C-111 marl prairie wetlands with Florida Bay, and represents an important region of Everglades study and management (SFWMD and FDEP, 2004; CRGEE and NRC, 2002). Though Taylor Slough is substantially smaller than Shark River Slough, in both discharge and areal extent, it plays an important role in regulating water-quality in Florida Bay (Fourqurean and Robblee, 1999). Additionally, the region encompasses thousands of acres of habitat that support dwindling populations of saltwater and freshwater animal species (van Lent et al., 1998), fifteen of which are listed as threatened or endangered with extinction (Beccue, 1999), including the Federally protected Cape Sable Seaside Sparrow (Pimm et al., 2004).

Flow through the southern Everglades has been increased as part of the Comprehensive Everglades Restoration Plan (CERP), with further increases imminent. The potential effects of these changes on nutrient conditions in Taylor Slough, the neighboring wet marl prairies, or the estuaries of Florida Bay is not well understood and the subject of ongoing research (Childers, 2006). Studies suggest that the SICS area is already under intense ecological stress from past management decisions that have impacted flow and nutrient conditions (Childers, 2006; Gaiser et al., 2006; Armentano et al., 2006). In addition, gradual reductions in freshwater inputs flowing southwards have contributed to the encroachment of saltwater tolerant species, primarily mangrove forest, into previously freshwater marsh vegetation (Smith, 1998). Of particular concern

are the possible consequences of additional nutrient loading to Florida Bay (SFWMD and FDEP, 2004), which has seen an increase in the incidence of harmful algal blooms and mass seagrass die-off (Fourqurean and Robblee, 1999).

The Everglades are a highly oligotrophic system (Noe et al., 2001) due to a natural scarcity in bioavailable phosphorus. The concentration of phosphorus in the surface-water is therefore a principal consideration in the Everglades restoration. Freshwater marshes in the SICS region are characterized by unique macrophyte and periphyton communities that are adapted to phosphorus-scarce conditions. Periphyton taxa have been shown to be very sensitive to phosphorus conditions (Gaiser et al., 2004), with cascading ecological consequences resulting from even low levels of nutrient enrichment (Gaiser et al., 2005). Additionally, the low phosphorus loading with freshwater inputs to the estuaries of Florida Bay means that water from the Gulf of Mexico is their most important source of phosphorus, as opposed to the upstream watershed as is normally the case (Chen and Twilley, 1999; Fourqurean et al., 1992). This reversal in the source of the limiting nutrient, compared with typical estuaries (biogeochemically speaking), is the reason they are referred to as “upside-down” estuaries (Childers, 2006). It is believed that phytoplankton and seagrasses in eastern Florida Bay, which is most isolated from the Gulf of Mexico, are therefore phosphorus-limited (Fourqurean et al., 1992). Higher natural or anthropogenic loadings of phosphorus that may accompany increasing freshwater inputs could potentially increase the frequency, intensity, and duration of phytoplankton blooms in regions of Florida Bay.

However, significant increases in the volume of freshwater inflow relative to the nutrient additions from upstream sources could make terrestrial phosphorus inputs

negligible, and may possibly even suppress the natural marine phosphorus supply by dilution. Recent research has shown that freshwater inflows have been found to enhance oligotrophy where Taylor Slough sufficiently flushes the area and suppresses the intrusion of water from Florida Bay (Childers, 2006). As such, any increase in freshwater inflows could enhance oligotrophic conditions in the ecotone between fresh and marine waters, especially during the wet season.

Time-series water-quality and soil phosphorus data shows a general pattern of low phosphorus availability along Taylor Slough during the wet season except near the marine source (Boyer et al., 1999), and the influence of marine phosphorus moving upstream during the low-flow dry season. This was not expected for the southern Everglades ecotone as light easily penetrates the clear shallow waters above seagrass pastures, which are known to efficiently sequester marine phosphorus (Fourqurean and Robblee, 1999). New research in the area has indicated that surface-water phosphorus concentrations were unexpectedly high in the Taylor Slough ecotone during the dry season (Childers, 2006). It is conjectured that relatively phosphorus-rich ground-water inputs to this ecotone are significant during the dry season, when surface-water hydraulic heads are lowest and residence times are long enough to deplete dissolved organic matter, thus reducing productivity and phosphorus consumption (Price et al., 2006; Childers, 2006). Strong interactions between ground-water and surface-water in this region mean that increased surface-water heads may impact this ground-water exchange, and thereby affect phosphorus conditions.

Opportunities for Spatially-Distributed Mechanistic Modeling of Phosphorus in SICS

A model of spatially-distributed surface-water phosphorus conditions for the region is required to study these issues. Spatially-distributed mechanistic modeling of wetland water-quality remains a challenging field of hydrology. Modeling the movement of solutes both within and with the water is contingent upon reliable flow modeling, which is a difficult task unto itself in the vegetated and hydrodynamically complex SICS wetlands (Swain et al., 2004; Langevin et al., 2005). In addition, water-quality constituents are subject to a multitude of chemical, physical and biological processes in wetlands where unique biogeochemistry and ecology are drivers of, as much as driven by, water-quality.

Hydrologic Modeling of SICS

Numerical models for simulating water flow south of Lake Okeechobee have been developed for three distinct regions. The South Florida Water Management Model (SFWMM) (SFWMD, 2005) and its successor, the South Florida Regional Simulation Model (SFRSM) (Lal et al., 2005), simulate the highly managed hydrology between Lake Okeechobee and Everglades National Park (ENP). The southern and western offshore waters of Florida Bay are modeled with the Florida Bay Hydrodynamic Model (Hamrick and Moustafa, 2003). The hydrologically complex region between these models' domains is encompassed by SICS, and is characterized by surface-water/ground-water and freshwater/saltwater interactions within a highly vegetated and hydrodynamically unsteady environment. A further specialized modeling effort was therefore required (Swain et al., 2004; Langevin et al., 2005; Wang et al., 2007), which culminated in the Flow and Transport in a Linked Overland-Aquifer Density Dependent

System (FTLOADDS) model (Langevin et al., 2005). FTLOADDS links the managed hydrology of the mainland with that of Florida Bay; outputs from SFWMM are applied as boundary conditions in FTLOADDS, the outputs from which are in turn applied as boundary conditions for the Florida Bay Hydrodynamic Model. In this way, an integrated hydrologic modeling framework of the region was produced that could propagate the hydrologic consequences of upstream management scenarios onto the downstream systems. Furthermore, detailed hydrologic conditions can be simulated for use by mechanistic ecological models that rely on such information, and which is typically not practically obtainable at the desired resolution (Swain et al., 2004).

FTLOADDS is itself composed of two models; the Surface-Water Integrated Flow and Transport in Two Dimensions (SWIFT2D) model (Schaffranek, 2004) adapted for coastal wetlands (Swain, 2005), and the variable-density ground-water model SEAWAT (Langevin and Guo, 2006). An application of FTLOADDS to the SICS area that uses only SWIFT2D, and thus neglects surface-water/ground-water interactions, has been shown to provide acceptable hydrodynamic results (Swain et al., 2004).

Water-Quality Modeling of SICS

Models of the Everglades hydrology and hydrodynamics have and continue to be addressed, but analogous tools for water-quality are still needed (McPherson and Torres, 2006). One approach to addressing this need is to develop a detailed ecosystem model (Wang and Mitsch, 2000). This approach simulates a large number of biogeochemical processes and therefore requires many parameters, which make the model cumbersome to apply and prone to overparameterization (Beven, 2006a). Such conceptually complex models often use free-form tools such as STELLA (Doerr, 1996), which can be readily tailored to the specific water-quality considerations at hand.

However, the versatility often comes at the expense of spatial heterogeneity, which is an untenable simplification in the context of the scale and spatial complexity of SICS.

For instance, the spatial variation in microtopography, landcover, and complex flow boundaries that include canals, pumping stations, and tidal effects, are known to be important factors that determine water-level (and therefore whether conditions are wet or dry) and velocity in SICS (Swain et al., 2004). Flow velocity is crucial for accurate solute transport when using the advection-dispersion equation. Water-level is biogeochemically important because it determines whether conditions are dry or wet, which has implications for the presence or absence of aquatic biota and senescence and decomposition processes (Reddy et al., 1999). Both velocity and water-level are important for accurate estimation of discharge, which with concentration determines loading rates that would be of interest to Florida Bay. Additionally, the original SICS hydrodynamic modeling effort demonstrated the striking effect of wind shear on water-levels and the directionality of discharges through coastal creeks, and in turn, important wind-driven mixing (Swain et al., 2004). In order to accurately capture these transient effects in the transport solution a mechanistic hydrodynamic model is required that accounts for their effects. Consequently, a spatially-distributed and mechanistic hydrodynamic foundation was considered requisite.

A more common and simplified approach is to aggregate all phosphorus cycling mechanisms into a single lumped process that captures net uptake or release (Kadlec and Knight, 1996; Mitsch et al., 1995; Walker, 1995), or some combination of lumping and mechanistic methods (Kadlec, 1997). This simplification in biogeochemistry is counterbalanced by the complexity of spatial heterogeneity in hydrology. However, the

modeling efforts cited simulated surface-water flow using simplified mass balance approaches (Walker, 1995; Wang and Mitsch, 2000) or as nondispersive, unidirectional plug flow (Kadlec, 1997), which are not suitable for the complex conditions in SICS. In addition to homogeneous hydrology, there is also no accounting for spatial heterogeneity in wetland components and processes that may be important or desirable (for example, soil phosphorus concentration or accretion and macrophyte or periphyton biomass).

With the arrival of spatially-distributed mechanistic models of Everglades hydrology, the logical step to develop a mechanistic water-quality model that built on this foundation was undertaken. The result was TaRSE, the Transport and Reaction Simulation Engine (Muller and Muñoz-Carpena, 2005; Jawitz et al., 2008; James et al., 2009). The term "reaction simulation engine" alludes to a novel characteristic of TaRSE; the state-variables and equations relating them are user-defined. To our knowledge, this was the first time a spatially-distributed mechanistic water-quality model had been developed with the built-in flexibility of a free-form simulation model for defining the system of biogeochemical water-quality processes. This pairing represents an important new management and research tool for the SFWMD to address phosphorus related water-quality issues. Though originally integrated into SFRSM, a version of TaRSE without the transport (now a Reaction Simulation Engine - aRSE) has subsequently been extricated from SFRSM and modularized.

Model Selection

A critical consideration in the selection of a model is the choice of appropriate complexity. In the context of mechanistic water-quality modeling, which entails a two-step process of simulating hydrology and biogeochemistry, this choice must be made

twice. Historically, the complexity of each of these components has often been mutually exclusive, though the greater prevalence of spatial data and computational power have seen a move towards models with complex treatments of both hydrology and biogeochemistry (Costanza et al., 1990). Figures 1-2 and 1-3 present a number of phosphorus water-quality models that were reviewed and classified according to their overall complexity. They demonstrate the wide range of complexities and approaches that exist for modeling phosphorus-related water-quality.

A distinguishing feature in the design of models that is associated with their complexity is whether they are “fixed-form” (usable as-is only), or “free-form” (intentionally user-definable). The fixed-form development paradigm is generally applied for complex spatially-distributed models (of which hydrologic models are a prime example), which require computationally efficient numerical solutions. Many hydrologic models are based on fundamental laws of physics, and consequently are quite versatile despite their rigid design. Free-form models are sometimes referred to as dynamic systems models, and are more suitable to simulating systems where spatial heterogeneity can be neglected. The relatively light computational demands of a spatially-lumped model compared with a spatially-distributed one make it amenable to a more flexible design. The user is therefore able to specify state-variables of interest and how they are related, with the result that such tools are highly adaptable to a variety of system applications, including biogeochemical cycling. The extensive and varied application of STELLA, a widely used example of a free-from model, is indicative of this versatility (Doerr, 1996).

The complexity of SICS hydrology calls for a fixed-form spatially-distributed mechanistic hydrodynamic model. Yet the lack of a clear indication of what, exactly, a phosphorus water-quality model should look like (Figures 1-2 and 1-3), and the looming need for models of other water-quality constituents and ecological components, calls for a free-form solution. It was therefore proposed that a fusion of the fixed-form and free-form development paradigms be attempted by linking the SWIFT2D model within FTLOADDS with aRSE.

Important SICS Modeling Considerations

Since the initial application of SWIFT2D to SICS (Swain et al., 2004) the model has been further adapted for application to the larger Tides and Inflows to the Mangroves of the Everglades (TIME) domain (Wang et al., 2007), which includes the SICS model domain but is applied using a somewhat larger cell size (500 m as opposed to 304.8 m). These changes include a number of potentially important simplifications; rainfall and evapotranspiration (ET) rates are now applied homogenously, and the Manning's coefficient no longer varies with flow-depth, though it is now treated anisotropically where before it was considered isotropic. The implications of the changes to rainfall and evapotranspiration have been sufficiently justified for SICS (Wang et al., 2007). The consequences of depth-invariant Manning's coefficients are unclear though, particularly since this proved to be an important factor in the original SICS hydrologic modeling effort (Swain et al., 2004). Depth-varying Manning's *n* was also found to be important under similar assumptions of homogeneous rainfall and ET in the ridge and slough Everglades landscape (Min et al., 2010). Of particular concern is how this change affects the ability of SWIFT2D to accurately capture dry versus wet conditions, which are important for phosphorus cycling (Reddy et al., 1999).

A second important consideration pertain to atmospheric deposition of total phosphorus (TP). This is a crucial input for modeling water-quality under the oligotrophic conditions found in SICS (Sutula et al., 2001; Noe and Childers, 2007). However, atmospheric deposition of phosphorus is notoriously difficult to quantify due to persistent sample contamination and limitations in the sampling methods (Redfield, 1998; Ahn, 1999). Bulk phosphorus deposition in Florida is estimated to be comprised of as much as 30-50% dry deposition from resuspended agricultural soils, phosphogypsum mining, urban emissions and transported dust (Landing, 1997; Meyers and Lindberg, 1997). However, rainfall is known to scavenge aerosol phosphorus and incorporate dry deposition into wet deposition estimates, further complicating quantification of the process.

Measured rates of bulk atmospheric deposition in the Everglades exhibit great variability, ranging from 0.017 to 0.07 g TP/m^2/yr, with an average of 0.03 g TP/m^2/yr (Sutula et al., 2001). Fitz and Sklar (1999) estimated total phosphorus deposition to be 0.03 g TP/m^2/yr for the Everglades, which is similar to an estimate by Davis (1994) of 0.036 g TP/m^2/y, and the same as that of 0.03 g TP/m^2/yr found for the Kissimmee region 100 miles north of the Everglades (Moustafa et al.. 1996). Rates as low as 0.0006 g P/m^2/yr have been estimated for the Bahamas (Graham and Duce, 1982). South Florida weather is characterized by frequent convection thunderstorms, which can scavenge aerosol phosphorus from the upper atmosphere (Poleman et al., 1995), and the location of SICS in the proximity of Miami could subject it to higher deposition rates associated with adjacent urban or industrial areas (Paerl, 1995; Redfield, 1998).

Consequently, there is great uncertainty in the quantification of atmospheric deposition of phosphorus, and the process will therefore represent a major source of uncertainty in any phosphorus water-quality modeling effort. How best to input this source remains an open question. Another important open question is, given the free-form of aRSE, what complexity of water-quality model to select. This raises the issue of how to balance model complexity and relevance.

Model Relevance

A principal tenet of model development is the establishment of *relevance* (Zadeh, 1973). Relevance is determined by balancing the *complexity* of a model against its *uncertainty*, given the modeling objectives at hand. This topic is introduced and discussed in great detail in Chapter 5, which is presented as a standalone paper, but is briefly reviewed here to clarify the motivation.

Model complexity is a property of the degree of detail implicit to the conceptualized rendition of reality, including the number of state variables and processes simulated. Increasing complexity implies ever more variables and processes, and therefore ever fewer simplifying assumptions. This results in a modeled version of reality with greater mechanistic integrity and thus less structural uncertainty. However, each new state-variable and process introduced requires additional calibration and parameterization data, all of which are subject to some measurement uncertainty. These measurement uncertainties accumulate and eventually outweigh any reductions in structural uncertainty gained by increasing complexity (Hanna, 1988). The sensitivity of model outputs also accumulates with consequences for the practicability of the model (Snowling and Kramer, 2001). Each added process that exerts some influence over a state-variable, either directly or through interactions with other processes, represents

additional flexibility in the model that can lead to overparameterization issues that can seriously undermine the validity of a model (Beven and Binley, 1992).

Two model evaluation methods exist that are ideally suited to elucidating these relationships. Uncertainty analysis applies Monte Carlo simulations to propagate the uncertainty inherent to model inputs onto outputs of interest. In this way, the uncertainties in an output for a given model structure, and subject to the given model input requirements, can be assessed and compared. Global sensitivity analyses determine where the uncertainty in an output originates from (Saltelli et al., 2000). Together, these evaluation methods can shed light on how much uncertainty is in the model, and why it is there (Muñoz-Carpena et al., 2007). When performed in the context of varying model complexity we are then able study how additional complexity affects the model's inner workings (Jawitz et al., 2008).

The process of defining a model is also the process of defining a model's complexity; the ultimate source to which many modeling considerations and challenges can be traced. This tripartite web of interacting complexity, uncertainty, and sensitivity has not been well-studied in very complex models (Lindenschmidt, 2006)precisely because they have typically been fixed-form. A flexible model structure presents a novel opportunity to subtly experiment with advanced levels of model complexity and to assess how complexity affects uncertainty, sensitivity, and ultimately relevance.

Research Questions and Objectives

Research Questions

There is urgent need for modeling tools to simulate a variety of water-quality issues of interest in the southern Everglades, and in particular phosphorus conditions in the sensitive of oligotrophic freshwater marshes. Assessing likely phosphorus

conditions in the surface-water in response to CERP flow management decisions is a pressing concern. Though a suitable hydrodynamic model of SICS has been identified and tested for hydrological outputs (Swain et al., 2004), its suitability to supporting spatially-distributed water-quality simulations needs to be assessed. Furthermore, as indicated atmospheric deposition of phosphorus is an important process in the oligotrophic freshwater Everglades that remains very difficult to quantify. How best to handle this crucial input is therefore a major source of uncertainty. Finally, with the flexibility of a free-form water-quality model the definition of the phosphorus conceptual model becomes a moving target, yet a suitable complexity must eventually be settled upon. Open questions to be addressed in this dissertation include:

- What are the consequences of recent changes to the SWIFT2D code that included removal of depth-varying Manning's roughness? In particular, how do these changes affect the hydrodynamic prediction of wet versus dry conditions in SICS, which are important distinctions for a water-quality simulation?
- Given the acknowledged uncertainty associated with quantifying atmospheric deposition of phosphorus, what methods of inputting this source to the water-quality model produce the most accurate simulated concentrations?
- What is the simplest phosphorus water-quality model that would produce acceptable results for SICS? Can a more complex and mechanistic model of water-quality produce comparable or better results than a simpler one?
- Given the tradeoffs between complexity and uncertainty, how does one choose what model complexity is appropriate, and how does uncertainty and sensitivity change with the addition of further complexity?

Objectives

1. Development of a combined fixed-form/free-form spatially-distributed hydrologic and biogeochemical model, validated against analytical testing, which is suitable for application to simulate phosphorus water-quality in SICS (Chapter 2).
2. Application of the new tool to study the importance of depth-varying Manning's roughness in hydrodynamic simulations of SICS surface-water (Chapter 3).

3. Application of the new tool to determine how best to input phosphorus additions by atmospheric deposition, and to determine what complexity of phosphorus water-quality model best captures measured phosphorus conditions in SICS surface-waters (Chapter 4).

4. Formal evaluation of the effect of using different complexity biogeochemical conceptual models on output uncertainty, global sensitivity, and model relevance (Chapter 5).

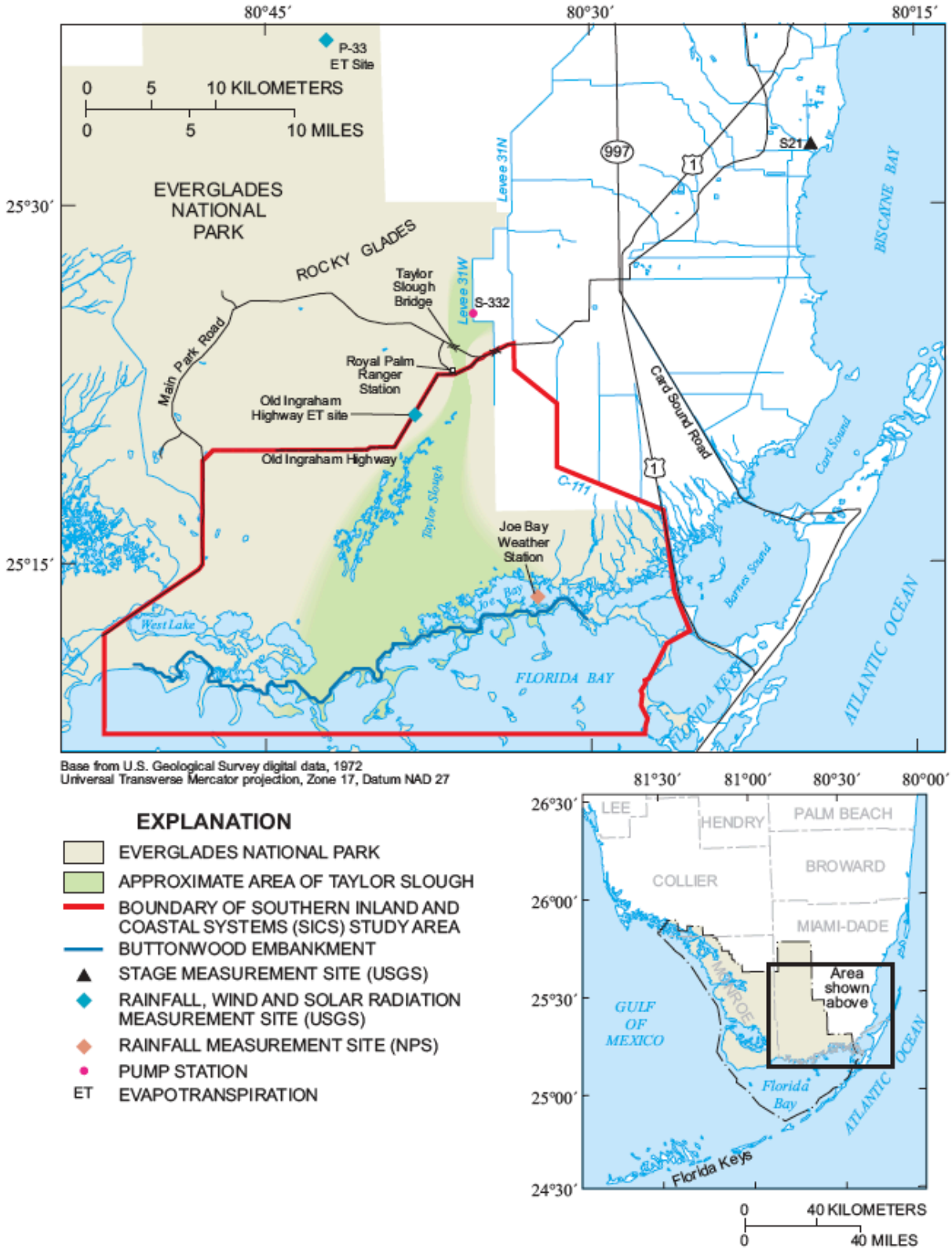

Figure 1-1. Location of the Southern Inland and Coastal Systems study area (from Swain et al., 2004).

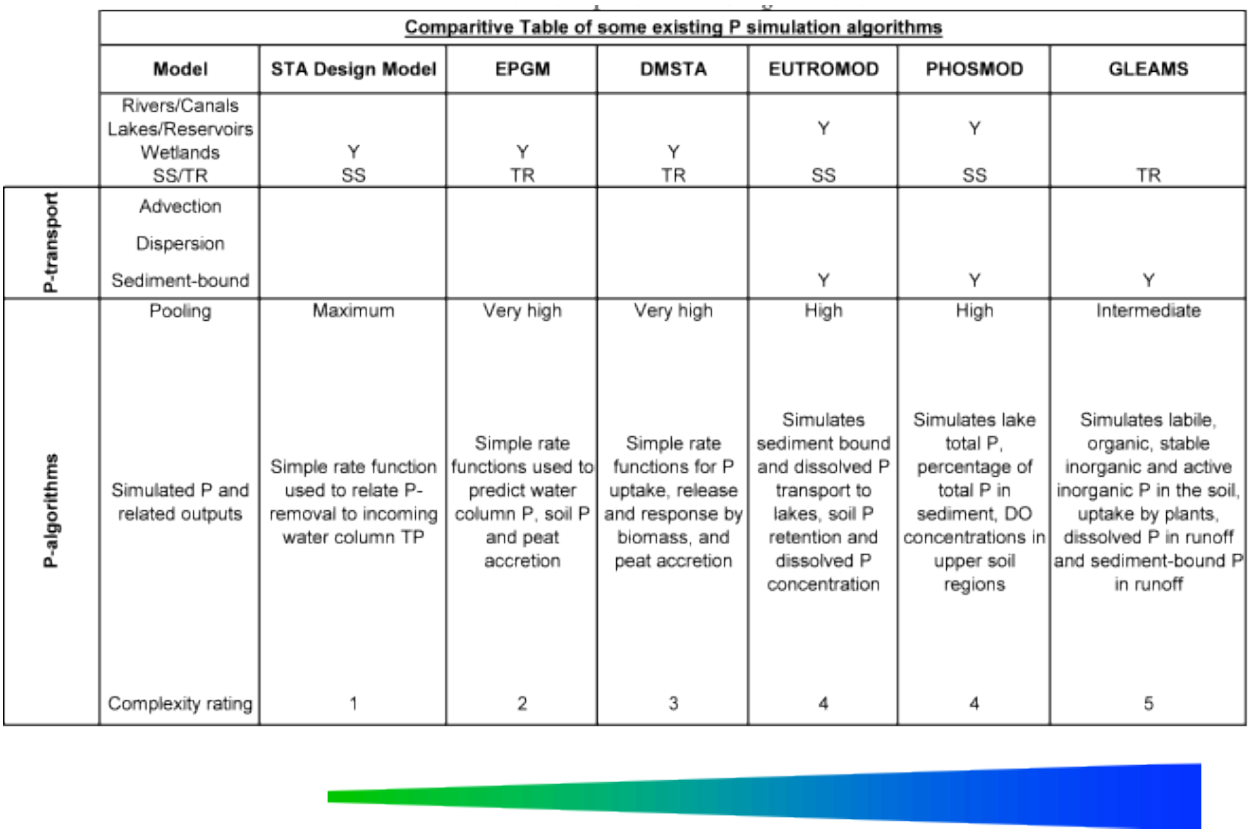

Comparitive Table of some existing P simulation algorithms							
	Model	**STA Design Model**	**EPGM**	**DMSTA**	**EUTROMOD**	**PHOSMOD**	**GLEAMS**
	Rivers/Canals				Y	Y	
	Lakes/Reservoirs						
	Wetlands	Y	Y	Y			
	SS/TR	SS	TR	TR	SS	SS	TR
P-transport	Advection						
	Dispersion						
	Sediment-bound				Y	Y	Y
P-algorithms	Pooling	Maximum	Very high	Very high	High	High	Intermediate
	Simulated P and related outputs	Simple rate function used to relate P-removal to incoming water column TP	Simple rate functions used to predict water column P, soil P and peat accretion	Simple rate functions for P uptake, release and response by biomass, and peat accretion	Simulates sediment bound and dissolved P transport to lakes, soil P retention and dissolved P concentration	Simulates lake total P, percentage of total P in sediment, DO concentrations in upper soil regions	Simulates labile, organic, stable inorganic and active inorganic P in the soil, uptake by plants, dissolved P in runoff and sediment-bound P in runoff
	Complexity rating	1	2	3	4	4	5

Figure 1-2. Reviewed phosphorus water-quality models and algorithms (from simple to complex from left to right).

	Comparitive Table of some existing P simulation algorithms continued						
	Model	**WASP6**	**HSPF**	**ELM**	**CE-QUAL-RIV1**	**CE-QUAL-W2**	**CE-QUAL-ICM**
	Rivers/Canals	Y	Y		Y		Y
	Lakes/Reservoirs	Y	Y			Y	Y
	Wetlands	Y		Y		Y	Y
	SS/TR	TR	TR	TR	TR	TR	TR
P-transport	Advection	y	y		y	y	y
	Dispersion	y			y	y	y
	Sediment-bound	y		y	y	y	y
P-algorithm	Pooling	Low	Low	Low	Low	Low	Very low
	Simulated P and related outputs	Simulates dissolved P,N and organic P,N in the water column, benthic algae, periphyton and detritus, accounting for DO, salinity temperature and sediment bonding	Simulates dissolved inorganic and organic P in surface and soil water, accounting for temperaure, DO, sediment bound transport, N-cycle, zooplankton, phytoplankton and pH	Simulates water column, soil, floc, periphyton, macrophyte and detrital P and C, as well as peat accretion, periphyton communities and biomass, and macrophyte communities and biomass	Simulates (for 1-D flow) phytoplankton, bacteria, DO-carbon balance, N, P cycle accounting for salinity and temperature. Also accounts for sediment/water O,N and P flux	Simulates phytoplankton, bacteria, DO-carbon balance, N, Si, P cycle accounting for salinity and temperature. Also accounts for sediment/ water O,N and P flux	Simulates up to 3 species of phytoplankton, zooplankton, bacteria, DO-carbon balance, N, Si, P cycle accoutning for salinity and temperature. Also accounts for sediment/water O,N and P flux
	Complexity rating	8	9	9	9	9	10

Figure 1-3. Reviewed phosphorus water-quality models and algorithms (from intermediate to complex from left to right).

CHAPTER 2
FUSION OF FIXED-FORM AND FREE-FORM MODELS FOR ADAPTIVE SIMULATION OF SPATIALLY-DISTRIBUTED WETLAND WATER-QUALITY

Introduction

Spatially-distributed mechanistic water-quality modeling of wetlands, such as those in southern Florida, requires simulating three distinct, yet inter-related, aspects: 1) the quantity and timing of water distribution ("hydrodynamics"); 2) the motion of constituents with and within the water by advection, dispersion and diffusion ("transport"); and 3) local biogeochemical processes that change the nature or state of constituents ("reactions"). Mechanistic hydrodynamics and transport of large-scale wetland systems generally requires spatially-distributed modeling. The numerical considerations associated with this, in conjunction with the generality of the underlying physics, results in models that are hard-coded – or "fixed-form" – with little or no freedom on the part of the user to influence the theoretical concepts driving the simulation. By contrast, biogeochemical reactions can be more readily conceptualized as a non-spatial system by relying on hydrodynamics and transport to provide the spatial connection. Water-quality reactions are therefore more amenable to non-spatial dynamic systems simulation, for which user-definable – or "free-form" – modeling tools are regularly used. The need for spatially-distributed mechanistic water-quality models therefore offers an excellent opportunity to integrate the versatility of a "free-form" dynamic systems model with the mechanistic and numerical rigor of a spatially-distributed fixed-form modeling.

Fixed-Form Versus Free-Form

Truly mechanistic models of hydrology apply theoretically derived equations of flow dynamics, which are generally well-understood and are based on uniformly

applicable laws of physics. For instance, the Surface-Water Integrated Flow and Transport in Two Dimensions (SWIFT2D) model (Leendertse, 1987; Schaffranek, 2004; Swain, 2005) applies the St. Venant equations, which are derived from Newton's Second Law (Conservation of Momentum) and the Principle of Conservation of Mass. Spatial discretization of the model domain is necessary to capture variability in space, and transience is captured by repeatedly solving the equations in successive time-steps. This approach is contingent on limitations to the size of both spatial and temporal discretizations in order to maintain mathematical stability of the numerical solutions. Stability considerations in conjunction with simulations of large areas or long periods can therefore become computationally intensive, even limiting, despite the modern computational capacities we have at our disposal.

To ensure numerical efficiency such hydrologic models are generally hard-coded into a fixed-form. This limits the model's application to only those conditions that meet the underlying (and fixed) assumptions. However, given the universality of physics, mechanistic flow models that use equations derived from theoretical principles remain generally versatile. For example, SWIFT2D has been applied to a multitude of water bodies and locations, including: Jamaica Bay, New York (Leenderste, 1972), the Dutch Delta Works of the Netherlands (Dronkers et al., 1981; Leendertse et al., 1981), the Dutch Wadden Sea (with modifications to evaluate mixing) (Riddererinkhof and Zimmerman, 1992), the Eastern Scheldt estuary in the Netherlands (Leendertse, 1988), the Pamlico (Bales and Robbins, 1995) and Neuse River (Robbins and Bales, 1995) estuaries of North Carolina, Tampa Bay (Goodwin, 1987), Hillsborough Bay (Goodwin, 1991), and the upper Potomac estuary in Maryland (Schaffranek, 1986).

Transport of dissolved and suspended constituents can be mechanistically simulated with the theoretically derived advection-dispersion equation (Equation 2-1). A reaction term can be introduced (now the advection-dispersion-reaction equation) to simulate first-order growth or decay reactions. Given the dependence on velocity, transport modeling within spatially-distributed systems is often integrated into existing hydrologic models, and inherits a fixed-form structure. This is the case for both SWIFT2D (Schaffranek, 2004) and SEAWAT (Langevin and Guo, 2006). However, the underlying simple and generic mathematical formulation of linear growth and decay kinetics make the reactive transport universally applicable for any constituent, provided first-order reaction kinetics are appropriate for the process.

The introduction of biogeochemical processes, which are fundamental to wetland water-quality (Mitsch and Gosselink, 2000), greatly complicates matters because such processes are too complex to be mechanistically derived from a physics-based foundation. The biology, chemistry and physics of the aquatic environment all interact to form a byzantine web of feedbacks that constitute some of the most complex natural systems science has endeavored to conceptualize. Simulating such complex biogeochemical systems requires substantial simplification and abstraction, and even then presents a significant technical challenge (Arhonditsis and Brett, 2004).

Matters are further confounded by the sheer variety of water-quality subjects – sediments, nutrients, pesticides, bacteria, pH, salinity, dissolved oxygen, dissolved organic matter, and algae, to name but a few – each of which are involved in their own unique biogeochemical processes. Spatially-distributed modeling of water-quality issues has therefore also generally been of the fixed form. Particular water-quality functionality

is to address a particular water-quality issue hard-coded into a given hydrologic model, which limits the applicability of the water-quality model to the range of appropriate hydrologic applications, and limits the conceptual model of the water-quality constituent to the hard-coded form.

Rarely have the power of free-form dynamic system models and fixed-form spatially-distributed hydrologic models been integrated. The aforementioned development of TaRSE (Jawitz, et al., 2008; James et al., 2009) in Chapter 1 was, to the best of our knowledge, the first instance of this. The reasons for this are unclear, although it is sufficiently intriguing to warrant some conjecture. Dynamic simulation models have generally been written in object-oriented programming languages since these are conceptually well matched to the task. By comparison, spatially-distributed mechanistic models have been written in linear programming languages such as FORTRAN, which carry benefits for numerically efficient processing of the large arrays of data associated with a spatially discretized domain.

Many of the most popular hydrologic models have their foundations in the early days of hydrologic model development, when the fusion of linear and object-oriented programming philosophies was uncommon because computational limitations of the day demanded the highest possible efficiencies. More often than not this meant coding in FORTRAN. The two sub- models of FTLOADDS, both coded in FORTRAN, are classic examples of this: SIMSYS2D (Leendertse et al., 1987) is based on model development from the 1970s (Leendertse, 1970) and is the progenitor of SWIFT2D; and SEAWAT is ultimately an adapted version of a 1983 modular ground-water model that would become MODFLOW (McDonald and Harbaugh, 1988). Mixed-language programming

has become increasingly common with ever-growing computational capacity (Zimmermann et al., 1992; Cary et al., 1997). Although languages such as FORTRAN still offer the greatest control over computational efficiency, many higher-level programming and even scripting languages are becoming popular alternatives for applications that are not critically limited by computational considerations (Oliphant, 2007).

It is also the case that model development is never without a purpose, and it is difficult to conceive of developing a water-quality model without a particular water-quality issue as the objective. In hindsight, it seems that a combination of serendipity and naïveté was at play in the development of TaRSE. The lack of experience at the time in both biogeochemistry and water-quality modeling on the part of this author, who was tasked with researching and formulating the preliminary water-quality conceptualization (Muller and Muñoz-Carpena, 2005), lead to particular attention and frustration associated with the choice of model complexity. This was amplified by the express intention of the project to develop a tool for application to water bodies throughout the Everglades, including wetlands, canals, and reservoirs, all of which are subject to their own biogeochemical idiosyncrasies (Reddy et al., 1999). It would appear that these factors combined with the object-oriented programming paradigm brought to the project by the team programmer to inspire the notion of a truly free-form spatially-distributed water-quality model.

Materials and Methods

In this section we describe the models selected for linkage and the processes by which their integration was achieved. Following this we present the results of testing conducted to validate the reactive transport of the fixed-form model against known

analytical solutions. Validation of the linkage between the fixed- and free-form models is then presented.

Description of the Models

The fixed-form hydrologic model used was Flow and Transport in a Linked Overland-Aquifer Density Dependent System (FTLOADDS) (Wang et al., 2007), and the free-from water-quality model was a Reaction Simulation Engine (aRSE) (Jawitz, et al., 2008). Together, they constitute a novel and potentially powerful new water-quality modeling tool for the coastal Everglades wetlands; Flow, Transport and a Reaction Simulation Engine in a Linked Overland-Aquifer Density Dependent System (FTaRSELOADDS).

Fixed-form hydrology and transport model: FTLOADDS

The USGS has recently developed FTLOADDS as a tool for simulating linked surface and subsurface hydrology and transport. Surface hydrology in FTLOADDS is modeled using the Surface-water Integrated Flow and Transport in Two Dimensions (SWIFT2D) model (Swain, 2005), which simulates vertically-averaged, variable-density, transient overland flow and transport of solutes. Subsurface hydrology in FTLOADDS is modeled using SEAWAT (Langevin, 2001; Guo and Langevin, 2002; Langevin and Guo, 2006), which simulates three-dimensional, variable-density, transient ground-water flow and transport through a porous media. The two models are linked through the exchange of water and constituent mass between the surface and subsurface (Langevin et al., 2005).

A number of different versions and implementations of FTLOADDS, SWIFT2D within FTLOADDS, and the SICS application using these tools are referred to. Appendix A contains a detailed breakdown of the distinguishing features of each version

and the nomenclature adopted by the USGS, and adapted herein. In this chapter, reference to “FTLOADDS” will imply FTLOADDS v1.2, which implements the latest SWIFT2D code used in FTLOADDS v2.2 (Wang et al., 2007) but with leakage and ground-water flow disabled, hence FTLOADDS v1.2 and SWIFT2D v1.2 (see Appendix A). In Chapter 3 some code changes were implemented that constituted a new sub-version, v1.2.1. Each version of each model is graphically outlined in Appendix A to facilitate clarification of the sub-models that comprise each model and application version.

Free-form water-quality reactions model: aRSE

With support from SFWMD and USGS, a group at UF recently developed a biogeochemical component, the Transport and Reaction Simulation Engine (TaRSE), for simulating the water-quality processes that control phosphorus concentrations and fate in Everglades wetlands (Jawitz et al., 2008; James et al., 2009). The term “simulation engine” alludes to the generic nature of the tool, which permits the user to define the conceptual biogeochemical system by controlling both the state-variables and the mathematical form of the processes that connect them. Given the existence of a number of proven hydrologic models for the Everglades, TaRSE was developed as a water-quality module, and therefore relies on a suitable hydrologic model to simulate flow and provide the necessary hydrodynamic inputs. The South Florida Regional Simulation Model (SFRSM) was selected as the first such hydrologic model. However, the absence of any solute transport functionality in SFRSM necessitated this be incorporated into the development of TaRSE. This transport functionality is contingent on the triangular mesh geometry employed by SFRSM for spatial discretization, which became a significant restriction on the portability of TaRSE for use by other hydrologic

models, many of which already have transport functionality of their own and a square spatial discretization geometry. The modularity of TaRSE was therefore re-established by extricating it from SFRSM and removing the transport functionality, leaving it as simply a Reaction Simulation Engine (aRSE). Portability of aRSE was finalized through its modularization into a dynamically linked library (DLL), which is callable by any model, hydrologic or otherwise, to which it offers a powerful and flexible simulation engine.

Fusing Fixed- and Free-Form Models

Figure 2-1 presents a schematic of the linkage implemented to integrate FTLOADDS and aRSE. Blue portions correspond to FTLOADDS code, green to aRSE code, and yellow to the linkage code. Black text and lines indicate FORTRAN, red text and lines indicate C++, solid lines indicate models, dashed lines indicate subroutines, solid line arrows indicate calls to subroutines in the same language, and mixed-dash arrows indicate calls from one language to another.

Full details of the technical considerations in the linkage are presented in Appendix A, but are briefly reviewed here in reference to Figure 2-1:

- An additional method for inputting aRSE parameters and state-variables was required for this information to be available to FTLOADDS at the beginning of the simulation. This was important for correctly exchanging hydrodynamic information between the models, and is achieved through a new input file that is read by the READIWQ subroutine during setup of SWIFT2D.

- FTLOADDS and its sub-models are all coded in FORTRAN, whereas aRSE is coded in C++. Mixed-language programming methods were therefore required to facilitate communication between the two models (indicated by the color-coding and mixed-dash lines in Figure 2-1).

- Since aRSE computes water-quality reactions for one cell at a time, it was necessary to establish a framework that would efficiently repeat this process for each of the cells in the spatially-distributed hydrodynamic domain. A temporary storage array is used to hold the latest values required by aRSE for each cell, which are in turn overwritten after each cell is processed by aRSE and returned to FTLOADDS once all cells have been reacted.

The general functionality of the linkage is described in detail in Appendix B (Section B1). The code comprising the various subroutines of the linkage is given in Appendix B (Section B2). An explanation of the IWQ input file is given in Appendix B (Section B3).

Analytical Testing of the FTaRSELOADDS Linkage

In order to verify that the code used to integrate FTLOADDS and aRSE was valid, a series of comparisons between numerically modeled results and known analytical solutions were conducted. While TaRSE has been previously tested, no published analysis of aRSE exists. Similarly, though widely used and thoroughly tested in practice, no published comparison of SWIFT2D reactive transport against known analytical solutions were identified. Therefore, the procedure outlined was intended to test both models in addition to their linkage. This process consisted of two main steps: 1) testing the reactive transport of SWIFT2D against an established analytical solution; and 2) reproducing these results using aRSE to perform the reactions calculations previously performed by SWIFT2D. In this way, the SWIFT2D code was verified against an analytical solution and could be used as a benchmark against which to verify the linkage. If FTaRSELOADDS reproduced the same results by relying on SWIFT2D for transport and the linked code of aRSE for the reactions, then both the linkage and the reactions code of aRSE will have been validated since a failure of either would preclude matching results.

Analytical solution

Reactive transport of dissolved constituents in two dimensions is described according to the advection-dispersion-reaction (ADR) equation (Equation 2-1):

$$\frac{\partial C}{\partial t} = -v_x \frac{\partial C}{\partial t} - v_y \frac{\partial C}{\partial t} + D_x \frac{\partial^2 C}{\partial x^2} + D_y \frac{\partial^2 C}{\partial y^2} - k_r C \qquad (2\text{-}1)$$

where C is concentration of the solute of interest; t is time; x is distance in the x-direction; y is distance in the y-direction; v_x is local velocity in the x-direction; v_y is local velocity in the y-direction; D_x is effective dispersion in the x-direction; D_y is effective dispersion in the y-direction; and k_r is the solute reaction rate.

The controlled velocity conditions implemented in SWIFT2D to ensure uniform velocity throughout the domain required using a type-three (flux-averaged) concentration boundary condition. Leij and Bradford (1994) present a suitable analytical solution for third-type boundary conditions in three dimensions, with a rectangular source area (Figure 2-2) of width *a* (in the y-direction), height *b* (in the z-direction), and flow in the x-direction, and provide the 3DADE software for numerically solving the solution. This software is now available as part of the STANMOD suite of numerical tools (Simunek et al., 1999; available at http://www.pc-progress.com/en/Default.aspx?stanmod) for solving various analytical solutions to the ADR equation.

In order to implement the 3-D solution for the horizontal 2-D conditions that SWIFT2D simulates, the *x*-direction was oriented in the direction of horizontal longitudinal flow, the *y*-direction as horizontally transverse to the direction of flow, and *z*-direction as the vertical plane over which the depth-averaged Navier-Stokes equations are integrated. In such an orientation vertically integrated conditions can be approximated by setting *b* sufficiently large compared with the dimension *a* to produce an effectively infinite height. This negated any variability in the *z*-direction and reduced the solution to an effective 2-D case. Additionally, the dispersion rate in the *z*-direction

was set to a value sufficiently low (Table 2-1) compared with that specified for the *x*- and *y*-directions to further negate any solute mass movement in the *z*-direction that might have occurred despite the large *b*-value. The value for vertical dispersion could not be set to zero exactly because it appears in the denominator of the analytical solution (see Equation 2-3 below). The analytical solution (Equation 2-2) solved using 3DADE is given in Leij and Bradford (1994) as follows:

$$C = \frac{C_o}{4}\int_{P(t)}^{t}\frac{v}{R}\Lambda_1(\tau)\Gamma(\tau)d\tau + \frac{\lambda}{2R}\int_0^t \Lambda_2(\tau)d\tau \tag{2-2}$$

for:

$$C(x,y,z,t)\big|_{x=0} = \begin{cases} C_0 & y<0, z<0, 0<t\le t_0 \\ 0 & \text{otherwise} \end{cases}$$

where:

$$\Gamma(\tau) = \left[\operatorname{erfc}\left(\frac{y-a}{(4D_y\tau/R)^{1/2}}\right) - \operatorname{erfc}\left(\frac{y+a}{(4D_y\tau/R)^{1/2}}\right)\right]\times \left[\operatorname{erfc}\left(\frac{z-b}{(4D_z\tau/R)^{1/2}}\right) - \operatorname{erfc}\left(\frac{z+b}{(4D_z\tau/R)^{1/2}}\right)\right] \tag{2-3}$$

$$\Lambda_1(\tau) = \exp\left(-\frac{\mu\tau}{R}\right)\left[\left(\frac{R}{\pi D_x\tau}\right)^{1/2}\exp\left(-\frac{(Rx-v\tau)^2}{4RD_x\tau}\right) - \frac{v}{2D_x}\exp\left(\frac{vx}{D_x}\right)erfc\left(\frac{Rx+v\tau}{(4RD_x\tau)^{1/2}}\right)\right] \tag{2-4}$$

$$\Lambda_2(\tau) = \exp\left(-\frac{\mu\tau}{R}\right)\left[\operatorname{erfc}\left(\frac{v\tau-Rx}{(4RD_x\tau)^{1/2}}\right) + \left(1+\frac{v}{D_x}(x+v\tau/R)\right)\times \exp\left(\frac{vx}{D_x}\right)\operatorname{erfc}\left(\frac{Rx+v\tau}{(4RD_x\tau)^{1/2}}\right) - \left(\frac{4v^2\tau}{\pi RD_x}\right)^{1/2}\exp\left(-\frac{(Rx-v\tau)^2}{4RD_x\tau}\right)\right] \tag{2-5}$$

and where R is the retardation factor; τ is time; v is porewater velocity; x is the position in the direction of flow; D_x, D_y, and D_z are dispersion coefficients in the x-, y-, and z-directions, μ is the first-order decay rate coefficient; and λ is the zero-order production rate coefficient.

Setup for testing of SWIFT2D

An important assumption implicit in the analytical solutions presented is that of uniform uni-directional velocity. However, given the complexity of SWIFT2D's mechanistic approach to hydrology, establishing a precisely uniform velocity field was not possible. To overcome this, and considering that the reactive transport was being tested and not the underlying hydrology, velocity was controlled by overwriting hydrodynamic values calculated by SWIFT2D at each time-step. In this way a uniform velocity was established, and observed discrepancies between numerical and analytical solutions were therefore known to be attributable to the numerical implementation of the reactive-transport equation, and not to variability in velocity.

A square test domain was established for SWIFT2D consisting of 101 x 101 cells, with each cell 100-m in length (Figure 2-3). Such a large domain was necessary given the decision to test the model for conditions approximating those under which it would be applied, namely low velocity and high dispersion (Swain et al., 2004), and the disparity in boundary conditions at the upper and lower borders of the domain. The analytical solution assumes open boundaries, but modeled domain was applied with no-flow boundaries. A constant velocity of 0.05 m/s was applied with a molecular diffusion of 20 m^2/s. For these conditions, the central fifty cells, justified to the left and centered around the source (Figure 2-3), were the focus region of the domain, and ensured

sufficient area remained in the domain to prevent any effect on concentrations within the focus region due to the discrepancy in boundary conditions.

Molecular diffusion in SWIFT2D is input as a single value that is applied isotropically in both dimensions of flow. The longitudinal dispersion coefficient (D_l) is computed in each cell (Equation 2-6) and in each principal direction of flow according to a function established by Elder (1959) relating flow conditions, depth, velocity, and the Chezy resistance coefficient according to:

$$D_l = \frac{C_d H \bar{u} \sqrt{(2g)}}{C}, \tag{2-6}$$

where C_d is a coefficient relating longitudinal dispersion to the local velocity; $\bar{u}$ is the local velocity; H is the temporal flow depth; g is acceleration due to gravity; and C is the Chezy resistance coefficient, related to the Manning's n according to (Leendertse, 1987):

$$C = \frac{H^{1/6}}{n}. \tag{2-7}$$

A representative value of 14.3 has been determined for C_d (Harleman, 1966). The total effective dispersion implemented in the advection-dispersion-reaction equation is then the sum of the longitudinal dispersion, which may be different for each direction, and diffusion, which is constant.

The 2-D analytical solution is valid for uni-directional flow. The absence of transverse velocity therefore prevented any dispersion from occurring in the transverse direction. In order to simulate 2-D solute transport it was therefore necessary to rely on the diffusion coefficient to generate dispersion in the transverse dimension. A reaction rate of -0.000001 s^{-1} was used to generate constituent decay for the reactive transport.

Setup for testing of FTaRSELOADDS

A first-order decay equation was input to aRSE through the XML input file. One state-variable was specified to represent the transported solute. One parameter, the reaction rate k_r, was input to reproduce the decay reaction. All other conditions were kept the same as those used for testing SWIFT2D

Results and Discussion

Conservative and reactive transport were simulated using SWIFT2D (Figures 2-4 and 2-5, respectively), and reactive transport using FTaRSELOADDS (Figure 2-4). Results using SWIFT2D confirm that the model correctly simulates solute transport, and that these results are reproducible using FTaRSELOADDS.

Benchmarking SWIFT2D

Results for 2-D transport of a non-reactive solute obtained using SWIFT2D (Figure 2-4) compared well with the analytical solution, but showed some disparity at the concentration front due to the effects of numerical dispersion (Fischer et al., 1979). To confirm that this was the source of the discrepancy in results the numerical dispersion (D_n) was calculated as per Swain et al. (2004):

$$D_n = \frac{0.5\left(\sigma_{i+1}^2 - \sigma_i^2\right)}{\Delta t}, \tag{2-8}$$

where σ^2 is the variance of the constituent concentration distribution and i is the computational cell number. When numerical dispersion was added to the value for dispersion allocated to the analytical solution the discrepancy at the concentration front is absent, confirming that numerical dispersion is the source of the differences. Close to the source boundary the differences are greater and cannot be mitigated by compensating for numerical dispersion.

Verifying FTaRSELOADDS

Results of reactive transport obtained using FTaRSELOADDS were essentially identical to those obtained using SWIFT2D by visual comparison (Figure 2-5). The ADI solution method implemented by SWIFT2D splits the transport step into two half-steps for each time-step, with one half-step used to calculate velocity in the x-direction, and the other the y-direction. This naturally lends itself to comparing the accuracy of alternate ways of integrating the reactions step of aRSE into the transport step of SWIFT2D. Three methods were identified and implemented: 1) applying the reactions after each half-step using the half-step time-step (TRTR, where T=transport and R=reactions); 2) applying the reaction step once in between the two transport steps, using the full time-step, (TRT); and 3) applying the reaction step once after both transport steps using the full time-step (TTR).

Given the closeness of results, visual analysis was unsuitable for comparison. To quantitatively assess how well the simulated results compared against the analytical solution throughout the entire model domain, a program was written making use of the CORSTAT (see Appendix B, Section B4) code (Aitken, 1973) to calculate the Root Mean Square Error (RMSE) and Nash-Sutcliffe (*E*) efficiencies (Nash and Sutcliffe, 1970) for each of the concentration points in the SWIFT2D domain, compared with analytical value at equivalent spatial points in the 2-D analytical domain, according to Equation 2-9:

$$E = 1 - \frac{\sum_{t=1}^{T} \left(O_t - S_t\right)^2}{\sum_{t=1}^{T} \left(O_t - \overline{O}\right)^2}, \qquad (2\text{-}9)$$

where O is the observed, $\overline{O}$ the mean observed, and S the simulated value.

Figures 2-6 and 2-7 depict the spatially-interpolated RMSE and Nash-Sutcliffe results at each grid-point in the domain after 150 and 300 minutes respectively, for the TRT case. Visual comparison of these results and those obtained using the SWIFT2D reactions, or either the TTR or TRTR methods, showed no visible differences. To quantify differences in overall numerical performance between the methods, the average Nash-Sutcliffe efficiencies for all the domain points were calculated for each case using the Nash-Sutcliffe values determined for each point after 300 minutes (Table 2-2). In this way it was possible to quantify the performance of each of the linkage options, from which it appears that the TRTR implementation is the best when taking all three statistical measures into account.

The two-dimensional presentation of time-variant error statistics in this way also offers insights into the location of relatively greater and lesser error, as well as its propagation throughout the domain in time. For instance, in all figures it is clear that the region closest to the source is subject to the greatest errors. The Nash-Sutcliffe results in Figure 2-6 also show the expected result of greater discrepancy at the concentration front (red ring) and the best match in the centre of the domain where source boundary effects and numerical dispersion effects at the front are least felt. Black regions of the Nash-Sutcliffe figures indicate that no values were calculated because no solute had yet reached those points in the domain, thereby generating a null denominator in the Nash-Sutcliffe calculations.

The Nash-Sutcliffe results in both figures also offer validation of the assumption in the model setup that an enlarged model domain of 101x101 cells would be sufficient to

prevent any effects from the no-flow boundaries above and below interfering with the focus region of the fifty cells centered on the source (Figures 2-4 and 2-5). At these boundaries, the assumption of an infinitely open horizontal plane implicit to the analytical solution is no longer met, and we see this disparity reflected in degraded Nash-Sutcliffe efficiencies in the region of the boundary. However, throughout the bulk of the domain, and certainly within the central 50 cells (25 cells above and below the source region), we find excellent matching between numerical and analytical results.

Close comparison of Figure 2-5 and 2-6 corroborates the directionality of the error propagation that is so visually striking in Figure 2-6. The isolines of Figure 2-5 match best at approximately +/- 45 degrees to the horizontal, taken from the solute source point. Greater than this angle and we see the numerical (black and orange) solutions under-predict compared with the analytical isoline (green). Less than 45 degrees (i.e. towards the extreme right of the concentration front) we see the models over-predict relative to the analytical solution. This pattern is clearly reflected in the Nash-Sutcliffe figure, where we see clear darker blue (higher Nash-Sutcliffe efficiency) arms projecting out into a lighter blue surrounding area.

Conclusions

A free-form, non-spatial water-quality model was integrated with a spatially-distributed hydrodynamic model. The resultant tool, FTaRSELOADDS, is a novel water-quality tool that is spatially-distributed, driven by mechanistic hydrodynamics, and user-definable. Linkage of the models was validated by demonstrating the ability of the linked tool to replicate results obtained using the reactive transport functionality of SWIFT2D when using aRSE to perform the reactions and SWIFT2D the transport.

Table 2-1. Quantities and values used in the comparison of SWIFT2D and FTaRSELOADDS against the analytical solution for 2-D conservative and reactive transport. Variable names as required by SWIFT2D, aRSE or STANMOD are included where appropriate

Case	Velocity [m/s]	Retardation Factor	Pulse length	Decay rate [s^{-1}]	Longitudinal (x) dispersion [m^2/s]	Transverse horizontal (y) dispersion [m^2/s]	Transverse vertical (z) dispersion [m^2/s]	Unit concentration source dimension [m]
Analytical solution	v = 0.05	RetFac = 1	T0 = 60000 s	μ = 1E-5	D_x = 20.5332	D_y = 20	D_z = 1E-10	-a to a (y-direction): |a| = 100 m; -b to b (z-direction): |b| = 1E+10 m
SWIFT2D transport and reactions	U,UP = 0.05 V,VP = 0.0	N/A	TRBNDA = 1 for TITI = 0 to 1000 min	AKK = 1E-5	DIFDEF = 20 D_l = 0.5332*	DIFDEF = 20	N/A	2 x 100 m cells (N,M): Cell (50,1) and (51,1)
SWIFT2D transport with aRSE reactions	U,UP = 0.05 V,VP = 0.0	N/A	TRBNDA = 1 for TITI = 0 to 1000 min	K_r = 1E-5	DIFDEF = 20 D_l = 0.5332*	DIFDEF = 20	N/A	2 x 100 m cells (N,M): Cell (50,1) and (51,1)

*D_l calculated from Equations 2-6 and 2-7 for n = 0.03 s/$m^{1/3}$, H = 0.50 m, $\bar{u}$ = 0.05 m/s, g = 9.801 m/s^2, C_d = 14.3

Table 2-2. Nash-Sutcliffe efficiencies obtained for different methods of integrating aRSE reactions into FTLOADS

	SWIFT2D	aRSE: TTR	aRSE: TRTR	aRSE: TRT
Average	0.92843577	0.94792578	0.94790868	0.94789519
Mode	0.99854711	0.98674260	0.99906814	0.99443873
Median	0.99463456	0.99467713	0.99466211	0.99464882

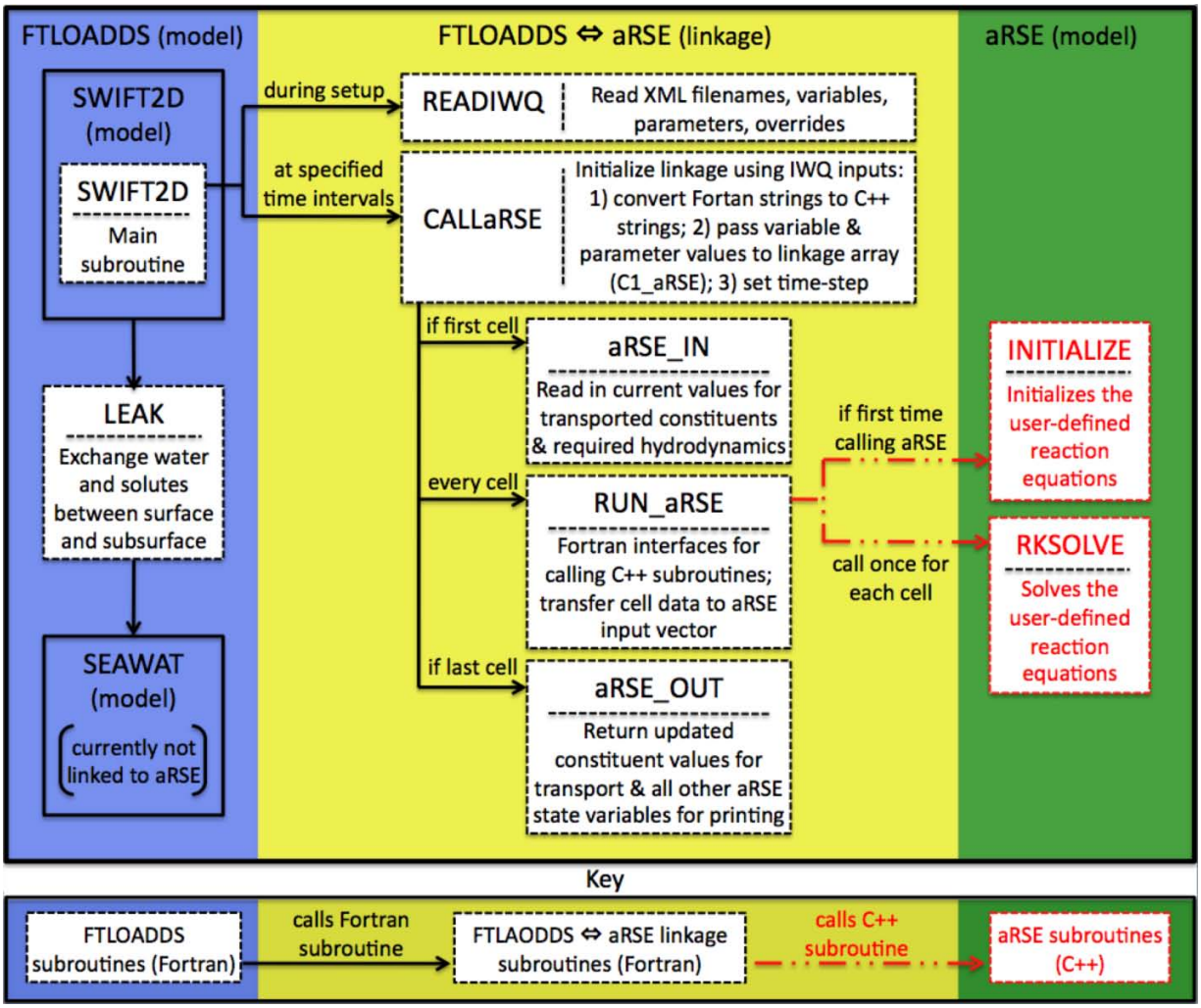

Figure 2-1. Schematic detailing the architecture of the code linking the surface-water model in FTLOADDS (SWIFT2D) with a Reaction Simulation Engine (aRSE).

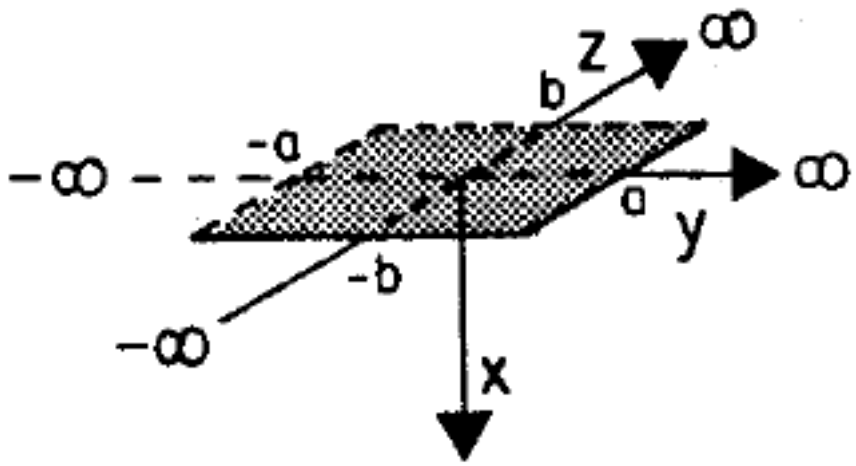

Figure 2-2. Source boundary condition for analytical solution: Third-Type, flow in the x-direction, source dimension a = 100 m in horizontal transverse y-direction, source dimension b = 1E+10 (~infinity) in the vertical transverse z-direction (from Leij and Bradford, 1994).

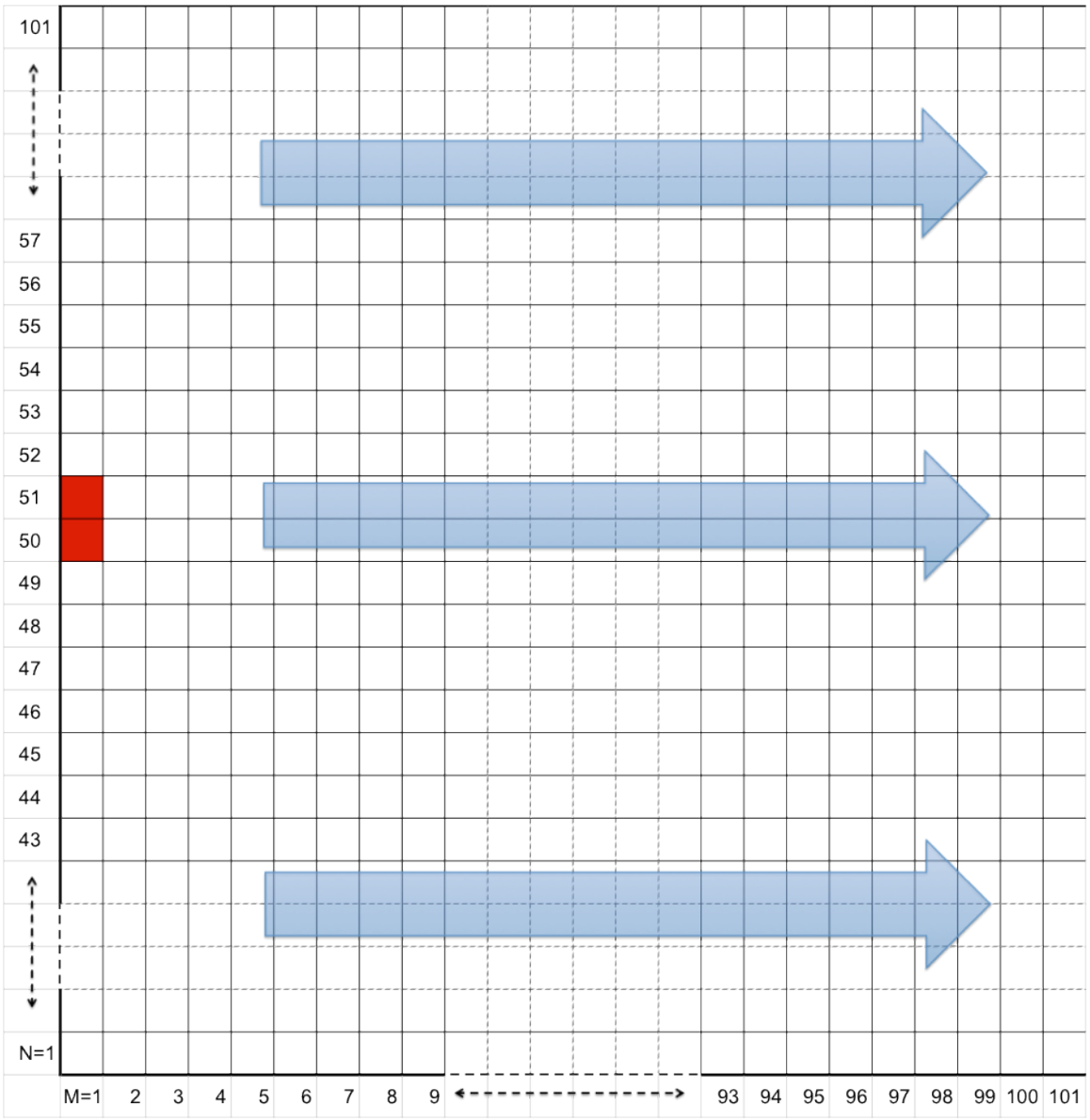

Figure 2-3. SWIFT2D model domain used for comparison of conservative and reactive transport simulations with analytical solutions; red indicate source cells, all cells 100 m square, total domain 10,000 m, no-flow boundaries at N=1 and N=101, and M=1.

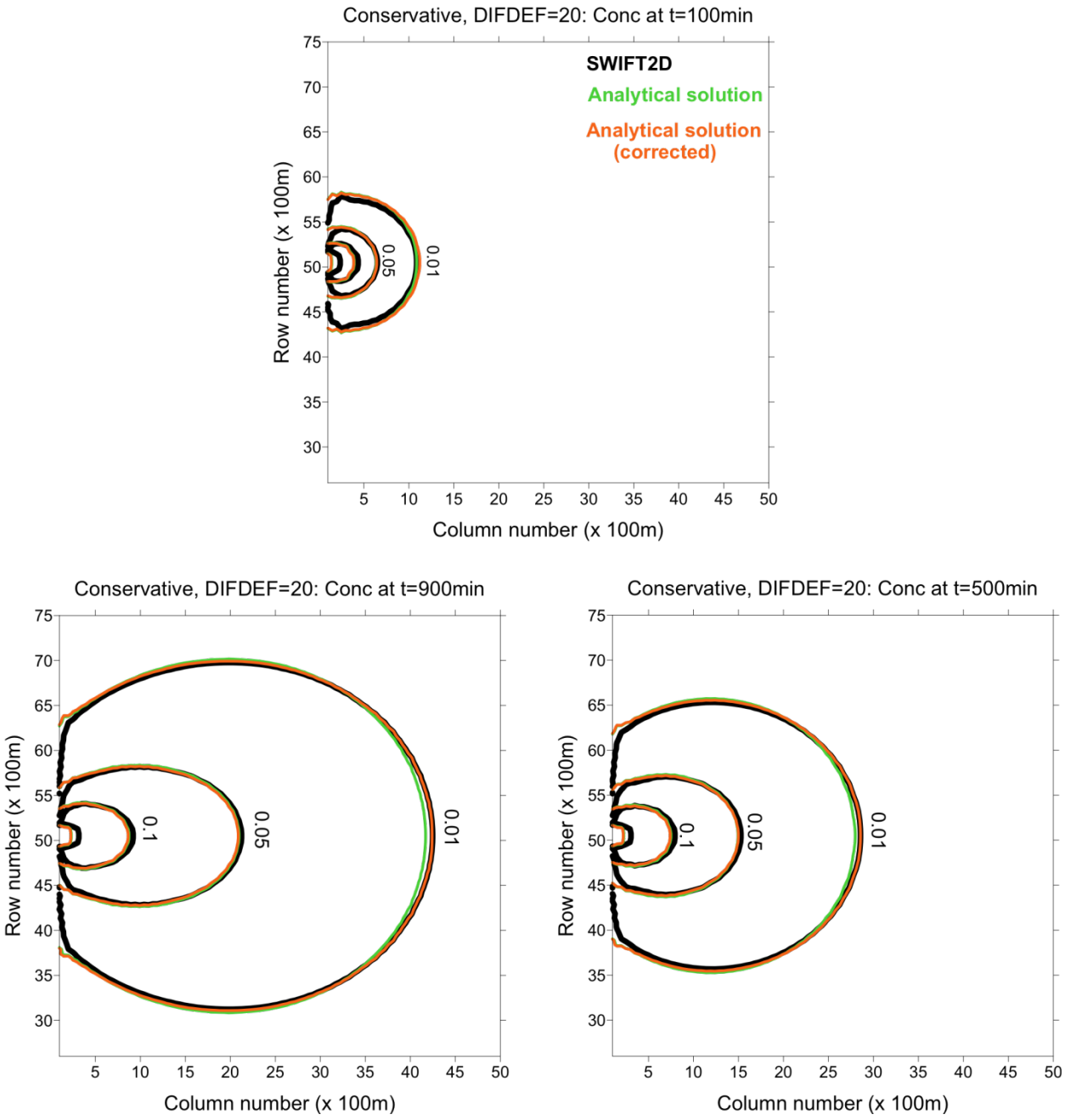

Figure 2-4. Concentration isolines for 2-D conservative transport from a small rectangular source as determined by SWIFT2D (black), the analytical solution (green), and the analytical solution with numerical dispersion effects accounted for (orange).

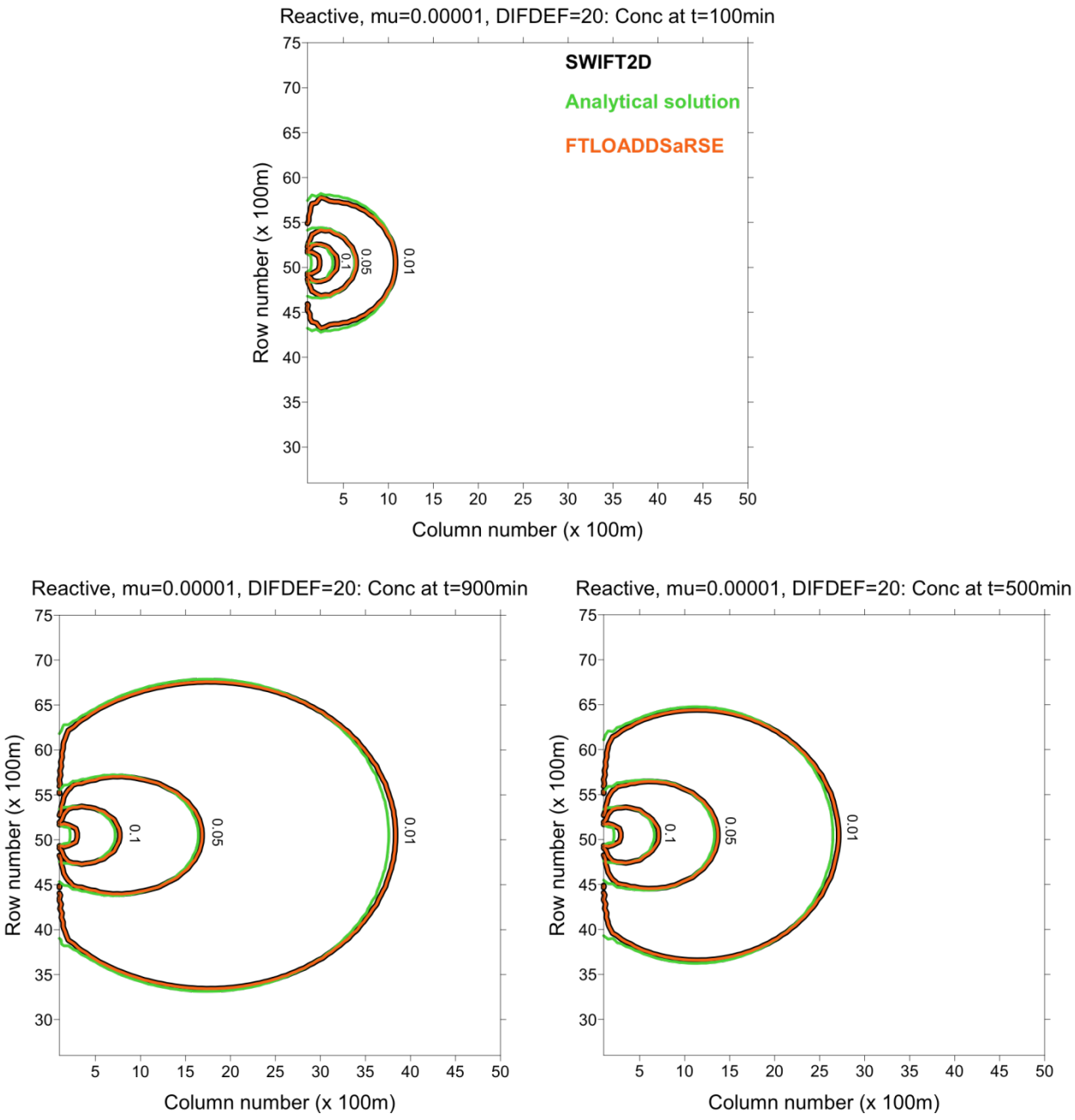

Figure 2-5. Concentration isolines for 2-D reactive transport from a small rectangular source as determined by SWIFT2D (black), the analytical solution (green), and the coupled version of FTLOADDS and aRSE (orange).

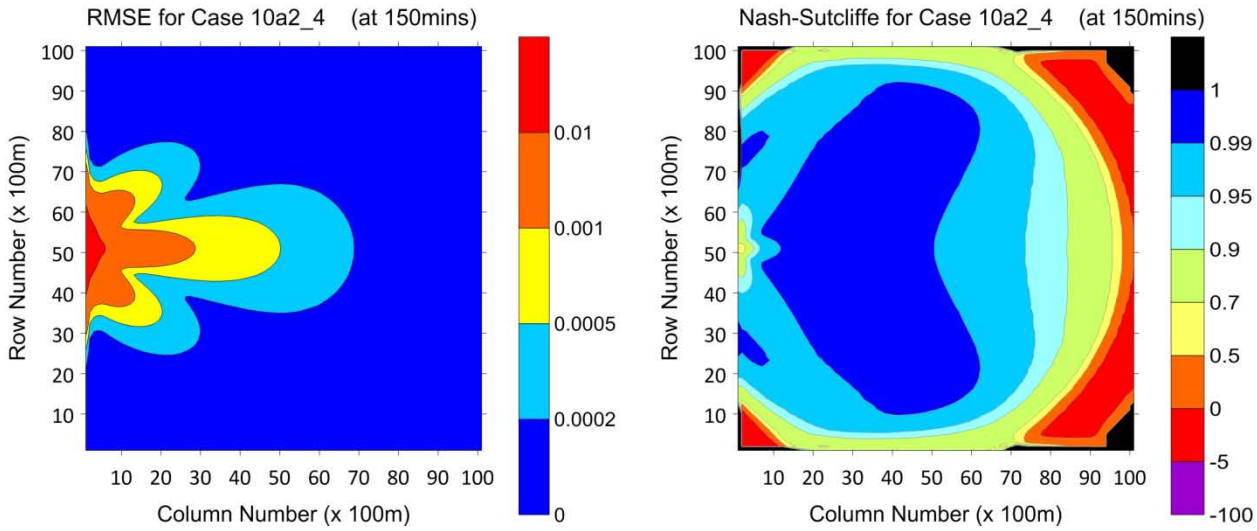

Figure 2-6. Spatially-interpolated RMSE (left) and Nash-Sutcliffe efficiencies (right) after 150 minutes of simulation for the case of transport-reactions-transport-reactions.

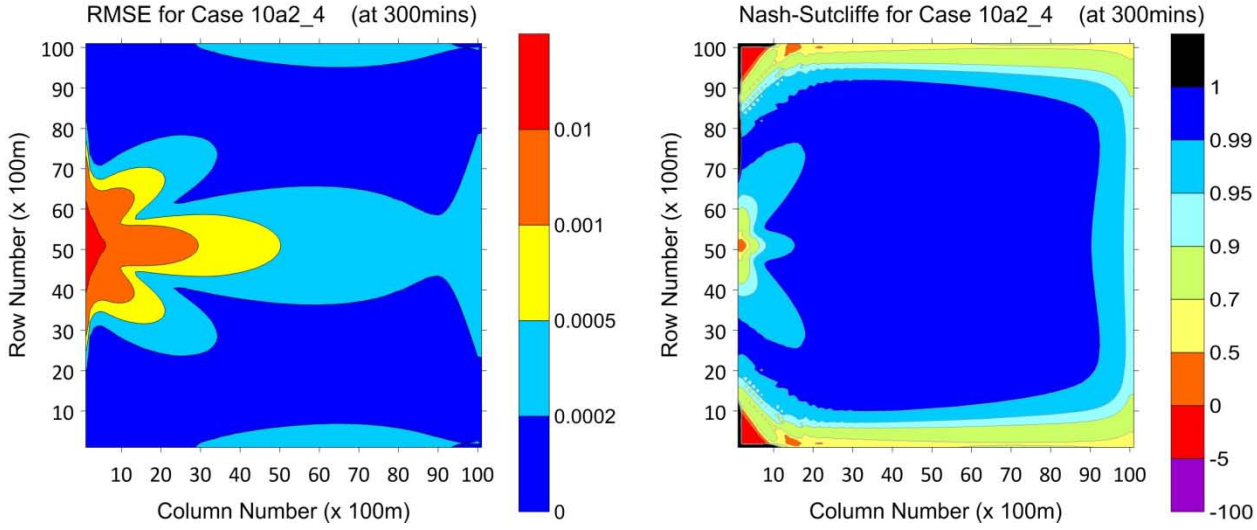

Figure 2-7. Spatially-interpolated RMSE (left) and Nash-Sutcliffe efficiencies (right) after 300 minutes of simulation for the case of transport-reactions-transport-reactions.

CHAPTER 3
MODELING HYDROLOGY IN THE SOUTHERN INLAND AND COASTAL SYSTEMS

Introduction

There are two major paths of natural freshwater flow from the Everglades into Florida Bay. One pathway, Taylor Slough, empties directly into the Bay, while the other pathway, Shark River Slough, contributes a portion of its flow to Florida Bay, but discharges primarily into the Gulf of Mexico. Freshwater inputs are vital to the coastal Everglades ecosystem, having important impacts reaching as far as the Florida Keys (SFWMD and FDEP, 2004). In particular, changes to the flow patterns are expected to have consequences for water-quality in Taylor Slough, adjacent wet prairies, and the coastal estuaries into which they empty (Childers, 2006). Modeling the region's hydrology is the first phase of an effort to model the phosphorus water-quality using a new water-quality model for the region.

Previous Hydrological Modeling of SICS

Numerous modeling and experimental studies have been undertaken to better understand the hydrodynamics within the SICS region. For many years, the South Florida Water Management Model (SFWMM; MacVicar et al., 1984) was used to provide regional hydrologic information at a 2-mile by 2-mile spatial scale. The coarse spatial resolution made SFWMM unsuitable for the detailed analysis required to determine local water management needs and support mechanistic water-quality modeling efforts.

The South Florida Regional Simulation Model (SFRSM; Brion et al., 2000) was, and continues to be, developed to replace the SFWMM. Though SFRSM employs a variable-resolution triangular mesh for spatial discretization, like its predecessor it too

neglects inertial forces, and flow volumes are consequently less accurate. Also neglected are variable-density and unsteady flow conditions, which are important characteristics of the SICS region because of tidal interactions with Florida Bay and wind-shear effects (Swain et al., 2004). Results from efforts to simulate coastal flows to Florida Bay using SFWMM (Hittle, 2000) were undermined by greatly amplified freshwater flows, which in turn diluted coastal salinities. Lin et al. (2000) attempted to use FEMWATER123 for the region, but the computational demands of the model, which simulates 1-D canal flow, 2-D overland flow, and 3-D finite-element ground-water flow, were restrictive.

The failure of these models to meet the persistent need for greater accuracy and spatial resolution of the simulated hydrologic conditions in SICS (as a necessary input for ecological modeling efforts using ATLSS) and freshwater inputs to Florida Bay (needed for hydrodynamic modeling of Florida Bay) led to an extensive modeling effort by the USGS that included a number of field studies to quantify physical parameters. The major product of this effort was the development of the SICS model, an application of the USGS-developed Surface-Water Integrated Flow and Transport in 2-Dimensions (SWIFT2D) hydrodynamic/transport model with additional enhancements specifically for the coastal wetlands of the Everglades (Swain et al., 2004; Swain 2005).

Variable-density ground-water simulation was integrated into the SICS application by Langevin et al. (2005). The effort entailed linking SWIFT2D with SEAWAT, a version of the 3-D modular ground-water flow model MODFLOW integrated with the 3-D modular transport model MT3DMS, which can simulate variable-density ground-water hydrology. The resultant tool is known as Flow and Transport in a Linked Overland-

Aquifer Density Dependent System (FTLOADDS), which was subsequently adapted further for the Tides and Inflows in the Mangroves of the Everglades (TIME) application (Wang et al., 2007). The TIME application not only encompasses the SICS region, but greatly expands the domain to include all of Everglades National Park and Big Cypress National Preserve. Versions 1.0 and 1.1 of FTLOADDS refer to the original SICS applications using only SWIFT2D. Version 2.1 refers to the coupled surface-water/ground-water SICS application, and version 2.2 the coupled surface-water/ground-water TIME application (see Appendix A for further details on versions).

Remodeling the Hydrology of SICS

The proposed effort to model water-quality in the SICS region using FTaRSELOADDS requires a suitable hydrologic application to provide the necessary hydrodynamic drivers of water-quality. The original SICS application, which did not include ground-water simulation, was selected for the inaugural application of FTaRSELOADDS based on a number of considerations: 1) the surface-water results obtained with this simplified version of FTLOADDS were considered sufficient for such testing; 2) the water-quality focus was on surface-water conditions, so only SWIFT2D had been coupled with aRSE (see Chapter 2); 3) the concerns about compounding computational times given the addition of aRSE to an already computationally intensive tool.

However, a number of changes have been made to the SWIFT2D code in FTLOADDS as the tool has evolved to the current form (version 2.2), which were not present when the original SICS application (version 1.1) selected for testing FTaRSELOADDS was established. It was therefore necessary to evaluate the effects of these changes, many of which were simplifications, on the simulation of surface-water

hydrology in SICS. In particular, the effect of removing depth-varying Manning's *n* needed to be evaluated to assess the implications for water-quality modeling.

Materials and Methods

Model Description

The 2-D, vertically integrated, unsteady flow and transport model SWIFT2D has its origins in SIMSYS2D (Leendertse, 1987), which in turn built on earlier work conducted throughout the 1970's by Leendertse and his colleagues at The Rand Corporation to develop a water-quality simulation model for well mixed estuaries and coastal seas (Leendertse, 1970; Leendertse and Gritton, 1971; Leendertse, 1972).

SWIFT2D governing equations

Thorough descriptions of the SWIFT2D governing equations and their numerical implementation are variously provided in Leendertse (1987), Goodwin (1987), Bales and Robbins (1995), and Schaffranek (2004). Four partial-differential equations are used to describe unsteady, non-uniform, variable-density, turbulent fluid motion (Equations 3-1 to 3-3) and solute transport (Equation 3-4), which are formulated according to the laws of Conservation of Mass and Conservation of Momentum. Hydrodynamics are described with the two-dimensional Saint-Venant equations (de Saint-Venant, 1871; Equations 3-2 and 3-3), which are derived from the Navier-Stokes equations by applying temporal averaging of velocity, pressure and mass over time-intervals that are long relative to the time-scale of turbulent fluctuations, and assuming negligible vertical accelerations. Transport is described by the advection-dispersion-reaction equation (Equation 3-4). The resultant formulations retain nonlinear advective and bottom-stress terms, which permit the simulation of eddies and residual circulation, and coupled motion and transport with time-varying horizontal density gradients:

$$\frac{\partial \zeta}{\partial t} + \frac{\partial (HU)}{\partial x} + \frac{\partial (HV)}{\partial y} = 0\,, \tag{3-1}$$

$$\frac{\partial U}{\partial t} + U\frac{\partial U}{\partial x} + V\frac{\partial V}{\partial y} - fV + g\frac{\partial \zeta}{\partial x} + \frac{gH\partial \rho}{2\rho \partial x} + gU\frac{\sqrt{U^2+V^2}}{C^2 H} - \frac{\theta \rho_a W^2 \sin\psi}{\rho H} - k\left(\frac{\partial^2 U}{\partial x^2} + \frac{\partial^2 V}{\partial y^2}\right) = 0\,, \tag{3-2}$$

$$\frac{\partial V}{\partial t} + U\frac{\partial U}{\partial x} + V\frac{\partial V}{\partial y} - fU + g\frac{\partial \zeta}{\partial y} + \frac{gH\partial \rho}{2\rho \partial y} + gV\frac{\sqrt{U^2+V^2}}{C^2 H} - \frac{\theta \rho_a W^2 \cos\psi}{\rho H} - k\left(\frac{\partial^2 V}{\partial x^2} + \frac{\partial^2 U}{\partial y^2}\right) = 0\,, \text{ and} \tag{3-3}$$

$$\frac{\partial (HP)}{\partial t} + \frac{\partial (HUP)}{\partial x} + \frac{\partial (HVP)}{\partial y} - \frac{\partial (HD_x \partial P / \partial x)}{\partial x} - \frac{\partial (HD_y \partial P / \partial y)}{\partial y} + HS = 0\,, \tag{3-4}$$

where:

C = Chezy resistance coefficient coefficient;
D_x, D_y = diffusion coefficients of dissolved substances;
f = Coriolis parameter;
g = acceleration due to gravity;
h = distance from horizontal reference plane to channel bottom;
H = temporal flow depth ($h + \zeta$);
k = horizontal exchange coefficient;
P = vector of vertically averaged dissolved constituent concentrations;
S = source of fluid with dissolved substances;
U = vertically averaged velocity component in x direction;
V = vertically averaged velocity component in y direction;
W = wind speed;
ζ = water - surface elevation relative to horizontal reference plane;
θ = wind stress coefficient;
ρ = density of water;
ρ_a = density of air; and
ψ = angle between wind direction and the positive y direction.

SWIFT2D numerical solution technique

The governing differential equations cannot be solved analytically unless subjected to simplifying assumptions that are unacceptable for the intended applications. A finite difference numerical solution technique is therefore applied to a computational domain of equally spaced grid points. The finite-difference equations are solved on a space-staggered grid (Figure 3-2) using the alternate-direction implicit (ADI) method. Velocity points are located between water-level points to produce an efficient solution of the continuity equation (Leendertse, 1987). The ADI method splits the time-step to obtain a multidimensional implicit solution that provides second-order accuracy, and requires only the inversion of a tridiagonal matrix in order to solve each set of finite-difference equations (Roache, 1982). Detailed descriptions of the finite difference equations are provided in Swain (2005).

Though the ADI method is unconditionally stable (Leendertse, 1987) there are practical limitations to the time-step (Roache, 1982), particularly when applied to irregularly shaped domains (Weare, 1979) or complex bathymetries (Benque et al., 1982).

SWIFT2D code enhancements and simplifications

The FTLOADDS code presently available is that of version 2.2. The original SICS application represents FTLOADDS version 1.1, which included enhancements to SWIFT2D but no ground-water linkage (see Chapter 2). These enhancements were maintained with only minor changes to the SWIFT2D code due to the coupling process in FTLOADDS version 2.1. However, SWIFT2D code was significantly modified in the course of the model's evolution to version 2.2. This has implications for this effort to reproduce SICS surface-water results originally obtained using SWIFT2D v1.1.

SWIFT2D in FTLOADDS v1.1. The original effort to model surface-water flow in the SICS region required a number of modifications to the SWIFT2D model (Swain et al., 2004):

- Precipitation: The rainfall code was adapted to permit spatially-distributed values for rainfall volume to be added to individual cells. Rainfall inputs were calculated at 15-minute intervals by kriging the rainfall from 14 different rainfall stations in the region. Rainfall was not added to dry cells, which implicitly assumed that when rainfall fell on dry cells it infiltrated into the ground-water.

- Evapotranspiration: Evapotranspiration (ET) was not included in the original SWIFT2D v1.0 code, which was intended for application to estuaries and coastal waters where evaporation could be considered negligible and macrophytes sufficiently sparse to ignore transpiration. For SWIFT2D v1.1 an equation regressing ET with solar radiation and depth (German, 2000) was applied to each cell to determine spatially-distributed, time varying ET.

- Depth-varying Manning's *n*: When up-scaling point measurements of frictional resistance to grid-scale representative values, microtopography can increase the effective frictional resistance at lower depths. To address this, an empirical relation was applied to determine an effective Manning's *n* (n_{eff}) based on a reference input value (*n*, measured or estimated), a reference depth (d_{ref}, the assumed depth at which measurement or estimation was conducted), the actual depth (*d*), and a power variable (*p*) to capture non-linear effects (Swain et al., 2004):

$$n_{eff} = n\left(\frac{d}{d_{ref}}\right)^{p}, \tag{3-5}$$

- Wind-sheltering: To account for the sheltering effects of vegetation (Jenter, 1999), which were not considered for open-water applications of SWIFT2D v1.0, a spatially uniform sheltering coefficient was applied to all vegetated cells (considered those having a Manning's *n* greater than 0.1).

- Other: Other changes included technical modifications to the treatment of flow adjacent to barriers (which were not previously permitted to go dry), wind friction in cells adjacent to water-level boundaries (set to zero to avoid numerical oscillations), and output printing routines.

SWIFT2D in FTLOADDS v2.2. The coupling of SWIFT2D to SEAWAT through leakage required additional code, but left each of the models intact such that SWIFT2D could be run without the need to call SEAWAT if so desired. However, the progression

from SICS application to TIME application introduced new changes to SWIFT2D (Wang et al., 2007):

- Precipitation: Rainfall in version 2.1 was specified at 15-minute intervals and spatially-interpolated from 14 stations for each cell. Rainfall in version 2.2 is spatially uniform over defined zones, of which SICS represents one (i.e. uniform rainfall over the entire domain), and is specified as 6-hour averages. Additionally, the wetting and drying algorithm has been modified such that rewetting is now permitted to occur directly from rainfall recharge.

- Evapotranspiration: In analogous fashion to rainfall, ET is now applied regionally, and therefore uniformly over the SICS domain, also as 6-hour averages. Additionally, the modified Penman method (Eagelson, 1970) has replaced the cell-by-cell ET calculations (Swain et al., 2004). When depth of ET is greater than 10 percent of the remaining depth of water then ET is instead removed from the first layer of the ground-water to avoid making the cell go dry or the depth go negative. When the ground-water module is turned off this effectively means no ET occurs.

- Manning's *n*: The functionality to treat variation of Manning's *n* with depth of flow was removed from SWIFT2D due to concerns over its empirical nature (E.D. Swain, U.S. Geological Survey, personal commun., 2010). Frictional resistance (Chezy) terms, which are calculated using depth and Manning's *n*, are now defined at cell faces rather than at cell centers. This permits a different resistance in each of the principal directions of flow, but also requires a second Manning's *n*-value for each cell. In version 2.1 obstruction to surface-water flow, most notably the Buttonwood Embankment, was defined using the original SWIFT2D barrier formulation intended to represent weirs. Coastal rivers and creeks were defined as low barriers with calibrated flow coefficients. In version 2.2 the coastal embankment is defined by a modified cell-face frictional resistance term, with creeks represented as gaps with specified (reduced) friction terms.

Considering the important roles played by both precipitation and ET in the south Florida water budget (Sutula et al., 2001), and of Manning's *n* in determining flow velocities and wet/dry conditions, the modifications to v2.2 described above represent significant hydrological simplifications to the SWIFT2D model. This effort to model SICS hydrology therefore represented an effort to study the effects of these model simplifications on the ability of SWIFT2D to simulate hydrodynamics in the SICS region for future water-quality application.

Model Setup

The SWIFT2D v1.1 model setup used in the original SICS application was reapplied as consistently as possible in an effort to reproduce the original results for the period of August 1996 through August 1997. All effort was made to maintain the same model setup and parameterization, and the integrity of the original SICS application should be assumed intact unless changes are specified below. Figures from the USGS' SICS modeling report (cited as Swain et al., 2004) are reproduced where model setup is appropriately consistent, and original figures have been produced where necessary.

Computational domain

The previously established SICS model (Swain et al., 2004) domain (Figure 3-3), comprising 9,738 square computational cells of length 304.8 m (1000 ft) for a total domain area of 905.8 km^2, was applied with minimal changes to the model boundary. The new treatment of frictional resistance terms at cell faces, rather than cell centers, generated a number of points on the domain boundary where floating point problem arose due to the underlying space-staggered grid geometry. The original version required resistance terms for each cell in the computational domain, which is defined row-by-row, and column-by-column, to produce the irregular boundary required. Resistance terms were calculated based on input Manning's *n* values, which were specified as zero outside the active domain. Since the original computational domain was not defined to intentionally account for the additional cell face values required by the current version, and given that the space-staggered grid used by SWIFT2D attributes values originating in, for example, cell (m, n+1) to cell (m, n), instances of Chezy resistance terms being calculated using Manning's *n* values of zero in the

denominator arose. This was resolved by eliminating the offending individual boundary cells from the computational row or column as the case arose.

Land-surface elevations were measured at about 400-m intervals (Desmond et al., 2000) and a linear distance-weighted four-point interpolation was applied to assign land surface elevations to each computational cell (Figure 3-4). The Buttonwood Embankment (Figure 3-1) is a significant hydrologic barrier in the region, which separates the freshwater wetlands from Florida Bay. Most exchange of water occurs through the many creeks that traverse the embankment. Physically, the embankment is an elevated region, but in SICS it is simulated by barriers based on large resistance terms in the direction of flow, interspersed with lower resistance values where creeks cut through the barrier.

Boundary conditions

Boundary conditions (Figure 3-5) were provided at the water surface and lateral boundaries. The water surface boundary is assumed to be horizontal in each cell; water is permitted to move vertically but no deformation of the water surface within the cell is considered. Physically, this implies that high-frequency surface waves are not accounted for in the model.

A uniform rainfall rate was supplied as a model input file containing values calculated as the arithmetic mean of all stations in the SICS region, averaged over 6-hour intervals. A uniform ET rate was similarly supplied as an input file, rather than calculated within the model. Input ET values were calculated as the regional mean of ET values calculated according to the modified Penman method (Wang et al., 2007). Wind conditions are represented as spatially uniform across the entire domain, and the data from the Old Ingram Highway site was used to define the wind field. A moving

average wind speed was used for the boundary condition since fluctuations in wind conditions at sub-hourly time-scales are considered to not generally be representative of regional patterns, which is the scale implied when uniformly applying wind.

Lateral boundaries are described as open (free exchange with water and solutes across the boundary) or closed (no flow or exchange). Open boundaries were described by time-series inputs for either discharge or water-level. The SICS model lateral boundaries are identified in Figure 3-5, and include seven constant head boundaries and three discharge source boundaries. The discharge sources (Figure 3-6) are at Taylor Slough Bridge, the C-111 pumping station, and within the L-31W canal. Inflow at Taylor Slough Bridge was determined from stage-discharge data at the Taylor Slough Bridge site, and at the L-31W site according to stage-discharge relationship at the S-175 hydraulic gate structure, where this flow originates. Input of discharge at C-111 source is based on the discharge from pumping station S-18C, occasionally adjusted to compensate for flows directly out of the canal and into Florida Bay when the S-197 structure is opened. The levee on the southern side of the C-111 section has been removed to promote delivery of additional water to the SICS region. An artificial topographic low along the SICS boundary was applied to facilitate more uniform flow distribution along the lower section of C-111.

Several regional model parameters are required and applied as per Swain et al. (2004): air density, latitude (single value), kinematic viscosity of water, wind stress coefficient, unadjusted horizontal mixing coefficients, isotropic mass dispersion coefficient, a coefficient relating mass dispersion to flow conditions, a resistance

coefficient for each computational cell and for tidal creeks, and marginal depth (Swain et al., 2004).

Stability considerations

Although the ADI method is unconditionally stable (Leendertse, 1987), the treatment of flow barriers introduces practical limitations. Experimentation with the time-step eventually lead to selection of a half-step of 1.5 minutes, which demonstrated sufficiently stability in the region of the creeks and barriers. The next-largest possible half-step was 2.5 minutes, based on the fact that full time-steps needed to be compatible with the time-steps defined for tidal boundary conditions, which are read in at 15-minute intervals, and this proved to be unstable.

Given the simulation of salinity transport it was also necessary to consider numerical dispersion. A diffusion coefficient of 10 m^2/s was applied based on the previous application of SICS v1.1. (Swain et al., 2004). Considering the cell dimensions of 304.8 m, and a conservative (high) estimate for average velocities on the order of 0.05 m/s (based on previous results in Swain et al., 2004), a Péclet number of approximately 1.5 was obtained, which even though conservative was below the generally applied upper limit of 2.

Results and Discussion

Water-level results at the 12 observation stations in the SICS domain are presented first, followed by an assessment of the flow through the creeks linking Florida Bay to Taylor Slough. Following thereafter are 2-D results for water-level, flow, and salinity.

Water-Level Results

Simulated stages at each of the 12 water-level stations are presented in Figures 3-7 and 3-8. Results are divided between those stations that fall within Taylor Slough (Figure 3-7), which are more directly subject to discharges from the TSB source, and stations east of the slough (Figure 3-8) that are more directly affected by flows originating from the C-111 canal. The area of the time-series figures shaded in brown indicates the subsurface. Where brown meets blue corresponds to ground-surface elevation for the cell containing the location of the station. The area shaded in blue indicates the maximum observed water-level during the model validation period from July of 1996 to August 1997. Observed water-levels are depicted in blue, and can drop below the ground surface because water-level observations are recorded by wells. The results obtained using SWIFT2D v1.2 are shown in black. Periods where simulated results are not depicted correspond to conditions that SWIFT2D considers dry, which occur when water depth drops below 5 cm. As can be seen in both figures, this happened regularly for a number of locations, including two critical phosphorus concentration observation locations, the EPGW and P37 stations.

Significant effort was expended attempting to resolve this. The final solution was to reintroduce the functionality of depth-varying Manning's *n*, which had been removed in the present version (v1.2). The reintroduction of depth-varying Manning's constitutes an updated version of 1.2, and is designated version 1.2.1 (red results in Figures 3-7 to 3-10). In the original SICS v1.1 modeling effort, the variables applied to the nominal Manning's input, d_{ref} and p (Equation 3-5), were 0.6 m and 2 respectively. In this version 1.2.1 the reference depth was set to 0.4 m given the absence of almost any depths of

0.6 m in the simulated year, making such an assumption for the reference depth questionable. The simple non-linear quadratic power was maintained.

A comparison of the results obtained in this work with those from the original SICS modeling effort (Swain et al., 2004) is given in Figures 3-9 and 3-10, with statistics comparing all three versions – original SICS application (v1.1), present SICS application with depth-constant Manning's *n* (v1.2), and present SICS application with depth-varying Manning's *n* (v1.2.1) – are presented in Table 3-1, and summarized in Table 3-2.

Visual comparison of the results in Figures 3-7 to 3-10 with the statistics in Table 3-1 reveals some contradictions. Visually, it is clear that the results obtained using depth-varying Manning's *n* (in both SICS 1.1 and 1.2.1) are a better representation of reality insomuch as periods of wetness and dryness are captured more reliably, particularly for the critical water-quality stations EPGW and P37. In SICS v1.1 (Figures 3-9 and 3-10) we see a tendency on the part of the model to over-predict water-levels, especially at the beginning of the simulation and the beginning of the second wet-season. The current application performs much better in this regard. Conversely, in SICS v1.2 (Figures 3-8 and 3-9), the lack of depth-dependency in flow resistance results in excessively rapid drying out of the system when data clearly shows that wet conditions prevail. Version 1.2.1 avoids the drawback of both of these versions, better predicting the dry-down following wet periods compared with SICS v1.2 and avoiding the over-predictions that were characteristic of SICS v1.1.

The Nash-Sutcliffe efficiencies presented in Table 3-1 and summarized in Table 3-2 do not capture this, instead implying that v1.2 offers the best results. This is a

consequence of the fact that periods of dry conditions are not accounted for in the Nash-Sutcliffe calculations because there is no simulated depth value against which to compare the observed value. The result is a failure to capture the full extent of the error, and exposes a weakness of this error statistic for assessing results in shallow systems where wetting and drying is frequent. Additionally, the EP12R station has very low Nash-Sutcliffe results which disproportionately reduce the Nash-Sutcliffe statistics (Tables 3-1 and 3-2) considering how little data is actually present for this station (Figure 3-9). Furthermore, the station is located very close to the boundary of the model, a region that is known to be susceptible to greater errors due to boundary effects (Leendertse, 1987).

Figure 3-11 to 3-13 shows the frequency and cumulative distribution of Nash-Sutcliffe results for all stations, Taylor Slough stations, and C-111 wetlands stations respectively, from SICS v1.2.1. Over 40 percent of all the stations attained Nash-Sutcliffe efficiencies of 0.7 or higher, and approximately 60 percent of 0.5 or higher. Performance of the model for simulating water-levels in Taylor Slough (Figure 3-12) was comparable to that for the C-111 wetlands (Figure 3-13).

It is known that bias can lead to misleading Nash-Sutcliffe efficiencies (McCuen et al, 2006). Furthermore, indication of a tendency to over-predict or under-predict would be useful in interpreting how the changes made to SICS have affected the models ability to capture particular conditions, which would be useful in future water-quality modeling efforts.

Simulated results from SICS v1.1. and v1.2.1 were plotted against analogous observational data. For the 6 stations in the vicinity of Taylor Slough (Figure 3-12) we

see a general reduction in variability about the 1:1 line for SICS v1.2.1 compared with v1.1. Stations higher up the slough (R127 and TSH) are the exception, tending towards over-prediction at shallow depths and under-prediction otherwise. For the C-111 stations (Figure 3-13), the current SICS v1.2.1 offers marked improvements, indicating that v1.2.1 is better equipped to handle the conditions of both slough (Taylor Slough area of SICS) and marl prairie (C-111 wetlands area). In particular, results were greatly improved for the EVER4 station and, importantly for water-quality, the EPGW station. The poor results obtained for EP12R appear to be a problem in both versions of the model. Since both versions apply some form of depth-varying Manning's coefficient, while version 1.2, which has better results for EP12R according to the Nash-Sutclife efficiencies previously discussed, does not account for changing resistence with depth, this may be a consideration. If the EP12R site is sparsely vegetated then the depth-varying effect will be less important, and may then be a reason for this discrepancy.

Water-levels throughout the SICS region are presented on the first of each month, from August 1996 to July 1997, in Figures 3-14 (first wet season), Figure 3-15 (dry season), and Figure 3-16 (end of dry season and start of wet season). Two-dimensional results are presented beneath time-series figures depicting precipitation and discharge source inputs to the domain during that period to facilitate visual comparison between inputs and hydrologic conditions.

Discharge Results

Discharge data were available for five creeks in the Buttonwood Embankment. Figure 3-17 compares the simulated daily averaged flow rates in SICS v1.2.1 with the observed daily averaged flow rates. These results are important for assessing the accuracy of fluxes, which are critical if loading rates are to be estimated. They are also

an important consolidation of depth and velocity simulations; given the reliable depth results described above, reliable flux results therefore indicate reliable velocities, which are important for the transport of solutes in water-quality modeling.

In all creeks except McCormick Creek, the magnitude and timing of daily average fluxes were satisfactory. Vector diagrams depicting flow direction and magnitude are given for the first of each month in Figures 3-18 to 3-20. Results reproduce well the trends found in Swain et al. (2004) that show tendency for flow from both Taylor Slough and C-111 to congregate in the region of Joe Bay. It is therefore important that the two primary creeks in this region, Taylor Creek and Mud Creek, are well modeled since they represent a significant portion of the Taylor Sough flow output to Florida Bay. The large fluxes through Trout Creek and the directionality of fluxes towards it from the C-111 canal indicate its importance for inputs to Florida Bay originating from the eastern region of SICS. Fluxes are probably particularly large through Trout Creek because of its position between two large water bodies that hold relatively deep water permanently compared with the shallow and intermittently wet/dry conditions on the landward side of Taylor Creek and Mud Creek.

Salinity Results

Figures 3-21 to 3-23 present the two-dimensional spatial results for salinity distribution throughout SICS on the first of each month. These results illustrate the significant diluting effect of freshwater inputs from Taylor Slough and C-111 to Florida Bay during high flow periods. Salinities were substantially higher throughout the Bay in the dry season. Dilution emanated from the region of Joe Bay following high freshwater flows, as would be expected given the previously discussed flow results. During peak dry periods there is marked intrusion of salinities into the coastal wetlands in the eastern

regions of SICS. Particularly high salinities may be due to evapotranspiration of water with increased salinity due to tidal influxes during low-flow periods. Such water may also become trapped in depressed regions by surrounding dry land after tides have withdrawn.

Conclusions

The current working version of SWIFT2D (v1.2) does not contain depth-varying Manning's resistance. This proved to undermine the ability of the mode to accurately capture wet and dry conditions, which are important for both practical considerations (given the paucity of phosphorus data points for testing in Chapter 4) and biogeochemical considerations (since wet conditions determine the presence or absence of aquatic processes). When depth-varying Manning's *n* was reintroduced into the model in version 1.2.1 this problem was overcome. Water-levels throughout the SICS region and discharge rates for important creeks were captured well. The reliable simulation of wet and dry conditions and velocities therefore established a satisfactory foundation for mechanistic water-quality modeling of the region.

It is possible that the reintroduction of ground-water exchange may negate the need for depth-varying Manning's *n*. Under very shallow flow conditions, which is when depth-varying Manning's would be most important, the small surface-water hydraulic head may lead to ground-water upwelling into the water column. Other modeling efforts in the region have shown that ground-water inputs likely occur during the dry season (Langevin et al., 2005), with possible implications for phosphorus loading to the surface water as well (Prince et al., 2006). In the absence of ground-water exchange, the calibration of the depth-varying Manning's parameters d_{ref} and p to maintain surface-water heads that would otherwise dissipate (as shown in the results for v1.2) equates to

compensating for the lack of ground-water upwelling that may actually be occurring. Consequently, a fully coupled surface-water/ground-water simulation of SICS using version 1.2 may be sufficient to justify the assumption of depth-invariant Manning's *n*. However, for the purpose of testing the phosphorus water-quality model, water-levels under shallow conditions are sufficiently sensitive to require that depth-varying Manning's be included.

Table 3-1. Nash-Sutcliffe efficiencies for water-level observation points in SICS

Station	SICS v1.1*	SICS v1.2**	SICS v1.2.1***
CP	0.7201337	0.901839	0.8771178
P67	0.2144507	0.7837026	0.8087565
TSH	0.7313131	0.8232658	0.7899594
P37	0.7620635	0.863053	2.44E-02
E146	0.778919	0.8662752	0.8897558
EVER5A	-0.1176481	0.6932715	0.3337759
EVER7	0.5472993	0.7139693	0.8710759
EPGW	0.4939922	9.81E-02	0.4452754
EVER6	0.8514937	0.6204761	0.8550127
EP12R	-2.930052	-1.618115	-4.148942
EVER4	0.5493984	0.8272943	0.6898439
R127	0.5810636	0.5898135	0.4134087

* Calculated from digitized results in Swain et al., 2004
** Manning's *n* held constant with depth of flow
*** Manning's *n* varied with flow depth according to Equation 3-5

Table 3-2. Nash-Sutcliffe statistics for stations in the viciniy of Taylor Slough, stations in the vicinity of C-111, and all stations in the SICS region.

	SICS v1.1*	SICS v1.2**	SICS v1.2.1***
Taylor Slough stations			
Mean	0.6313	0.8047	0.6339
Standard Error	0.2159	0.1128	0.3463
Median	0.7257	0.8432	0.7994
Kurtosis	3.7805	3.4693	1.0346
Skewness	-1.9502	-1.7921	-1.4219
C-111 stations			
Mean	-0.1009	0.2225	-0.1590
Mean (excl EP12R)	0.4649	0.5906	0.6390
Standard Error	1.4219	0.9371	1.9666
Median	0.5206	0.6569	0.5676
Kurtosis	4.9453	4.4112	5.7462
Skewness	-2.1940	-2.0892	-2.3836
All stations			
Mean	0.2652	0.5136	0.2375
Mean (excl EP12R)	0.5557	0.7074	0.6362
Standard Error	1.0423	0.7052	1.4085
Median	0.5652	0.7488	0.7399
Kurtosis	9.9357	9.1905	10.8236
Skewness	-3.0767	-2.9601	-3.2369

* Calculated from digitized results in Swain et al., 2004
** Manning's *n* held constant with depth of flow
*** Manning's *n* varied with flow depth according to Equation 3-5

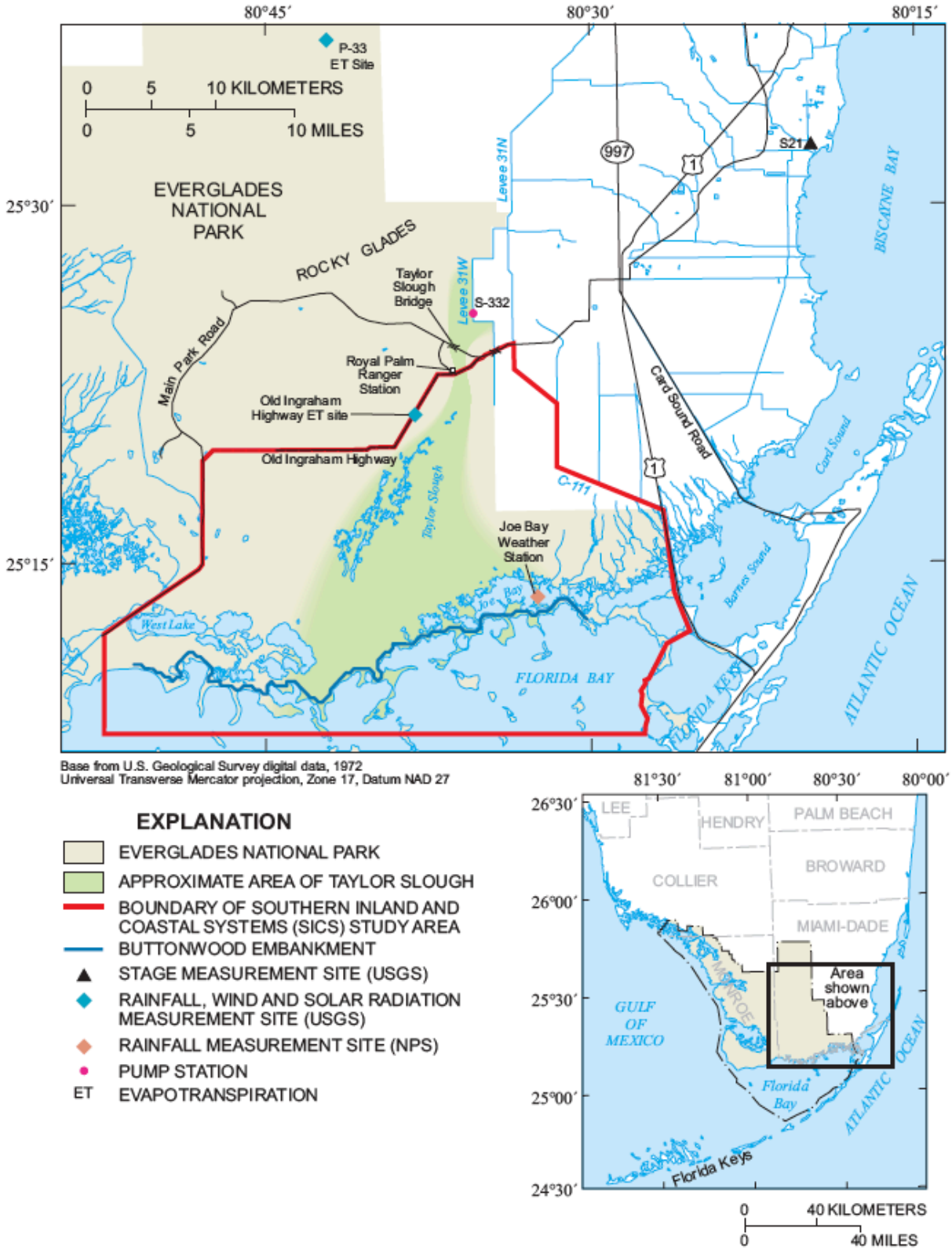

Figure 3-1. Location of the Southern Inland and Coastal Systems study area (from Swain et al., 2004).

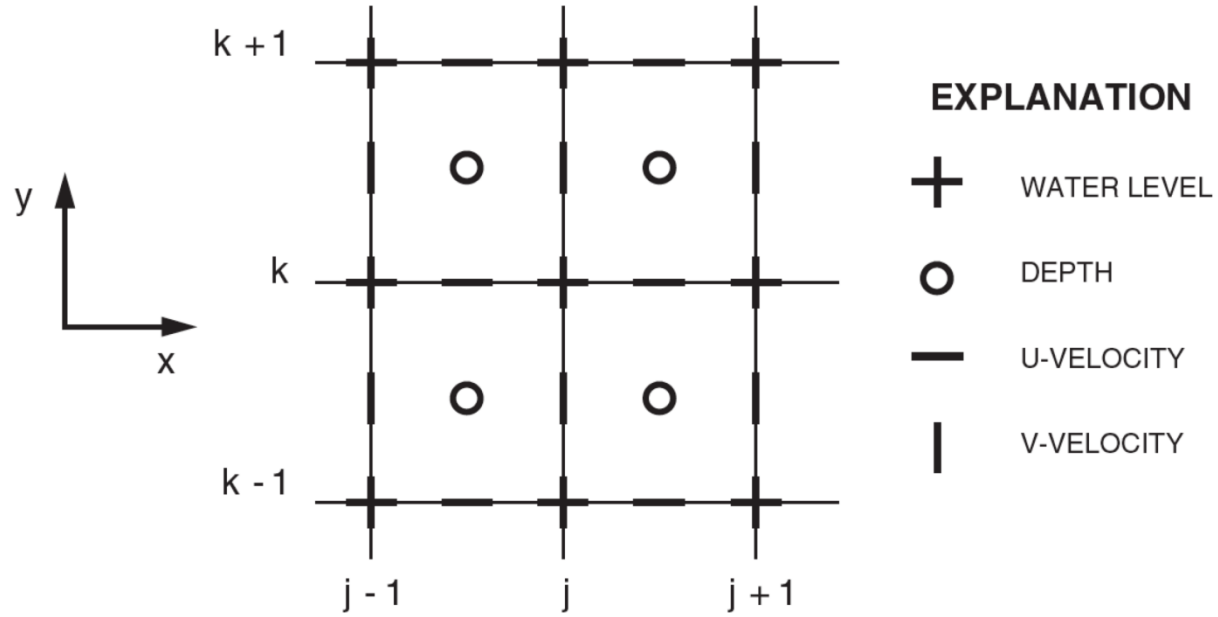

Figure 3-2. Space-staggered grid system showing relative locations of hydrodynamic characteristics.

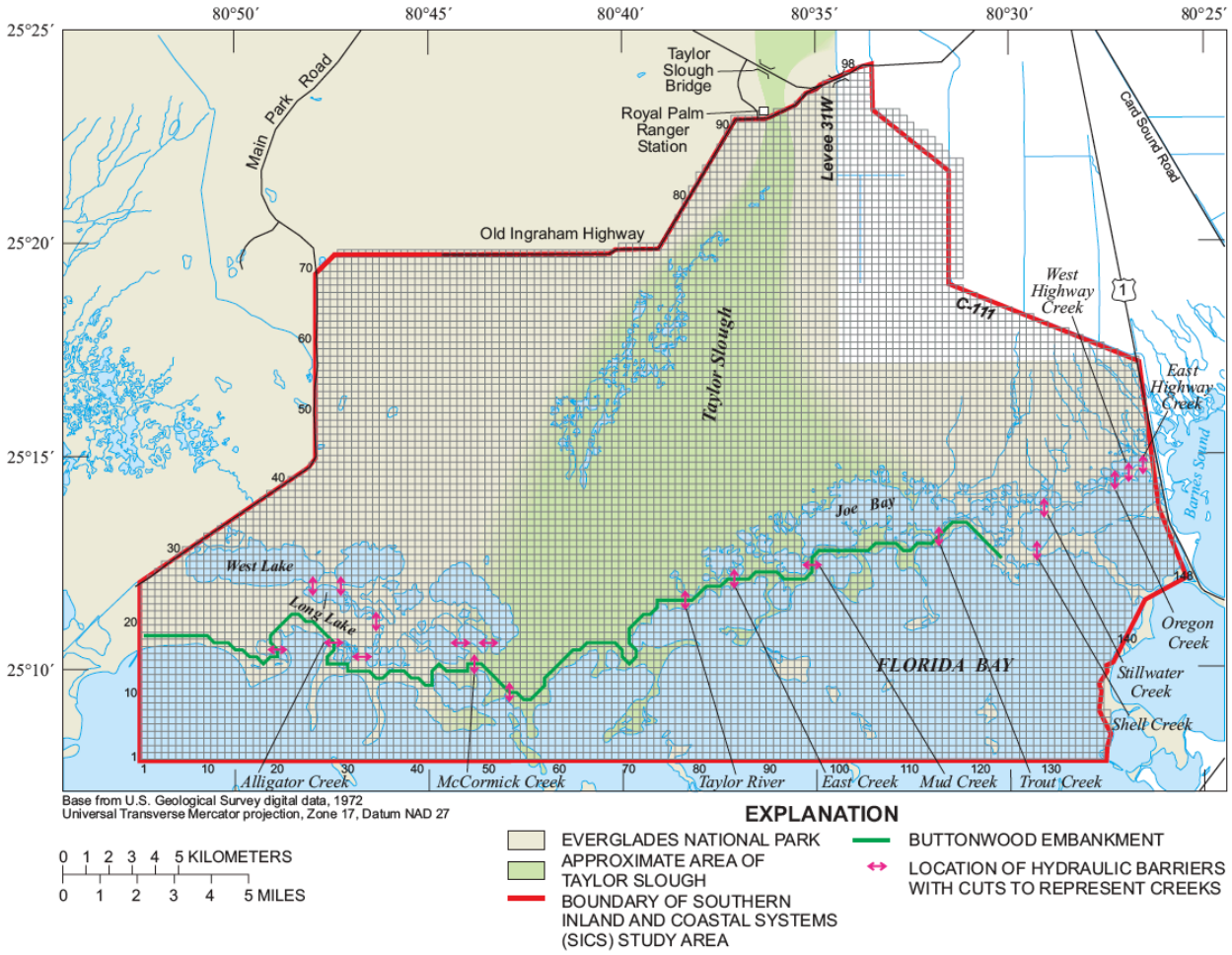

Figure 3-3. The SICS computational grid, showing the location of Taylor Slough, the Buttonwood Embankment and the coastal creeks (from Swain et al., 2004).

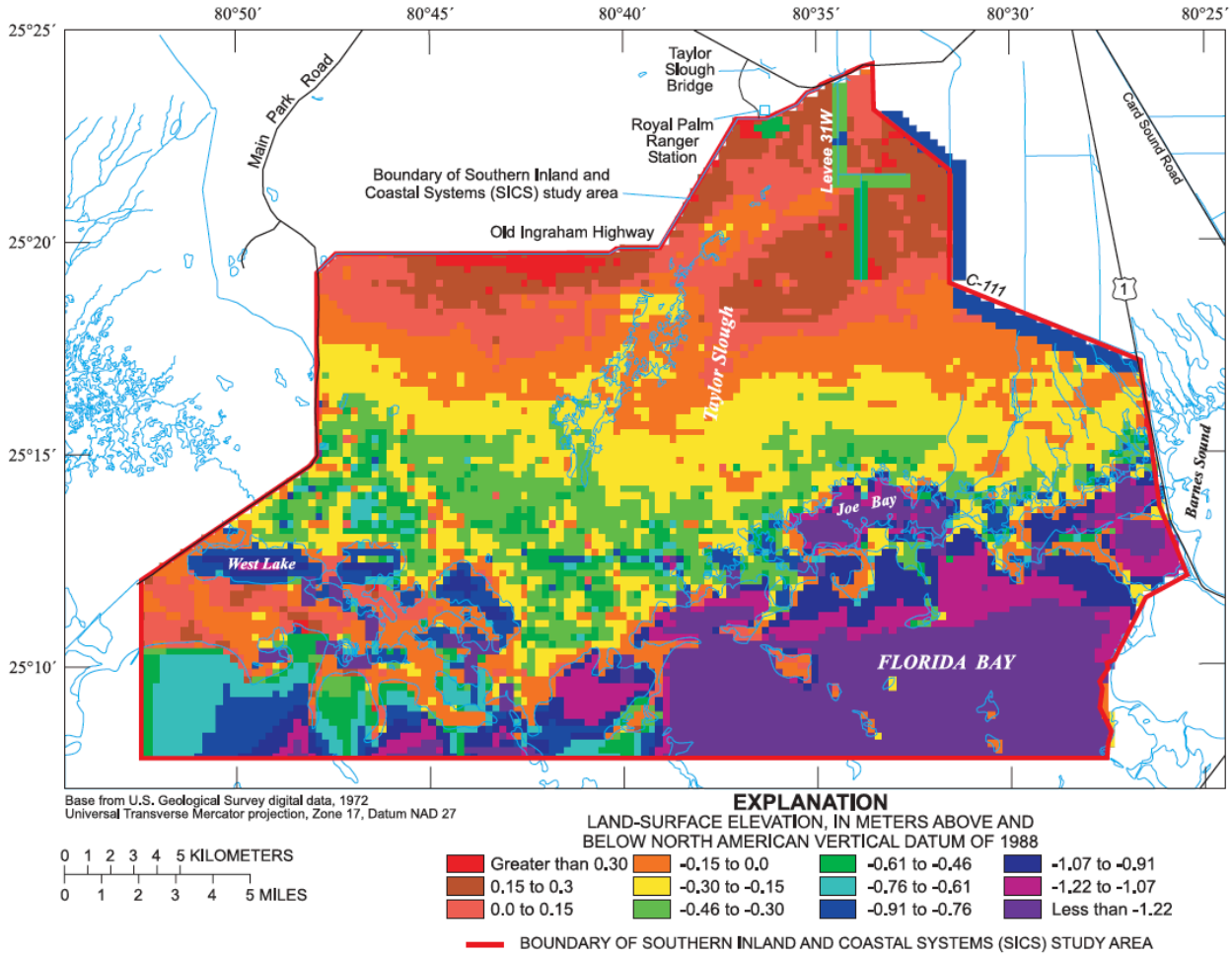

Figure 3-4. Land-surface elevations (from Swain et al., 2004).

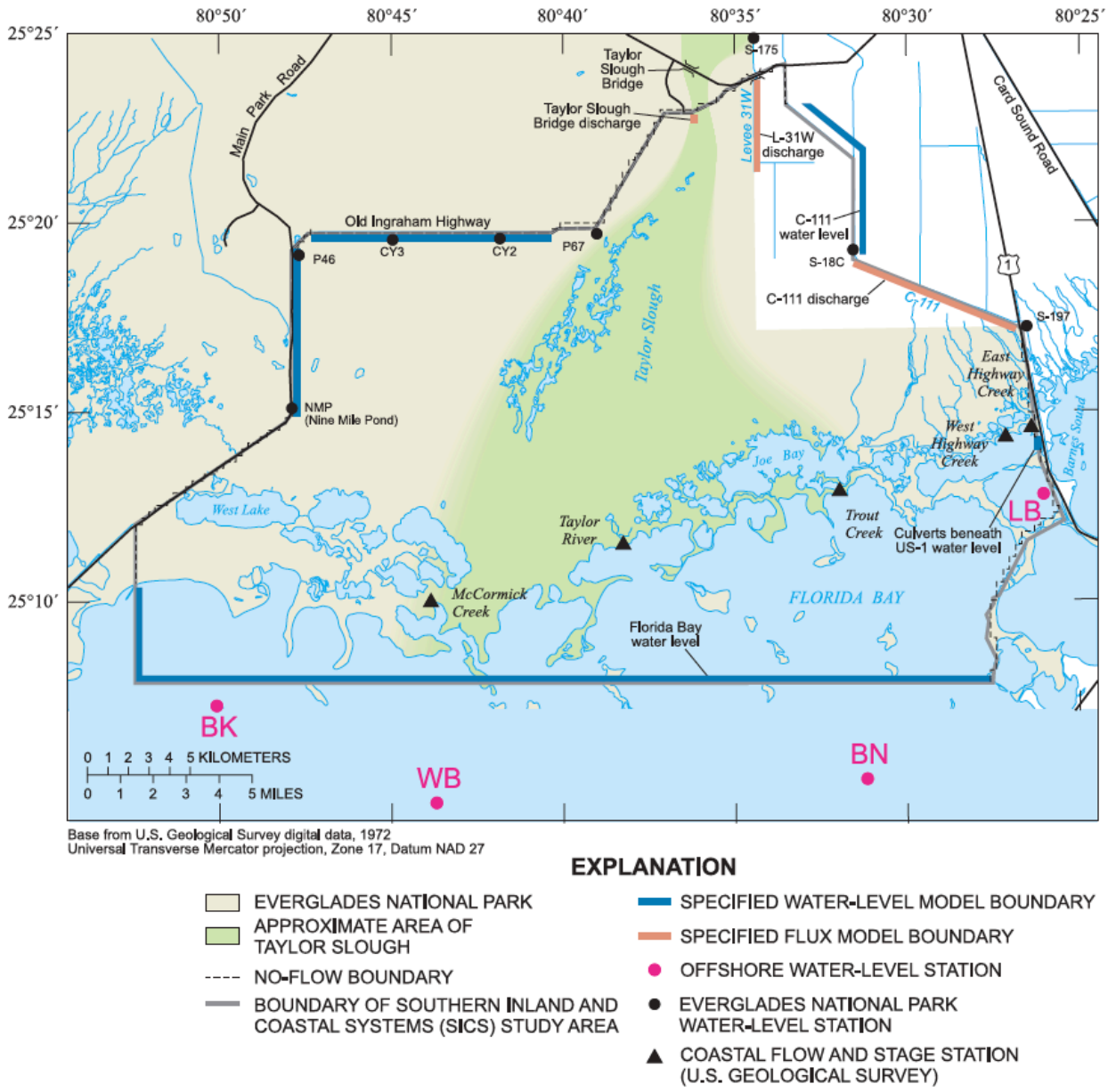

Figure 3-5. Location of SICS model boundary conditions, including specified water-level boundaries and discharge sources (from Swain et al., 2004).

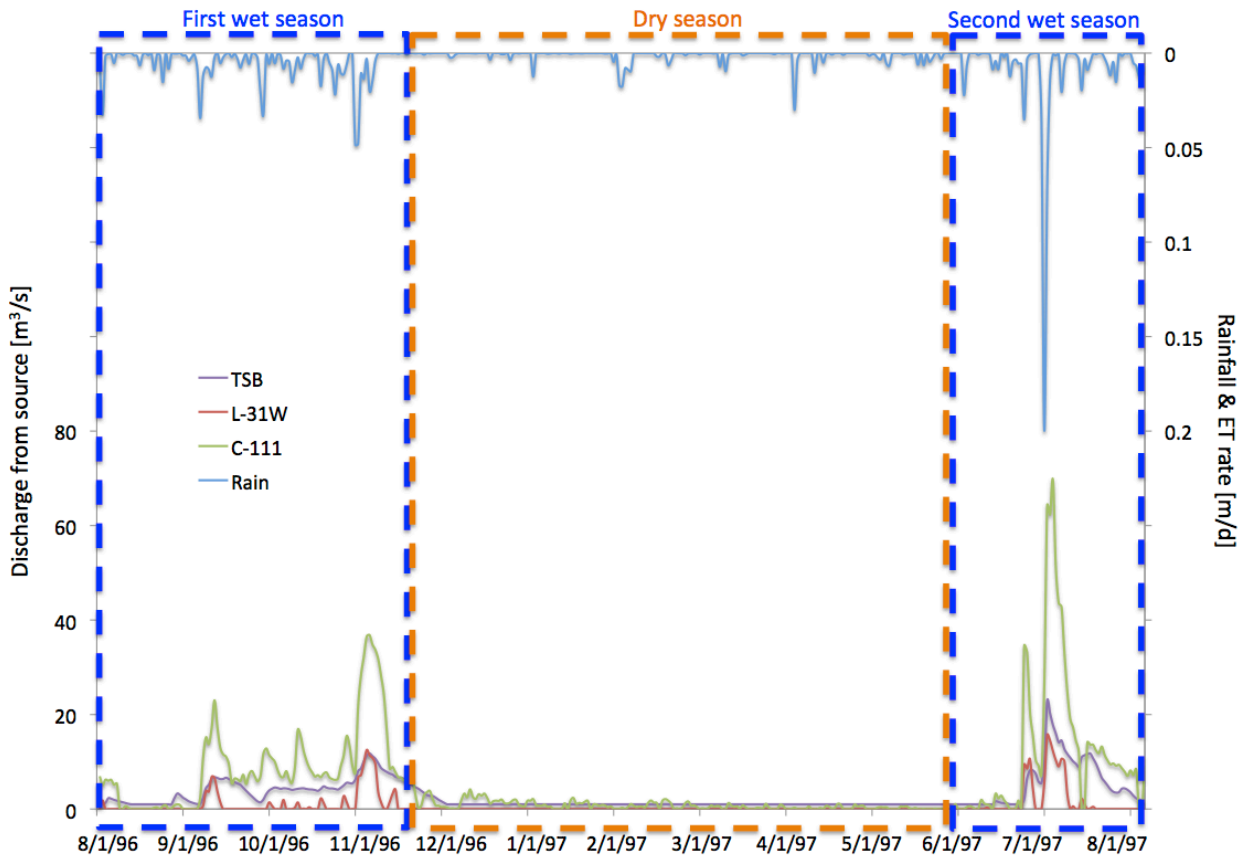

Figure 3-6. Specified hydrologic inputs to SWIFT2D: discharge on the bottom axis and rainfall on the top axis. The three principal seasons, wet interspersed by dry, during the course of the simulation are depicted.

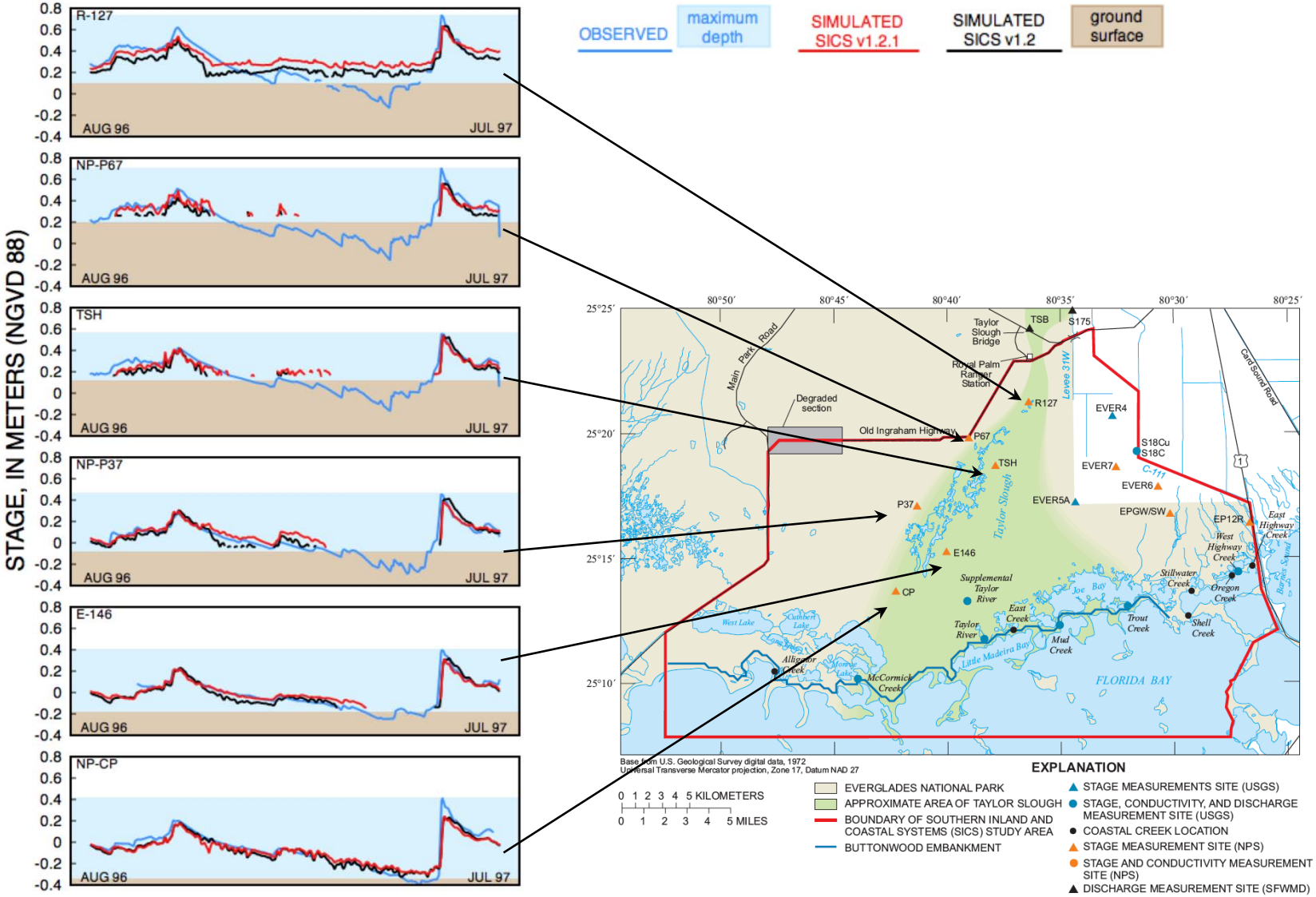

Figure 3-7. Water-levels at the six stations in the vicinity of Taylor Slough, simulated with depth-varying Manning's *n* (v1.2.1 - red) and with constant Manning's *n* (v1.2 – black).

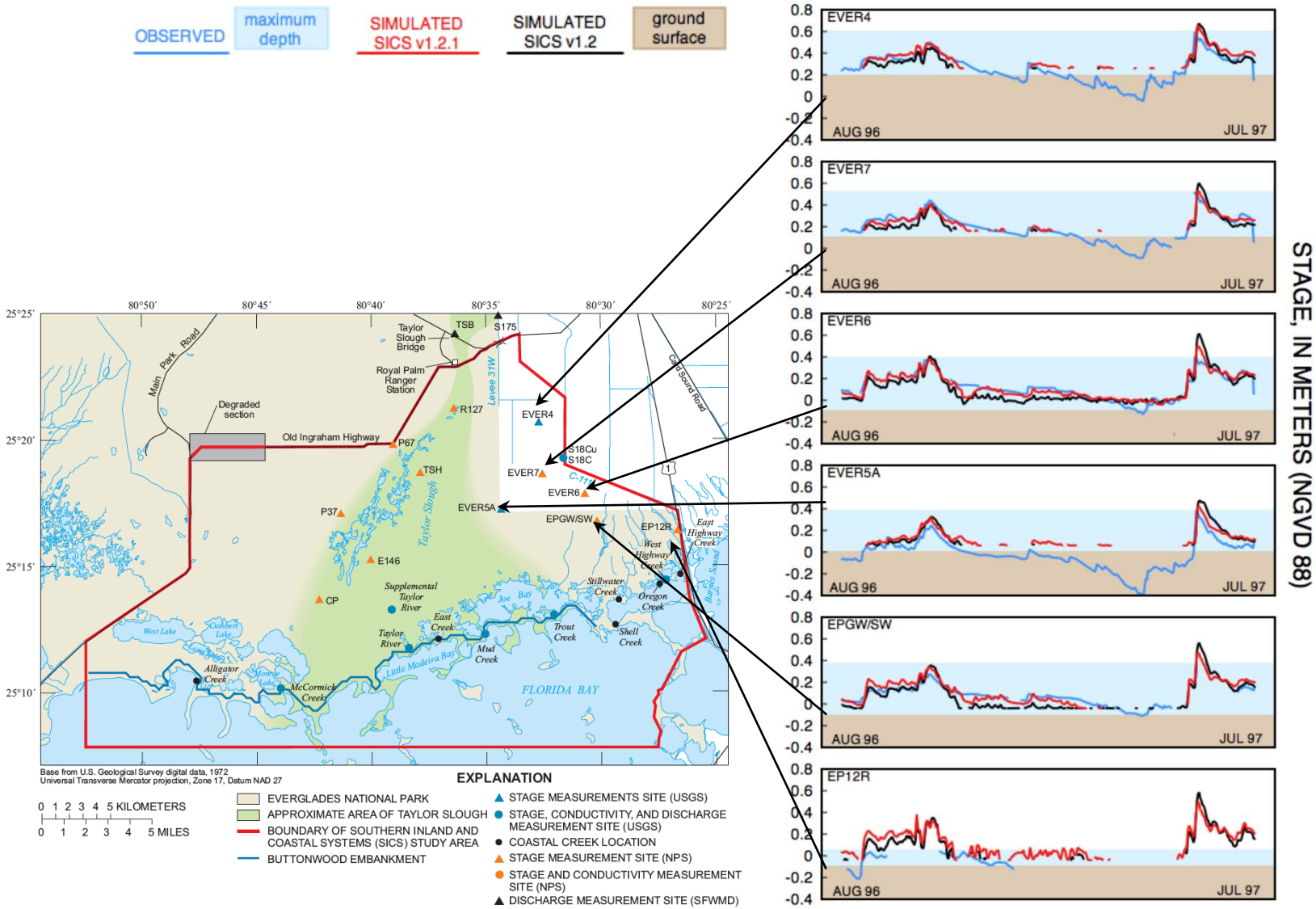

Figure 3-8. Water-levels at the six stations in the vicinity of C-111, simulated with depth-varying Manning's *n* (v1.2.1 - red) and with constant Manning's *n* (v1.2 – black).

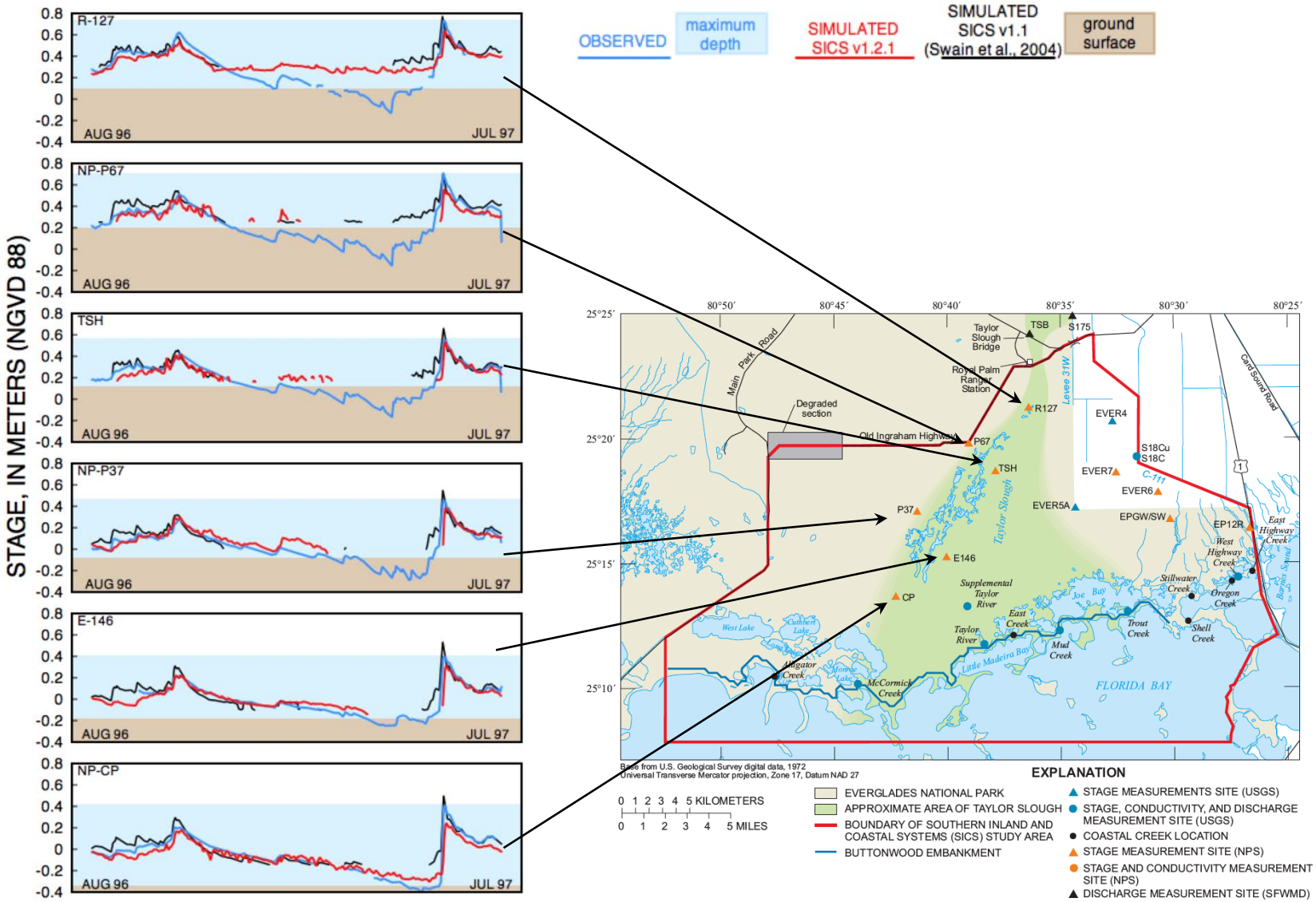

Figure 3-9. Water-levels at the six stations in the vicinity of Taylor Slough, simulated with depth-varying Manning's *n* in the current version (v1.2.1 - red) and the original SICS application (Swain et al., 2004; v1.2 – black).

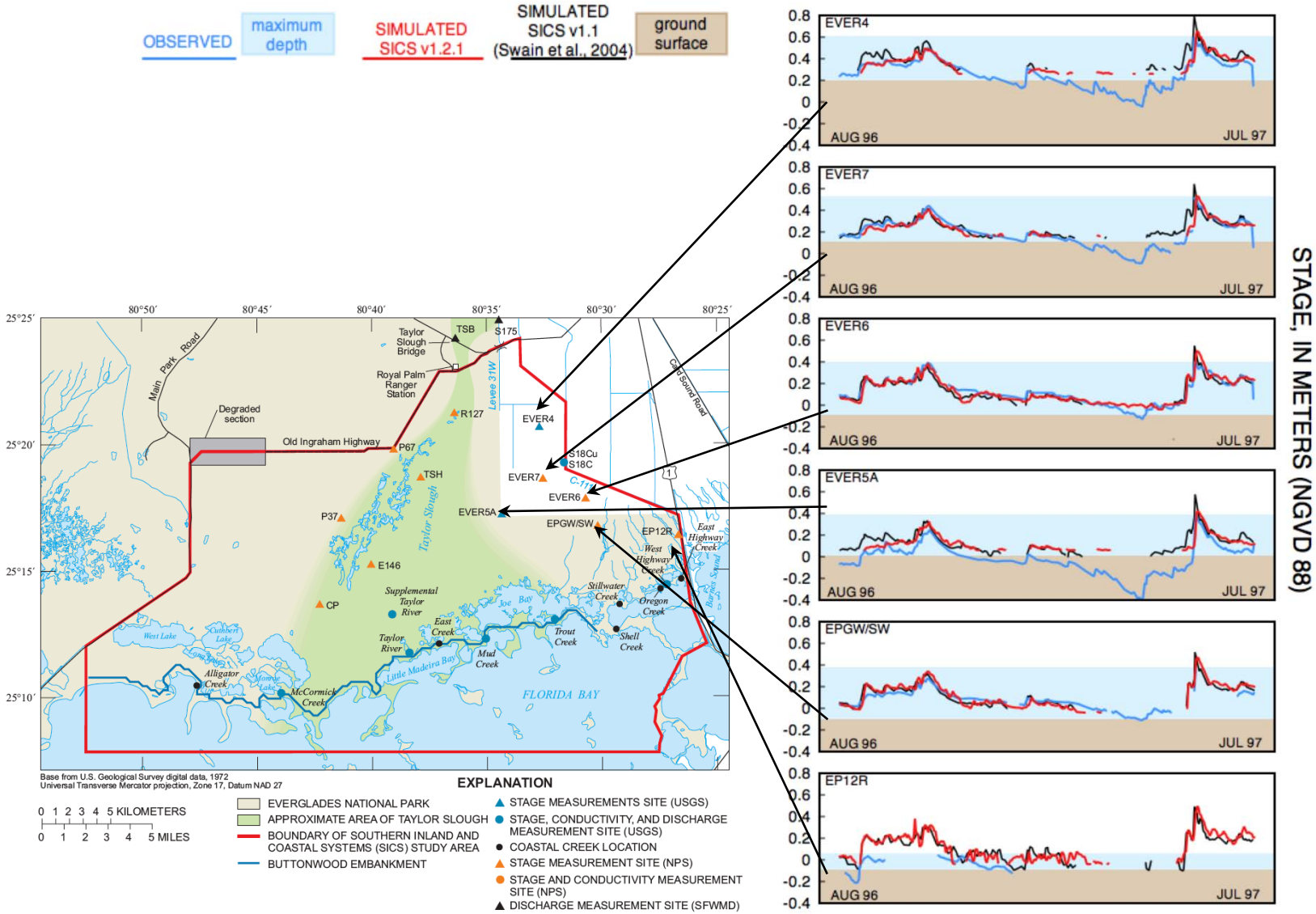

Figure 3-10. Water-levels at the six stations in the vicinity of C-111, simulated with depth-varying Manning's *n* in the current version (v1.2.1 - red) and the original SICS application (Swain et al., 2004; v1.2 – black).

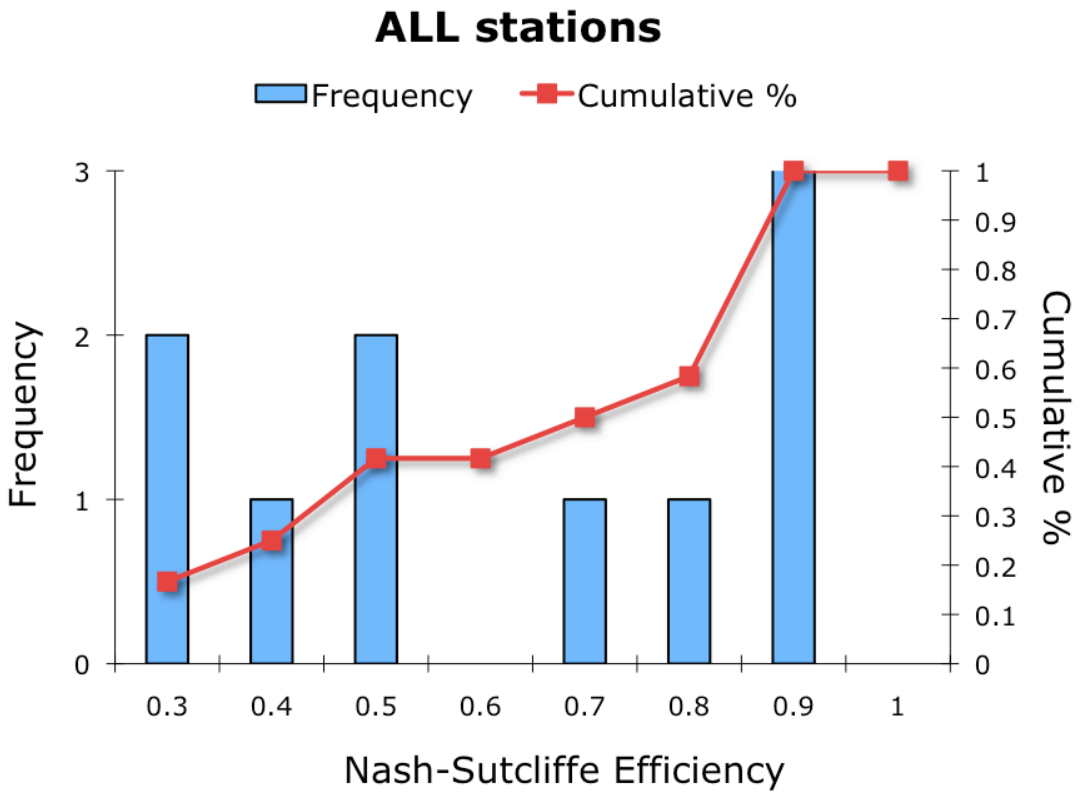

Figure 3-11. Frequency and cumulative distribution of Nash-Sutcliffe efficiencies attained with SICS v1.2.1, for all 12 water-level stations.

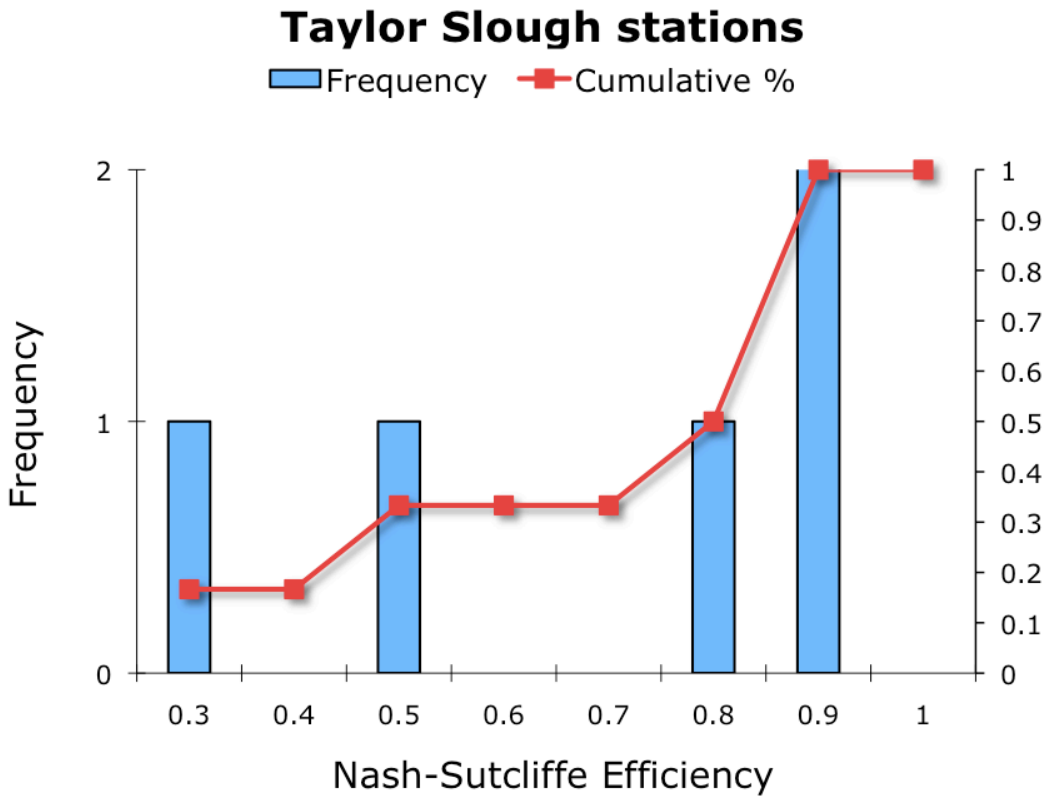

Figure 3-12. Frequency and cumulative distribution of Nash-Sutcliffe efficiencies attained with SICS v1.2.1, for 6 water-level stations in the vicinity of Taylor Slough.

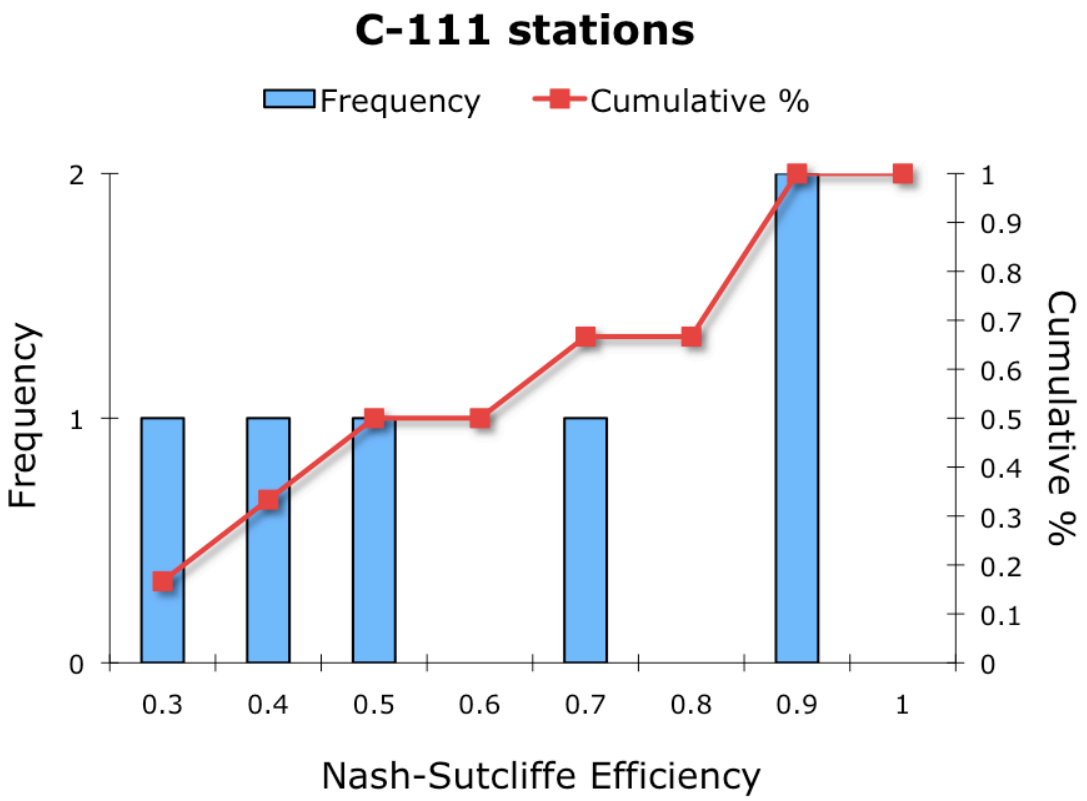

Figure 3-13. Frequency and cumulative distribution of Nash-Sutcliffe efficiencies attained with SICS v1.2.1, for 6 water-level stations in the vicinity of C-111.

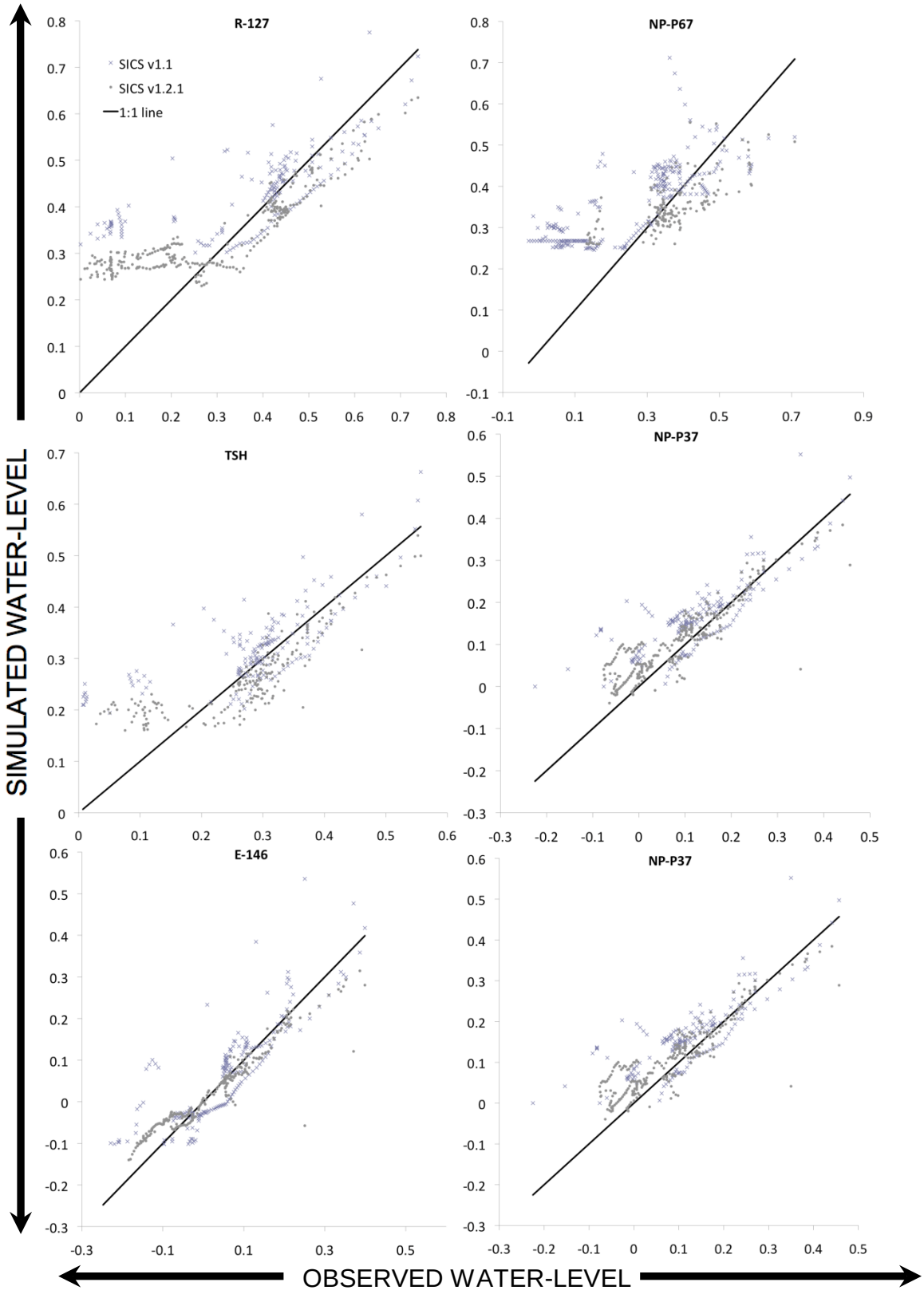

Figure 3-12. Trends in prediction bias for the 6 stations in the vicinity of Taylor Slough.

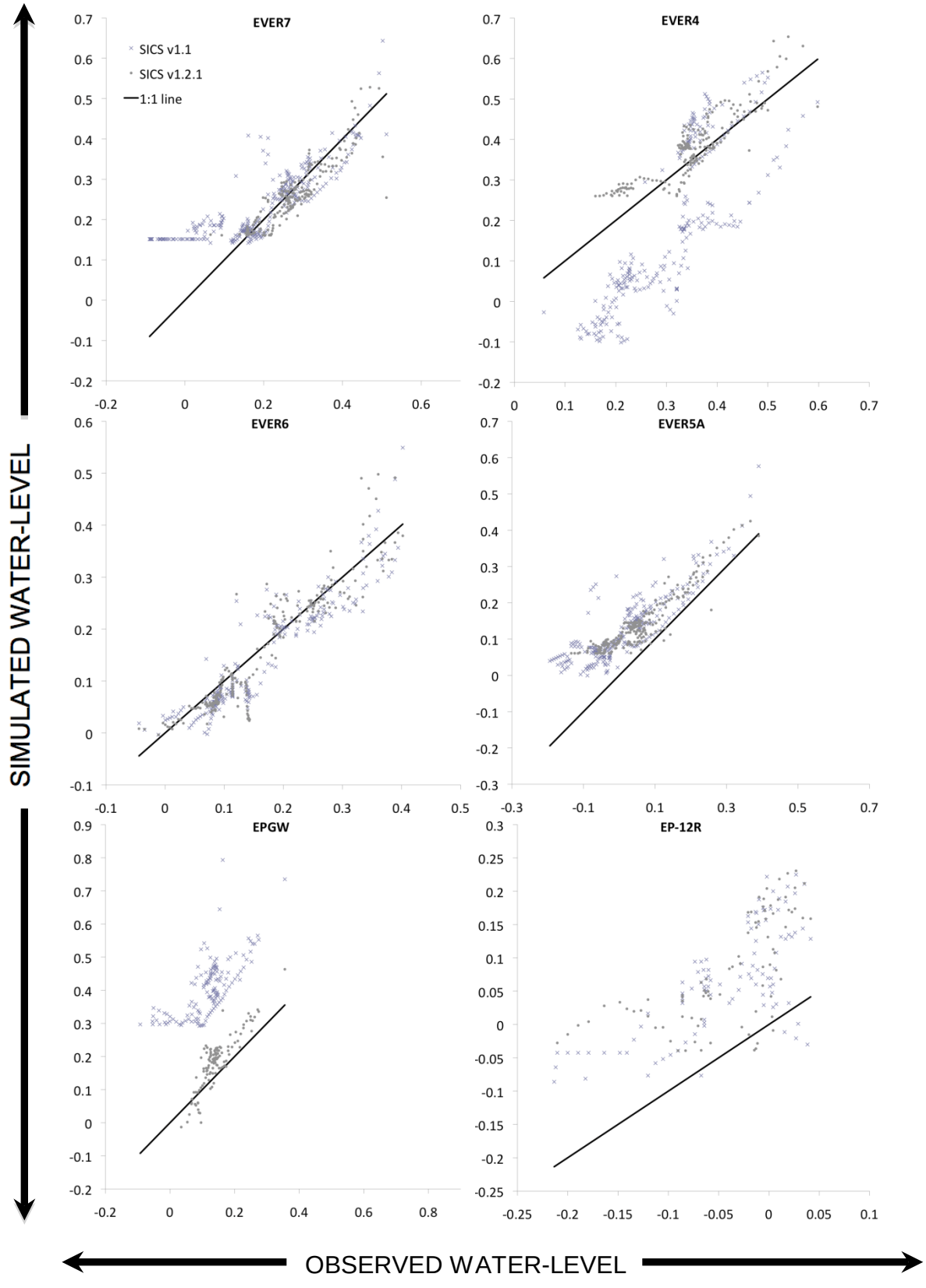

Figure 3-13. Trends in prediction bias for the 6 stations in the vicinity of C-111.

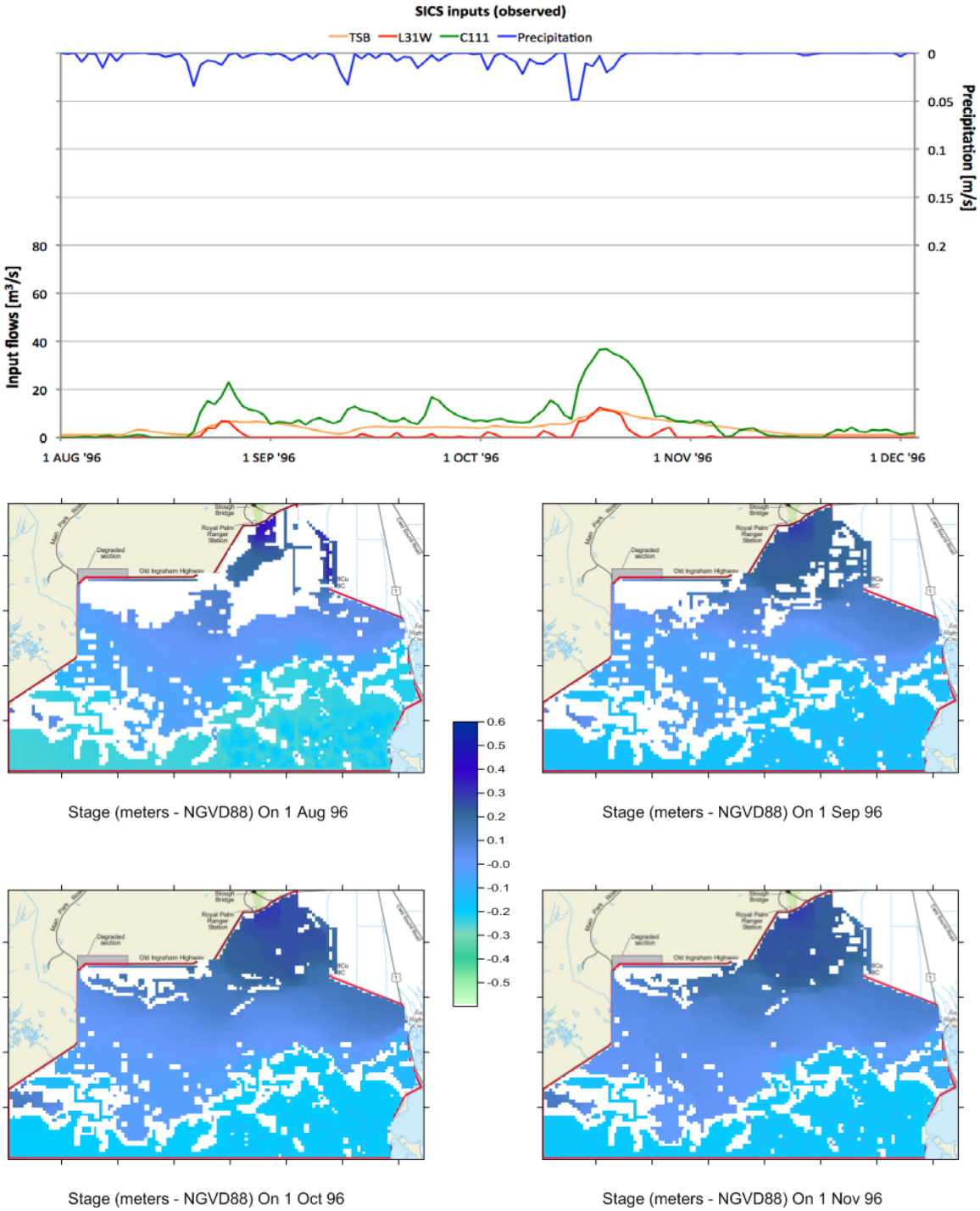

Figure 3-14. Rainfall and discharge inputs, and corresponding 2-D water-level distributions for the first four months (first wet season). White space within the domain indicates dry cells.

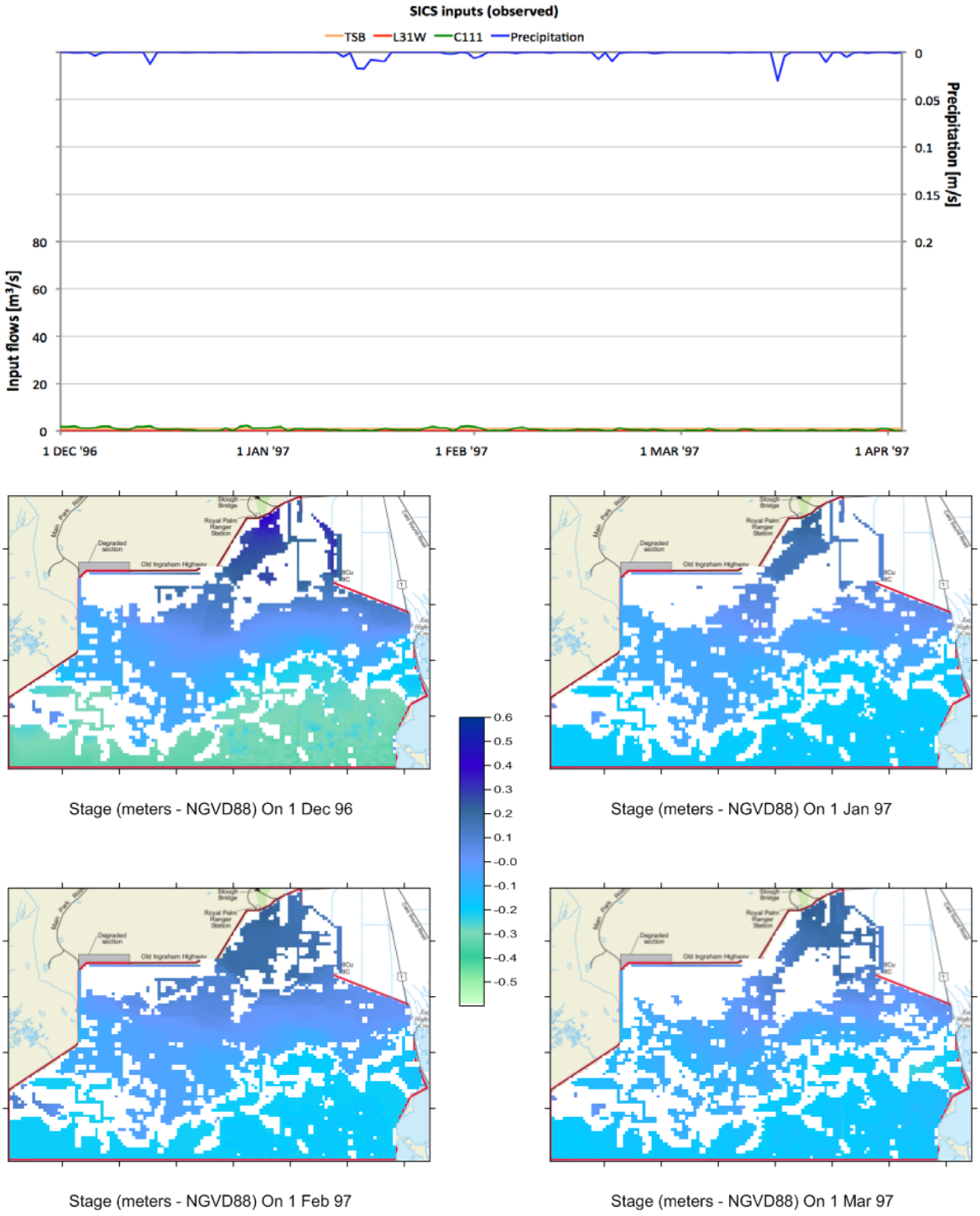

Figure 3-15. Rainfall and discharge inputs, and corresponding 2-D water-level distributions for the middle four months (dry season). White space within the domain indicates dry cells.

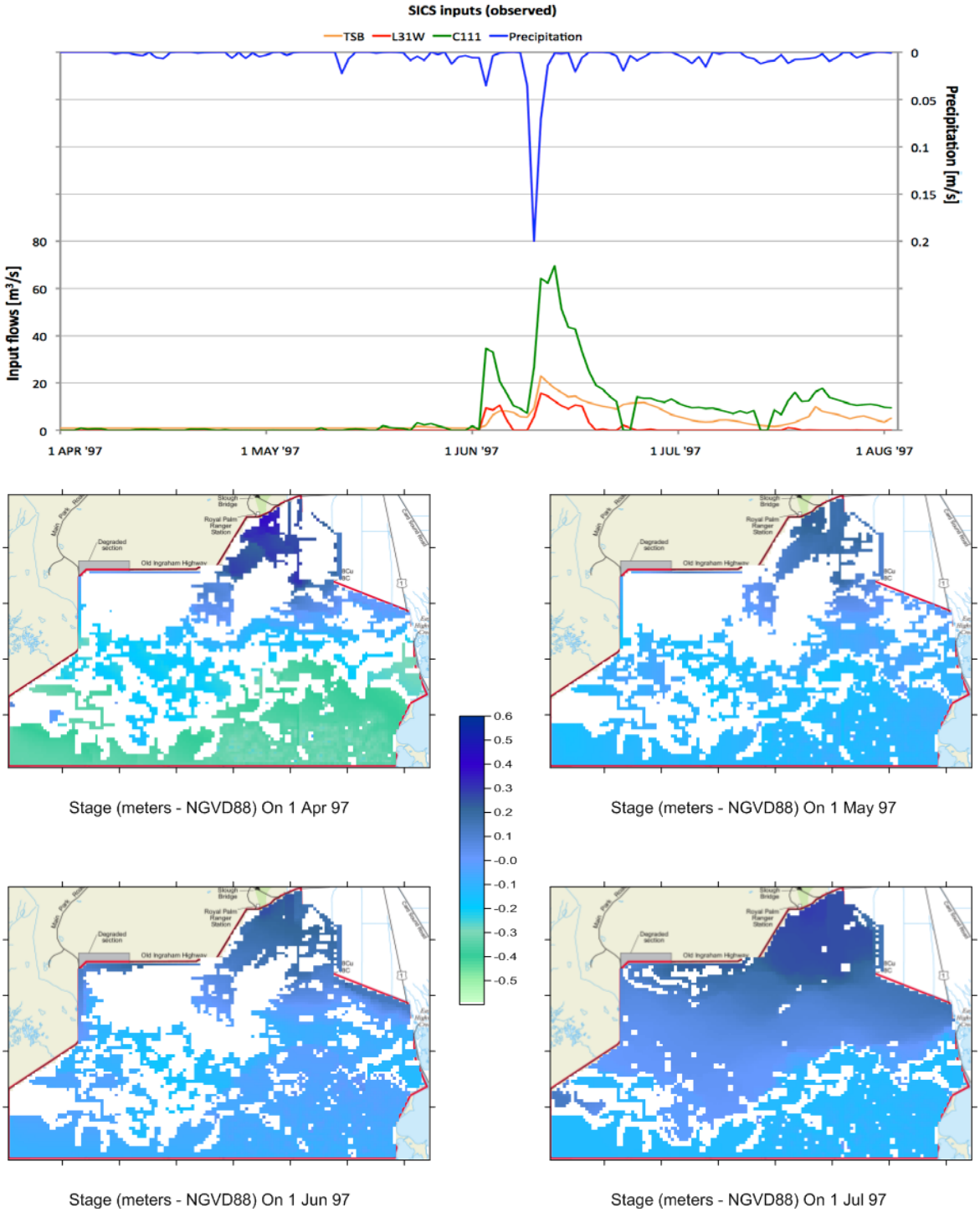

Figure 3-16. Rainfall and discharge inputs, and corresponding 2-D water-level distributions for the final four months (up to the second wet season). White space within the domain indicates dry cells.

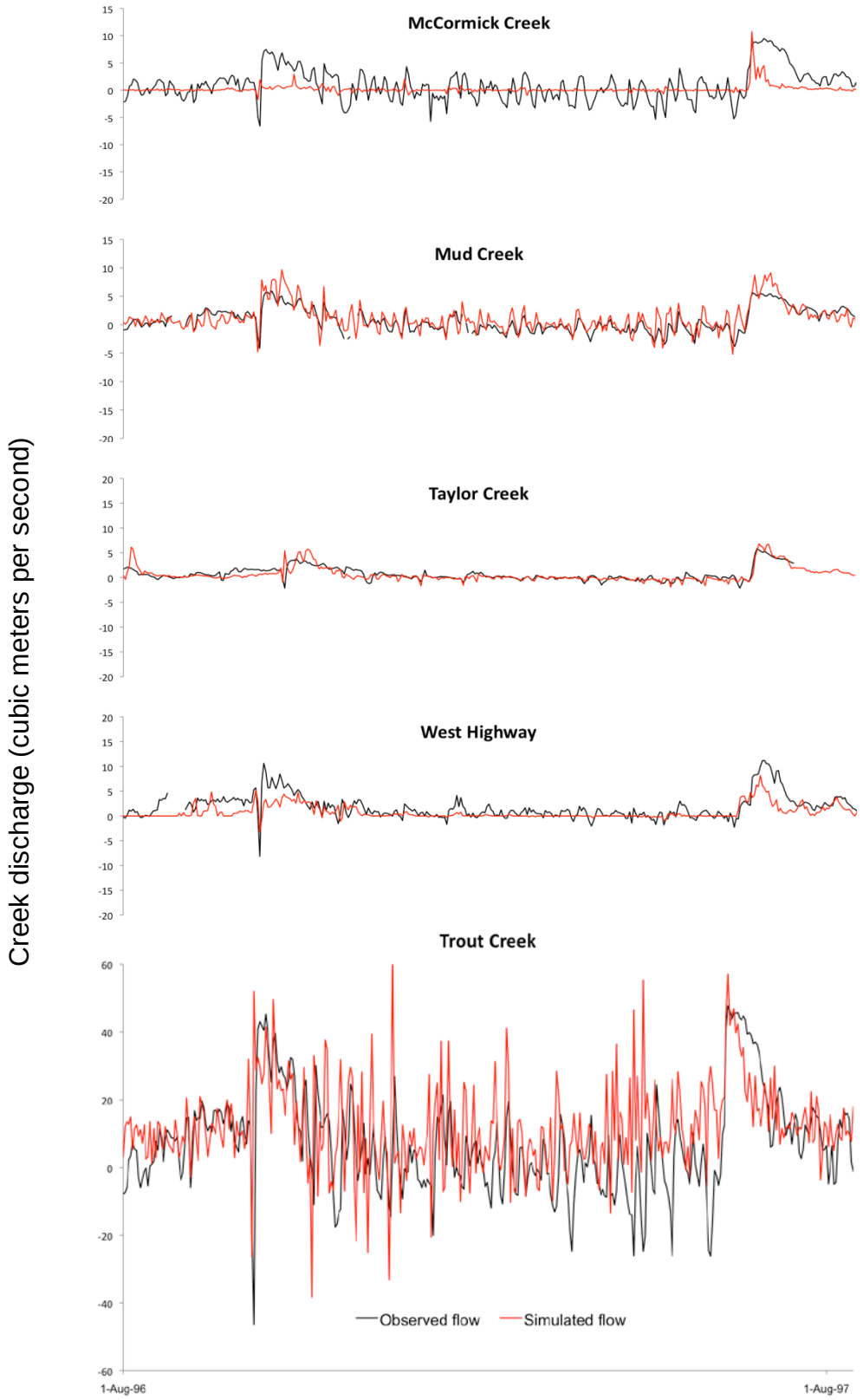

Figure 3-17. Simulated and measured discharges through five gauged creeks in the Buttonwood Embankment

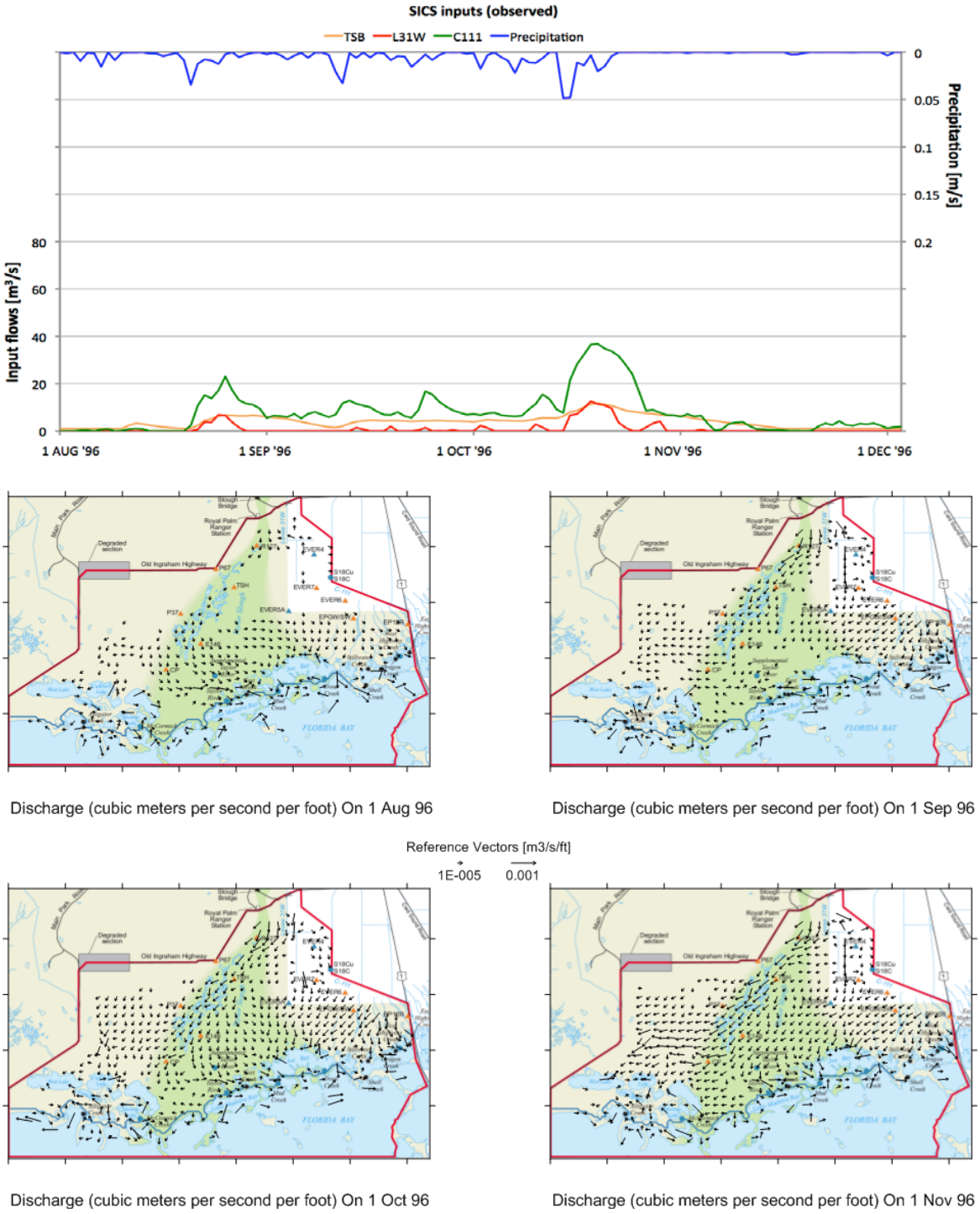

Figure 3-18. Rainfall and discharge inputs, and corresponding 2-D discharge vector distributions for the first four months (first wet season).

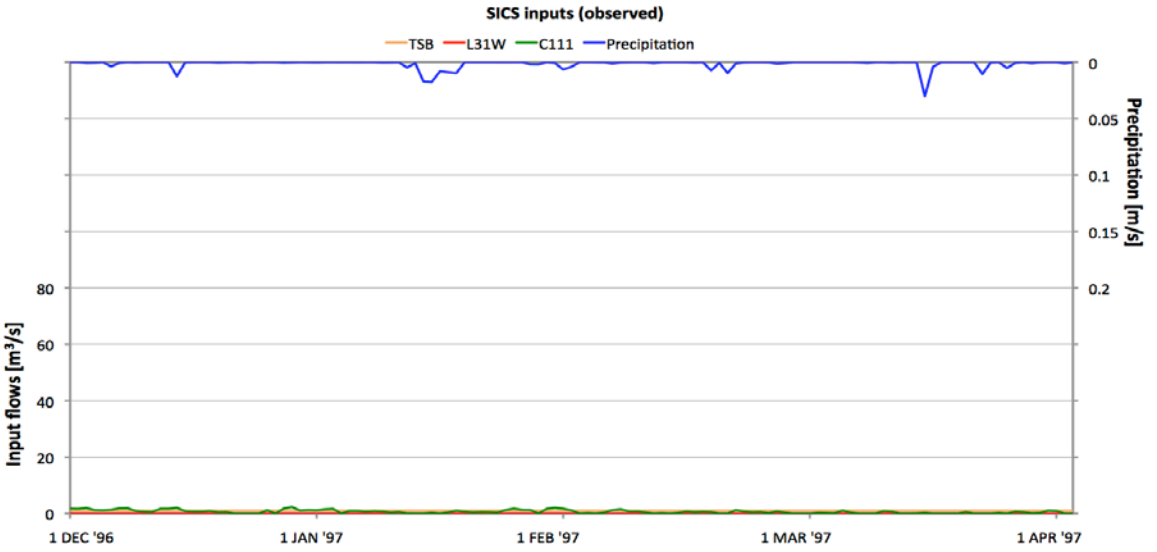

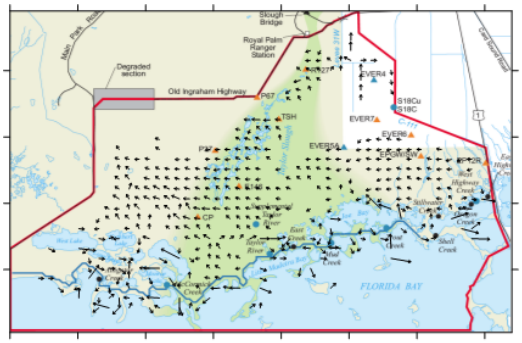

Discharge (cubic meters per second per foot) On 1 Dec 96

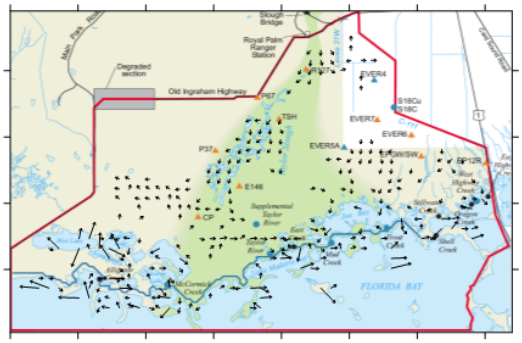

Discharge (cubic meters per second per foot) On 1 Jan 97

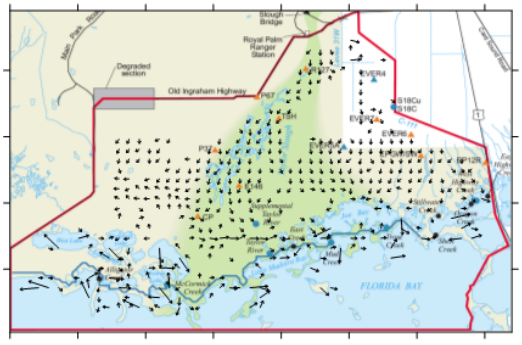

Discharge (cubic meters per second per foot) On 1 Feb 97

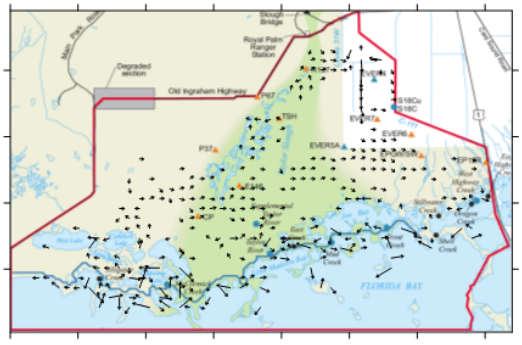

Discharge (cubic meters per second per foot) On 1 Mar 97

Figure 3-19. Rainfall and discharge inputs, and corresponding 2-D discharge vector distributions for the middle four months (dry season).

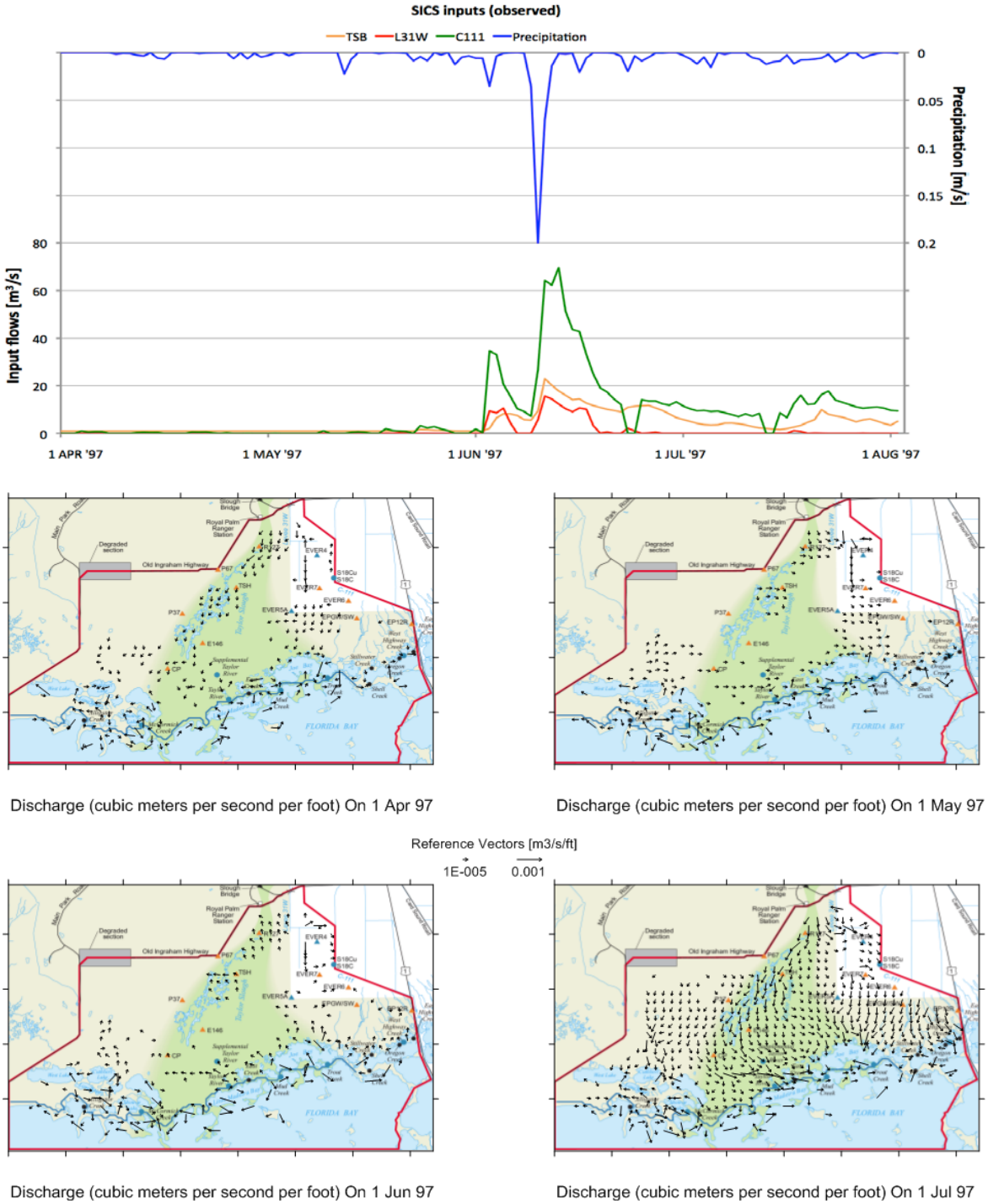

Figure 3-20. Rainfall and discharge inputs, and corresponding 2-D discharge vector distributions for the final four months (up to the second wet season).

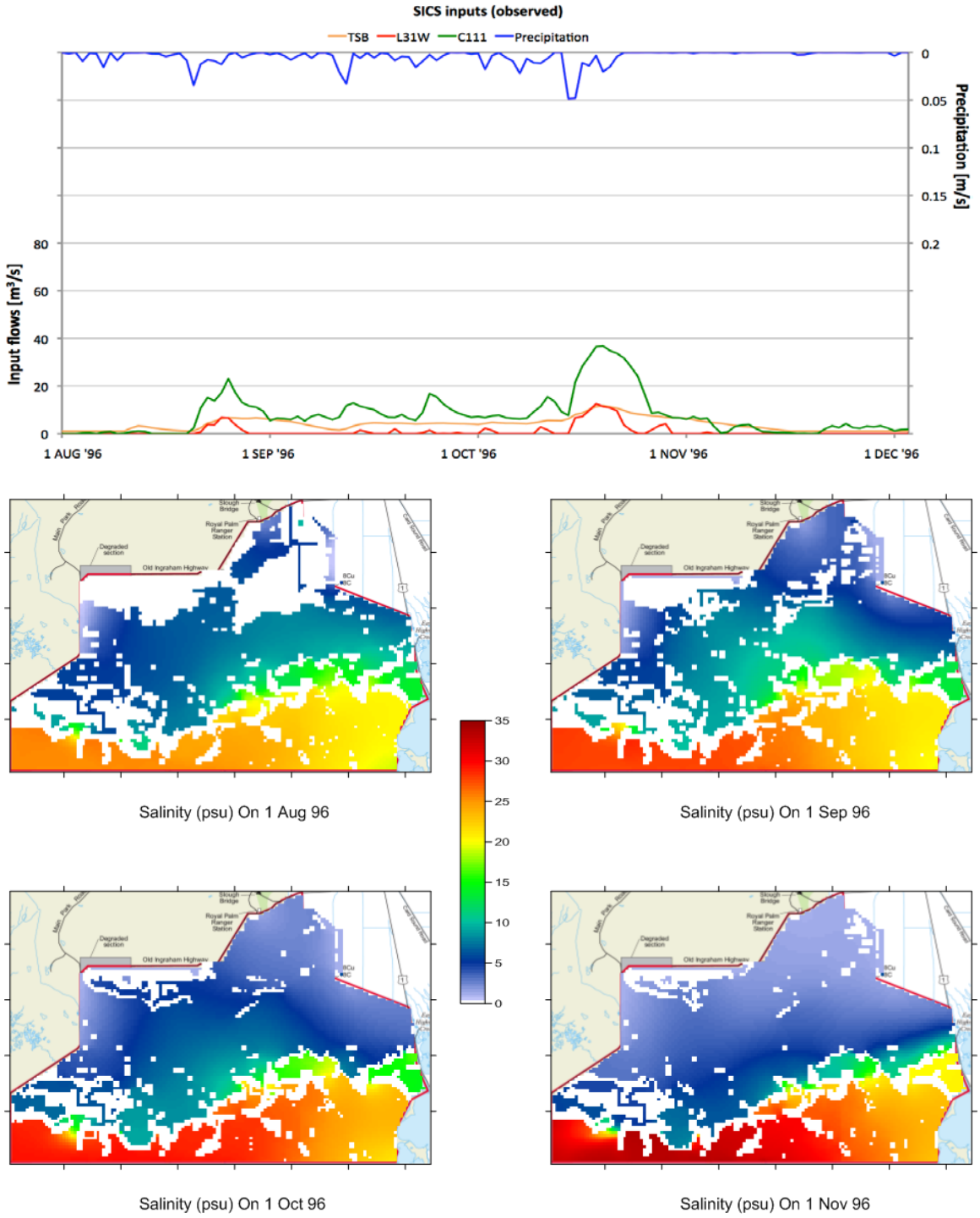

Figure 3-21. Rainfall and discharge inputs, and corresponding 2-D salinity distributions for the first four months (first wet season). White space within the domain indicates dry cells.

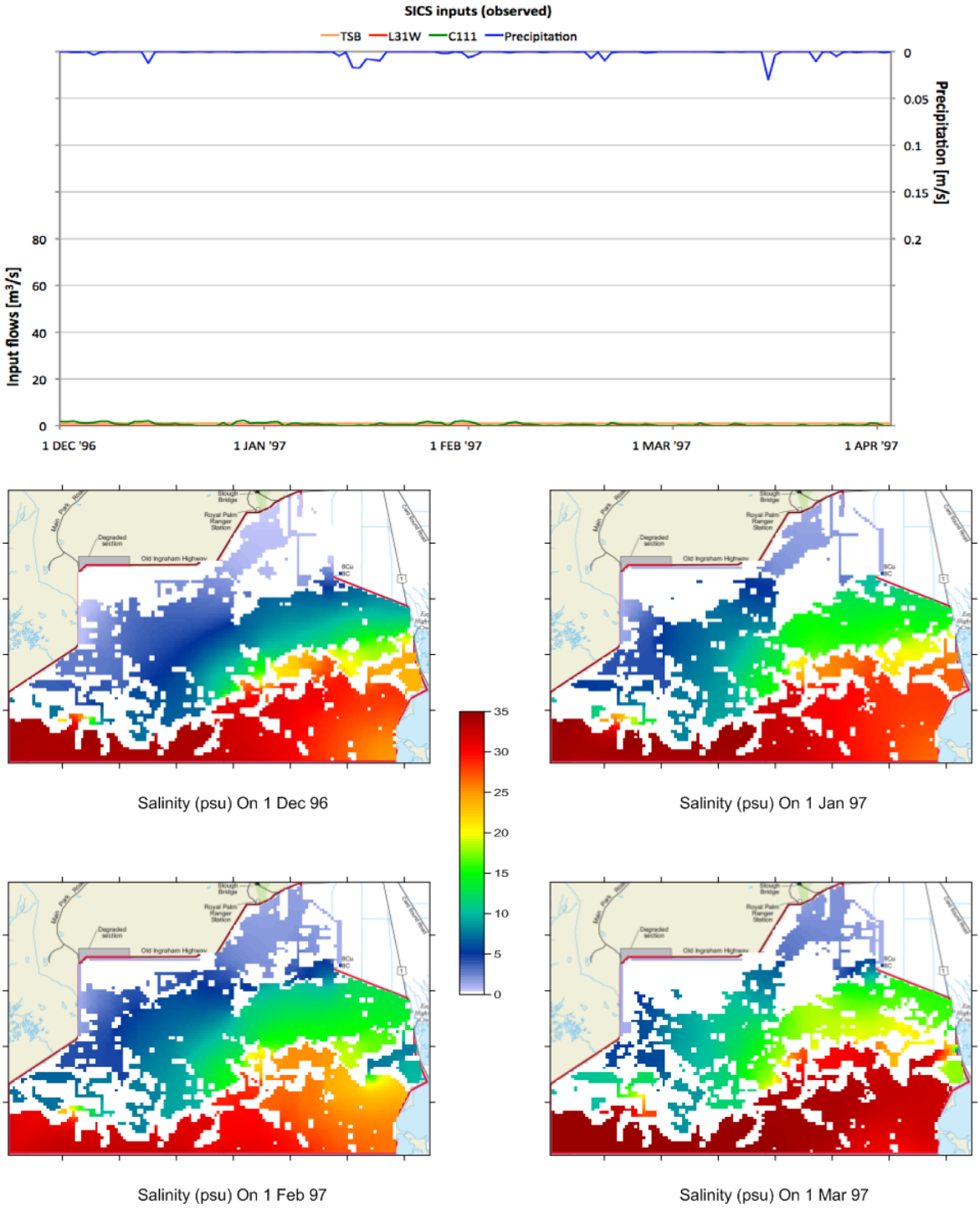

Figure 3-22. Rainfall and discharge inputs, and corresponding 2-D salinity distributions for the middle four months (dry season). White space within the domain indicates dry cells.

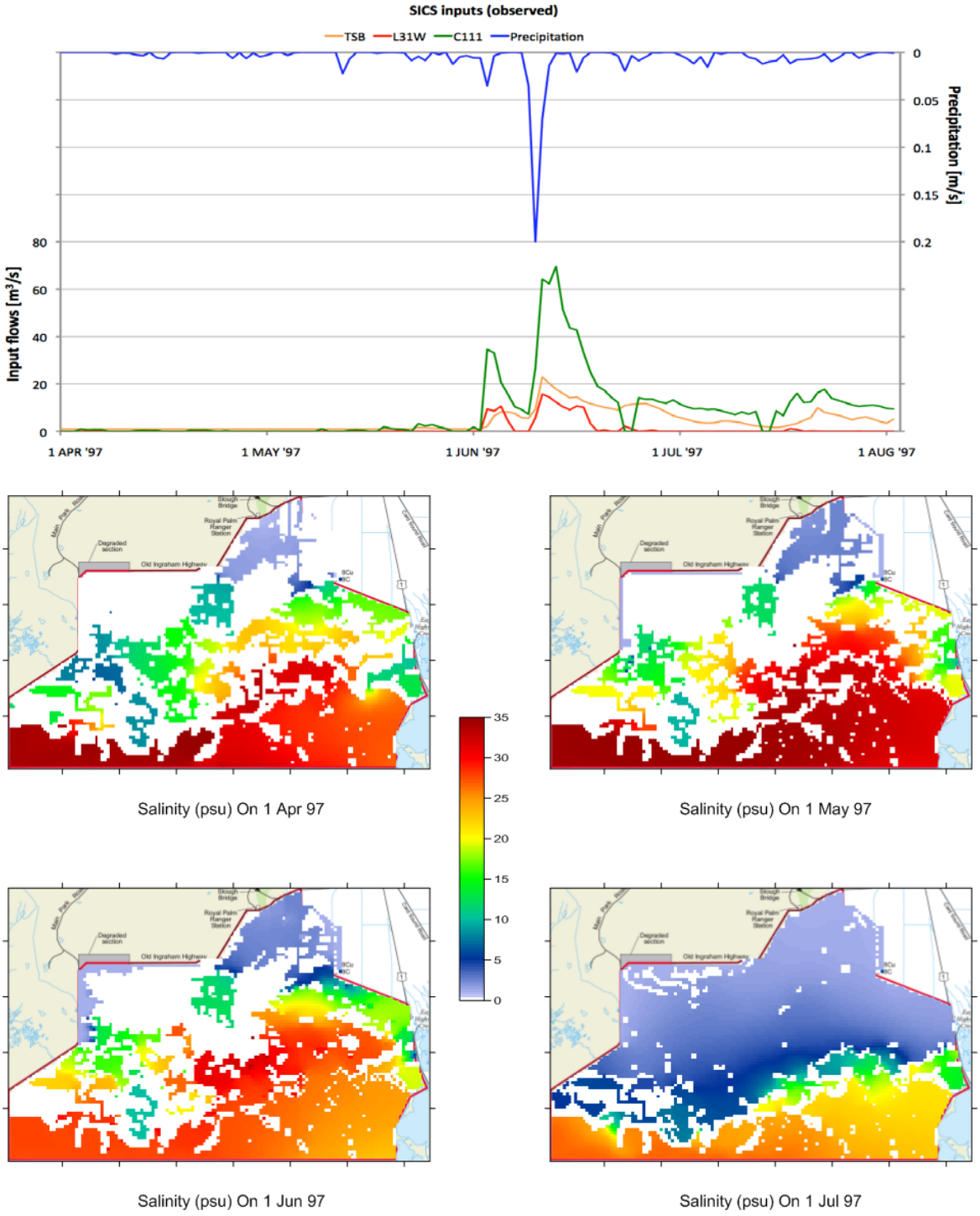

Figure 3-23. Rainfall and discharge inputs, and corresponding 2-D salinity distributions for the final four months (up to the second wet season). White space within the domain indicates dry cells.

CHAPTER 4
MODELING PHOSPHORUS WATER-QUALITY IN THE SOUTHERN INLAND AND COASTAL SYSTEMS

Introduction

The freshwater Everglades are oligotrophic due to the strong affinity for phosphorus exhibited by the carbonate substrate underlying the system (de Kanel & Morse, 1978). The cycling of phosphorus is a complex mix of physical, chemical, and biological processes (Figure 4-1) that is too complex to describe based on fundamental physics and chemistry. However, many processes can be functionally lumped together to simplify and abstract the system of cycling to a manageable degree of complexity.

The Southern Inland and Coastal Systems (SICS) region encompasses two principle habitat structures; slough and marl prairie. Taylor Slough, running southwards through the center of the region (Figure 3-1 in Chapter 3), has proportionately less emergent macrophyte biomass and more floating macrophyte and periphyton biomass than adjacent marl prairie, which is a complex of sawgrass (predominantly) and calcareous periphyton (Swain et al., 2004). Both systems have significant layers of flocculent material (floc), a loose conglomerate of bacteria, periphyton and partially decomposed litter (Noe et al., 2003). Uptake of surface-water phosphorus in both systems is dominated by periphyton and floc (Noe et al., 2003; Noe and Childers, 2007). Emergent macrophytes in the marl prairies obtain the majority of their phosphorus from porewater (Richardson and Marshall, 1986). Floating macrophytes absorb phosphorus directly from the water column, but turnover is rapid (Mitsch, 1995).

In Taylor Slough, periphyton and macrophyte litter accrete and produce organic soils. The periphyton in the marl prairies co-precipitate phosphorus with calcium, which accrete to form marl soils. Both forms of soil store phosphorus and do not readily release it unless conditions become dry (Sutula et al., 2001).

Atmospheric deposition is probably the most important source of nutrients to the southern Everglades (Noe and Childers, 2007; Sutula et al, 2001). Under historic conditions atmospheric deposition is estimated to have accounted for up to 90% of total phosphorus inputs to the Everglades (Davis, 1994). Flow into the southern Everglades does not generally exhibit the amplified nutrient loading more prevalent further north, where wetlands receive waters directly from the EAA.

Ground-water and surface-water in the region are also readily exchanged because of the combination of shallow topography and particularly high hydraulic conductivity (Fennema et al., 1994), though the extent to which such exchange contributes nutrients is unclear. Recently, Price et al. (2006) have suggested that phosphorus inputs from ground-water may increase during the dry season due to a reversal of hydraulic gradient that causes upwelling rather than leakage. Integrated ground-water and surface-water modeling of SICS (Langevin et al., 2005) have also indicated that there is upwelling during low-flow periods. However, the effects on productivity that this ground-water input of nutrients is suggested to drive are found largely in the mangrove/marshland ecotone in the southern portion of Taylor Slough, and are not thought to be as significant in the freshwater wetlands that are the focus of this modeling work.

Together, these biological, chemical, and physical processes interact to determine the concentration of phosphorus in the water column, and in turn the mass exported out of the system. By considering simplified representations of these processes an abstracted yet functionally mechanistic water-quality model can be developed that is sufficiently simple to remain manageable and justifiable, yet sufficiently complex to provide insights into internal biogeochemical processes that cannot be captured by simple reactive-transport models. However, such simple models are not without merit, and depending on the objectives of the modeling exercise may prove sufficient in themselves. We explore the value of a number of models for the purpose of simulating total phosphorus concentrations in SICS surface-waters, from the simple reactive-transport model to a more detailed model of conceptualized biogeochemical cycling.

Materials and Methods

The integrated surface-water flow, transport and reaction simulation engine that was described in Chapter 2, and applied to model hydrology in in Chapter 3, was applied to simulate surface-water total phosphorus concentrations in the SICS region for the period of August 1996 through October 1997. Two locations were identified with measured total phosphorus concentrations in the surface-water against which to compare simulated results. These were the P37 and EPGW hydrologic stations introduced in Chapter 3, and depicted in Figure 4-2.

Boundary Conditions

Concentration boundary conditions were required for each of the surface-water boundary locations described in Chapter 3 (Figure 4-2). These boundary

conditions were associated with either specified head or specified discharge boundary conditions at the lateral boundaries. Atmospheric deposition of phosphorus is input to describe the vertical inputs.

Specified water-level boundaries

For boundaries in Florida Bay (specified head boundaries 1 to 4 in Figure 4-2), time-series data was obtained for relevant water-quality observation stations in Florida Bay (Table 4-1). These data were interpolated and input into the SWIFT2D input file as time-varying data. Time-varying concentration data at specified water-level boundaries are specified in Record 2A of Part 3 of the SWIFT2D input file (Swain, 2005) at the same time intervals at which time-varying tidal (water-level) boundary conditions are read in. A FORTRAN program was therefore written to do this efficiently and reliably given the very large number of required inputs at this interval (see Subroutine EDIT_INPUTFILE in Appendix C, Section C1).

Time-series data for concentrations at specified head boundaries within the oligotrophic marsh areas (boundaries 6-8) were not available. However, analysis of long-term concentration trends at stations situated within oligotrophic marshlands (EPGW and P37) show that concentrations tend to be either below detection limit (i.e. less than 4 ppb), or on the order of 5 ppb. Total phosphorus concentrations well below 10 ppb are common in the Everglades (McCormick et al., 1996) with any excess phosphorus rapidly taken up (Rudnick et al., 1999). Given that discharge sources are the dominant lateral hydrologic input and that measured boundary concentrations are available for these (see below), and

considering the known importance of atmospheric deposition, a background concentration of 5 ppb was considered justifiable.

Specified discharge boundaries

Time-series concentration data for discharge sources were obtained for the pumping stations used to specify boundary condition flow rates. The TSB discharge source was specified using pumping data from the Taylor Slough Bridge site, the L-31W source with data from the S-175 pumping station, and the C-111 source with data from the S18C pumping station (Swain et al., 2004). Total phosphorus concentrations for these stations were obtained from the SFWMD water-quality database, DBHydro (Tables 4-2 to 4-4). Additional data sets used in a Florida Bay water-quality model (Walker, 1998) were identified that contained supplementary data for the period of interest (Tables 4-2 to 4-4). These data sources were consolidated and the time-series data interpolated for daily input to the water-quality model. Additional code had to be written into SWIFT2D to handle the addition of total phosphorus mass at the discharge sources. Mass of phosphorus added to the cell containing the discharge source was calculated based on the volume discharged and the input concentration. The mass was then added to the existing mass within the cell and the updated cell concentration determined, accounting for dilution and concentration effects due to additions and losses of water, from precipitation and ET, respectively. The subroutine STRUCTCONCS (see Appendix C, Section C1) was written to read daily discharge source concentration inputs from a new input file INPUTFLOWCONCS.dat (see Appendix C, Section C2). For consistency with the existing methods within SWIFT2D for handling sources of water, including

discharge sources, the format of the concentration data input file and its processing by the STRUCTCONCS subroutine were based on the methods used for input and handling of water sources.

Atmospheric deposition

A value of 0.03 g TP/m^2/yr was chosen given past application of this value for phosphorus budgets in southern Florida (Sutula et al., 2001 ; Noe and Childers, 2007). Given the known uncertainty of this input and the system's reported sensitivity to it, the sensitivity of the water-quality model to this input was explored by evaluating three different options for applying this average annual rate: Option 1) a fixed daily rate of 8.219E-5 g TP/m^2/d based on the annual deposition of 0.03 g TP/m^2/yr distributed evenly over 365 days; Option 2) a fixed rate of 9.709E-5 g TP/m^2/d applied only on days on which rain occurred, based on the annual deposition of 0.03 g TP/m^2/yr and the number (309) of rain days; and Option 3) a rate proportionate to the rainfall volume on each given day, summing to 0.03 g TP/m^2/yr. In this way, mass of phosphorus added to system in each case was the same.

Conceptual Models of Water-Quality Processes

Wetland biogeochemical processes are extremely complex. It is therefore necessary to abstract and simplify the many processes into a conceptual model of manageable and useful complexity. Noe and Childers (2007) have calculated annual phosphorus budgets for oligotrophic sloughs that contain phosphorus pools for water, floc, periphyton, soil, consumers, dead aboveground macrophytes, live aboveground macrophytes, and live macrophyte root biomass. Such complexity is unjustifiable in this instance given the absence of data against

which to compare the simulated results in a spatially heterogeneous and transient simulation. Furthermore, without data to constrain the many parameters that describe the flux of phosphorus between so many pools, fluxes that are themselves often very uncertain estimates (Noe and Childers, 2007; Noe et al., 2003; Sutula et al., 2001), there is a likelihood of generating non-identifiability and non-uniqueness issues in such a complex spatially-distributed model due to overparameterization (Beven, 1992).

Given the adaptable nature of the water-quality functionality in FTaRSELOADDS, a number of water-quality models (Figures 4-4, 4-5 and 4-6) were tested with increasingly complex conceptualizations of phosphorus cycling following the approach adopted in Jawitz et al. (2008) and recommended as good practice by Chwif et al. (2000).

Model 1

Applying the principle of Occam's Razor, the most simple case possible treated total phosphorus as a conservative tracer (Figure 4-4). In this case, the implicit assumption is that phosphors uptake from the surface-water through the many processes described in the introduction is balanced with atmospheric deposition and other internal sources. This is a reasonable assumption given the efficient uptake of available phosphorus reported for oligotrophic Everglades wetlands (Davis, 1994; Noe et al., 2001) and the consistently low and relatively invariant concentrations recorded for the region (McCormick, 1996). Atmospheric deposition was therefore not added to the water column in this application, though inputs with lateral flow through the specified head and concentration boundaries were maintained.

Model 2

The second tested model (Figure 4-5) accounted for atmospheric deposition as a model input, and simulated phosphorus extraction from the surface-water with a simple first-order sink term, intended to capture the lumped effect of biotic uptake and physical processes that remove phosphorus from the water column. This method was used to explore the three atmospheric deposition options described above. The time-step at which reactions were applied was that implemented for the transport and hydrology in SWIFT2D, being 1.5 minutes (see Chapter 3). To facilitate comparison, a single uptake rate that best fit all three methods was determined rather than individual rates for each case. Manual calibration showed that a rate 1.5E-6 s^{-1} offered the best result.

Model 3

The most complex case made full use of aRSE to simulate a conceptual water-quality system of processes including lumped biotic uptake of phosphorus, senescence, burial, and release of phosphorus from the dead biomass back into the water column (Figure 4-6).

Although aRSE includes methods to solve partial differential equations using the Runge-Kutta 4^{th} order solution methods, testing for numerical stability indicated that a maximum time-step of 15 minutes was permissible. This proved to be an untenable time-step for computational time considerations. Alternatively, aRSE offers simple equation solving in two separate steps, known as “presolve” and “postsolve”. This offered a means of solving the system of equations at a more reasonable daily time-step using a mass-balance approach. This was the method adopted.

Noe et al. (2003) conducted a radioisotope tracing study to examine the cycling and partitioning of phoshorus in an oligotrophic Everglades wetland (Figure 4-7). Peak tracer signals were obtained after 10 days (Noe et al., 2003), at which point the partitioning of the tracer between what remained in the surface-water and what had been removed was used to estimate an average daily uptake rate of 0.084375 day^{-1}.

The measured partitioning of phosphorus in Noe et al. (2003) was applied to determine rates of uptake by living biomass, considered to be the lumped pool of macrophytes, all forms of periphyton, consumers, and floc. The observed rate of flux from living to dead material was used to estimate the senescence rate and burial rate as a function of the uptake rate (Noe et al., 2003). DeBusk and Reddy report rates for sawgrass decomposition of 0.00067 to 0.003 d^{-1}. McCormick et al. (1996) reported aerobic decomposition of periphyton mats ranging from 0.006 go 0.11 d^{-1}, and Newman and Pietro (2001) report periphyton decomposition on the order of 0.0003 d^{-1}. After calibration a value of 0.001 d^{-1} was chosen.

Parameters, their values and their sources are presented in Table 4-5. State-variables, their initial conditions, and their definition in the XML input file are given in Table 4-6. The full system of equations input to aRSE are given in the XML input file (XMLINPUT.xml) in Appendix C (Section C3). The IWQ input file (IWQINPUT.iwq) which contains the definitions of model parameters and their values for access by SWIFT2D (see Chapter 2) is also given in Appendix C (Section C3), as well as the SWIFT2D input file (WETLANDS.inp).

Results and Discussion

Results for each of the 3 model complexities applied are presented. The simulation periods were extended beyond the 12-month hydrologic period presented in Chapter 3 up to mid-October of 1997. In this way an additional validation data-point for the P37 station was obtained. No such data was available for the EPGW station until much later (and beyond the maximum simulation length for this work). Table 4-7 summarizes the Nash-Sutcliffe efficiencies obtained for each of the models applied.

Model 1

Simulated results for a location in Taylor Slough (P37) and the marl prairies of the C-111 wetlands (EPGW) for the case of conservative transport are shown in Figure 4-8. The quality of results indicates the assumption that atmospheric deposition and internal sources are balanced by internal sinks is justifiable. The model performed better in the marl prairies (Nash-Sutcliffe of 0.74) than in the slough environment (Nash-Sutcliffe of 0.58), but the average efficiency of 0.66 implies that conservative transport may be an acceptable approximation for estimating loadings assuming that the mechanistic hydrodynamics are sufficiently accurate.

Model 2

Figure 4-9 compares the simulated concentrations achieved at stations P37 and EPGW using Model 2 and the three options for atmospheric input. Option 1 input a fixed daily mass irrespective of weather conditions, Option 2 applied a fixed mass only on rain-days, and Option 3 applied mass relative to the amount of rainfall on a given day. All three methods were applied such that total mass

added over a year summed to 0.03 g TP/m^2/yr to ensure comparable loadings to the system despite the different methods.

Option 1 was the simplest approach to adding deposition, simply dividing the annual flux equally over each day. This method provided the best results, with an average Nash-Sutcliffe across both stations of 0.66. Later efforts to refine the calibrated value of the uptake rate (1.5E-6 s^{-1}) produced no significant improvement in results so this value and these results were used as the final simulation of total phosphorus concentrations for Model 2.

Nash-Sutcliffe efficiencies for Option 2 ranged fro 0.06 to 0.46, which were poorer than those of the first method, but still reasonable, especially for EPGW. Nash-Sutcliffe efficiencies for Option 3 were uniformly less than -5 and therefore unacceptable. Efforts to improve performance by calibrating the rate constant specifically for this method proved futile because the lag in peaks could not be shifted through this factor. This method introduced strong spikes and troughs during periods of sparse rainfall that degraded results in the dry season. The lack of input given rare rain events and low volume events when rain did occur lead to significant reductions in concentrations with time. Rainfall events that then occurred under drier conditions added a disproportionate amount of phosphorus to low water-level conditions and produced large spikes in concentration that tended to lag behind the observed values. During wet periods this problem was mitigated: peaks were not as high due to the diluting effect of larger volumes of standing water, and troughs were not as low because the regular input of mass with frequent rainfall kept the mass topped up. By volume-

weighting the deposition with rainfall this method implicitly assumes that deposition is strongly related to rainfall and therefore disproportionately made up of wet deposition. The failure of this method corroborates the suggested importance of dry deposition in the SICS region.

Model 3

Results for the most complex model applied are presented in Figure 4-10. Results for the prairie (Nash-Sutcliffe = 0.73) were comparable in quality to those obtained using Model 1 (0.74) and better than those obtained with Model 2 (0.70). However, results for the slough environment (Nash-Sutcliffe = 0.23) were poorer than those obtained using Model 1 (0.58), though comparable to those obtained with Model 2 (0.28). The average efficiency for both measurement stations using Model 3 was a respectable 0.47.

As was the case for all the other models, results for the marl prairie station (EPGW) were noticeably better than those obtained for the slough station (P37). While it is unclear why this trend should be present for Models 1 and 2, it can be explained in Model 3 by noting that the radioisotope study conducted by Noe et al. (2003) was performed in wet prairie marshes in Shark River Slough. The location of this study within marshes within a slough was originally thought to be useful because of the presumed aggregating effect of the habitat being a marsh within a slough, and the fact that SICS is comprised of marsh and slough. However, given the modeling results it appears that the measured rates were more appropriate for marsh/wet prairie conditions than for slough conditions, and this hoped for aggregating effect was not present, or remained biased towards marsh conditions.

Conclusions

Three different models of increasing complexity were applied to the modeling of phosphorus water-quality in the SICS region. Average Nash-Sutcliffe efficiencies ranged from 0.47 to 0.66, indicating that phosphorus water-quality could be reasonably simulated with multiple models of differing complexity. Considering this result, the additional complexity inherent to applying a model akin to Model 3 must be justified by the objectives of the modeling effort or theoretical considerations pertaining to the underlying conceptual model.

For instance, though the best results were obtained with the simplest model, this version is subject to the greatest structural uncertainty because of the sweeping assumptions implicit in its simple form. Model 3 also remains subject to significant simplifying assumptions, but there is a degree of mechanistic process to the conceptual model at this higher complexity that imbues the model with greater theoretical justification. Alternately, if the objectives are to assess how frequently conditions exceed a specified threshold, say for example the CERP-mandated maximum TP concentration of 10 ppb, we see that the more dynamic results from Model 3 capture multiple exceedence events that were missed by the simpler versions.

The question of how best to handle the problematic but important input of atmospheric deposition appears to be best answered with the most simple solution; an annual average evenly distributed across all days of the year. Occam's Razor would tend to support this approach in any event given the great uncertainties, but the comparison of input methods yielded some valuable insights into the problem. Despite the conjectured role of convection storms in

harvesting phosphorus from the upper atmosphere, and the regularity of rainfall in the wet season, results indicated the a rainfall volume-weighted approach was not advisable. The second deposition method, which assumes rainfall captures and flushes the dry deposits, performed well but not as well as daily average. This work, however, remains founded on an annual average that is itself subject to significant uncertainty, and requires further study and experimentation to assess the full extent of model sensitivity to this source of uncertainty.

The issue of model complexity is an important one in the context of model development, and the availability of a tool such as FTaRSELOADDS, which provides the user with the freedom to define and experiment with model structure demands of the user a greater understanding of the role of complexity on model performance. Despite the reduced structural uncertainty, additional complexity is known to also introduce uncertainty into models through the additional parameters that are needed, each subject to some measurement uncertainty. In this case, the uncertainty associated with atmospheric deposition may well be the underlying reason for the simplest model, which neglected to account for atmospheric deposition, performing the best. Any effort to mechanistically model water-quality in the oligotrophic Everglades is surely going to be greatly hampered using such uncertain measures for such an important input.

Further complexity could be introduced into the water-quality model to produce more biogeochemically detailed models, and these may well improve results despite the uncertainty of deposition, but such an effort needs to be constrained with sufficient data to prevent sensitivity in the model from

undermining the integrity of calibration. The paucity of phosphorus data against which to evaluate model performance in this period is a challenge, though more recent research in the region of Taylor Slough (Childers, 2006) has produced much data that would probably be sufficient to test greater complexity. The following chapter will explore the issue of model complexity, uncertainty and sensitivity in greater detail.

As discussed in Swain et al. (2004), accurate capture of flow reversals in the tidal creeks is largely due to wind driven effects and not simply tidal fluctuations. The importance of wind-shear in this environment has implications for wind-induced mixing effects in the transport solution that cannot be captured by hydrologic models that do not account for this hydrodynamic effect. It is therefore quite possible that the good results obtained in all models, but particularly the conservative transport approach, would be eroded were a less hydrodynamic model simulating the transport. This would require further testing to confirm given that both phosphorus observation stations are located some distance from the tidal creeks where this effect is most prominent.

Table 4-1. Stations and total phosphorus concentration data (g/m^3) used for interpolation of daily concentrations for specified head boundary conditions in Florida Bay. Station numbers correspond with those of Figure YY and boundary condition numbers with those of Figure XY.

Date	TP [g/m^3] Station 3	TP [g/m^3] Station 6	TP [g/m^3] Station 13	TP [g/m^3] Station 15	TP [g/m^3] Station 23	TP [g/m^3] Station 24
7/4/96	0.00597	0.00822	0.01108	0.01256	0.00481	0.00411
8/21/96	0.00566	0.00628	0.01651	0.03294	0.00760	0.00395
9/13/96	0.00698	0.00698	0.02077	0.01333	0.00465	0.00349
10/14/96	0.00612	0.00806	0.01992	0.03216	0.00581	0.00558
11/8/96	0.00411	0.00806	0.00891	0.01201	0.00457	0.00434
12/5/96	0.00496	0.00581	0.00736	0.01744	0.00527	0.00527
1/7/97	0.00419	0.00512	0.01116	0.01620	0.00388	0.00349
2/14/97	0.00496	0.00535	0.02534	0.01767	0.00388	0.00473
3/13/97	0.00581	0.00605	0.00891	0.01240	0.00450	0.00558
4/15/97	0.00411	0.00481	0.00783	0.01380	0.00349	0.00186
5/23/97	0.00380	0.00349	0.00845	0.00907	0.00264	0.00271
6/11/97	0.01604	0.00636	0.01015	0.01116	0.00473	0.00473
7/9/97	0.00667	0.00884	0.02255	0.02612	0.00767	0.00550
8/20/97	0.00752	0.00868	0.02108	0.02860	0.00690	0.00837
9/9/97	0.00798	0.00822	0.02093	0.02031	0.00535	0.00605
10/22/97	0.00860	0.00512	0.01643	0.03534	0.00729	0.00620
11/24/97	0.00581	0.00930	0.01232	0.01759	0.00628	0.00496
12/11/97	0.00915	0.00977	0.01256	0.01411	0.00682	0.00558
BC no.	BC 4**		BC 2	BC 1	BC 3***	

* Data provided by the Southeast Environmental Research Center monitoring program in Florida Bay (http://serc.fiu.edu/wqmnetwork/SFWMD-CD/Pages/FB.htm)

** Applied the average of station 3 and station 6

*** Applied the average of station 23 and station 24

Table 4-2. Data sources and values used for boundary conditions concentrations at the L-31W discharge source

S175: From DBHYDRO (SFWMD)		S175: From Walker (1998)		Averaging per month**	
Date	TP [ppm]	Date	TP [ppm]	Date	TP [ppm]
7/11/96	0.0090	7/96	0.0034	7/96	0.0062
7/24/96	BDL				
8/7/96	BDL	8/96	0.0031	8/96	0.0031
8/20/96	BDL				
9/11/96	0.0040	9/96	0.0039	9/96	0.0040
9/24/96	BDL				
10/9/96	0.0080	10/96	0.0050	10/96	0.0065
10/22/96	BDL				
11/6/96	BDL	11/96	0.0033	11/96	0.0033
11/19/96	BDL				
12/4/96	0.0070	12/96	BDL	12/96	0.0070
12/17/96	BDL				
1/8/97	0.0040	1/97	BDL	1/97	0.0055
1/21/97	0.0070				
2/12/97	0.0040	2/97	BDL	2/97	0.0040
3/12/97	BDL	3/97	BDL	3/97	0.0040
--	--	4/97	BDL	4/97	0.0040
5/21/97	BDL	5/97	0.0084	5/97	0.0062
6/12/97	0.0090	6/97	0.0084	6/97	0.0071
6/25/97	0.0040				
7/8/97	BDL	7/97	0.0035	7/97	0.0043
7/22/97	0.0050				
8/5/97	BDL	8/97	0.0063	8/97	0.0052
9/2/97	0.0040				
9/17/97	0.0064	9/97	0.0050	9/97	0.0051
9/30/97	BDL				
Annual mean	0.0061*		0.0050*		0.0050

BDL="below detection limit"

* Excluding BDL

** If value from Walker (1998) > 0.004 ppm and all SFWMD records BDL then the assumed detection limit of 0.004 ppm was included in the average. If no data was recorded by SFWMD then the Walker (1998) value was used. If only BDL records existed then 0.004 ppm was used.

-- No data sampled by SFWMD that month

Table 4-3. Data sources and values used for boundary conditions concentrations at the C-111 discharge source.

S18C: From DBHYDRO (SFWMD)		S18C: From Walker (1998)		Averaging per month**	
Date	TP [ppm]	Date	TP [ppm]	Date	TP [ppm]
7/11/96	BDL	7/96	0.0030	7/96	0.0030
7/24/96	BDL				
8/7/96	BDL	8/96	0.0032	8/96	0.0032
8/20/96	BDL				
9/11/96	0.0040	9/96	0.0035	9/96	0.0038
9/24/96	BDL				
10/9/96	0.0040	10/96	0.0034	10/96	0.0037
10/22/96	BDL				
11/6/96	BDL	11/96	0.0040	11/96	0.0045
11/19/96	0.0050				
12/4/96	0.0040	12/96	0.0038	12/96	0.0039
12/17/96	BDL				
1/8/97	0.0050	1/97	0.0041	1/97	0.0044
1/21/97	0.0040				
2/12/97	BDL	2/97	0.0031	2/97	0.0031
3/12/97	BDL	3/97	0.0033	3/97	0.0033
--	--	4/97	0.0068	4/97	0.0068
--	--	5/97	0.0115	5/97	0.0115
6/12/97	0.0290	6/97	0.0214	6/97	0.0185
6/25/97	0.0050				
7/8/97	BDL	7/97	0.0031	7/97	0.0031
7/22/97	BDL				
8/5/97	BDL	8/97	0.0063	8/97	0.0052
09/2/97	0.0041	9/97	0.0046	9/97	0.0046
09/17/97	0.0051				
Annual mean	0.0075*		0.0058		0.0056

BDL="below detection limit"

* Excluding BDL

** If value from Walker (1998) > 0.004 ppm and all SFWMD records BDL then the assumed detection limit of 0.004 ppm was included in the average. If no data was recorded by SFWMD then the Walker (1998) value was used. If only BDL records existed then 0.004 ppm was used.

-- No data sampled by SFWMD that month.

Table 4-4. Data sources and values used for boundary conditions concentrations at the TSB discharge source.

TSB: From DBHYDRO (SFWMD)		TSB: From Walker (1998)		Averaging per month**	
Date	TP [ppm]	Date	TP [ppm]	Date	TP [ppm]
7/9/96	BDL	7/96	0.0047	7/96	0.0044
8/6/96	0.0120	8/96	0.0081	8/96	0.0101
9/10/96	0.0040	9/96	0.0041	9/96	0.0041
10/15/96	BDL	10/96	0.0031	10/96	0.0031
11/5/96	BDL	11/96	0.0045	11/96	0.0043
12/3/96	0.016	12/96	0.0152	12/96	0.0156
--	--	1/97	0.0138	1/97	0.0138
--	--	2/97	BDL	2/97	0.0040
--	--	3/97	0.0058	3/97	0.0058
--	--	4/97	0.0081	4/97	0.0081
--	--	5/97	0.0067	5/97	0.0067
6/24/97	BDL	6/97	0.0040	6/97	0.0040
7/29/97	BDL	7/97	0.0030	7/97	0.0030
8/19/97	BDL	8/97	0.0029	8/97	0.0029
09/16/97	BDL	8/97	0.0035	8/97	0.0035
Annual mean	0.0107*		0.0063*		0.0062

BDL="below detection limit"

* Excluding BDL

** If value from Walker (1998) > 0.004 ppm and all SFWMD records BDL then the assumed detection limit of 0.004 ppm was included in the average. If no data was recorded by SFWMD then the Walker (1998) value was used. If only BDL records existed then 0.004 ppm was used.

-- No data sampled by SFWMD that month.

Table 4-5. Parameters used in the model

Parameter	Definition	XML input	Value	Units	Source
k_u	P uptake rate	k_uptake	0.083475	d-1	Noe et al., 2003
k_{sn}	Senescence rate as a function of uptake	k_senesc	0.25	--	Noe et al., 2003
k_{dc}	Decomposition rate	k_decomp	0.001	d-1	Calibration; Debusk and Reddy, 2005; Newman et al.; 2001
k_b	Burial rate as a function of uptake	k_soil	0.13	--	Noe et al., 2003
K_w	Wet/dry factor	K_wet	1 or 0	--	From SWIFT2D based on ICLSTAT*

* ICLSTAT(N,M) is 0 if a cell is considered wet at the time by SWIFT2D, or >0 if dry.

Table 4-6. State-variables with initial conditions as used in Model 3

State variable (Figure 4-6)	Definition	XML input	Initial condition (aRSE)	Units
$[TP_{sw}]$	TP concentration in the surface-water at t	TP_sw_conc	0.005	g TP/m^3
TP_{sw}	Mass of TP in the surface-water at t-1	TP_sw_mass1	0.01	g TP/m^2
	Mass of TP in the surface-water at t	TP_sw_mass2	0.01	g TP/m^2
TP_u	TP uptake from the surface-water for t	TP_uptake1	0.0008	g TP/m^2/d
	TP uptake from the surface-water for t-1	TP_uptake2	0.0008	g TP/m^2/d
TP_{bio}	TP in live biomass at time t	TP_live1	0.04	g TP/m^2
	TP in live biomass at time t-1	TP_live2	0.04	g TP/m^2
TP_{dead}	TP in dead biomass at time t	TP_dead1	0.014	g TP/m^2
	TP in dead biomass at time t-1	TP_dead2	0.014	g TP/m^2
TP_{sn}	TP flux by senescence at time t	TP_senesc	0.0002	g TP/m^2/d
TP_{dc}	TP flux by decomposition at time t	TP_decomp	0.0001	g TP/m^2/d
TP_b	TP flux by burial at time t	TP_bury	0	g TP/m^2/d
TP_s	TP in the soil at time t	TP_soil1	0.0001	g TP/m^2
	TP in the soil at time t-1	TP_soil2	0.0001	g TP/m^2

Table 4-7. Nash-Sutcliffe efficiencies for the water-quality models applied to simulate total phosphorus in the Southern Inland and Coastal Systems

	Model1	Model 2 (Option 1)	Model 2 (Option 2)	Model 2 (Option 3)	Model 3
P37	0.583531	0.285041	0.062226	-5.183816	0.226110
EPGW	0.737771	0.697249	0.460871	-5.612662	0.733882
Combined	0.658693	0.484382	0.255956	-5.364559	0.471255

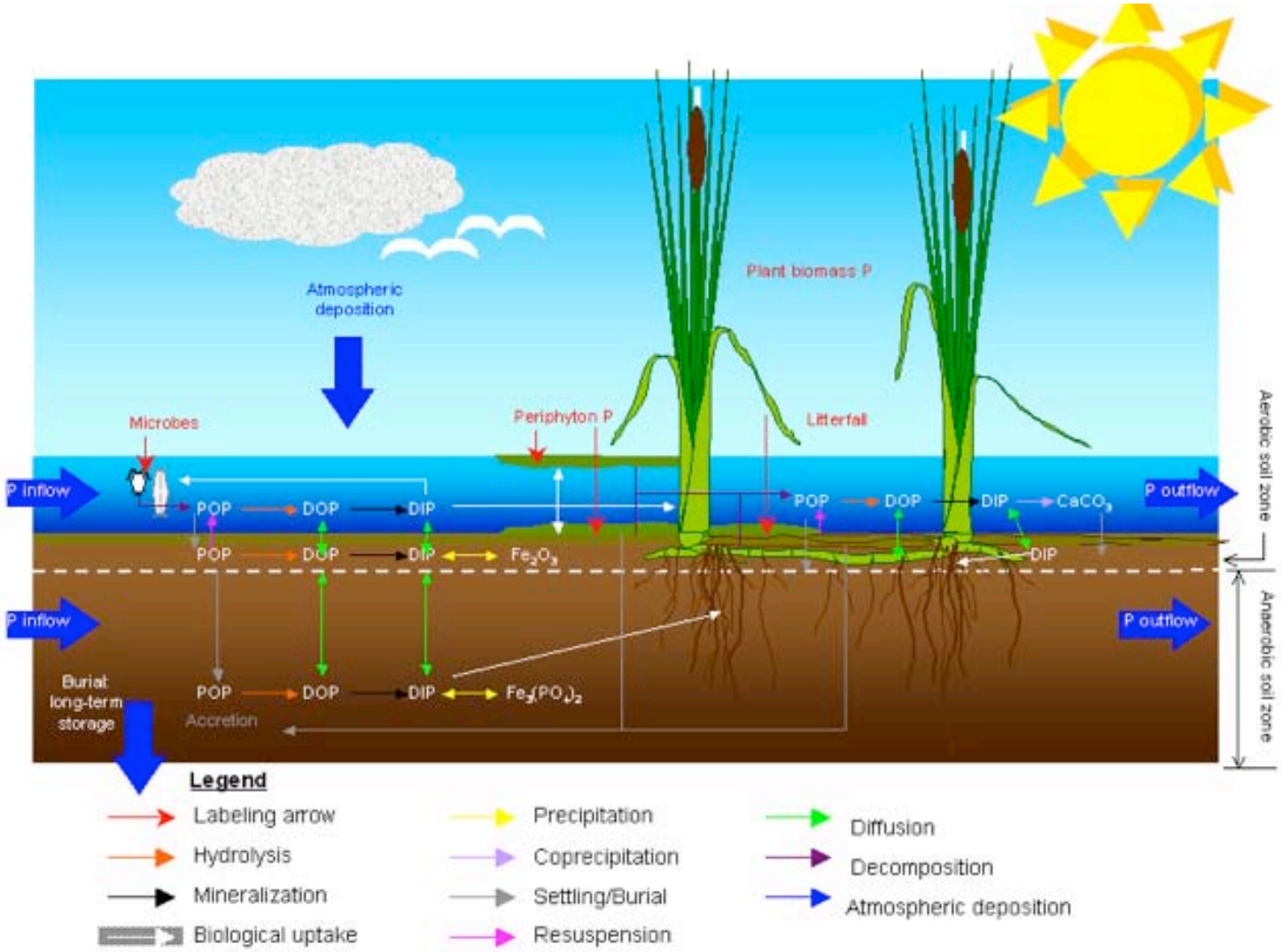

Figure 4-1. Schematic of phosphorus cycling processes in Everglades wetlands.

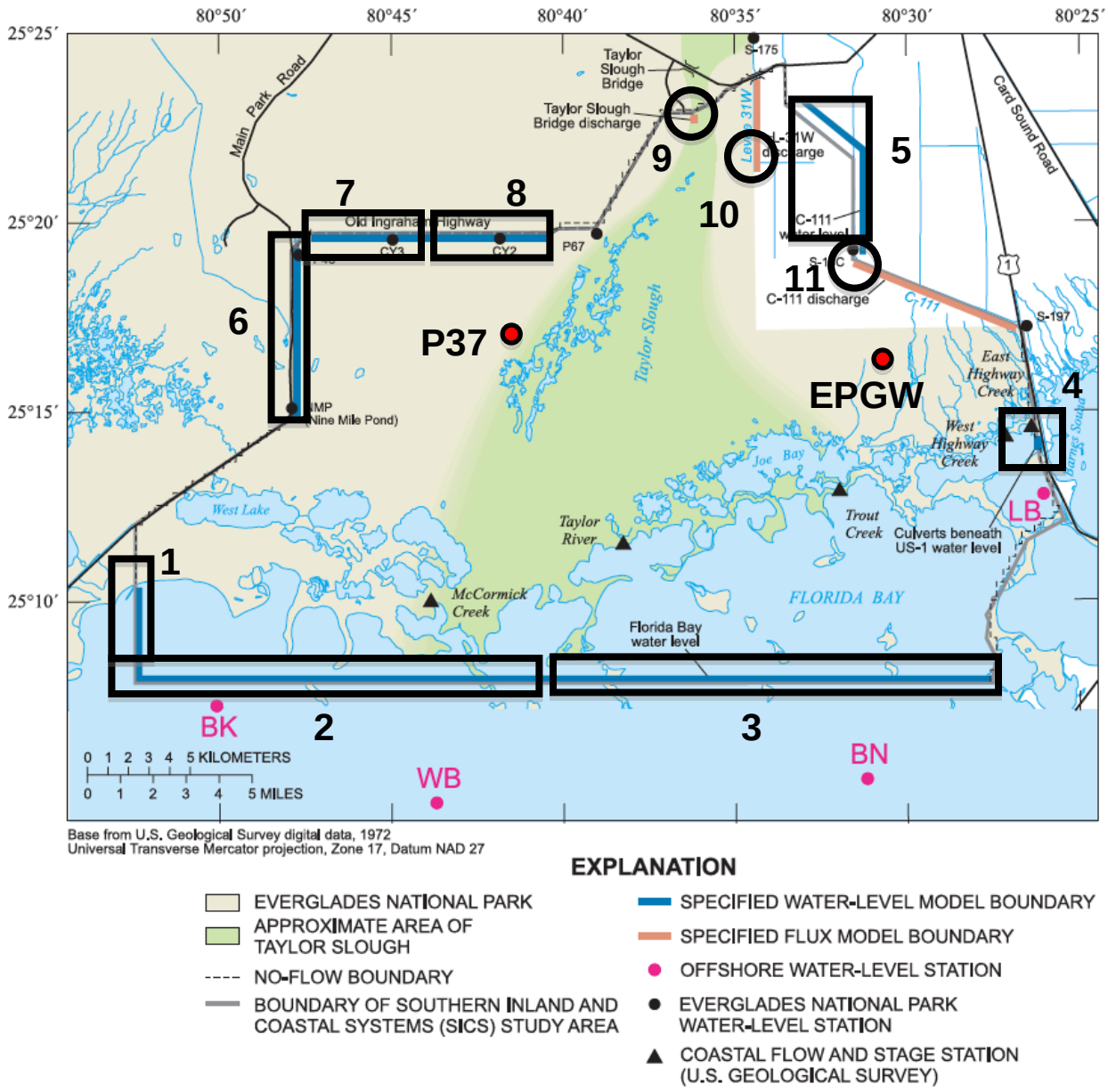

Figure 4-2. Location of SICS model boundary conditions including specified head boundaries (blue), discharge sources (orange), and the associated total phosphorus concentration boundary conditions (black – squares indicate specified head and circles discharge sources; numeric references refer to Table 4-1) at each of these (map and hydrologic boundaries from Swain et al., 2004).

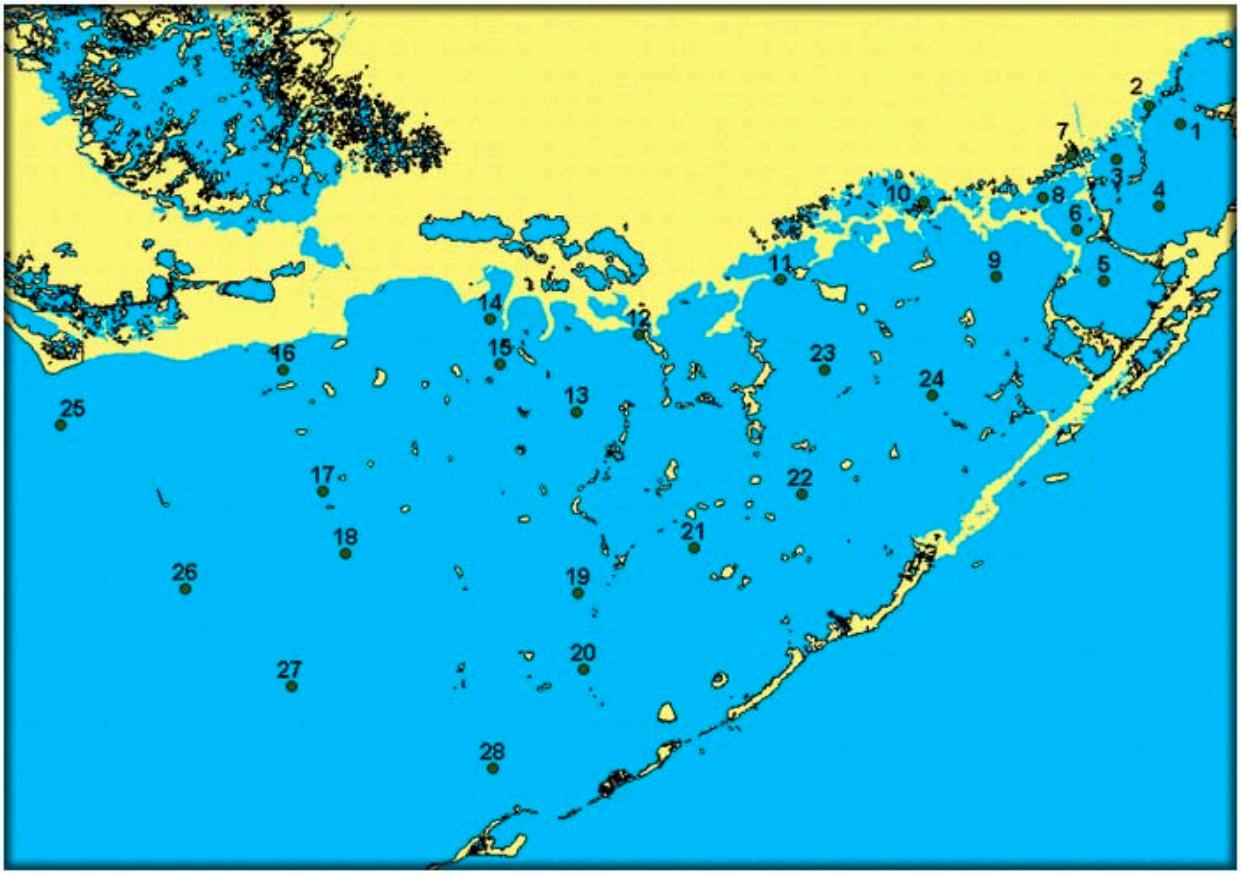

Figure 4-3. Location of water-quality observation points in Florida Bay. Data are provided by the Southeast Environmental Research Center (http://serc.fiu.edu/wqmnetwork/SFWMD-CD/Pages/FB.htm)

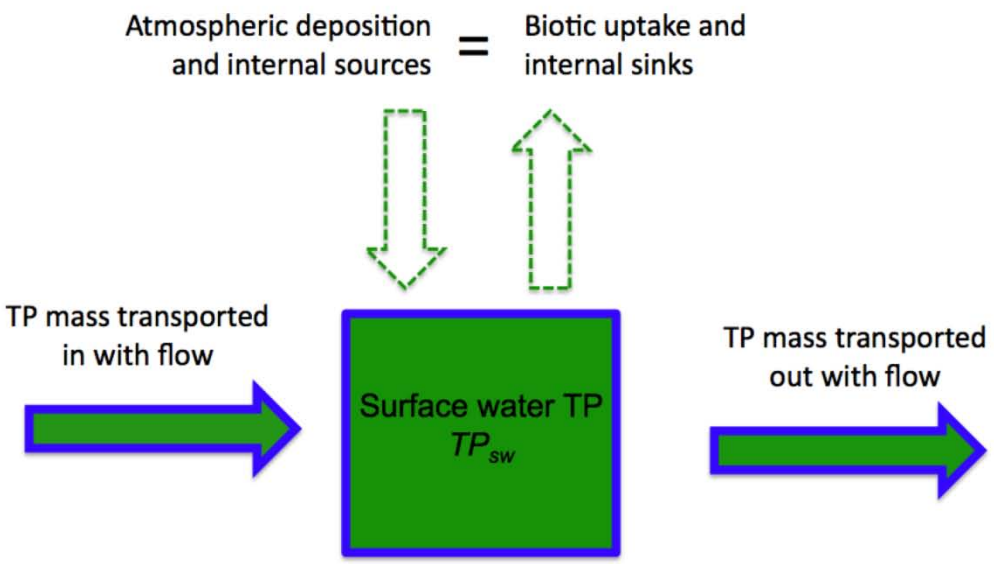

Figure 4-4. Model 1: Conservative transport assuming deposition and internal sources are in equilibrium with biotic uptake and internal sinks. Green fill indicates total phosphorus, and blue lines indicate the medium is water.

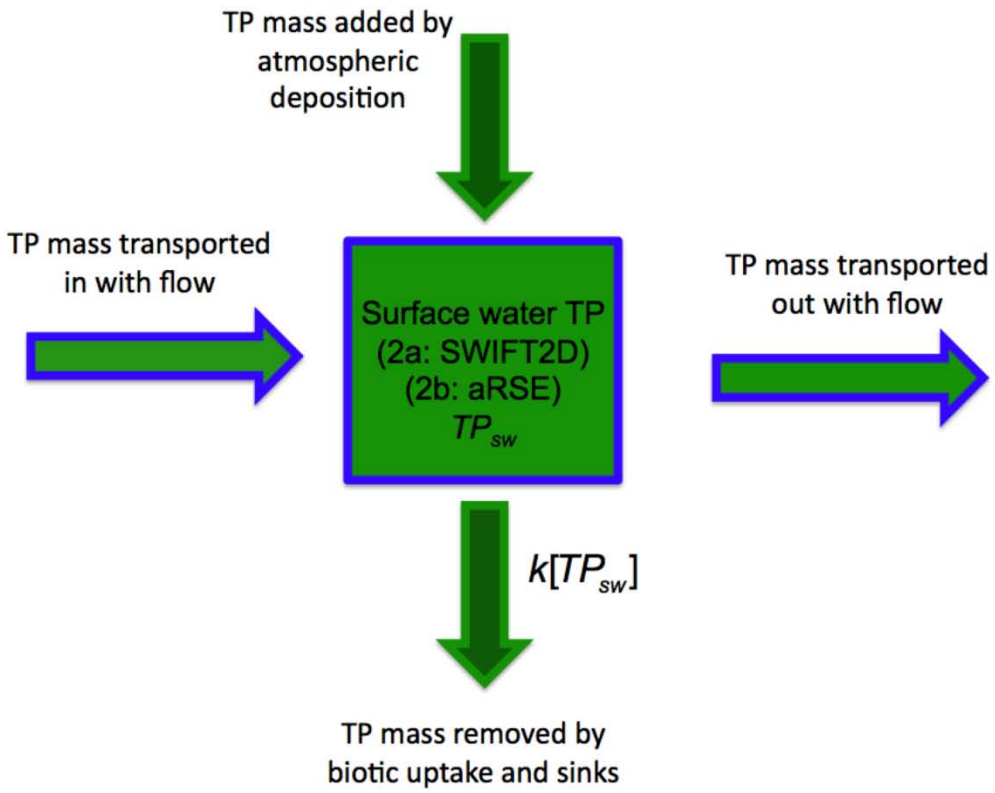

Figure 4-5,. Model 2: First-order uptake from the water column using the reactive transport functionality of SWIFT2D (Model 2a) or aRSE for reactions and SWIFT2D for transport (Model 2b).

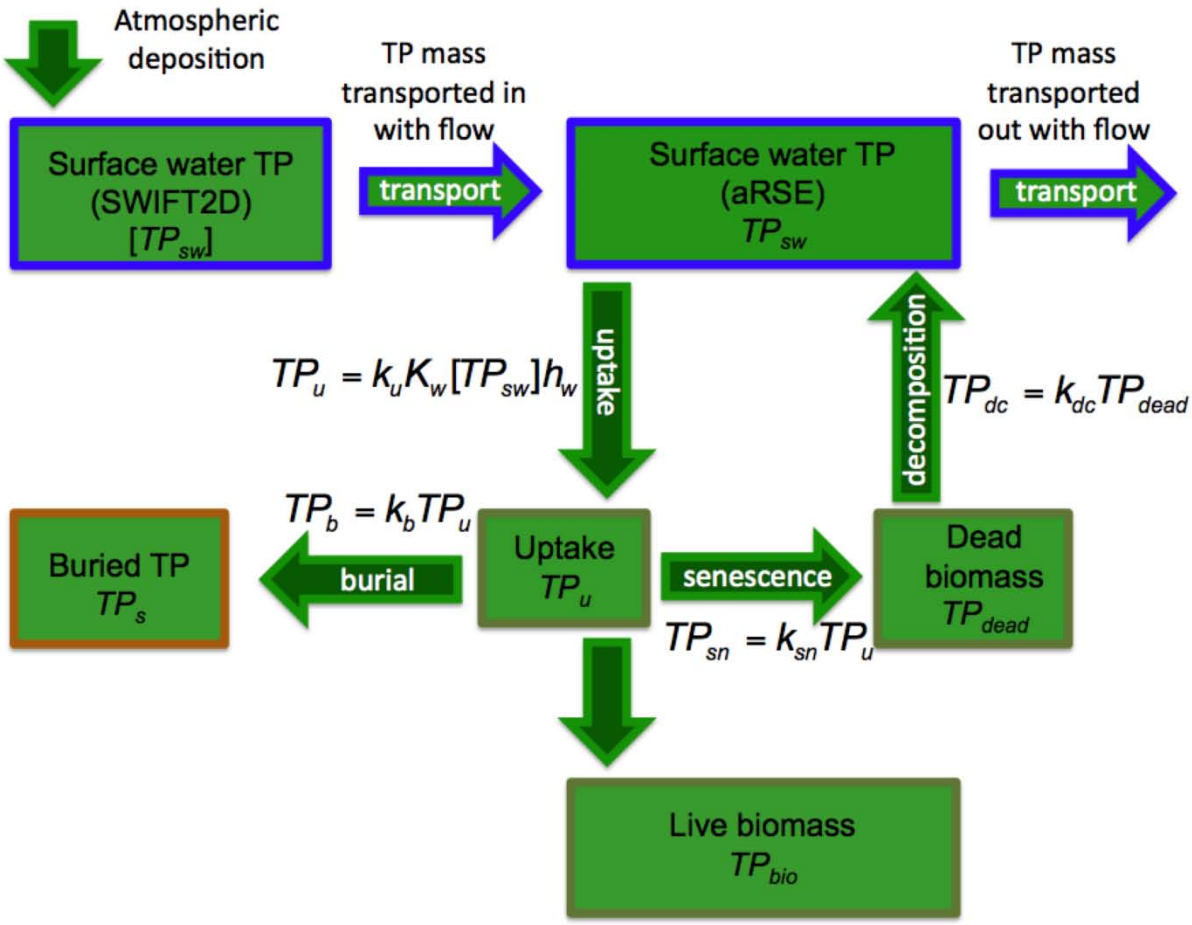

Figure 4-6. Model 3: Reactions simulated by aRSE with transport by SWIFT2D. For XML equations see Appendix C (Section C3). Variables and parameters defined in Tables 4-5 and 4-6.

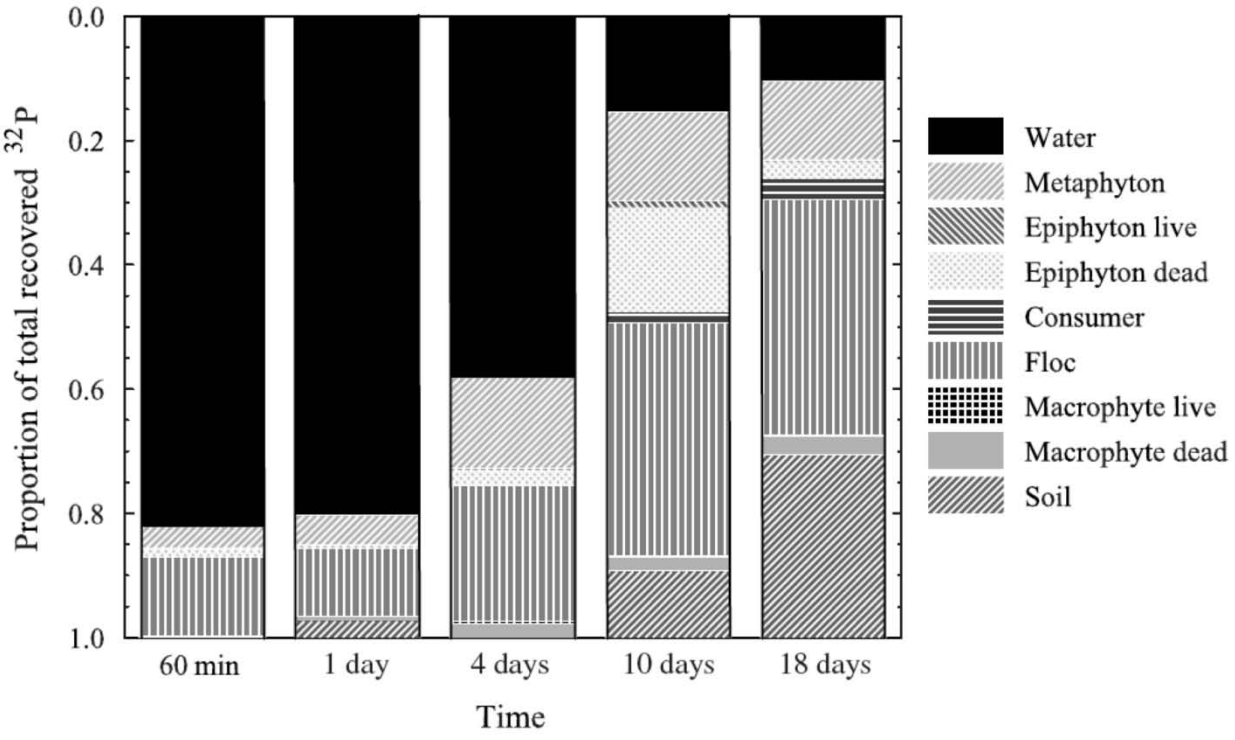

Figure 4-7. Mean proportion of total recovered radioisotope (^{32}P) per mesocosm found in different ecosystem components over time (from Noe et al., 2003).

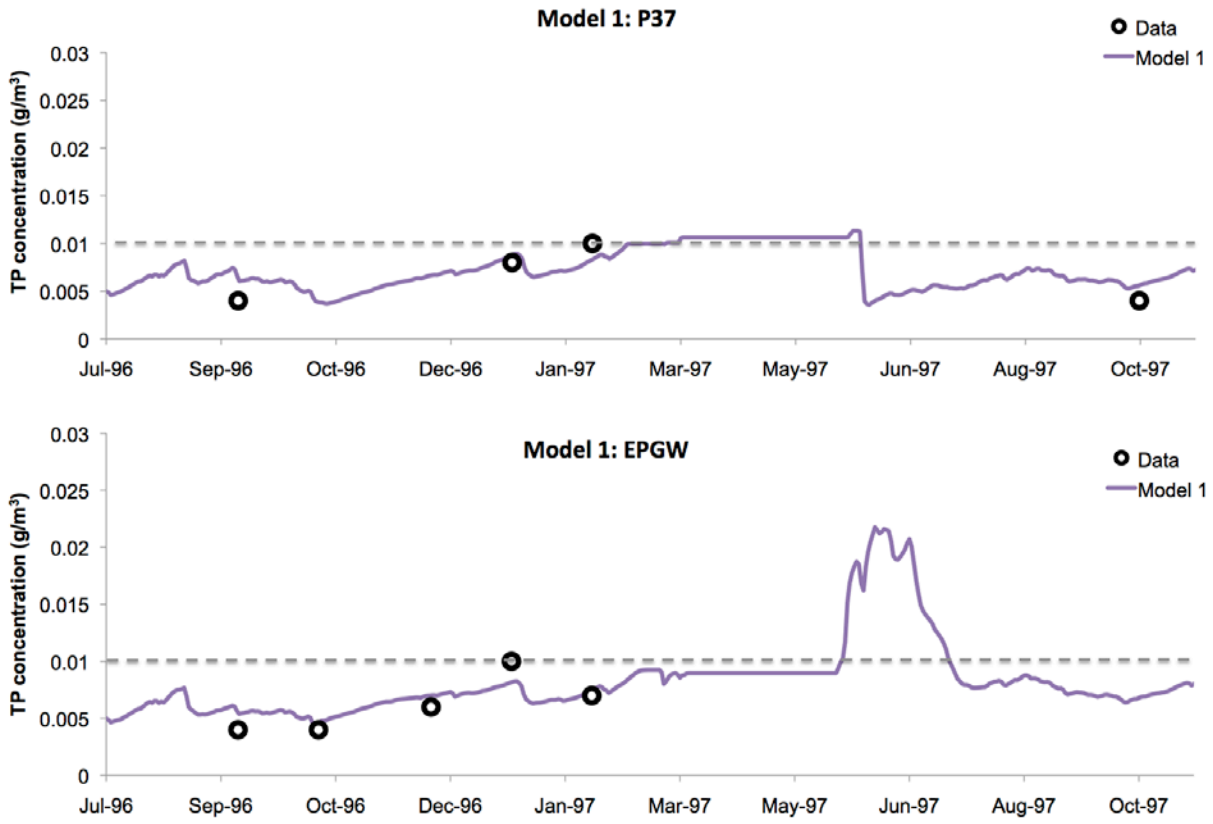

Figure 4-8. Simulated TP concentrations obtained with Model 1 at observation stations in Taylor Slough (P37) and C-111 wetlands (EPGW).

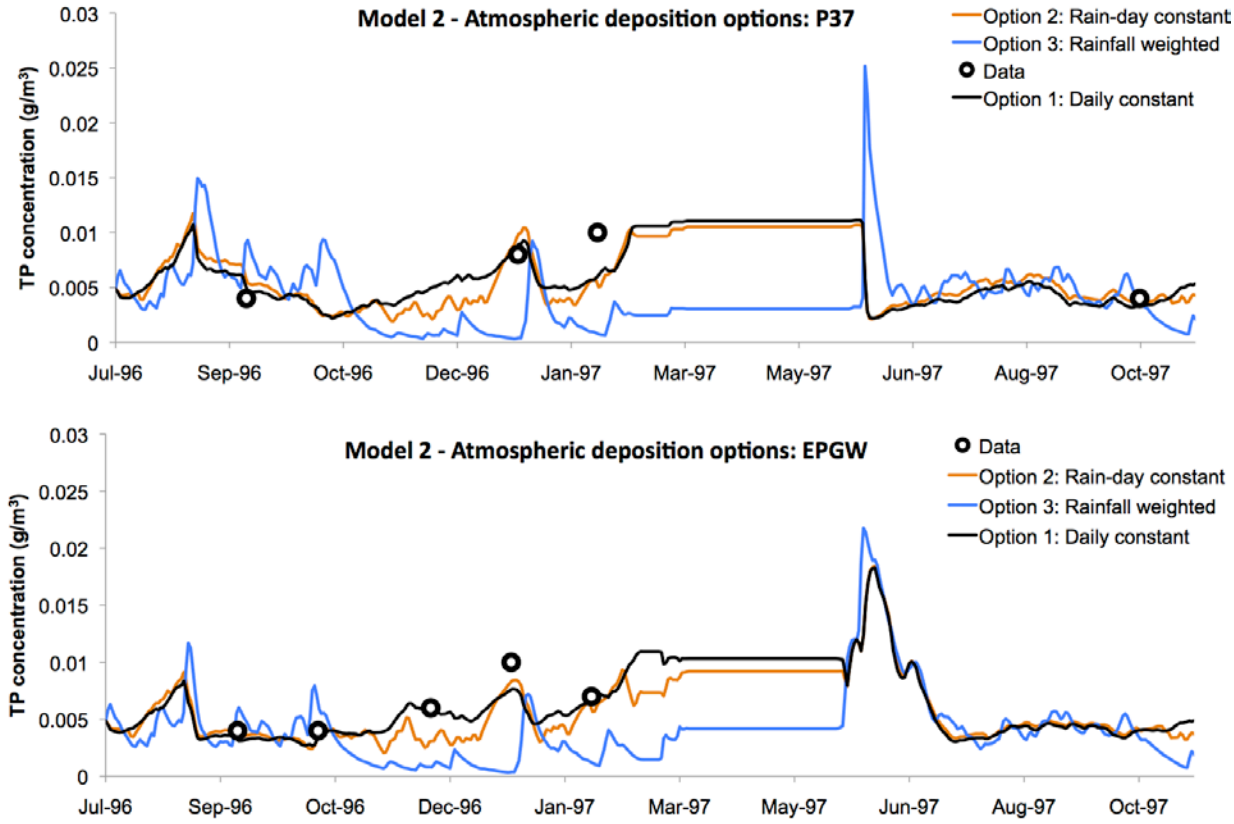

Figure 4-9. Simulated TP concentrations obtained with Model 2 for each of the atmospheric deposition options explored at observation stations in Taylor Slough (P37) and C-111 wetlands (EPGW).

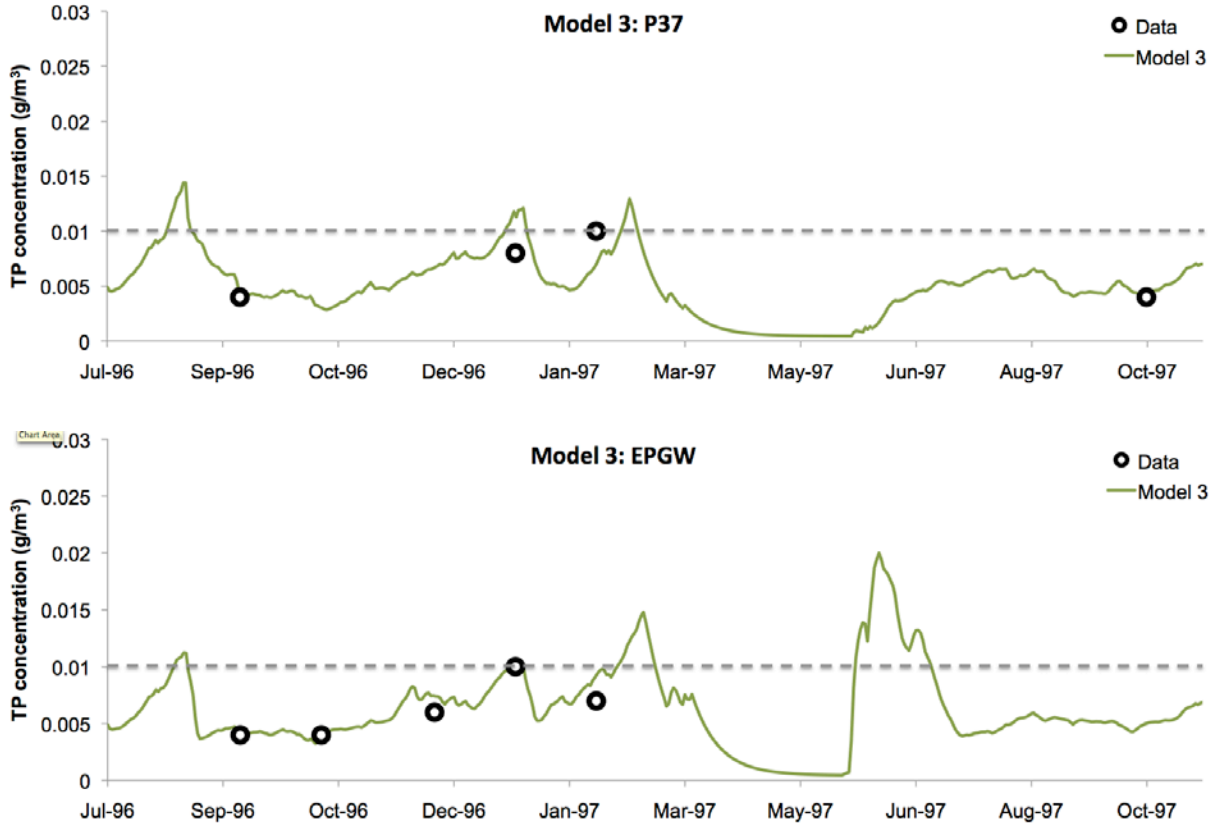

Figure 4-10. Simulated TP concentrations obtained with Model 3 at observation stations in Taylor Slough (P37) and C-111 wetlands (EPGW).

CHAPTER 5
UNRAVELING MODEL RELEVANCE: THE COMPLEXITY-UNCERTAINTY-SENSITIVITY TRILEMMA

Introduction

At its heart, our inability to truly simulate environmental (open) systems (Oreskes et al., 1994; Konikow and Bredehoeft, 1992) is due to our inability to reproduce their complexity. There are many reasons for this shortcoming: a lack of understanding in poorly studied systems or the inability to either conceptualize or reproduce the intricacies of well-studied systems; the inability of our instruments and methods to obtain true observations needed for parameterization and calibration due to measurement uncertainties and heterogeneities in space and time and scale; and the discontinuous nature of numerical solutions that imperfectly reproduce the continuity of reality. Such limitations prohibit true model validation (Oreskes et al., 1994). In lieu of confirming such validity, we strive instead for confidence in model results, which we consider by evaluating the extent of our doubt, as indicated by the degree of uncertainty associated with the generated results (Naylor and Finger,1967; Beven, 2006a). There is growing unease among developers and users of dynamic simulation models about the cumulative effects of various sources of uncertainty on model outputs, which inherit these underlying uncertainties (Manson, 2007 and 2008; Cressie et al., 2009; Messina et al., 2008). In particular, this issue has prompted doubt over whether the considerable effort going into further elaborating complex dynamic system modeling will in fact yield the expected payback, viz. new insights about the complicated systems they are intended to simulate (Ascough et al., 2008). The concern is that insufficient heed has been paid to the balance between investment (complexity) and return (uncertainty),

which was succinctly captured by Zadeh (1973), who first presented the notion of *relevance* as part of his “principle of incompatibility”:

> ... the conventional quantitative techniques of system analysis are intrinsically unsuited for dealing with humanistic systems or, for that matter, any system whose *complexity* [emphasis added] is comparable to that of humanistic systems [author’s note: e.g. environmental systems]. The basis for this contention rests on what might be called the "principle of incompatibility". Stated informally, the essence of this principle is that as the complexity of a system increases, our ability to make precise and yet significant statements about its behavior diminishes until a threshold is reached beyond which precision and significance (or *relevance* [emphasis added]) become almost mutually exclusive characteristics.

The relevance of a model is contingent on the balance between its power to address questions and the power of its answers. The former is dependent on model complexity – the degree of detail to which the real system is reproduced in the model structure. The latter is dependent on model uncertainty – the accuracy, precision and confidence associated with output results. Our failure to attend more closely to this balance is due largely to insufficient understanding of how complex models gain and lose relevance. Failure to advance this understanding has been at least in part due to the practical limitations associated with complex models. In particular, mechanistic environmental models are among the most complex, demanding specialized numerical code of spatially-distributed domains, numerous state variables, and a plethora of input parameters and data. Such complex tools are typically developed by specialists and, once complete, are not very amenable to adjustments in structure. The choice of complexity in such tools has therefore more commonly been the responsibility of model developers, while users simply have to deal with the consequences. Users do have a choice between potential tools of differing complexity, but that decision is still based on fixed choices, and is generally the product of a multitude of other considerations that

comprise what most modelers understand as the “art of modeling” (Getz, 1998; Basmadjian, 1999). We believe that suitable tools now exist to support controlled experimentation with model complexity, as well as more rigorous investigation into the consequences for uncertainty. Using such tools, we propose and demonstrate that meaningful new progress can be achieved toward unraveling the issue of relevance.

The Complexity-Uncertainty-Sensitivity Trilemma

To this point, we have used the term “uncertainty” to encompass various types of uncertainty, some quantifiable and some less so, which collectively contribute to the epistemic uncertainty in model results (that is, uncertainty associated with our knowledge about the state of a simulated system; Regan et al., 2002). To better investigate total epistemic uncertainty, it becomes necessary to distinguish between specific forms of uncertainty. The most commonly encountered form of uncertainty in modeling is error, which is a measure of model accuracy (i.e., the discrepancy between simulated results and observed data). Another prevalent form of uncertainty is that due to the uncertainties inherent to the values of input parameters, which are propagated through a model and onto the outputs and manifest as precision (i.e., the irreducible uncertainty in any model result that determines the range of possible values the actual result might inhabit). This is the sense of the word most commonly intended in the context of uncertainty analysis, and is the meaning adopted in all following sections unless specified otherwise. Other forms of uncertainty exist, most of which are difficult to assess because they are conceptually more qualitative, for example: uncertainty due to the underlying assumptions and structure of a model; uncertainty in the interpretation of voluminous and complicated results; and uncertainty in the validity of a model’s calibration due to model sensitivity. All are influenced by model complexity, but

sensitivity is particularly interesting in the context of investigating relevance. Methods of sensitivity analysis now exist to rigorously quantify sensitivity in such a way as to not only characterize the flexibility inherent to the model, and thereby the risk of overparameterization issues, but also to illuminate how the sensitivity is caused and possible ways for improving the precision of results (Saltelli et al., 2004). This feedback, linking sensitivity and uncertainty, completes a tripartite dialectic between complexity, uncertainty, and sensitivity – the relevance trilemma that guides this work.

Uncertainty

There is growing interest in evaluating the contributions of model inputs (uncertainty in data) and model structure (uncertainty from the simplifying assumptions necessary to abstract reality into model design and algorithms) to the overall uncertainty of model outputs (Beven and Binley, 1992; Beven, 1993; Draper, 1995; Cressie et al., 2009). However, the sources and magnitude of uncertainty and their effect on dynamic model outputs have not been comprehensively studied (Haan et al., 1995; Beven, 2006a; Shirmohammadi et al., 2006; Muñoz-Carpena et al., 2007; Valle et al., 2009). Uncertainty analyses endeavor to address this by propagating the various uncertainties onto a model output, and many methods exist to achieve this end (Haan, 1989; Shirmohammadi et al., 2006; Cressie et al., 2009). Systems that are better described and characterized (as physical systems such as hydrology tend to be) are more suitable for variance-based methods that apply Monte-Carlo simulations, such as the Generalized Likelihood Uncertainty Estimation method (GLUE; Beven and Binley, 1992). However, many systems (such as ecosystems) are poorly understood and modeler experience and subjectivity play an important role in their simulation. Uncertainty assessments that employ Bayesian methods are better suited to

incorporate subjectivities and are therefore often favored in such circumstances (Cressie et al., 2009). Merely quantifying the uncertainty in model outputs is insufficient to fully understand where and how the uncertainty is propagated or to understand the role of complexity. Sensitivity analysis can be used to determine how uncertainty in model outputs is apportioned to different sources of uncertainty in the model inputs (Saltelli et al., 2008). Whereas uncertainty analysis quantifies the overall uncertainty, sensitivity analysis identifies the key contributors to uncertainty; together they constitute a reliability assessment of a model (Scott, 1996).

Sensitivity

The sensitivity of a model output to a given input parameter has traditionally been expressed in terms of the derivative of the model output with respect to the input variation (Haan et al., 1995; Cariboni et al., 2007). Such sensitivity measurements are "local" because they are fixed to a point or narrow range where the derivative is taken. Local sensitivity indices are generally classified as "one-at-a-time" (OAT) methods, because they quantify the effect of varying a single parameter by altering only its value while holding all others fixed. Local OAT sensitivity indices are effective only if all factors in a model produce linear, direct responses in the output, or interest is in the model response under specific conditions (Saltelli et al., 2004). However, if changes produced in an output are non-linear, or parameters exhibit interaction effects on model output response, or an extensible assessment of sensitivity patterns is required, then a global sensitivity approach is needed (Leamer, 1990; Saltelli et al., 2004). Global sensitivity analyses (GSA) simultaneously vary all inputs and explore the entire parametric space of a model, thereby making no assumptions about linearity, additivity, or monotonicity. In complex models, the output response is often non-linear and non-

additive, so local OAT techniques are not appropriate, and global techniques should be used (Saltelli et al., 2004). Different GSA methods can be selected based on the objective and context of the analysis (Saltelli et al., 2000 and 2004; Cacuci, 2003).

Output sensitivity is inextricably tied to uncertainty, representing as it does the "paths of greatest influence" on the output (those parameters to which the output is most sensitive). An alternative perspective is that sensitivity represents the "paths of least resistance" through which input uncertainty will be propagated onto outputs during an uncertainty analysis. Sensitivity therefore plays an important role in another source of epistemic uncertainty: model overparameterization, which is variously captured in both forward and inverse solutions as non-identifiability, non-uniqueness, and equifinality (Brun et al., 2001; Omlin et al., 2001; Beven, 2006b; Ebel and Loague, 2006). Overparameterization issues are the result of too many degrees of freedom in a model due to the number of variable parameters. Each additional parameter introduces an additional source of influence over model outputs. This effect accumulates and can result in excessive flexibility in the model, which is counterproductive to parameterization and calibration efforts and can produce poorly defined calibrations or multiple irresolvable model characterizations (Beven, 2006a).

A poorly calibrated model, or one with a number of calibrated states that may be physically irreconcilable, undermines confidence in the model's projections. GSA methods uniquely capture the internal model relationships between input and output, as well as between different inputs. These can be used as indicators of a model's flexibility, and thereby the risk of non-identifiability and other overparameterization issues (Snowling and Kramer, 2001). Though it is an important and neglected (Luo et

al., 2009) source of epistemic uncertainty, sensitivity quantified in this form remains a qualitative measure of uncertainty. However, we can surmise that given sufficient complexity, uncertainty associated with a model's total sensitivity might be expected to reach a point that inhibits the model's relevance, overwhelming any gains in accuracy from added complexity in analogous fashion to Hanna's (1998) usual uncertainty suspects (Figure 5-2). The sensitivity of outputs to interactions between parameters is a key contributor to overparameterization, and total sensitivity measures that capture this effect are therefore a useful proxy for assessing the risk over over-sensitivity. By contrast, greater direct sensitivity implies stronger direct links between input and output, which is not only less likely to generate overparameterized conditions, but is also necessary for identifiability (Brun et al., 2001).

Complexity

Model complexity has proved challenging to quantify, or even define (Chwif et al., 2000). In a sense, complexity remains an abstract quality that can be assessed according to many factors, with no single definition proving useful for all contexts. However, when considering the structural complexity of a model, the number of parameters is generally considered a useful indication of relative complexity, since the number of parameters is tied to the number of processes included (Fisher et al., 2002). Incorporating the complexity of the equations themselves can be achieved using a Petersen matrix, which accounts for the number of mathematical operations (Snowling and Kramer, 2001). Subjective allocation of complexity "levels" can also be assigned based on users' knowledge of the number and nature of the processes included (Lindenschmidt et al., 2006). In this work, a simple measure of relative complexity is

sufficient, and thus distinct complexity levels were defined according to the number of parameters required.

Given the limitations inherent to simulating reality with simplified tools, it is not surprising that more complex models are pursued (Arthur, 1999; Beck, 1987). Models that are too simple may not capture important processes and cannot be proven to reproduce the measured data for the correct reasons (Nihoul, 1994). The complexity of a model fundamentally defines (and limits) the potential realities that can be reproduced. Environmental systems are particularly challenging to simulate, not only because they contain profound numbers of processes and constituents, but also because they can shift between alternate stable states, a complex emergent process (Scheffer, 2009). Such shifts can fundamentally change the nature of a system (i.e., the shift from an aquatic system dominated by algae to one dominated by macrophytes). Models that simulate ecological or biogeochemical systems like these within a physically dynamic environment, such as a hydrodynamic aquatic environment, are already highly complex. Yet, as we will show, failure to incorporate sufficient (additional) complexity can have important consequences for a model's ability to resolve certain simulated conditions.

The growing interest in optimizing model complexity relative to uncertainty (Cox et al., 2006; Lawrie and Hearne, 2007) is particularly pertinent today because of the growing availability of adaptable computational modeling tools, which give the user the freedom to define model structure, and thus complexity. Dynamic systems that can be conceptualized without a spatial domain have had such adaptable tools for many years, with systems such as STELLA finding application in a wide array of fields (Doerr, 1996).

Similar versatility has been pursued with GIS modeling tools (e.g., Wesseling et al., 1996). However, for the case of mechanistic, numerical models of complex environmental systems, with large, spatially-distributed domains and numerous state variables, the degree of model complexity has remained largely imposed on model users.

Nonetheless, the value and amount of specialist time required for such model development; the dramatic advances in computing capacity (Schaller, 1997) and data acquisition by remote sensing (Pohl & Van Genderen, 1998); and the economics of computer code reusability have compelled continued evolution of even the most complex models toward greater adaptability. Recently, Jawitz et al. (2008) developed a spatially-distributed numerical water-quality model, the Transport and Reactions Simulation Engine (TaRSE), with user-definable state variables and biogeochemical processes. To the authors' knowledge, this degree of control is novel in such a complex environmental model. Another driver of increased interest in the effects of model complexity is the development of multi-disciplinary integrated models that combine environmental and socio-economic drivers, sometimes through coupling of existing specialty models into a multi-modeling framework that can incorporate larger uncertainty than conventional models (Lindenschmidt et al., 2007).

Relevance dilemmas

Previous work has sought to begin the process of elucidating the relationships between complexity and various forms of epistemic uncertainty. Model complexity has been long recognized as having important consequences for output uncertainty. Hanna (1998) illustrated (Figure 5-1a) that increasing complexity by incorporating more state variables and processes can initially reduce uncertainty, but can have the opposite

effect after a certain critical point (Fisher et al., 2002). Greater complexity improves a model's conceptual rendition of reality, meaning the model has fewer simplifying assumptions and therefore less structural uncertainty. However, each additional process requires parameters to characterize the mathematics, and the uncertainty associated with each of these accumulates, eventually exceeding any gains. This makes identification of a potential "inflection point" important, for it reveals the optimal degree of complexity for modeling a system that incorporates sufficient detail to gain information while avoiding greater uncertainty and loss of relevance.

Snowling and Kramer (2001) proposed general relationships relating complexity and two forms of uncertainty: error and sensitivity (Figure 5-1b). The authors showed that as complexity was increased, model error decreased while model sensitivity increased. Snowling and Kramer based their hypothesis on the general concept that reduced structural error increased accuracy in analogous fashion to the reduction of uncertainty presented by Hanna. Conversely, sensitivity would increase because the additional parameters required to simulate the additional processes have some effect on the model outputs, and therefore represent additional degrees of freedom.

This hypothesis has since been supported by work in Lindenschmidt (2006) and Lindenschmidt et al. (2006). However, all corroborating results presented thus far (Snowling and Kramer, 2001; Lindenschmidt, 2006; Lindenshcmidt et al., 2006) are subject to limitations in generality, having been produced for limited ranges of parameter variation, centralized around calibrated applications, or based on local OAT sensitivity analyses. Furthermore, existing support for this hypothesis does not address how the nature of sensitivity changes with model complexity. Improving our

understanding of these dilemmas, between complexity and uncertainty, complexity and error, and complexity and sensitivity, is crucial to improving our understanding of relevance. However, it is also necessary that we acknowledge the links between such dilemmas, which further complicate the problem but cannot be ignored is we wish to address it. To this end we propose a trilemma, relating complexity, uncertainty, and sensitivity, as the first step toward a more integrated assessment of relevance.

The relevance trilemma

In this paper we propose the following relationships relating uncertainty, sensitivity, and model complexity, which together we believe represent a useful characterization for model relevance (Figure 5-2): 1) Total global sensitivity, being the net sum of all input effects on an output, increases with complexity due to the additive influence of additional parameters; 2) Interactions increase with increasing complexity (for the same reason), and will diminish the role of direct sensitivity as progressively more parameters interact to control the output and detract from the direct influence of individual parameters.

To test these hypotheses, we integrated a step-wise model-building approach using TaRSE, GSA and UA to investigate the role of complexity, and to better guide development across multiple levels of model complexity. Given doubt associated with model input factors, such as structural complexity and uncertainty input parameters, model development that is closely coupled to GSA and UA can reveal important unintended effects, not only in terms of model sensitivity and uncertainty, but also the capacity of a model to reproduce real, and complicated, system responses.

Materials and Methods

Global Sensitivity and Uncertainty Analysis Methods

Two state-of-the-art global sensitivity and uncertainty methods were used in this analysis: the qualitative method of Morris (1991) and a quantitative, variance-based method called the extended Fourier Amplitude Sensitivity Test (FAST; Saltelli, 1999). A brief summary of each method is given below (further details summarized by Muñoz-Carpena et al. (2007), and an in-depth treatment of the methods is provided in Saltelli et al., 2004).

The Morris (1991) method, extended by Campolongo and Saltelli (1997), is intended to elucidate qualitative global sensitivity, sacrificing quantification in lieu of dramatically improved computational demands. This method is therefore suitable for assessing the *relative* importance of input parameters, and for this reason it is an efficient screening method often used to filter out unimportant parameters before conducting the more computationally intensive, and quantitative, FAST analysis (Jawitz et al. 2008; Saltelli et al., 2005). The Morris method applies a frugal sampling technique to obtain unique sets of parameter values by varying each within their prescribed range and probability distribution. The multiple simulations then performed using these unique sets produce "elementary effects" in the outputs, attributable to changes in each input parameter, the absolute values of which are averaged to produce a qualitative global sensitivity statistic, μ^*. The magnitude of μ^* indicates the relative order of importance for each parameter with respect to the model output of interest (Campolongo et al., 2007). The standard deviation of the elementary effects, σ, can be used as a statistic indicating the extent of interactions between inputs. A higher σ implies variability in the elementary effects attributed to a particular parameter. Since the values of all other

tested parameters are simultaneously varied, this variability implies that the observed effect is dependent on the values held by other varied parameters (the parametric context), and thus interaction effects between them. Conversely, an invariant μ* implies that interactions between parameters do not affect the parameter's influence on the output, and that the output is therefore directly sensitive to it. For each output of interest, pairs of (μ*i, σi) for each input parameter can be plotted in a Cartesian plane to indicate the relative importance of each output (distance from the origin on the X-axis), and the prevalence of interaction effects (distance from the origin on the Y-axis).

The variance-based extended FAST method provides a *quantitative* measure of the direct sensitivity of a model output to each parameter, using what is termed a first-order sensitivity index, Si, defined as the fraction of the total output variance attributable to a single input parameter (i). In the rare case of an additive model, where the total output variance is explained as a summation of individual variances introduced by varying each parameter alone, $\Sigma S_i = 1$. Such additivity is a requisite condition if *local* sensitivity analysis results are to be generally applied to a model (Saltelli et al., 2004). Given that even relatively simple models rarely meet this requirement, the application of *global* sensitivity methods should be the preferred approach. In addition to the calculation of first-order indices, the extended FAST method (Saltelli, 1999) calculates the sum of the first- and all higher-order indices for a given input parameter (i), called the total sensitivity index (ST_i), (Equation 5-1),

$$S_{Ti} = S_i + S_{ij} + S_{ijk} \ldots + S_{i \ldots n}, \tag{5-1}$$

where S_i is the first-order (direct) sensitivity, S_{ij} is the second-order indirect sensitivity due to interactions between parameters *i* and *j*, S_{ijk} the third-order effects to due to interactions between *i* and *k* via *j*, and so forth to the final varied parameter, *n*.

Based on Equation 5-1, total interaction effects can then be determined by calculating $S_{Ti} - S_i$. It is interesting to note that μ* of the Morris (1991) method is a close estimate to the total sensitivity index (S_{Ti}) (Campolongo et al., 2007). Since the extended FAST method applies a randomized sampling procedure, it provides an extensive set of outputs that can then be used in the global uncertainty analysis of the model. Thus, probability distribution functions (PDFs), cumulative probability distribution functions (CDFs), and percentile statistics can be derived for each output of interest with no further simulations required.

In general, the analysis procedure followed six main steps: (1) PDFs were constructed for uncertain input parameters; (2) input sets were generated by sampling the multivariate input distribution according to the selected global method; (3) model simulations were executed for each input set; (4) global sensitivity analysis was performed according to first the Morris method and then 5) the extended FAST method; and (6) uncertainty was assessed based on the outputs from the extended FAST simulations by constructing PDFs and statistics of calculated uncertainty. The free software Simlab (Saltelli et al., 2004; http://simlab.jrc.ec.europa.eu/) was used for multivariate sampling of the input parameters and post-processing of the model outputs. Sample sets were created for all the parameters in each of the complexity levels tested (see subsequent section and Figure 5-3) and for both methods, resulting in a total of six sets of analyses. The number of model runs was selected based on the number of

parameters in each complexity level according to Saltelli et al. (2004). A total of 1,170 simulations were conducted for the Morris method and 45,046 simulations for the extended FAST method.

Model Description, Application, and Selection of Complexity Levels

Model description: TaRSE

A water-quality numerical modeling framework, the Transport and Reactions Simulation Engine (TaRSE), has been developed to simulate the biogeochemistry and transport of phosphorus in the Everglades wetlands of south Florida (Jawitz et al., 2008; James et al., 2009). The US$10 billion Comprehensive Everglades Restoration Plan (CERP) is the largest ecosystem restoration effort in the world, and aims to restore historic flows and P levels to the ecosystem. The freshwater wetlands of the Everglades have evolved under phosphorus-scarce nutrient conditions and are especially sensitive to labile phosphorus in the surface-water (Munsen et al., 2002; Noe et al., 2003). An important component of CERP therefore entails modeling the water-quality with respect to phosphorus levels, and TaRSE was developed to meet this need.

The design of TaRSE is comprised of two functional modules; one that simulates the advective and dispersive movement of solutes and suspended particulates in flowing water (the "Transport" module; James et al., 2009), and one that simulates the transfer and transformation of phosphorus between biogeochemical components (the "Reactions" module) (Jawitz et al., 2008). The term "Simulation Engine" refers to the generic nature of the reactions module, which has been designed such that the user is responsible for specifying (in XML input files) the model's state variables and the equations relating them. State variables cam be grouped in conceptual stores, such as surface-water or soil, and are classified as "mobile" if they are to be transported or

"stabile" if they are not. Thus, even though the inaugural implementation of TaRSE was intended for phosphorus-related water-quality modeling, this variable structure means it can be easily adapted for different applications. The user selects from a suite of equations to describe exchanges between state variables, including zeroth-order, first-order, Michelis-Mentin growth and decay, sorption-desorption kinetics and rule-based relations (Jawitz et al., 2008). When applied in a hydrodynamic environment, TaRSE requires that necessary hydrologic state variables, such as stage and velocity, be provided by a coupled hydrologic model. TaRSE employs a triangular mesh to discretize the spatial domain for the Godunov-mixed finite element transport algorithm (James, et el., 2009), but the reactions module is independent of mesh geometry. Once the reactions have been simulated and mobile quantities updated within each cell, they are transported.

Model application

This effort to study the effects of increasing model complexity was carried out as part of a comprehensive testing process during the development of TaRSE. In addition to the necessary quality control provided by sensitivity and uncertainty analyses, the intention of this analysis was to study potential consequences resulting from the novel freedom afforded by TaRSE's flexible design (i.e., user-defined complexity). In order to isolate the effects of complexity, an artificial domain was created in which the sources of variability extrinsic to complexity could be controlled and excluded. A 1,000 × 200-m generic flow domain (Figure 5-3) was created and discretized into 160 equal rectangular triangles (cells). Flow was set from left to right so that the inflow boundary consisted of cells 1, 41, 81, and 122, and the outflow boundary consisted of cells 40, 80, 120, and 160. A no-flow boundary was applied to the top and bottom (longer) edges of the

domain. To exclude the effects of transient flow, steady-state velocity was established, and the effect of heterogeneities were managed by assuming spatially homogeneous conditions. A constant velocity of 500 m/d was established to approximate Everglades flow conditions (Leonard et al., 2006) with an average water depth of 1.0 m. Simulations were run for 30 days with a 3-hour time-step.

Levels of complexity

Three models of increasing complexity were created (Figure 5-4a-c). Following the recommendations of Chwif et al. (2000), complexity was progressively added to the model in an organized and step-wise fashion. Each new complexity level corresponded to the addition of one new state variable and the associated processes relating the variable to the pre-existing system. The simplest case (Level 1) contained no biotic components (Figure 5-4a). The intermediate-complexity case (Level 2) contained surface-water biota in the form phytoplankton (Figure 5-4b). The most complex case (Level 3) contained additional macrophytes rooted in the soil (Figure 5-4c). Table 2-1 lists the state variables and processes that appeared in each complexity level, including the boundary conditions for the mobile state variables (always quantified in g/m^3), viz. soluble reactive phosphorus (SRP) in the surface-water (C_{sw}^{P}) and plankton biomass (C_{pl}). Initial conditions for the stabile state variables (always quantified in g/m^2), viz. SRP in the porewater, adsorbed phosphorus, macrophyte biomass, and organic soil mass, were 0.05, 0.027, 500, and 30,000 g/m^2, respectively. Boundary and initial conditions were selected to represent reasonable Everglades conditions based on values cited in the extensive literature review conducted as part of parameterization effort required for the sensitivity analyses (see following section). For full details of the model equations and numerical solutions see Jawitz et al. (2008).

Parameterization of Inputs Across Complexity Levels

The application of TaRSE was done without prior calibration in order to avoid limiting the potential range of physical conditions the model might be applied to, and through which the effects of new complexity would be expressed. This also facilitated testing of the model across a wide range of possible scenarios as a necessary step in the development process prior to evaluation of its performance for a particular application (Saltelli et al., 2000). Results from the GSA and UA were evaluated to ensure that simulation results were consistent with the conceptual models and that unreasonable results did not emerge (see Jawitz et al., 2008 for extensive details). Before conducting a GSA or UA it is necessary to specify a range and distribution for each parameter, from which values can be statistically sampled.

The field-scale ambient variability of many inputs has been reported to be adequately modeled with log-normal or Gaussian distributions (Jury et al. 1991; Haan et al. 1998; Limpert et al. 2001; Loáiciga et al. 2006). When there is a lack of data to estimate the mean and standard deviation for such PDFs, the (beta) β-distribution can be used as an acceptable approximation (Wyss and Jørgensen 1998). When only the range and a base (effective) value are known, a simple triangular distribution can be used (Kotz and van Dorp 2004). Finally, a uniform distribution is recommended in cases where values are assumed equally distributed along the entire parametric range.

The input parameters used in the analysis of TaRSE (Table 5-2) were assigned ranges and probability distributions based on an extensive literature review found in Jawitz et al. (2008). Since the goal of this work was a general model investigation, and not a specific study of its application to a particular site, parameter ranges were selected to cover all physically realistic values for the intended target region (the

Everglades). Given the wide range of physical and ecological conditions that the data from such an all-encompassing approach include, and considering that values were derived from relevant literature rather than directly from sets of data, the more general β-distribution was adopted. Consequently, all biogeochemical parameters (i.e., excluding transverse and longitudinal dispersivity) were described using β-distributions. Dispersivity is related to the composition of the physical system, such as for example vegetation density, domain dimensions, and velocity. These characteristics are contingent on the site selection, rather than natural variation, and their probability was therefore considered to be random, and accordingly allocated a uniform distribution (Jawitz et al., 2008).

Several outputs were defined for the analysis, accounting for each of the model's state variables at each complexity level, and described in Table 5-1. In the context of this work to investigate the role of complexity, only those outputs that appear in all three complexity levels permit comparison and are presented. Outputs were defined to integrate both spatial and temporal effects. For outputs of mobile quantities, averages across the outflow domain (cells 40, 80, 120, and 160) were calculated at the end of the simulation period in order to integrate the effects of transport parameters and processes across the entire domain into the output. For stabile quantities, outputs were expressed as the difference between the initial and final value of averages across the entire domain.

Given the constancy of conditions applied to the model across all complexity levels through fixed parameter ranges and distributions; invariant scale, initial, and boundary

conditions; and steady hydrodynamics, any changes observed in the uncertainty and sensitivity are attributed to the effects of changes in model complexity.

Results and Discussion

Effects of Model Complexity on Sensitivity

Morris method

Figures 5-5a-c depict trends in the results from the Morris method analysis for soluble reactive phosphorus (SRP) in the surface-water, C_{sw}^{P}. This output is generally considered to be of greatest interest in management of water-quality for CERP (Perry, 2008), and is the official water-quality restoration target mandated by Congress (Sheikh and Carter, 2005). Immediately apparent is that the relative location of parameters in the μ^*-σ plane changed as the complexity increased. At lower complexities (Levels 1 and 2) inputs were found closer to the μ^*-axis, almost never approaching, and never exceeding, the 1:1 line. At Level 3 the parameters were generally above the 1:1 (shaded triangle in each graph) and associated with proportionally larger σ-values. Higher σ-values denote a greater role for interactions among input parameters. As the complexity increased, more parameters were drawn out into the μ^*-σ plane, particularly at Level 3. Since important parameters (i.e., those to which C_{sw}^{P} is most sensitive) are distinguished from unimportant ones by their relative distance from the origin, these results indicate that more parameters became relatively important as complexity increased. Conversely, fewer parameters were uniquely important in the more complex model. This trend is generalized in Figure 5-5d, a novel presentation of Morris method results that takes advantage of the geometry inherent to their interpretation. Multiple outputs were plotted collectively (C_{sw}^{P}, C_{pw}^{P}, S^{o}, and S^{P}) by normalizing the points to

conserve their relative Cartesian positions, and grouping them by complexity level for comparison. The same patterns observed in the C_{sw}^{P} results are exhibited by all the outputs lumped together in this way.

These results are in agreement with our hypothesis that as complexity increases, an increase in interactions is associated with a decrease in direct effects. The sensitivity of C_{sw}^{P} to different parameters at different complexities shows the changing role of certain parameters as others are added. In Level 1, the stabile parameters k_{ox}, k_{df}, ρ_b and X_{so} (oxidation rate, coefficient of diffusion, soil bulk density, and the soil phosphorus mass fraction, respectively) were the most important. In Level 2, plankton in the water column was added to the model, and parameters associated with plankton growth (k_g^{pl} and $k_{1/2}^{pl}$; plankton growth rate and plankton phosphorus half-saturation constant, respectively) became the most important to C_{sw}^{P}. With the addition of macrophytes in Level 3, it became difficult to separate obviously important parameters. Instead, the model became comparably sensitive to many parameters because of the increased role of interactions.

Extended FAST

Quantitative results for C_{sw}^{P} from the extended FAST analysis (Figs. 5-6a-h) corroborate the qualitative Morris method results. The percentage of total variance (Figure 5-6a) attributable to direct (first-order) effects (S_i) decreased with increasing complexity, slowly from Level 1 to 2, then rapidly from Level 2 to 3. The same trends were exhibited by C_{pw}^{P}, S^{o}, S^{P} (Figure 5-6b-d). Conversely, interaction effects (Figure 5-6a-d) rose slowly from Level 1 to 2, then rapidly from Level 2 to 3. These trends were consistent across all model outputs and provide further quantitative evidence in support

of the hypothesized sensitivity-complexity relationship, as posited by Snowling and Kramer (2001) and extended globally herein.

In Level 1, the sensitivity of C_{sw}^{P} to parameters associated with stabile state variables was limited by the coefficient of diffusion (see Figure 5-3a), because diffusion was the physical link between mobile surface-water and stabile subsurface state variables. In Level 2, the total sensitivity (Figure 5-6e) of C_{sw}^{P} increased because the addition of plankton introduced a number of parameters that could affect C_{sw}^{P} without first being channeled through, and thus dampened by, the slow process of diffusion. By contrast, the Level 2 sensitivity of stabile outputs (C_{pw}^{P}, S^{o} and S^{P}) to parameters more closely associated with either of the mobile state variables (C_{sw}^{P} or C^{pl}) remained mitigated by the diffusion rate (Fig 5-6f-h). This changed in Level 3, however, where the addition of macrophytes introduced new parameters to the subsurface. At this level of complexity, macrophytes represented a phosphorus-sink dominant enough to make all outputs sensitive to even those parameters whose influence was dampened by the slow rate of diffusion. Consequently, we see a consistent trend across all outputs of decreasing direct effects, and increasing interactions and total sensitivity. These results indicate that the system was more sensitive to the addition of macrophytes than to plankton. Furthermore, when viewed in conjunction with our understanding of the physical description of the system, they allow us to understand how the model's internal dynamics, expressed as output sensitivities, are shifting with increasing complexity.

Effects of Model Complexity on Uncertainty

Some of the uncertainty results (Figs. 5-6e-h), presented here using the 95% confidence interval, seem to question the conceptual trends in Hanna (1988) (Figure 5-1a), indicating that these relationships may not be as simple as proposed. In fact, this is

explainable by accounting for the fact that some outputs are integrative, in that all system components can participate in producing their final outcome, whereas others have inherent biases that inhibit such integration. The key output, C_{sw}^{P}, is an example of an integrative output, since it is subject to the influence of all other state variables, and the expected reduction of uncertainty holds. By comparison, accreted organic soil (S^{o}), which is defined in terms of mass that is several orders of magnitude larger than any other outputs, is not subject to comparable influence by other model components, and is therefore not integrative. Mechanistically, this discrepancy is due to the relative influence of turnover rates for the component compared with the fluxes into and out of the store.

The consistent increase in uncertainty exhibited by S^{o} (Figure 5-6f) therefore does not follow the conceptual trend. Interestingly, in Level 2 we saw that the stabile outputs closely associated with S^{o} (C_{pw}^{P} and S^{P}, which we might expect to be more integrated), followed the S^{o} trend and became more uncertain. This corresponds well with the physics of the model for that level, however; addition of phosphorus through oxidation is the predominant contributor to C_{pw}^{P}, to which S^{P} is in turn bound through equilibrium adsorption-desorption kinetics. Thus, their uncertainties *should* in fact be coupled with that of S^{o}. This demonstrates that the uncertainty effects in poorly integrated outputs can be passed onto related outputs, effectively dis-integrating them. With the introduction of macrophytes in Level 3, the effect of S^{o} on C_{pw}^{P} and S^{P} was broken by the addition of a major new sink for phosphorus released through oxidation of the organic soil, the process that physically linked the three outputs. The previously affected outputs in turn became more integrated, and we see their uncertainty drop as

originally expected (Figure 5-6h). It is therefore important to consider that outputs can be effectively dis-integrated, and therefore may not receive the consequences of increasing complexity in the same way. Similarly, outputs may not be affected by added complexity in other parts of the model.

Figures 5-7a-c depict the progression of output PDFs across complexity levels for the same key output, C_{sw}^{P}, from a simpler leptokurtic distribution at the lowest complexity level (represented by the lowest number of input parameters, eight), through the platykurtic distribution at the intermediate level (12 parameters), to a bimodal distribution at the highest complexity (16 parameters). The latter results represent different system states, combining the further platykurtic nature of the Level 2 stable-state, with a strongly leptokurtic end-point that corresponds to combinations of parameter values that push the simulation out of the original stable-state. In this case, the alternate state appears as a single value, and indicates that the complexity at this level was sufficient to capture the existence of a second state, but insufficient to capture any variability within the state.

Mechanistically, the presence of this second state demonstrates that a critical threshold existed for the state previously simulated as Level 2. Its presence was caused by combinations of parameter values working in conjunction with initial and boundary conditions, which resulted in the systemic depletion of the biotic components (plankton and macrophytes). This occurred because the range of values over which the parameters were varied was held constant across complexity levels, yet included values appropriate for both of the known stable-states that shallow water bodies can exhibit in the Everglades (Scheffer, 1990; Scheffer et al. 1993; Beisner et al., 2003;), namely

algae- and macrophyte-dominated systems (Bays et al. 2001; Cichra et al. 1995). Testing the full range of plankton-dominated conditions in Level 2 presented no problems to the model because the structure was mechanistically appropriate – there were no macrophytes. However, the incorporation of macrophytes into the model structure changed the definition of the simulated ecosystem, and without the necessary feedback mechanisms (i.e., complexity) in place to resolve the extreme conditions produced by unrealistic combinations of parameter values, phytoplankton biomass is all but eliminated. Without this surface-water sink for phosphorus, C_{sw}^{P} continuously input at the boundary remained essentially unchanged in these cases, depicted by the spike in outflow values matching the boundary concentration of 0.05 g/m^3 (Figure 5-7c) The platykurtic area represents model conditions under which the simulated system is not catastrophically overwhelmed. The results therefore mimic those of Level 2, where macrophytes were absent and phytoplankton dominated the surface-water phosphorus dynamics. It is noteworthy that the introduction of macrophytes still acts as a phosphorus sink in these cases, stressing the phytoplankton in terms of phosphorus availability and thereby dampening the frequency of lower C_{sw}^{P} values (a sign of greater phosphorus uptake due to growing plankton). Macrophytes also prevent the majority of C_{sw}^{P} results from exceeding the boundary input concentration (which can only occur when significant diffusion takes place due to high C_{pw}^{P}, as in Level 2, and as was never the case for Level 3 because of porewater SRP uptake by the macrophytes (Jawitz et al. 2008).

In this way, the addition of macrophytes to the set of tested model conditions represented the introduction of an alternate stable-state that could not be resolved. The

complexity was insufficient to permit the model to simulate a shift between stable-states, but (in conjunction with the parameter ranges tested for) was sufficient to simulate the existence of a second stable-state. Though these results express emergent characteristics of the simulated systems under the tested conditions, the forcing "functions" in this case (being the variously sampled parameter sets) are based on real values (albeit not necessarily real combinations of values) and therefore represent potential realities that match well with the known biotic states of the Everglades: mixed algae-macrophyte (the hump in Figure 5-7c) and macrophyte-dominated (the spike). Given the absence of any suitable feedback in the tested model's mechanisms that might permit plankton to dominate macrophytes, such a stable state is impossible to simulate. The emergence of alternate stable-states in the results only occurs once complexity has reached Level 3, clearly indicating that additional model complexity is required to capture the complicated, but real, behavior of the system.

Conclusions

Presented results have corroborated the sensitivity-complexity relationship, proposed by Snowling and Kramer (2001), using true global sensitivity methods and over a wide range of model conditions, thereby demonstrating the validity of the relationship in the most general context yet. We have also demonstrated that our hypotheses relating the global sensitivity indices for direct effects, interactions, and total sensitivity to model complexity are valid, providing a fresh global perspective to the relevance trilemma.

The combined GSA and UA framework applied herein produced valuable insights for interpreting both the meaning of the model results, and the meaning of how they were generated in the context of model relevance. This methodology is therefore

proposed as a useful way to glean insights into the external and internal dimensions of model performance.

The combined GSA and UA results presented indicate that uncertainty, on average, decreases with complexity, and that total sensitivity increases. This implies that we are still within the region of the trilemma space (Figure 5-2) that encourages us to persist with increasing complexity if so desired. These results emerged from an exploration of parametric spaces far larger than would be expected for any application to a specific site, and therefore constitute a worst-case-scenario, which is thus cause for further optimism. It is therefore reasonable to expect that refinement to a particular application will reduce uncertainty further and permit additional complexity without loss of relevance.

Given the benefits derived from the GSA/UA methods, it is proposed that these methods constitute a valuable framework (Figure 5-8) for exploring the Relevance Trilemma. In applying it herein, we gained useful information about the tested versions of TaRSE, including important considerations valuable to future work, such as the sensitivity of outputs to particular parameters, the strong effects caused by introducing macrophytes, and the importance of considering integration in output definitions. The sensitivity of the model to the addition of macrophytes calls for close attention to the associated initial conditions and parametric ranges. The emergence of alternate stable states in Level 3 results, and their absence in simpler levels, demonstrates the need for some minimal complexity if such real world patterns are to be reproduced in simulations, and highlights the unexpected potential for such patterns in the output response of even a relatively coarse biogeochemical model. Importantly, these

methods also provide insights into how one might reduce model uncertainty (Saltelli et al., 2004) by identifying important and unimportant parameters and processes. This information can be used to guide efforts to better measure important parameters or remove ineffectual complexity.

Important questions remain after the analyses presented here. Does Level 3 represent the optimum system description? Can this optimum be determined? Although answers to these questions fall, at least in part, into the subjective realm of the "art of modeling," the tools presented here offer the modeler an opportunity to better understand the sometimes unexpected tradeoffs introduced by increasing model complexity. We suggest that today we are in a better position to unravel the relevance trilemma, and indeed even to actively incorporate it into our art, than when Zadeh (1973) first presented his principle of incompatibility.

Table 5-1. Process description for the increasing levels of complexity studied

Process	Levels	Key, fig5-2	Affected variables	Process equation
Diffusion	1, 2, 3	1	Surface-water SRP concentration (mobile), C_{sw}^{P} (g/m^3) Soil porewater SRP concentration (stabile), C_{pw}^{P} (g/m^2)	$\frac{dC_{sw}^{P}}{dt} = \frac{k_{df}}{z_w z_{df}}\left(C_{pw}^{P} - C_{sw}^{P}\right)$
Sorption-desorption	1, 2, 3	2	Soil porewater SRP concentration (stabile), C_{pw}^{P} (g/m^2) Soil adsorbed P mass (stabile), S^{P} (g/m^2)	$\frac{dS^{P}}{dt} = \frac{\rho_b k_d}{\theta}\frac{dC_{pw}^{P}}{dt}$
Oxidation of organic soil	1, 2, 3	3	Soil porewater SRP concentration (stabile), C_{pw}^{P} (g/m^2) Organic soil mass (stabile), S^{o} (g/m^2)	$\frac{dS^{o}}{dt} = -k_{ox}S^{o}$
Inflow/outflow of surface-water SRP	1, 2, 3	4	Surface-water SRP concentration (mobile), C_{sw}^{P} (g/m^3)	BC: C_{sw}^{P} = 0.05 g/m^3
Uptake of SRP through plankton growth	2, 3	5	Surface-water SRP concentration (mobile), C_{sw}^{P} (g/m^3) Plankton biomass concentration (mobile), C^{pl} (g/m^3)	$\frac{dC^{pl}}{dt} = -k_g^{pl}C^{pl}\left(\frac{C_{sw}^{P}}{C_{sw}^{P} + k_{1/2}^{pl}}\right)$
Settling of plankton	2, 3	6	Plankton biomass concentration (mobile), C^{pl} (g/m^3) Organic soil mass (stabile), S^{o} (g/m^2)	$\frac{dC_{sw}^{pl}}{dt} = -k_{st}^{pl}C^{pl}$
Inflow/outflow of suspended particulates (plankton)	2, 3	7	Plankton biomass concentration (mobile), C^{pl} (g/m^3)	BC: C^{pl} = 0.043 g/m^3
Uptake of porewater SRP through macrophyte growth	3	8	Soil porewater SRP concentration (stabile), C_{pw}^{P} (g/m^2) Macrophyte biomass (stabile), C^{mp} (g/m^2)	$\frac{dC^{mp}}{dt} = -k_g^{mp}C^{mp}\left(\frac{C_{pw}^{P}}{C_{pw}^{P} + z_{as}\theta k_{1/2}^{mp}}\right)$
Senescence and deposition of macrophytes	3	9	Macrophyte biomass (stabile), C^{mp} (g/m^2) Organic soil mass (stabile), S^{o} (g/m^2)	$\frac{dC^{mp}}{dt} = -k_{sn}C^{mp}$

Table 5-2. Probability distributions of model input factors used in the global sensitivity and uncertainty analysis

Parameter definition	Symbol	Process in Fig5-4	Distribution	Units	Input present in		
					L1	L2	L3
Coefficient of diffusion	k_{df}	1	β (7×10^{-10}, 4×10^{-9})	m^2/s	x	x	x
Coefficient of adsorption	k_d	2	β (8×10^{-6}, 11×10^{-6})	m^3/g	x	x	x
Soil porosity	θ	2	β (.7, 0.98)	-	x	x	x
Soil bulk density	ρ_b	2	β (.05, 0.5)	-	x	x	x
Soil oxidation rate	k_{ox}	3	β (.0001, 0.0015)	1/d	x	x	x
P mass fraction in organic soil	X_{so}^{P}	3	β (.0006, 0.0025)	-	x	x	x
Longitudinal dispersivity	λ_l	4	U (70, 270)	m	x	x	x
Transverse dispersivity	λ_t	4	U (70, 270)	m	x	x	x
Plankton growth rate	k_g^{pl}	5	β (.2, 2.5)	1/d		x	x
Plankton half saturation constant	$k_{1/2}^{pl}$	5	β (.005, 0.08)	g/m^3		x	x
Plankton settling rate	k_{st}^{pl}	6	β (2.3×10^{-7}, 5.8×10^{-6})	m/s		x	x
P mass fraction in plankton	X_{pl}^{P}	6	β (.0008, 0.015)	-		x	x
Macrophyte growth rate	k_g^{mp}	8	β (.004, 0.17)	1/d			x
Macrophyte half saturation constant	$k_{1/2}^{mp}$	8	β (.001, 0.01)	g/m^3			x
Macrophyte senescence rate	k_{sn}^{mp}	9	β (.001, 0.05)	1/d			x
P mass fraction in macrophytes	X_{mp}^{P}	9	β (.0002, 0.005)	-			x

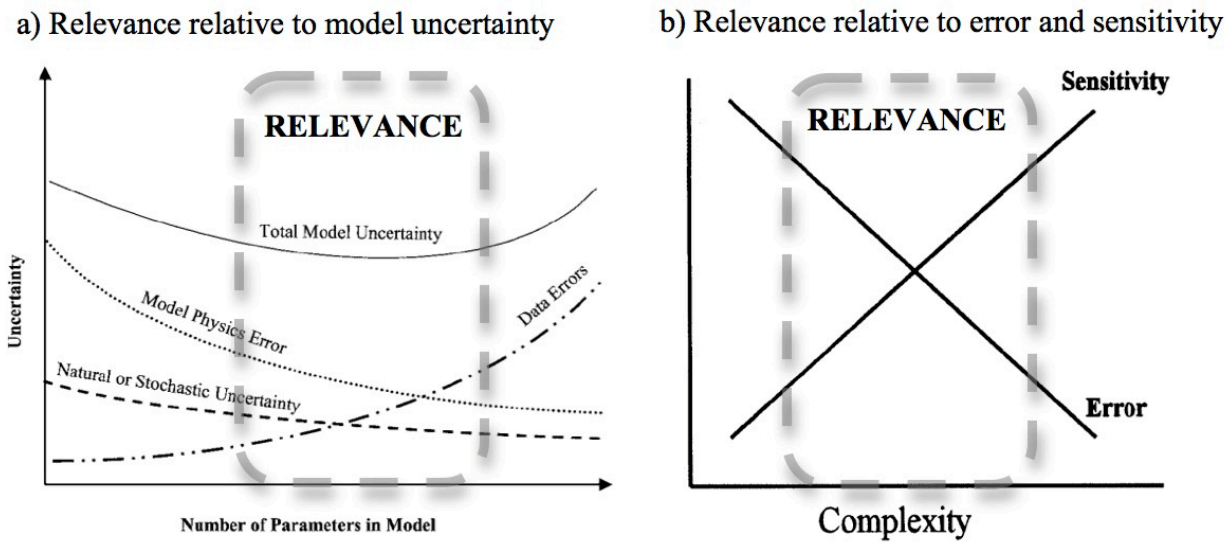

Figure 5-1. Relevance relative to a) sources of modeling uncertainty in relation to model complexity (Hanna, 1988 as cited in Fisher et al., 2002), and b) Snowling and Kramer's (2001) hypothesis relating error and sensitivity to model complexity.

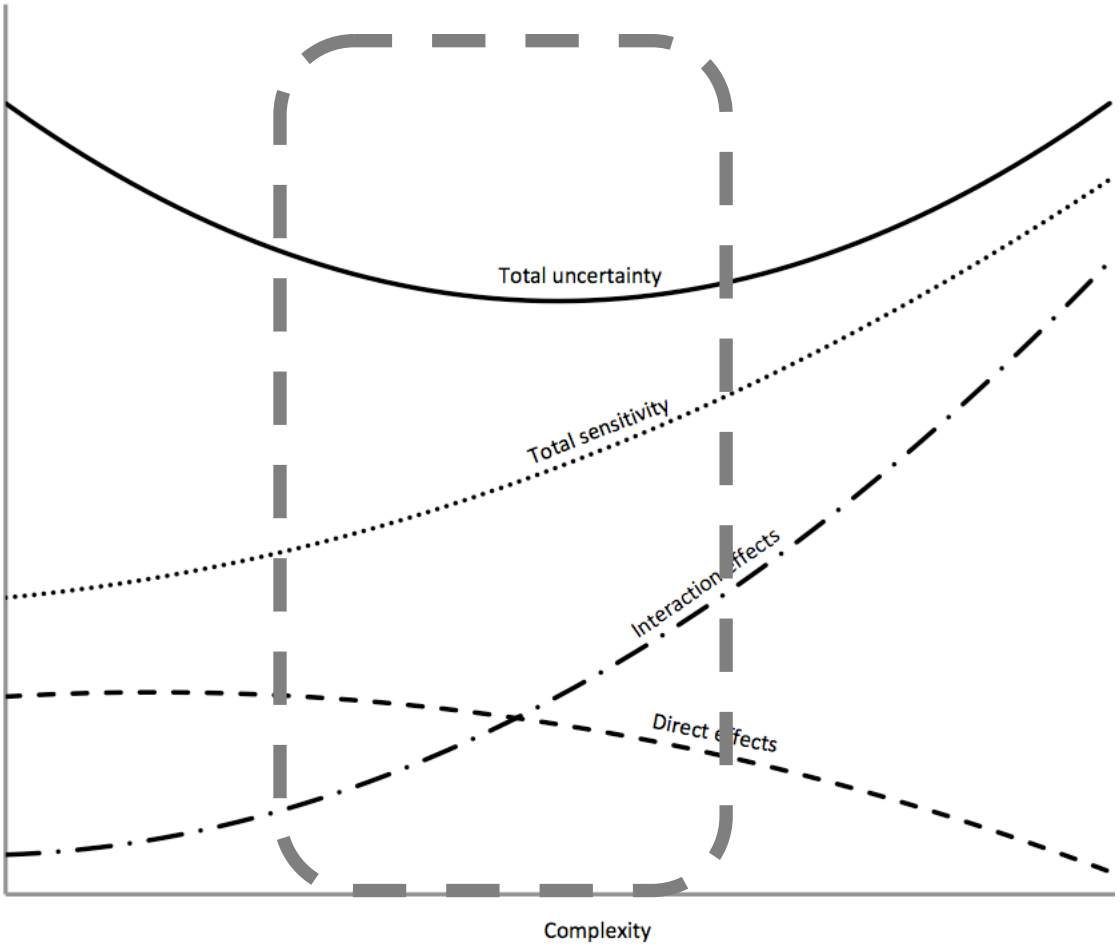

Figure 5-2. Hypothesized trends relating complexity to sensitivity from direct effects, sensitivity from interactions, and total sensitivity. Total uncertainty still follows the trends of Hanna (1988) but now includes total sensitivity as another source of uncertainty.

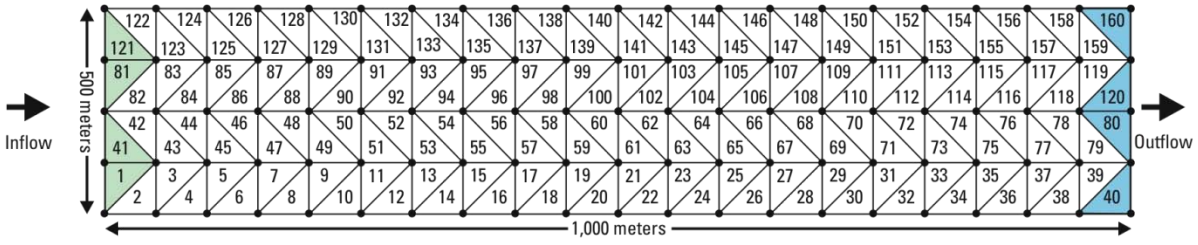

Figure 5-3. TaRSE application domain, with flow from left to right and bounded above and below by no-flow boundaries. Simulations were run for 30 days with a time-step of 3 hours.

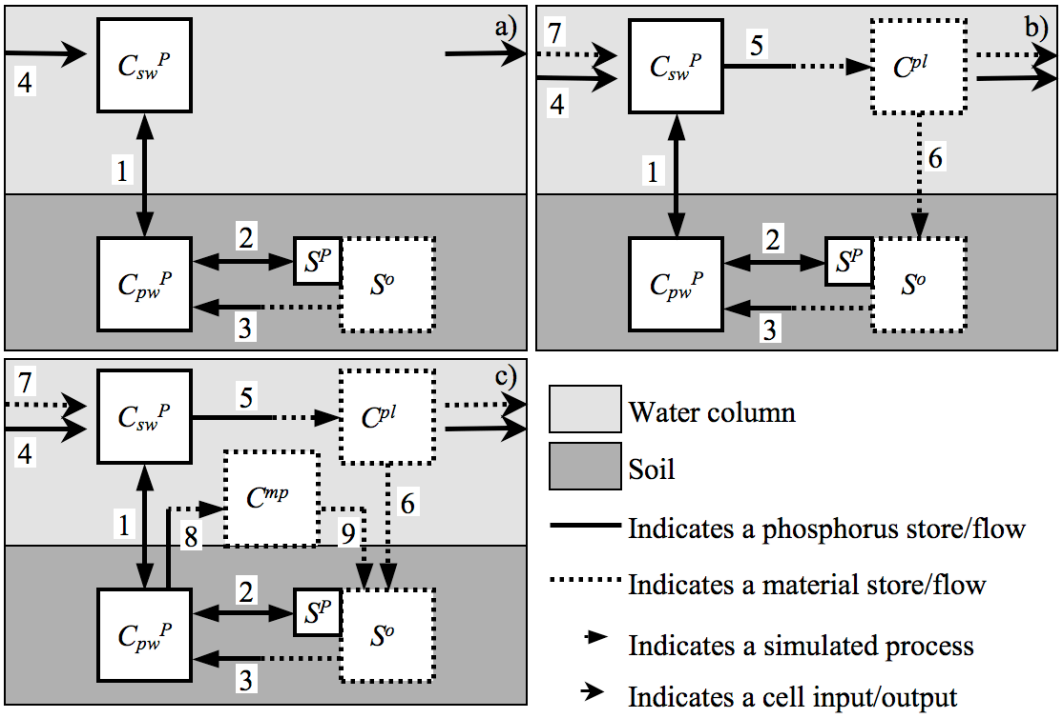

Figure 5-4. Levels of modeling complexity studied to represent phosphorus dynamics in wetlands. Levels include a) Level 1: interactions between SRP in the water column and SRP in the subsurface; b) Level 2: Level 1 with the addition of plankton growth and settling; c) Level 3: Level 2 with the addition of macrophyte growth and senescence. Notation and details on processes included in each Level are given in Table 2-1.

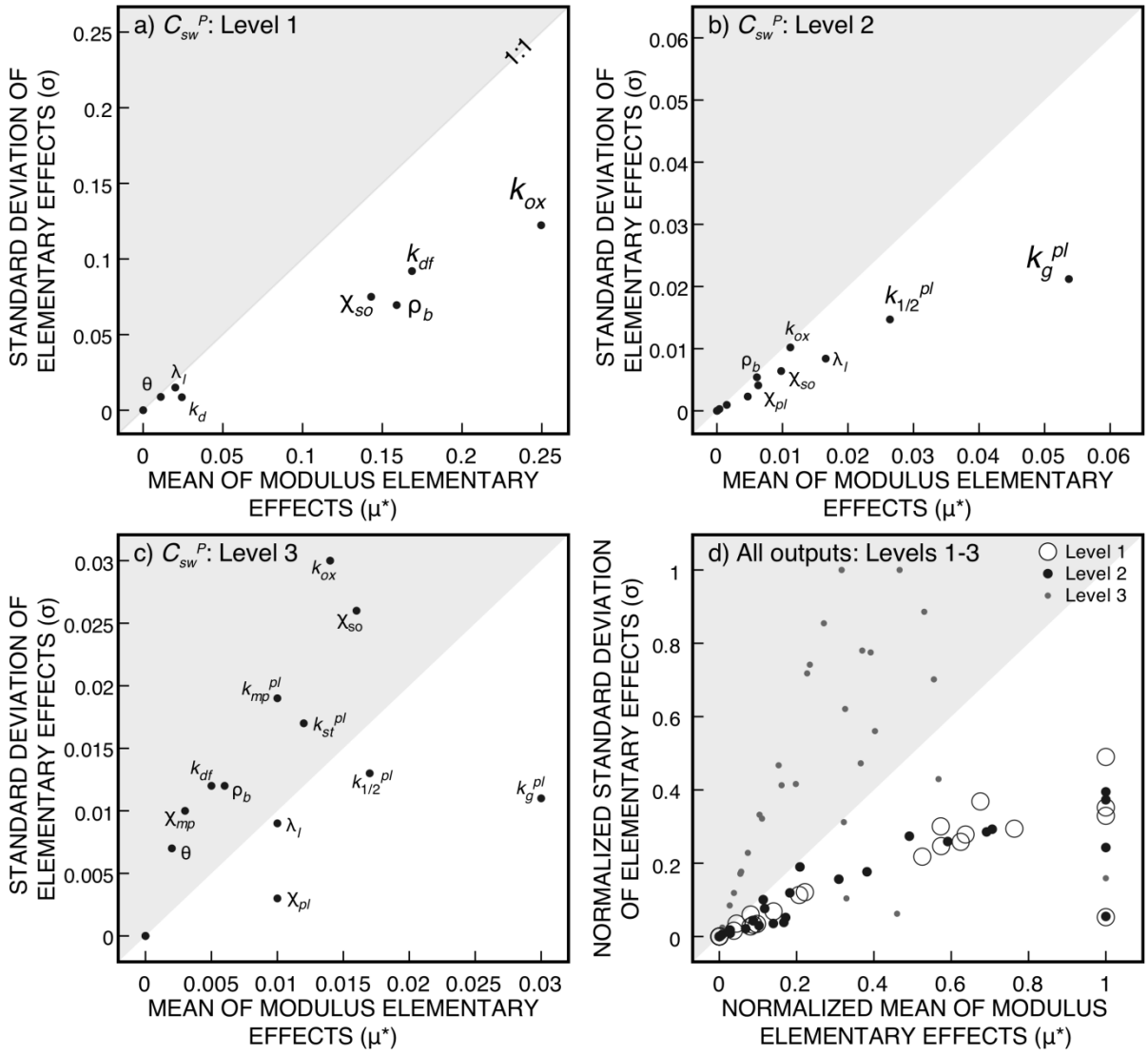

Figure 5-5. Morris method global sensitivity analysis results for surface-water soluble reactive phosphorus outflow (C_{sw}^{P}) in a) Level 1, b) Level 2, c) Level 3, and for d) all outputs and all levels combined. The grey triangles indicate the 1:1 line, font size of labeled parameters indicates their relative importance to C_{sw}^{P}.

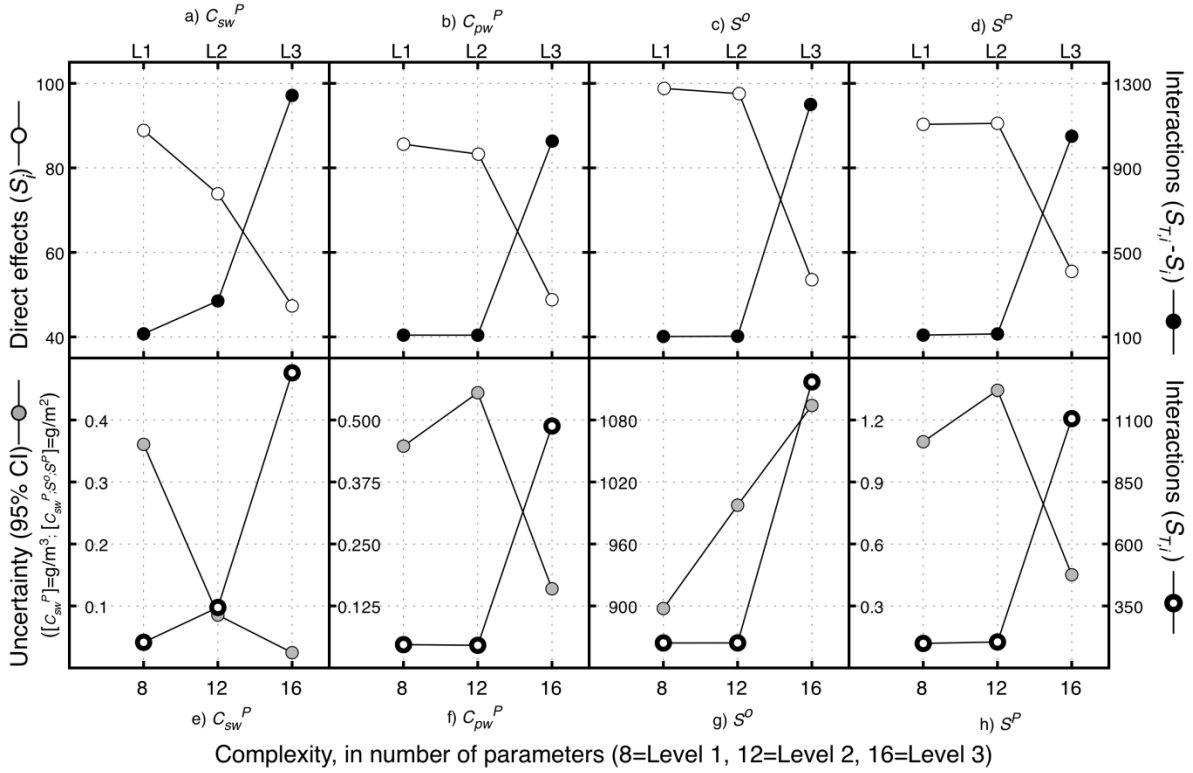

Figure 5-6. Results for a-d) sensitivity from direct effects (S_i, left y-axis) and sensitivity from interactions (S_T - S_i, right y-axis, and e-h) output uncertainty expressed as the 95% CI (left y-axis) and total sensitivity (S_T, right y-axis), as model complexity was increased.

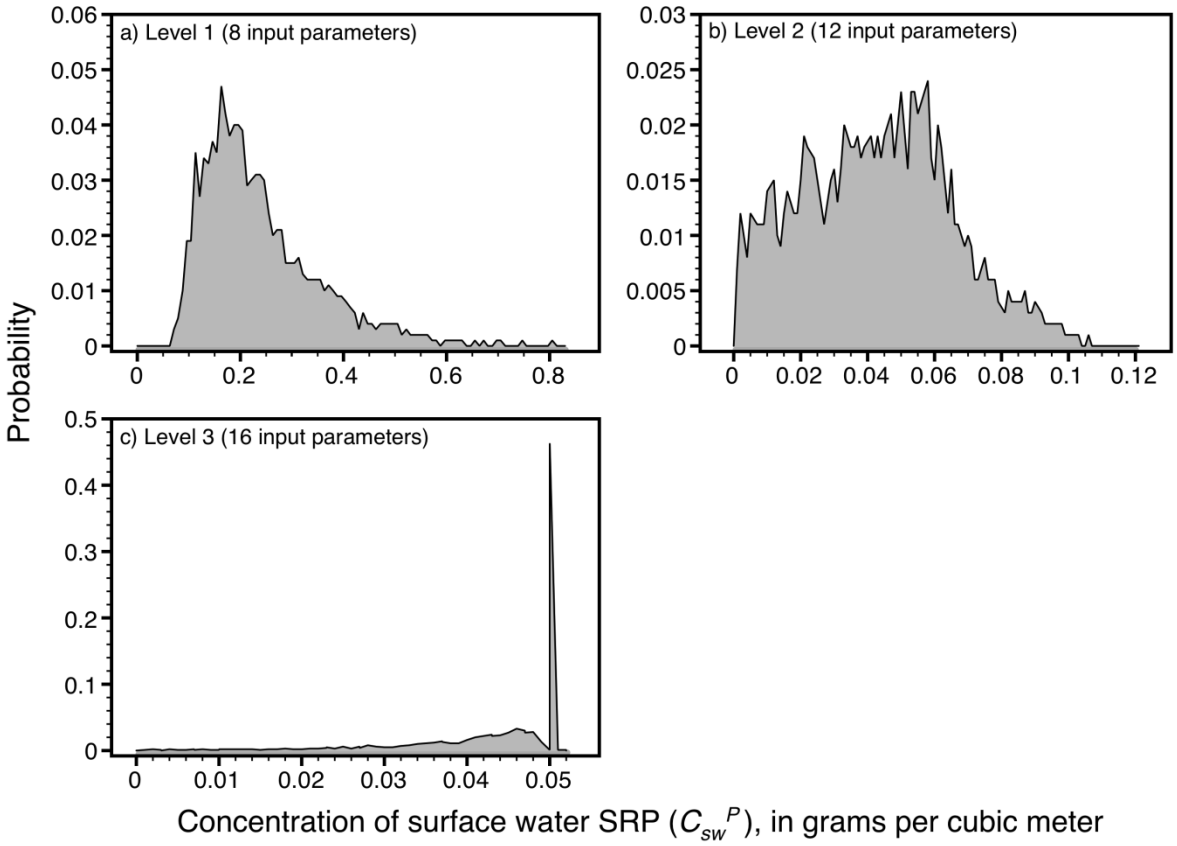

Figure 5-7. Output PDFs for SRP concentration in surface-water outflow (C_{sw}^{P}) for a) Level 1, b) Level 2 and c) Level 3.

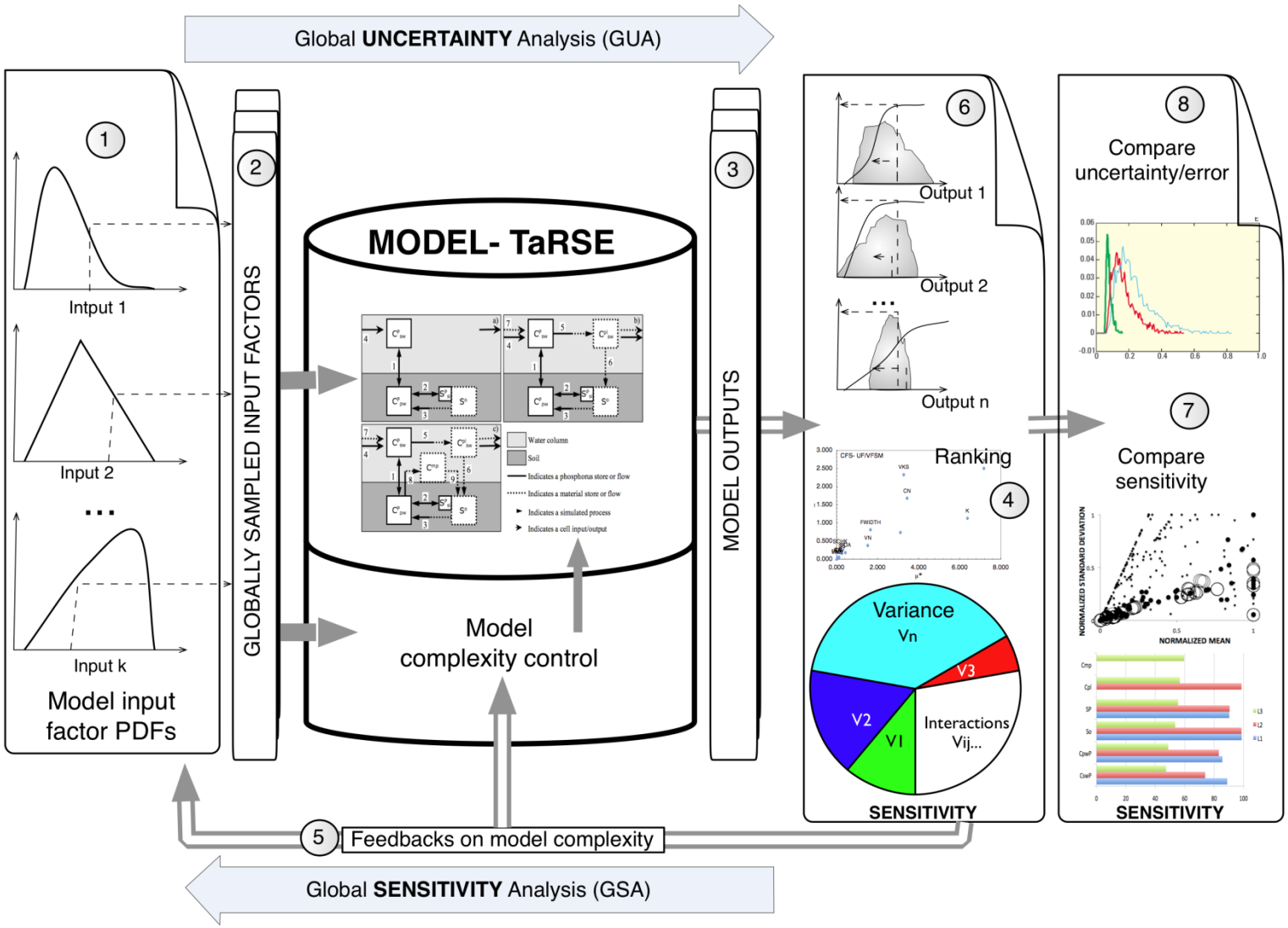

Figure 5-8. A suggested framework, employing global sensitivity and uncertainty analyses, for enhancing understanding of model performance studying model relevance in relation to complexity

CHAPTER 6
CONCLUDING REMARKS

Conclusions

A novel water-quality modeling tool has been developed for the coastal wetlands of the southern Everglades by linking the hydrologic model FTLOADDS with the water-quality model aRSE to create FTaRSELOADDS. FTaRSELOADDS combines the numerical efficiency and mechanistic rigor of a fixed-form spatially-distributed hydrodynamic model with the adaptability of a flexible free-form biogeochemical cycling model. In combination, the two models represent a tool that can be adapted and refined to best capture the water-quality issue of interest while accounting for the complex variable-density unsteady hydrodynamics that characterize the region's hydrology The linkage of the FTLOADDS and aRSE was validated by a series of comparisons between known analytical solutions and numerically simulated results that used FTLOADDS and a combination of FTLOADDS and aRSE. Thus Objective 1 was satisfied.

The linked models were tested with a field application to the SICS region, which provided answers to the questions underlying Objectives 2 and 3. Surface-water hydrodynamics were shown to be sensitive to depth-varying Manning's *n*, which had to be reintroduced into the hydrodynamic model in order to accurately capture wetting and drying processes and their effects on water-quality. Three different water-quality conceptual models of increasing complexity were implemented and the results compared. The simplest version employed conservative transport and produced the best match with data. However, this version also neglected all biogeochemical processes, including the important input of atmospheric deposition, and was therefore the weakest of the models from the perspective of mechanistic justifiability. The most

complex model produced acceptable results despite being subject to the significant uncertainty associated with including atmospheric deposition, implying that the greater mechanistic integrity may have helped mitigate this uncertainty. Experimentation with how to input atmospheric deposition indicated that the simplest approach of distributing an annual average equally over all days in the course of a year produced the best results and is justifiable based on the limited data available.

Given the freedom to manipulate model complexity, and the recognized relationship between this complexity and model uncertainty, sensitivity and relevance, a study was conducted to elucidate how additional complexity affects model performance (Objective 4). Global sensitivity and uncertainty analysis methods were applied, and a framework for formally exploring their results in the context of complexity was presented. Direct sensitivity was found to decrease and interaction effects to increase as complexity was added. Uncertainty was found to decrease in response to increased complexity, though considerations of turnover rates versus flux rates were shown to influence this result. The suggested framework demonstrated its value as a useful means of exploring and explaining model results and of assessing relevance with respect to complexity, thus satisfying Objective 4.

Limitations

Currently, the computational expense of a fully integrated fixed-form/free-form tool remains high. The required time-step for hydrodynamic simulations of SICS is small but the efficiency of solution methods keeps the investment manageable. With the addition of aRSE comes significant overhead since each cell in the SICS hydrodynamic model domain is individually processed. This process is exacerbated by the need to prepare and exchange large amounts of data between the two models. The presented effort

was limited to a daily time-step by these computational costs, which precluded using the Runge-Kutte 4th Order differential equation solution functionality within aRSE, which required a maximum 15-minute time-step and untenable cumulative computational times.

The paucity of surface-water phosphorus data was a significant limitation to the water-quality modeling effort. This was exacerbated by the fact that observed phosphorus concentrations fluctuated within a relatively small range of variation due to the oligotrophic conditions. A more rigorous testing of the water-quality against more phosphorus concentration data points, or against more types of data (such as biomasses or fluxes), would contribute valuable additional validation of the model.

Additionally, the sensitivity and uncertainty analyses performed did not evaluate the SICS water-quality application, but rather a theoretical application established in a generic testing domain. The SICS water-quality application would benefit from such a sensitivity and uncertainty analysis. Similarly, evaluation the complexity-relevance relationship for a field-tested application such as SICS would provide additional rigor to the testing of the suggested relevance framework.

Finally, there is currently no formal documentation for aRSE or FTaRSELOADDS. Documentation does exist for TaRSE and SWIFT2D individually, but a formal record of the linkage of the models and a user's manual to guide implementation of the linked tools is needed. Without this documentation the complexity of the tool prevents its wider application by any user not already familiar with it.

Future Research

Future work is required to either extend the simulation period to include more data points, or to shift the simulation period to more recent times when data is being

recorded at greater resolution. Additional time-series data pertaining to soil phosphorus, periphyton and macrophyte biomass in the SICS region would provide valuable additional testing of the more mechanistic water-quality modeling approaches. The current treatment of the water-quality reactions as a completely separate step to the transport means that parallelization of the reactions is possible. Considering that over 9,000 cells are currently processed in linear sequential order when they could all theoretically be processed simultaneously, the opportunities for greater computational efficiency are significant.

The work presented here has demonstrated the significant commitment required to get to the point of being able to make use of this tool. Future work must now explore and expose the potential within, especially as it pertains to the flexibility provided by aRSE. Most immediately, the mechanistic and spatially-distributed modeling of any number of water-quality issues in the southern Everglades can begin in earnest. Nitrogen and dissolved organic carbon input to Florida Bay are a major concern that has not been satisfactorily addressed. The proven ability of the hydrodynamic model to accurately capture wetting and drying is encouraging for future sulfur and mercury modeling in the region given the importance of these processes to mercury methylation (Cleckner et al., 1999).

The development of ecohydrological water-quality modeling is now also possible. The important role of Manning's *n* in the hydrological simulations was demonstrated in Chapter 3. Making the link between simulating biomass growth for water-quality and changes in flow resistance with seasonal growth and senescence is readily achievable

with FTaRSELOADDS. So too is the integration of spatially-distributed nutrient inputs to ecological models in the region, which have previously been limited to hydrologic inputs.

Finally, such flexibility within complex models is an important launching point for serious study of how model complexity, uncertainty, and sensitivity interact in complex spatially-distributed models. Given the paucity of work in this field and the clear benefits derived from the GSA and UA methodology that was applied in Chapter 5, the framework that was proposed for tackling questions related to the Relevance Trilemma should prove fruitful.

Philosophical Deliberations

The freedom to be creative is the source of progress. It is this tenet that underlies the very notion of Academia, and recognizes the profound role of creative freedom in advancing our technological, cultural, and intellectual evolution. It is the freedom to be creative that will prove to be the greatest strength of tools such as FTaRSELOADDS.

One need look no further than the kaleidoscope of problems to which STELLA has been applied to see the imagination unleashed by a tool that puts creative control in the user's hands. There is no reason why users of complex models, such as that applied herein, should be denied such creative freedoms as a matter of course, as has long been the case with the availability of only fixed-form spatially-distributed models. In fact, it is precisely because modeling of this highly complex sort is so arduous, and so challenging, that such freedoms should be encouraged. To have modelers who have invested such energy and expertise and life time into mastering a tool that is subject to claustrophobic specificity is to waste a glut of potential and opportunity.

The art of modeling will always entail balancing the pros and cons behind the choice of an appropriate tool for a given problem, whether it be developed from scratch

or picked off a shelf. With the freedom to uniquely tailor complex spatially distributed models comes a new dimension to the art modeling: the notion of optimizing these high levels of complexity with respect to uncertainty, sensitivity and relevance. It is important that we continue to delve more deeply into this tripartite conundrum or risk falling behind our tools. Modelers, and all who depend on their work, cannot fail to acknowledge and grasp the limitations to relevance inherent to the nascent generation of “super-complex” tools, including efforts to integrate many independent and spatially-distributed models into vast multi-model systems.

As complex model creation and modeler creativity become ever more entangled, better understanding of how models gain and lose relevance is critical both to the evolution of our tools and to the evolution of our modelers. We cannot forget that the science and art of modeling are one and the same.

APPENDIX A
MODEL VERSIONS

Model and Application Versions: Nomenclature

The following rules and naming conventions apply when referring to versions of either SWIFT2D, FTLOADDS, or their applications as SICS or TIME:

SWIFT2D: specifies only the surface-water model

SEAWAT: specifies only the ground-water model

FTLOADDS: specifies versions in which SWIFT2D and SEAWAT have been linked (one or the other may be on or off)

SICS: the Southern Inland and Coastal Systems application

TIME: the Tides and Inflows in the Mangroves of the Everglades application

Version 1.X: models or applications simulating only surface-water

Version 2.x: models or applications simulating coupled surface-water/ground-water

Version X.1: models or applications using SWIFT2D code adapted for the SICS application as per Swain et al. (2004)

Version X.2: models or applications using SWIFT2D code adapted for the TIME application as per Wang et al. (2007)

Version X.Y.1: models or applications using SWIFT2D code adapted for TIME but with variable-Manning's functionality from SICS adaptations reinstated

Model and Application Versions: Sub-models

The following figures offer a graphical overview of the model and application versions. Consistent colors are used to represent identical versions/models to facilitate identification across figures. Perpendicular blocks, generally oriented vertically, indicate models/versions that encompass adjacent horizontal blocks. Blocks crossed out in white indicate that the submodel is present but not used.

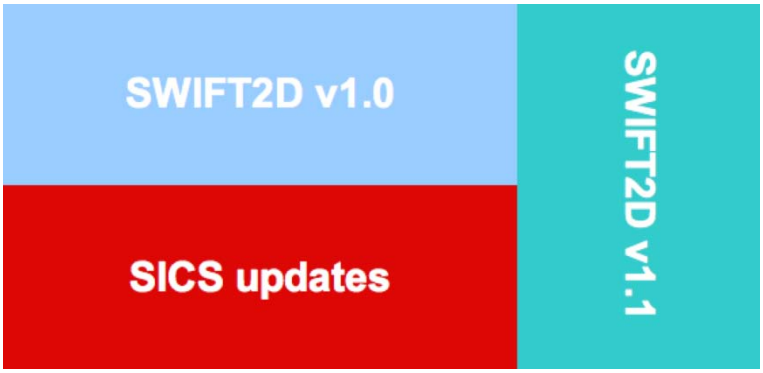

Figure A-1. SWIFT2D v1.1 comprises the SWIFT2D v1.0 (Schaffranek, 2004) code and additional code from SICS updates for coastal wetlands (Swain, 2005).

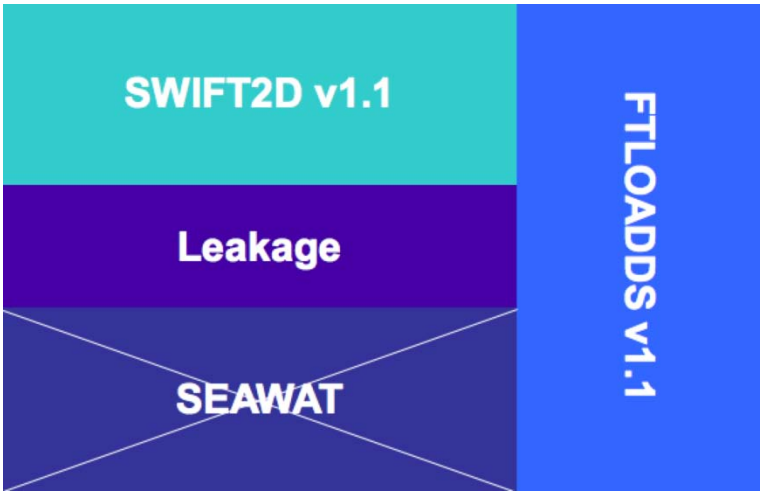

Figure A-2. FTLOADDS v1.1 comprises the SWIFT2D v1.1. code, leakage code linking SWIFT2D to SEAWAT, and SEAWAT, but represents applications in which SEAWAT is not implemented.

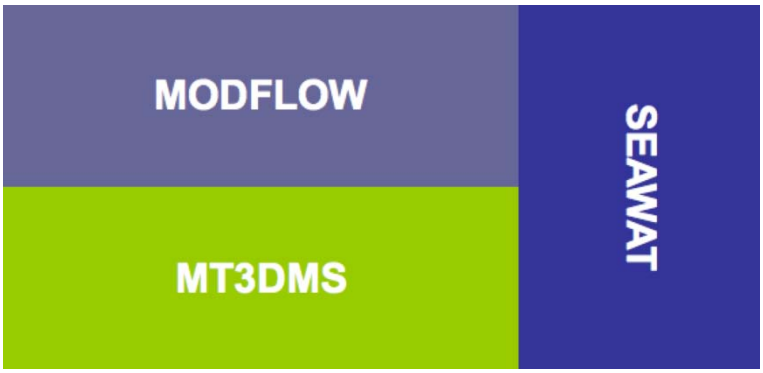

Figure A-3. SEAWAT comprises the MODFLOW code and the MT3DMS code (Langevin and Guo, 2006).

Figure A-4. FTLOADDS v2.1 comprises SWIFT2D v2.1 and SEAWAT, where SWIFT2D v2.1 is SWIFT2D v1.1 implemented with integrated leakage and ground-water simulation by SEAWAT.

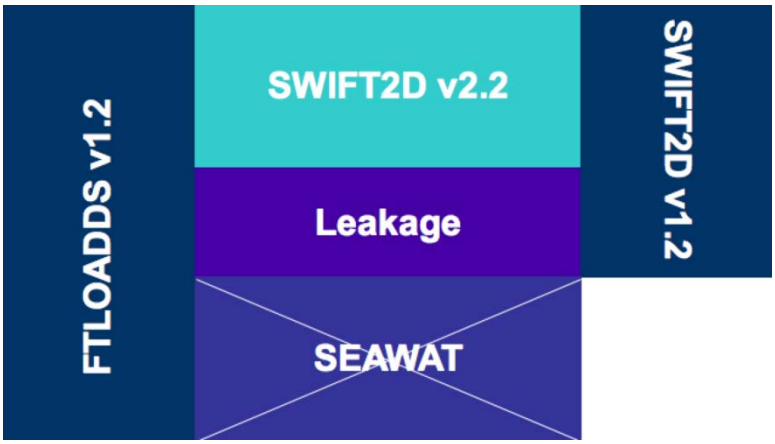

Figure A-5. FTLOADDS v1.2 comprises SWIFT2D v2.2 with updates for TIME but with the ground-water simulation turned off (thus SWIFT2D v1.2).

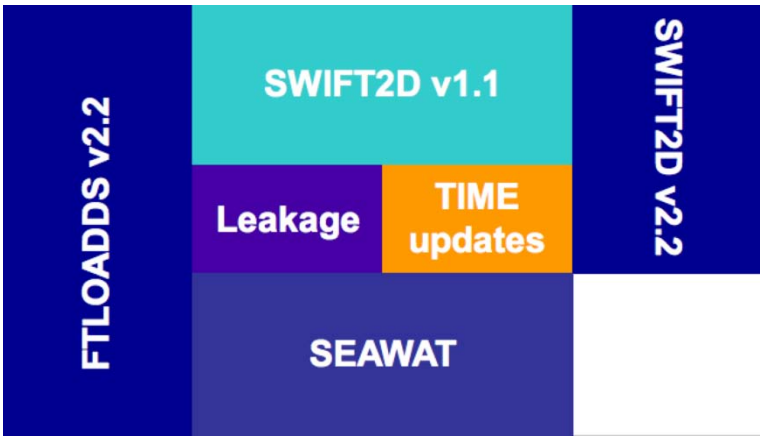

Figure A-6. FTLOADDS v2.2 contains SWIFT2D v2.1 linked with SEAWAT and containing TIME updates (thus SWIFT2D v2.2).

APPENDIX B
DETAILS OF THE FTARSELOADDS LINKAGE

Section B1

Technical Considerations in the Model Linkage

Since aRSE is callable as a DLL, and considering the primacy of hydrology and the role of FTLOADDS in controlling the integrated execution of SWIFT2D and SEAWAT, FTLOADDS was selected as the controlling program. Furthermore, the decision was taken to link aRSE with the surface-water model only, i.e. to SWIFT2D. This was done to keep the scope of the task manageable given the effort entailed in linking aRSE to even one of the two complex FTLOADDS sub-models. The choice of SWIFT2D is further justified by recognizing that the biogeochemical processes aRSE is intended to simulate are primarily associated with the surface-water in wetlands systems. Water-quality in the ground-water is generally not as sensitive to biological influence given the paucity of autotrophic organisms and was therefore not justified at this early stage development. Additionally, though vertical flow through the upper soil cannot be simulated given these assumptions, the flexibility of aRSE does permit soil phosphorus state-variables to be defined, which would permit soil biogeochemistry to be modeled under assumptions of negligible vertical advection processes.

A number of fundamental differences in the respective design of FTLOADDS and aRSE had to be overcome in order to successfully link the two models. These included an idiosyncratic artifact of the initial setup of aRSE that inhibited its automation within FTLOADDS, the absence of a spatial distribution in aRSE, and the use of different programming languages to code the models.

Consideration 1: Initial setup of aRSE

In order for the user to specify a unique system of water-quality processes it is necessary to input the state-variables that comprise the system, the parameters required to characterize the equations relating the state-variables, and the nature of the equations themselves. State-variables are classified as *mobile* if they represent constituents that would be moved with flow (solutes and suspended particulates – constituents), or *stabile* if they represent stationary quantities (e.g. rooted macrophytes, soil, benthos). There are also 30 additional implicit parameters that are always present, though only used if specified in the equations. These implicit parameters were originally necessary for transport processes and have been kept because they represent useful properties (mostly of hydrodynamics) that may be useful in future work and present little inconvenience with their presence. In the jargon of aRSE, state-variables and parameters are collectively referred to as *components*. Given that the number of both parameters and state-variables is a user choice, the total number of components is variable.

A single vector, VARS, is used by aRSE to store the values for all components. In order for updated values of transported constituents or hydrodynamic quantities to be passed from FTLOADDS to aRSE it is necessary to know which particular element of this vector corresponds with the given quantity. However, aRSE must be initialized once in order to determine these locations since they are subject to the number of user-specified components. In order to exchange information between the two models it is necessary to have some means to determine what quantity each element of the vector refers to.

Consideration 2: Spatially-distributed versus non-spatial

FTLOADDS is a spatially-distributed model, and therefore performs calculations on, and stores data about, many individual cells that together comprise the modeled domain. By contrast, aRSE is non-spatial, assuming that the system of reactions it simulates is carried out at a singular location with no consideration of spatial distribution.

Where FTLOADDS stores arrays of data for each model variable, aRSE stores a single vector containing the single value for each of the model components. The use of a one-dimensional vector, as opposed to a higher-dimensional array, is possible because there is essentially only ever one cell (hence non-spatial) under consideration. By contrast, SWIFT2D maintains two-dimensional arrays, dimensioned to the total number of cells used to discretize the model domain, for each of the hydrodynamic variables and three-dimensional arrays for the solute concentration variables (the third dimension is used to specify the particular constituent, since all concentrations for up to seven constituents are stored in a single array).

Since aRSE can only ever consider a single cell at a time it must be run repeatedly for each of the cells in the FTLOADDS domain. This in turn entails updating the VARS values with data appropriate to the cell in question, and then saving the values after the reactions step so they are not over-written by the results of the subsequent cell's reaction step.

Consideration 3: FORTRAN versus C++

The programming languages used to encode each of the models was not consistent. The FORTRAN language (in the form of both FORTRAN 77 and FORTRAN 90) was used to code FTLOADDS and its constituent sub-models, SWIFT2D and

SEAWAT. The generic design of aRSE is the product of object-oriented template functionality in the C++ language used to code it. The linkage of the two models therefore represents a mixed-language programming problem in which communication between the two structurally and syntactically foreign languages must be facilitated.

A number of inter-language calling conventions have been adopted by FORTRAN and C/C++ (Arnholm, 1997; Wang et al., 2005):

- Most FORTRAN compilers convert subroutine names to lower case and append an underscore. To make a C routine callable in FORTRAN, declare the name of the routine in lower case and append an underscore.
- FORTRAN passes arguments by reference, C++ by value. For a variable name in a subroutine call from FORTRAN, the corresponding C routine receives a pointer to that variable. When calling a FORTRAN routine, the C routine must explicitly pass addresses (pointers) in the argument list.
- C routines assume that character strings are delimited by the null character. From FORTRAN to C, the length of each character string is passed as an implicit additional INTEGER (KIND=4) value, following the explicit arguments. From C to FORTRAN, when a function returns a character string, the address of the space to receive the result is passed as the first implicit argument to the function, and the length of the result space is passed as the second implicit argument, preceding all explicit arguments.
- Arrays in FORTRAN are stored in a column-major order, whereas in C they are stored in a row-major order. Two types of communication between FORTRAN and C++ were required that called for special treatment.

Wang et al. (2005) outline a suggested manual procedure for overcoming these problems. The principle is to build a “wrapper” for the C++ library that hides the implementation details of the library from the FORTRAN code. The wrapper handles the request from a FORTRAN call to create and destroy the objects defined in C++, and then returns a FORTRAN pointer aliased to the memory allocated in the C++ library with support function overloading. The “wrapper” itself is made of two components, one “C” and one FORTRAN 90 component, written in “standard” C++ and FORTRAN 90,

together with the conventional inter-language calling method. Changes to the application source code are minimal and can be automated.

The FORTRAN 90 component contains a module that provides a set of public functions for the FORTRAN application to call. Each of these public functions corresponds to a function implemented in the C++ library, and it calls the corresponding function via the C++ component. The FORTRAN 90 module also holds one- or multi-dimensional FORTRAN pointers in its global space, and thereby provides an alias function for the C++ component to call that makes the one- or multi- dimensional FORTRAN pointer aliased to the memory space allocated dynamically in the C++ library.

Resolution 1: Initial setup of aRSE

To overcome this problem a FORTRAN subroutine, READIWQ, was written to read a new water-quality input file (IWQINPUT.iwq) that contains the necessary data also included in the XML input file, but which could be read without the need for aRSE to be executed. The XML output file was therefore no longer needed. Since aRSE still relies on reading the XML input file to correctly setup, this method requires that two input files containing some overlap in data be provided. However, the files are small and simple to produce, and allow the setup of aRSE to be automated and controlled from FTLOADDS. Furthermore, having such a file is also useful for overwriting aRSE parameters and state-variable initial conditions should this be desirable, and introduces some measure of control from within the calling FORTRAN code over the inputs to aRSE without having to tamper with the aRSE code at all.

The automation process in READIWQ makes use of the fact that aRSE distributes components in the VARS vector in an orderly manner that, given knowledge about the

number of state-variables and the number of parameters, permits the deduction of their future location in VARS vector. Mobile state-variables are always positioned first, followed by stabile state-variables, followed by a fixed number of implicit parameters (27 hydrodynamic and spatial properties), followed by the user-input parameters, followed by the remaining 3 implicit parameters (temporal properties). The subroutine READIWQ therefore requires, in order:

The number of mobile state-variables
The number of stabile state-variables
The paired name and initial value for each mobile state-variable
The paired name and initial value for each stabile state-variable
The number of user-specified parameters
The paired name and value for each user-specified parameters

Also permitted are override values for any of the implicit parameters, whose positions in VARS are fixed relative to each other, though contingent in absolute position on the number of state-variables that precede them. This process is conducted during the initial setup of SWIFT2D, thereby ensuring that data is correctly exchange and the linkage with aRSE is fully functional from the first time it is called from within SWIFT2D (though aRSE still requires its own initialization step the first time it is called to process the equations outlined in the XML input).

Resolution 2: Spatially-distributed versus non-spatial

A new two-dimensional vector was established, C1_aRSE, dimensioned to the number of components (i.e. the same size as the VARS vector) and the total number of cells in the FTLOADDS domain. Each time aRSE is called, which may or may not be coincident with the FTLOADDS hydrology and transport time-steps, all the appropriate data for each of the cells is moved from the various arrays within FTLOADDS to C1_aRSE prior to the simulation of reactions in the first cell. Since no exchange of

information between cells takes place during the reaction step, the order in which cells are processed for reactions does not matter with regards to the accuracy of the simulation. However, the order in which memory is accessed during computations does affect the speed of the process. It date are therefore transmitted in column-major order from FTLOADDS arrays to C1_aRSE in order to minimize computational time. Though FTLOADDS arrays are dimensioned with a rectangular shape (number of rows x number of columns), the model permits an irregularly shaped domain, which may result in many points within the rectangular memory array referring to cells that are not actually used by FTLOADDS. The subroutine CELLCOUNT therefore determines the number of active cells in the model and this number is used in the reactions step, thereby minimizing the computational iterations

Prior to each individual cell being processed the data appropriate to that cell is transmitted to the VARS vector that is used directly by aRSE. Once the reactions have been simulated the updated VARS values are used to overwrite old values in C1_aRSE. In this way old values are overwritten and new values stored until reactions have been performed on all cells. After the final cell has been processed, all updated values in C1_aRSE used transmitted back to their appropriate FTLOADDS arrays, where they are then used in subsequent transport calculations.

Currently, concentrations, depths, and velocity in the x- and y-directions are passed from FTLOADDS to aRSE, where concentrations are analogous to mobile state-variables, and the hydrodynamic variables to particular implicit parameters. Only concentrations are transmitted back to FTLOADDS for use in transport, though the freedom to return updated hydrodynamic variables should the reactions affect them

offers potentially exciting opportunities for simulating ecohydrological effects using these models.

Resolution 3: FORTRAN versus C++

Text strings in FORTRAN and C++ are represented differently. FORTRAN strings are character variables that are declared as a particular length, which is maintained by trailing blank space characters irrespective of the length of the text of interest within the string. By contrast, C++ strings are null-terminated following the final character of text. If FORTRAN strings are to be understood by C++ they must be converted to a null-terminated form. A subroutine to do so exists, and was used to convert the XML input filenames, which are now read in by the FORTRAN subroutine READIWQ, and convert them to a format acceptable to the C++ code of aRSE.

The second instance necessitating mixed-language communication was the calling of subroutines. In this case, aRSE is executed by calling one of a three C++ subroutines from within the FORTRAN linkage. FORTRAN 90 contains some built-in functionality to facilitate mixed-language programming, including the INTERFACE statement, which is useful for creating interfaces between FORTRAN and external subroutines. Interfaces were therefore defined for each of the external C++ subroutines. Compiler directives were specified within the interface to attribute C++ calling conventions, to specify the location of the subroutines as within a DLL, and to specify an alias for the called subroutine that was preceded with an underscore to match the C++ syntax.

General description of the linkage mechanism

- If aRSE is greater than zero then READIWQ is called during the setup of SWIFT2D to preprocess aRSE.

- The subroutine CALLaRSE is called at the time interval specified by the variable CaRSE.

- Prior to performing reactions on the first cell the subroutine aRSE_IN is called to transfer the values for all specified FTLOADDS variables in each of the domain cells to the storage array variable C1_aRSE.

- For each cell in turn the subroutine RUN_aRSE is called, which updates the vector VARS with the cell-specific values and calls the C++ subroutines PRESOVE, RKSOLVE and POSTSOLVE to execute aRSE. If it is the first time aRSE is being called then the subroutine INITIALIZE is called prior to these subroutines. After each cell has been processed the array variable C1_aRSE is updated with the updated values in the vector VARS.

- After reactions have been performed on the final cell the subroutine aRSE_OUT is called to update all appropriate FTLOADDS variables with the new values in the array variable C1_aRSE.

Section B2

FORTRAN Subroutines for Linkage

The following subroutines were written specifically for the linkage of aRSE and FTLOADDS. Additional code that was added to existing SWIFT2D subroutines is given in Section B3.

Module aRSEDIM

```
MODULE aRSEDIM
!***********************************************************************
*
! This MODULE is used for declaring variables used in the linkage of aRSE
! with SWIFT2D within FTLOADDS
!***********************************************************************
*
    IMPLICIT NONE

    INTEGER*4 INITIATE, NCALLS, NCELLS, NCELLST, NCOMPS, NCOMPST, NVARS
    INTEGER*4 CALLNO, CELLNO, RKORDER, NPAR, NMOB, NSTAB, NSTABMAX, K_WET,
ATM_NPAR

    PARAMETER (NCALLS = 1, NCELLST = 10201, NCOMPST = 60, RKORDER = 4,
NSTABMAX = 15)

    INTEGER*1 XMLINPUTC(50), XMLOUTPUTC(50), XMLREAC_SETC(50)
    INTEGER NPRZ(NSTABMAX)
    CHARACTER*120 PREPROCESS, XMLINPUT, XMLOUTPUT, XMLREAC_SET,
COMPNAME(NCOMPST)
    REAL*8 DTaRSE,DTFTLOADDS
```

```
!**************************************************************************
****

    REAL*8, DIMENSION (:), PUBLIC, ALLOCATABLE :: ZR(:,:,:),
C1_aRSE(:,:),ZRIC(:,:,:),RIC(:,:,:)
     PUBLIC :: SUB
     CONTAINS
      SUBROUTINE SUB (en,em,el,ze,comps,activecells)
        !integer, intent(in) :: en,em,te
        INTEGER :: en,em,el,ze,err,comps,activecells
        ALLOCATE ( ZR(en,em,ze), stat=err)
        ZR=0
            !IF (err /=0) PRINT *, "SUB allocate NOT successful."
        ALLOCATE ( C1_aRSE(comps,activecells), stat=err)
        C1_aRSE=0
            !IF (err /=0) PRINT *, "SUB allocate NOT successful."
        ALLOCATE ( ZRIC(en,em,ze), stat=err)
        ZRIC=0
            !IF (err /=0) PRINT *, "SUB allocate NOT successful."
        ALLOCATE ( RIC(en,em,el), stat=err)
        RIC=0
            !IF (err /=0) PRINT *, "SUB allocate NOT successful."
      END SUBROUTINE SUB

    END MODULE aRSEDIM
```

Subroutine READIWQ

```
SUBROUTINE READIWQ
!ccccccccccccccccccccccccccccccccccccccccccccccccccccccccccccccccccccccccccccccccccc
cccc
!C This subroutine  read a .IWQ file to extract the data needed to run RSE.
C
!C The data read are:
C
!C * A flag (to be used in vfsmod when RSE is used for simulation of
pollutants C
!C * 2 XML files (input [eq's included here, and output [to check indexed])
C
!C * the reaction set used (delclared in the XML input file
C
!C * number, name and data for the mobile variables (used in the reactions)
C
!C * number, name and data for the stabile variables (used in the reactions)
C
!C * number, name and data for the parameters (used in the reactions)
C
!C * Flag for reading 4 intrinsic parameters (depth, x_vel, time_step, area)
C
!C   that can be used in the equations (XML input files)
C
!C Once data are read, values are passed to the hydrodynamic driving program
C
!ccccccccccccccccccccccccccccccccccccccccccccccccccccccccccccccccccccccccccccccccccc
```

```
cccc
    USE aRSEDIM
    USE SWIFTDIM, ONLY: NMAX,MMAX,LMAX,VARZINT

    IMPLICIT NONE

    INTEGER(kind=4)     :: WQFLAG,M
    integer(kind=4)     :: s,i,j,k,l,n

    PREPROCESS='IWQINPUT.iwq'  !Moved this from CALLaRSE since moving READIWQ
to being called from SETUP2

!Opens and read input file .iwq for RSE
    OPEN (UNIT=50, FILE=PREPROCESS)
    READ(50,*) WQFLAG, NMOB, NSTAB, NPAR, K_WET, ATM_NPAR
    IF(NMOB.NE.LMAX)PRINT*, 'NMAX not equal to NMOB'
    NVARS=NMOB+NSTAB
    NCOMPS=NMOB+NSTAB+27+NPAR

    CALL CELLCOUNT
    CALL SUB(NMAX,MMAX,NMOB,NSTAB,NCOMPS,NCELLS)
!Read  XML input file, XML outout file to check indexes, react set to be used
in XML input file
    READ(50,*) XMLINPUT, XMLOUTPUT, XMLREAC_SET
!Read mobile variables
    READ(50,*) (COMPNAME(i),C1_aRSE(i,1),i=1,NMOB)

!Read stabile variables
    READ(50,*) (COMPNAME(j),C1_aRSE(j,1),j=(NMOB+1),(NMOB+NSTAB))
!Read stabile print flags
    READ(50,*) (NPRZ(s),s=1,NSTAB)    !Equivalent to the NPRR in FTLOADDS,
but for stabile components
! Output file always has user-defined variables first (j), then 27 intrinsic
params + 1
    j=NMOB+NSTAB
    n=NMOB+NSTAB
    k=j+27+1
    j=k
!Read parameter to be used (usually declared to be used in the set of
equatiuons)
    READ(50,*) (COMPNAME(k),C1_aRSE(k,1),k=j,(j+NPAR-1))
! Read intrincsic values of depth, x_vel_ol, time_step, area if m="1"
    READ(50,*)M
      IF(M.EQ.1) THEN
        READ(50,*) COMPNAME(n+2),C1_aRSE(n+2,1)&   !depth
                  !&,COMPNAME(n+16),C1_aRSE(n+16,1)& !x-vel
                  &,COMPNAME(n+20),C1_aRSE(n+20,1)& !time
                  &,COMPNAME(n+1),C1_aRSE(n+1,1)     !area
      ENDIF
    DTaRSE=C1_aRSE(n+20,1) !time step if not in .iwq

    CLOSE(50)

    IF(VARZINT.NE.99)THEN   !Read in STABILE ICs as uniform
        DO L=1,NSTAB
            DO N=1,NMAX
                DO M=1,MMAX
```

```
                    ZR(N,M,L)=C1_aRSE(NMOB+L,1)
                ENDDO
            ENDDO
        ENDDO
    ENDIF

    END
```

Subroutine CALLaRSE

```
SUBROUTINE CALLaRSE
!ccccccccccccccccccccccccccccccccccccccccccccccccccccccccccccccccccccccccccccccccccccccccccccccc
cccc
!C This program emulates a hydrodynamic calling program for using the
Reaction  C
!C Simulaiton Engine (RSE). The code structure of this program can be adapted
C
!C to other hydrodynamic calling programs.
C
!C This program reads a text file (.iwq) with the data needed to used
C
!C RSE. This .iwq file contains the name of the XML input file, the name of
C
!C the XML output file to check the indexes used, the name of the reaction
set  C
!C to be used (declared in the XML input file), the number(s), name(s) and
C
!C value(s) for the mobile, stabile and parameters used in the equation(s)
C
!C declared in the XML input file.
C
!C Once data is read, call MyReactionModTest subroutine, which initiate and
C
!C runs RSE.
C
!C RSE is called at each time step. Initiallitation occurs in time step 1
C
!ccccccccccccccccccccccccccccccccccccccccccccccccccccccccccccccccccccccccccccccccccccccccccccccc
cccc
    USE aRSEDIM
    USE SWIFTDIM, ONLY: HALFDT,aRSE,CaRSE,NMAX,MMAX

    IMPLICIT NONE

    INTEGER(KIND=4)  :: i,j,p,r,HALFSTEP
    DATA HALFSTEP/0/

    IF(INITIATE.EQ.0)THEN
        CALL FORT_CSTRING(XMLINPUT, XMLINPUTC)
        CALL FORT_CSTRING(XMLOUTPUT, XMLOUTPUTC)
        CALL FORT_CSTRING(XMLREAC_SET,XMLREAC_SETC)
        !IF (VARZINT.EQ.99) CALL READIC
        DO r=1,NCELLS
            DO p=1,NCOMPS
                C1_aRSE(p,r)=C1_aRSE(p,1)
```

```
            ENDDO
          ENDDO
          INITIATE=1
        ENDIF

        DO 100 CALLNO=1,NCALLS
          IF(aRSE.EQ.2) THEN
              HALFSTEP=HALFSTEP+1
          ELSEIF(aRSE.EQ.1) THEN
              HALFSTEP=HALFSTEP+2  !Initiated to zero, so +2 means always even,
so always uses R
          ELSEIF(aRSE.EQ.3) THEN
              HALFSTEP=1
          ELSE
              PRINT*, 'aRSE is neither 1, 2 or 3'
              PAUSE
          ENDIF

! Time step used by the controlling program
          IF (DTaRSE.GT.0) THEN
              DTFTLOADDS=DTaRSE
          ELSEIF (aRSE.EQ.1) THEN
!time_step in RUNaRSE is DTFTLOADDS*60. If aRSE=0 then no aRSE called so the
/aRSE should
!not be a problem and acts as a check; if aRSE=1 then CaRSE is used to
specify how many full
!time-steps (HALFDT*2) to wait.
              DTFTLOADDS=CaRSE*HALFDT*2
          ELSEIF (aRSE.EQ.2) THEN
              DTFTLOADDS=HALFDT*2/aRSE
          ELSEIF (aRSE.EQ.3) THEN  !use TRT split-operator
              DTFTLOADDS=HALFDT*2
          ENDIF

          DO 10 CELLNO=1,NCELLS
              IF(CELLNO.EQ.1) THEN
                  CALL aRSE_IN(HALFSTEP) !Halfstep needed to determine R or RP
              ENDIF

              CALL RUNaRSE

              IF(CELLNO.EQ.NCELLS) THEN
                  CALL aRSE_OUT(HALFSTEP)   !Halfstep needed to determine R or
RP
              ENDIF

10        CONTINUE
100     CONTINUE

101     FORMAT(500F8.4)

        END
```

Subroutine aRSE_IN

```
SUBROUTINE aRSE_IN(HALFSTEPIN)

!*********************************************************************
! This subroutine moves the necessary values into C1_aRSE for RSE
!*********************************************************************

      USE SWIFTDIM, ONLY:
IROCOL,NOROWS,MSTART,MEND,SEP,SEMIN,U,UP,V,VP,RP,R,LMAX,ICLSTAT,ATMDEP
      USE aRSEDIM

      IMPLICIT NONE

    INTEGER CELLNUMI, NUMCELLSIRK, CELLNUM, IRK_aRSE, HALFSTEPIN
    INTEGER M,N,L,S
    REAL DEPTHMIN
    DATA DEPTHMIN/0.05/

!*********************************************************************

    CELLNUMI=0

    IF(LMAX.NE.NMOB) THEN
        PRINT*,'LMAX (SWIFT2D) not equal to NMOB (aRSE)'
        PAUSE
    ENDIF
!*********************************************************************
!Read in mobile/transported variables from R (u-step) or RP (v-step)
!*********************************************************************
    IF(HALFSTEPIN/2*2.EQ.HALFSTEPIN) THEN    !Even = v-step, which uses RP to
create R in DIFV, so use R
        DO IRK_aRSE=1,NOROWS
            N=IROCOL(1,IRK_aRSE)
            MSTART = IROCOL(2,IRK_aRSE)
            MEND = IROCOL(3,IRK_aRSE)
            DO M=MSTART,MEND
                CELLNUMI=CELLNUMI+1
                !Mobile inputs
                DO L=1,LMAX
                    C1_aRSE(L,CELLNUMI)=R(N,M,L)
                ENDDO
                !Stabile inputs
                IF(NSTAB.GT.0)THEN
                    DO S=1,NSTAB
                        IF((S.EQ.NSTAB).AND.(K_WET.EQ.1)) THEN
                            IF(ICLSTAT(N,M).EQ.0) THEN
                                !Cell is wet: K_wet=1
                                C1_aRSE(LMAX+S,CELLNUMI)=1
                            ELSEIF(ICLSTAT(N,M).NE.0) THEN
                                !Cell is dry: K_wet=0
                                C1_aRSE(LMAX+S,CELLNUMI)=0
                            ENDIF
                        ELSE
                            C1_aRSE(LMAX+S,CELLNUMI)=ZR(N,M,S)
                        ENDIF
```

```
                    ENDDO
                ENDIF
                !Hydro inputs
                IF(ICLSTAT(N,M).NE.0) THEN
                    C1_aRSE(NVARS+2,CELLNUMI)=DEPTHMIN
                ELSE
                    C1_aRSE(NVARS+2,CELLNUMI)=(SEP(N,M)-SEMIN(N,M))  !depth
                ENDIF
                IF(ATM_NPAR.GT.0)
C1_aRSE(NVARS+27+ATM_NPAR,CELLNUMI)=ATMDEP(2)
                !C1_aRSE(NVARS+14,CELLNUMI)=U(N,M)  !u-vel moved from UP to U
after u-step, not changed in v-step
                !C1_aRSE(NVARS+16,CELLNUMI)=VP(N,M) !V-vel updated to VP in
SEPV earlier in v-step
            ENDDO
        ENDDO
    ELSE   !Odd = u-step, which uses R to create RP (in DIFU) so use RP
        DO IRK_aRSE=1,NOROWS
            N=IROCOL(1,IRK_aRSE)
            MSTART = IROCOL(2,IRK_aRSE)
            MEND = IROCOL(3,IRK_aRSE)
            DO M=MSTART,MEND
                CELLNUMI=CELLNUMI+1
                !Conc inputs
                DO L=1,LMAX
                    C1_aRSE(L,CELLNUMI)=RP(N,M,L)
                ENDDO
                !Stab inputs
                IF(NSTAB.GT.0)THEN
                    DO S=1,NSTAB
                        IF((S.EQ.NSTAB).AND.(K_WET.EQ.1)) THEN
                            IF(ICLSTAT(N,M).EQ.0) THEN
                                C1_aRSE(LMAX+S,CELLNUMI)=1
                            ELSEIF(ICLSTAT(N,M).NE.0) THEN
                                C1_aRSE(LMAX+S,CELLNUMI)=0
                            ENDIF
                        ELSE
                            C1_aRSE(LMAX+S,CELLNUMI)=ZR(N,M,S)
                        ENDIF
                    ENDDO
                ENDIF
                !Hydro inputs
                IF(ICLSTAT(N,M).NE.0) THEN
                    C1_aRSE(NVARS+2,CELLNUMI)=DEPTHMIN
                ELSE
                    C1_aRSE(NVARS+2,CELLNUMI)=(SEP(N,M)-SEMIN(N,M))  !depth
                ENDIF
                IF(ATM_NPAR.GT.0)
C1_aRSE(NVARS+27+ATM_NPAR,CELLNUMI)=ATMDEP(2)
                !C1_aRSE(NVARS+14,CELLNUMI)=UP(N,M)  !u-vel updated to UP in
SEPU earlier in u-step
                !C1_aRSE(NVARS+16,CELLNUMI)=V(N,M)   !v-vel moved from VP to
V after previous v-step, not changed in u-step
            ENDDO
        ENDDO
    ENDIF
```

```
    RETURN
    END
```

Subroutine aRSE_OUT

```
SUBROUTINE aRSE_OUT(HALFSTEPOUT)

!*********************************************************************
! This subroutine: moves the necessary values out of C1_aRSE for FTL
!*********************************************************************

      USE SWIFTDIM, ONLY: IROCOL,NOROWS,MSTART,MEND,RP,R,LMAX
      USE aRSEDIM

      IMPLICIT NONE

    INTEGER CELLNUMO, NUMCELLSIRK, CELLNUM, IRK_aRSE, HALFSTEPOUT
    INTEGER M,N,L,S

!*********************************************************************

     CELLNUMO=0
     IF(LMAX.NE.NMOB) THEN
        PRINT*,'LMAX (SWIFT2D) not equal to NMOB (aRSE)'
        PAUSE
     ENDIF

     IF(HALFSTEPOUT/2*2.EQ.HALFSTEPOUT) THEN    !even = v-step, which uses RP
to create R in DIFV so use R
        DO IRK_aRSE=1,NOROWS
            N=IROCOL(1,IRK_aRSE)
            MSTART = IROCOL(2,IRK_aRSE)
            MEND = IROCOL(3,IRK_aRSE)
            DO M=MSTART,MEND
                CELLNUMO=CEllNUMO+1
                !Mobile outputs
                DO L=1,LMAX
                    R(N,M,L)=C1_aRSE(L,CELLNUMO)
                ENDDO
                !Stabile outputs
                IF(NSTAB.GT.0)THEN
                    DO S=1,NSTAB
                        ZR(N,M,S)=C1_aRSE(LMAX+S,CELLNUMO)  !Use ZR always
because not transported so no ZRP
                    ENDDO
                ENDIF
            ENDDO
        ENDDO
    ELSE     !odd = u-step, which uses R to create RP in DIFU so use RP
        DO IRK_aRSE=1,NOROWS
            N=IROCOL(1,IRK_aRSE)
            MSTART = IROCOL(2,IRK_aRSE)
            MEND = IROCOL(3,IRK_aRSE)
            DO M=MSTART,MEND
                CELLNUMO=CEllNUMO+1
```

```
                !Mobile outputs
                DO L=1,LMAX
                    RP(N,M,L)=C1_aRSE(L,CELLNUMO)
                ENDDO
               !Stab outputs
                IF(NSTAB.GT.0)THEN
                    DO S=1,NSTAB
                        ZR(N,M,S)=C1_aRSE(LMAX+S,CELLNUMO) !Use ZR always
because not transported so no ZRP
                    ENDDO
                ENDIF
            ENDDO
        ENDDO
    ENDIF

    RETURN
    END
```

Subroutine RUNaRSE

```
    SUBROUTINE RUNaRSE

    USE IFPORT
    USE aRSEDIM

    IMPLICIT NONE

    Integer(kind=4)              :: a,x
    Integer(kind=4)              :: nvals
    Integer(kind=4)              :: rk_order !Either 2 or 4
    Real(kind=8)                 :: time_step
    Real(kind=8), Dimension(NCOMPST)    :: vars
    CHARACTER (len=120)          :: input_filename,input_filename1
    CHARACTER (len=120)          :: output_filename, output_filename1
    CHARACTER (len=120)          :: reaction_set, reaction_set1
    integer*1, Dimension (50):: input_filename1A, output_filename1A,
reaction_set1A

!REMEMBER: change Interfaces to syntax suggested by Steve on IVF forum
Interface to Subroutine Initialize ( input_xml, output_xml, rsname )
      !DEC$ Attributes C, DLLIMPORT, alias: "_Initialize" :: Initialize
      integer*1, Dimension (50):: input_xml, output_xml, rsname !new input
files as arrays of chars instead of strings

 !     Character*(*) input_xml       'old string file name
 !     Character*(*) output_xml      'old string file name
 !     Character*(*) rsname
      !DEC$ Attributes REFERENCE :: input_xml
      !DEC$ Attributes REFERENCE :: output_xml
      !DEC$ Attributes REFERENCE :: rsname
    END

    Interface to Subroutine PreSolve ( num_var, vars )
      !DEC$ Attributes C, DLLIMPORT, alias: "_PreSolve" :: PreSolve
      Integer(kind=4)                     :: num_var
      Real(kind=8), Dimension(num_var)    :: vars
```

```
    End

    Interface to Subroutine PostSolve ( num_var, vars )
    !DEC$ Attributes C, DLLIMPORT, alias: "_PostSolve" :: PostSolve
      Integer(kind=4)                     :: num_var
      Real(kind=8), Dimension(num_var)    :: vars
    End

    Interface to Subroutine RKSolve ( time_step, rk_order, num_var, vars )
    !DEC$ Attributes C, DLLIMPORT, alias: "_RKSolve" :: RKSolve
      Integer(kind=4)                     :: num_var
      Integer(kind=4)                     :: rk_order
      Real(kind=8)                        :: time_step
      Real(kind=8), Dimension(num_var)    :: vars
    End

    Interface to Subroutine SetGlobalValues ( num_var, vars )
    !DEC$ Attributes C, DLLIMPORT, alias: "_SetGlobalValues" ::
SetGlobalValues
      Integer(kind=4)                     :: num_var
      Real(kind=8), Dimension(num_var)    :: vars
    End

    nvals = NCOMPS
    rk_order = RKORDER
    time_step = DTFTLOADDS*60

!   Name of the input xml file (here, wq_input_file.xml)
    input_filename1A = XMLINPUTC
!   Name of the component output file, only used to double check the inputs
    output_filename1A = XMLOUTPUTC
!   Name of the reaction set to use - set to the same as in the input xml
file
    reaction_set1A = XMLREAC_SETC

!   MUST initialize the passed in values to 0.0
!   New values of conc's are stored here @ vars
    IF(INITIATE.EQ.1)THEN
        DO a = 1, NCOMPS !NCOMPST
            vars(a) = 0.0
        ENDDO
        INITIATE=2
    ENDIF

    DO a = 1, NCOMPS
        vars(a) = C1_aRSE(a,CELLNO)
    ENDDO

    IF (INITIATE.EQ.2) THEN
        CALL Initialize( input_filename1A, output_filename1A, reaction_set1A
)
        INITIATE=3
    ENDIF

    CALL PreSolve(nvals, vars)

    CALL RKSolve(time_step, rk_order, nvals, vars) !why nvals and not
```

```
num_var?

    CALL PostSolve(nvals, vars)

 !  Nvals should be replaced with nvarX equivalent because only vars(1) and
vars(2) are changed
    DO a = 1, NCOMPS
        IF(a.LE.NVARS) THEN
            IF(vars(a).LT.0) vars(a)=0.0
        ENDIF
        C1_aRSE(a,CELLNO) = vars(a)
    ENDDO

 20 FORMAT (I3, I3, E16.4, E16.4)
    RETURN
    END
```

Subroutine CELLCOUNT

```
SUBROUTINE CELLCOUNT

!*********************************************************************
! This subroutine: counts the number of active cells
!*********************************************************************

    USE SWIFTDIM
    USE aRSEDIM

    IMPLICIT NONE

    INTEGER NUMCELLS,NCELLSIRK,IRK_aRSE,COUNTCELLS,CELLSCOUNTED,COUNTOFF

!*********************************************************************

    COUNTOFF = 0
    IF(COUNTOFF.EQ.1) GOTO 10

    DO IRK=1,NOROWS
       MSTART = IROCOL(2,IRK)
        MEND = IROCOL(3,IRK)
        NCELLSIRK = MEND - MSTART + 1
        NUMCELLS = NUMCELLS + NCELLSIRK
    ENDDO
    NCELLS=NUMCELLS


 10 RETURN
    END
```

Section B3

READIWQ Input File

The nature of the XML interface, on which aRSE relies to obtain the names and values of the model components (i.e. state variables and parameters), is such that aRSE relies on the numeric order in which each component appears in order to correctly match name and value. Given that the number of user-defined state variables and parameters can change, so too then can the numeric reference and it is therefore necessary to run aRSE once in order to determine what the appropriate position is for the various components, unique to the given model setup. This is obviously undesirable for automated calling of aRSE (and is an artifact of the parent version TaRSE) because it requires that the user execute the model prior to using it.

This input file's purpose is to avoid the necessity for calling aRSE prior to using it, and is predicated on the fact that the number of intrinsic parameters in the model is constant (there are 27), that the state variables appear first in the input XML file, and that the user-defined parameters appears last. The appropriate numeric positions of all components can therefore be determined by knowing what and how many state variables there are, and what and how many user-defined parameters there are. This information is entered in this .IWQ file, read by the model, and used accordingly.

Table B-1. Explanation of the READIWQ input file structure and read in parameters

Line number	Variable	Explanation
1	WQFLAG	Flag for running water-quality module (unused)
	NMOB	Number of mobile state-variables specified in input XML
	NSTAB	Number of stabile state-variables specified in input XML
	NPAR	Number of user-specified parameters specified in input XML
	K_WET	Flag to exchange wet/dry conditions. If used, this parameter must be specified as the final user-input parameter (see code in aRSE_IN subroutine)
	ATM_NPAR	Flag to indicate atmospheric deposition, read in by FTLOADDS from ATMDEP.dat input file, must be passed to aRSE. If 0, then not, if > 0 then the input number must correspond with the position of the parameter in the list of user-input parameters e.g. ATM_NPAR=2 indicates that the second nput parameter in the input XML is the atmospheric deposition rate parameter (the name must match that used in Line 6 of the .IWQ)
2	XMLINPUT	Name of the XML input file
	XMLOUPUT	Name of the XML output file (not used)

Table B-1. Continued

Line number	Variable	Explanation
2	XMLREAC_SET	Name of the XML reaction set tag
3	VARNAME(i); C2(i)	For i=1 to NMOB, each mobile state-variable name must be given (VARNAME) along with it's corresponding initial condition (C2)
4	VARNAME(j); C2(j)	For j=NMOB to NMOB+NSTAB, each stabile state-variable name must be given (VARNAME) along with its corresponding initial condition (C2)
5	NPRZ(s)	For s=1 to NSTAB, the printing interval must be given. Currently not used, but included for anologous control to that offered by NPRR for constituent printing in SWIFT2D
6	VARNAME(k); C2(k)	For k=j+28 to j+28+NPAR, each user-specified parameter name must be given (VARNAME) along with its corresponding constant value (C2)
7	MM	Flag to specify whether intrinsic variables are read directly in from .IWQ file in Line 8. If MM=1 then values read in from Line 8
8	VARNAME(x); C2(x)	The position (x) of the desired intrinsic variable in the list of intrinsiic parmaters must be known, and its name (VARNAME) and value (C2) given if MM is 1

Section B4

Nash-Sutcliffe Calculation for Analytical Testing

The following program and and subroutines were written for the purpose of calculating spatially-distributed Nash-Sutcliffe efficiencies in the comparison of analytical and numerical solutions.

Program STUPOSTPROCESS

```
PROGRAM StuPOSTPROCESS

!***************************************************************************!
!                                                                           !
!  PROGRAM: StuPOSTPROCESS                                                  !
!                                                                           !
!  PURPOSE: To run stats on FTLOADDSaRSE results using CORSTAT.  When       !
!  called, the number of measurements in the time-series to be used in the  !
!  statistics (TOTALTIN), and the number of cells to be assessed by rows    !
!  (NMAXIN) and columns (MMAXIN)                                            !
!                                                                           !
```

```
!************************************************************************!
    USE GLOBAL
    IMPLICIT NONE

    integer :: err, SURFERVID,TOTALTI,YES

    !Read in the number of measurements in the time-series

55  CALL GETARG(1,ARGUMENT1)
    READ(ARGUMENT1,'(A6)') SURFERCASE

    CALL GETARG(2,ARGUMENT2)
    READ(ARGUMENT2,'(I5)') TOTALTF

    CALL GETARG(3,ARGUMENT3)
    READ(ARGUMENT3,'(I5)') NMAX

    CALL GETARG(4,ARGUMENT4)
    READ(ARGUMENT4,'(I5)') MMAX

    CALL GETARG(5,ARGUMENT5)
    READ(ARGUMENT5,'(I2)') SURFERVID

50  OPEN(300,FILE="C:\Users\Stuart Muller\Documents\Visual Studio
2008\Projects\FTLOADDSaRSE_v2.8\FTLOADDS_Test_Case_v3\FTLOADDS\SurferCases.tx
t",&
            STATUS='REPLACE')


    IF(SURFERVID.EQ.99) THEN
        GOTO 100
    ELSE
        CALL SUB(NMAX,MMAX,TOTALTF)
        TOTALT=TOTALTF
        GOTO 200
    ENDIF

100 DO TOTALT=2,TOTALTF
        CALL SUB(NMAX,MMAX,TOTALTF)

200     IF(TOTALT.LT.10) THEN
            TOTALTI=1
            WRITE(SURFERSTRING1,'(I<TOTALTI>)') TOTALT
        ELSEIF(TOTALT.LT.100) THEN
            TOTALTI=2
            WRITE(SURFERSTRING2,'(I<TOTALTI>)') TOTALT
        ELSEIF(TOTALT.GE.100) THEN
            TOTALTI=3
            WRITE(SURFERSTRING3,'(I<TOTALTI>)') TOTALT
        ENDIF


        CALL POSTPROCESS

        IF(SURFERVID.NE.99) GOTO 300

        DEALLOCATE(C1,C2)
```

```
    ENDDO

300 CONTINUE


    END PROGRAM StuPOSTPROCESS
```

Subroutine POSTPROCESS

```
    SUBROUTINE POSTPROCESS

    USE GLOBAL
!C**********************************************************************
********
! This subroutine combines the prepared results from FTLOADDSaRSE
(LCONR1_AN.txt)   !
! and 3DADE (CXTFIT.OUTe) into CORSTAT.TXT for statistical processing
!
!**********************************************************************
*******!

    IMPLICIT NONE

    CHARACTER*50 MODELFILE,MODFILE,ANALFILE,ANALYTFILE

    INTEGER t,i,j !!,TOTALT,NMAX,MMAX


!Input files must be of the format INTEGER, REAL(OBS), REAL(SIM)
!The integer is the code for a given time series of data (NCOD in CORSTAT),
and increments up when a new series is encountered (this
!is not used currently)

    MODELFILE='..\output\LCONR1_AN.txt'
    OPEN(100,FILE=MODELFILE,STATUS='OLD')

    ANALYTFILE='..\output\CXTFIT.OUTe'
    OPEN(101,FILE=ANALYTFILE,STATUS='OLD')

    DO t=1,TOTALT
        DO j=1,MMAX
            DO i=1,NMAX
                READ(100,'(F8.4)',END=1010) C1(i,j,t)   !Read in model
outputs
                READ(101,'(F8.4)',END=1010) C2(i,j,t)   !Read in analytical
model outputs
            ENDDO
        ENDDO
    ENDDO
    PRINT*, "Reads complete"
    !pause
    GOTO 1011

1010PRINT*, "Specified time-series exceeds either observed or simulated data
input"
```

```
1011CONTINUE


1020CONTINUE
    DO j=1,MMAX
        DO i= 1,NMAX
            CALL CORSTAT(i,j,TOTALT)
        ENDDO
    ENDDO

1008FORMAT(I3,F8.4,1X,F8.4)

    PRINT*, 't:',t,'m:',j,'n:',i

    END
```

Subroutine CORSTAT

```
SUBROUTINE CORSTAT(NN,MM,TOTALI)

!C**************************************************************************
!C*      WRITTEN FOR: Paper on VFSMOD development and testing (J.of Hyd) *
!C*      Last Updated:June 29, 1998.                                     *
!C*           CORSTAT, 5/20/87, VER. 0.1, J.E. PARSONS                   *
!C*           REVISED: 5/11/93, VER, 0.3, R. MUNOZ-CARPENA               *
!C*           UPDATED: 06/04/02, VER, 0.7, R. MUNOZ-CARPENA              *
!C*                                e-mail: carpena@ufl.edu
*
!C*           ADAPTED: 2/7/10 S. MULLER (!SJM) for FTLOADDSaRSE          *
!C*     CREDITS: (c) 1986-92 Numerical Recipes Software iPJ-5.1:#>0K!.   *
!C*     USES:(c)Numerical recipes: tptest, avevar, betai,gammaln, betacf *
!ccccccccccccccccccccccccccccccccccccccccccccccccccccccccccccccccccccccc
!C*           CORSTAT, 5/20/87, VER. 0.1, J.E. PARSONS                   *
!C*           REVISED: 5/11/93, VER, 0.3, R. MUNOZ-CARPENA               *
!C*           LAST UPDATED: 29/6/98, VER, 0.5, R. MUNOZ-CARPENA          *
!C*    THIS PROGRAM COMPUTES A NUMBER OF STATISTICS FOR THE              *
!C*     COMPARISON OF TWO TIME SERIES, FOR EXAMPLE, AN OBSERVED AND A    *
!C*     SIMULATED ONE.   THE STATISTICS ARE:                             *
!C*      1) MEAN ERROR                                                   *
!C*      2) STANDARD DEVIATION                                           *
!C*      3) SERIAL CORELATION COEF.                                      *
!C*      4) COEFICIENT OF PERFORMANCE                                    *
!C*      5) COEFICIENT OF PERFORMANCE CORRECTED FOR VARIATION OF THE     *
!C*          OF THE RECORDED PROCESS                                     *
!C*      6) PEARSON MOMENT AND THE WEIGHTED MOMENT                       *
!C*  RMC-7) Correlation coefficient for the 1:1 line                     *
!C*  RMC-8) Paired t-test to check for differences in series means       *
!C*          (from Numerical Recipes)                                    *
!C*                                                                      *
!C*    These are computed for the absolute value of the error and the    *
!C*    error.                                                            *
!C*    These measures are defined and discussed in:                      *
!C*                                                                      *
!C* 1. Aitken, A.P. 1973. Assesing systematic errors in rainfall-runoff  *
```

```
!C*    models. J. of Hydrology. 20:121-136.                              *
!C* 2. James, L.D. and S.J. Burges. 1982. Selection, calibration, and    *
!C*    testing of hydrologic models by. In Hydrologic Modeling of Small  *
!C*    Watersheds, Chapter 11,  ed. C. T. Haan, H. P. Johnson and D. L.  *
!C*    Brakensiek.  pages 435-472.  ASAE monograph no. 5. St. Joseph.    *
!C* 3. McCuen, R.H. and W.M. Snyder. 1975. A proposed index for          *
!C*    comparing hydrographs. Water Resour. Res. (AGU).11(6):1021-1024.  *
!C* 4. Press et al., 1992. Numerical Recipes in Fortran. 2nd, edition.   *
!C*    Cambridge: Cambridge University Press                             *
!C*                                                                      *
!C*   Definition of variables                                        *
!C**********************************************************************
      USE GLOBAL, ONLY:
C1,C2,SURFERSTRING1,SURFERSTRING2,SURFERSTRING3,TOTALT,SURFERCASE

      IMPLICIT DOUBLE PRECISION (A-H,O-Z)
      character*16 dummyf1
      CHARACTER*6 VARBLE
      CHARACTER*50 FLABEL
      PARAMETER(NPTS=500)
      REAL prob1,t1,data1(NPTS),data2(NPTS)
      DIMENSION NCOD(5000),OBS(5000),SIM(5000),AERR(5000),&
      ERR(5000),NCD(101),NTC(101),SUM(4),SUMSQ(4),CSS(4),DAERR(1000),&
      DREC(1000),VAR(4)

    INTEGER MM,NN,TOTALI,FILELABELS,ALLOCATEARRAY
    DATA FILELABELS/0/
    DATA ALLOCATEARRAY/0/


      OPEN (UNIT=10,FILE='NUL')

      IDIAG=0
      I=1
      INC=0
      KC=0
      NC=0
      mycount=0
    !SJM: Removing FLABEL read because CORSTATIN.txt not being written with
headers
      !READ(8,*)FLABEL
!10  READ(8,*,END=20)NCOD(I),OBS(I),SIM(I)

    !SJM: Instead of a READ now transferring data between arrays. Note, still
jumps to 20
    !when OBS and SIM are filled
    DO I=1,TOTALI
        NCOD(I)=1
        !!OBS(I)=OBSC1(NN,MM,I)
        OBS(I)=C1(NN,MM,I)
        !!SIM(I)=SIMC2(NN,MM,I)
        SIM(I)=C2(NN,MM,I)
!c-- Debug     ----
!c        print*,ncod(i),obs(i),sim(i)
!c-- End Debug ----
      ERR(I)=SIM(I)-OBS(I)
      AERR(I)=DABS(ERR(I))
```

```
!C*** COUNT THE DIFFERENT CODES
      IF (NC.EQ.NCOD(I)) THEN
            INC=INC+1
            NTC(KC)=INC
      ELSE
            KC=KC+1
            NC=NCOD(I)
            NCD(KC)=NC
            INC=1
      ENDIF
    !SJM: Deleted because DO loop automatically updates I
!     I=I+1
      ENDDO
20  CONTINUE
!C** ZERO OUT THE STATISTICS ARRAYS
      NOBS=I
      IST=1
      DO 25 K=1,KC
          DO 24 J=1,4
              SUM(J)=0.D0
            SUMSQ(J)=0.D0
24      CONTINUE
          CROSS=0.D0
          cosse=0.d0
          NOBK=NTC(K)+IST-1  !!!!!!!!!!!!GRRR
        KOUNT=0
        DO 30 I=IST,NOBK
            KOUNT=KOUNT+1
            DAERR(KOUNT)=AERR(I)
            DREC(KOUNT)=OBS(I)
            SUM(1)=SUM(1)+ERR(I)
            SUM(2)=SUM(2)+AERR(I)
            SUM(3)=SUM(3)+OBS(I)
            SUM(4)=SUM(4)+SIM(I)
            SUMSQ(1)=SUMSQ(1)+ERR(I)*ERR(I)
            SUMSQ(2)=SUMSQ(2)+AERR(I)*AERR(I)
            SUMSQ(3)=SUMSQ(3)+OBS(I)*OBS(I)
            SUMSQ(4)=SUMSQ(4)+SIM(I)*SIM(I)
            CROSS=CROSS+OBS(I)*SIM(I)
            cosse=cosse+(obs(i)-sim(i))*(obs(i)-sim(i))
            data1(KOUNT)=OBS(I)
            data2(KOUNT)=SIM(I)
30      CONTINUE
        mycount=mycount+1
        XPOINT=DFLOAT(NTC(K))
        ERMEAN=SUM(1)/XPOINT
        AEMEAN=SUM(2)/XPOINT
        OBMEAN=SUM(3)/XPOINT
        SIMEAN=SUM(4)/XPOINT
!C*** DO RESIDUAL MASS CURVES FOR ACCUMMULATED ERRORS
        CPAT=0
        CPBT=0
        CPCT=0
        SECOR=0.D0
        SAECOR=0.D0
        DO 37 I=IST,NOBK
            IF (I.GT.IST) THEN
```

```
                SECOR=SECOR+(ERR(I)-ERMEAN)*(ERR(I-1)-ERMEAN)
                SAECOR=SAECOR+(AERR(I)-AEMEAN)*(AERR(I-1)-AEMEAN)
              ENDIF
              ERS=0.D0
              ERD=0.D0
              ERD2=0.D0
              DO 36 II=IST,I
                   ERS=ERS+ERR(II)
                     ERD=ERD+OBS(II)
                   ERD2=ERD2+(OBS(II)-OBMEAN)
36            CONTINUE
              XJP=DFLOAT(I-IST+1)
              XJP2=XJP*XJP
              CPAT=CPAT+ERS*ERS/XJP2
              CPBT=CPBT+(ERS/ERD)*(ERS/ERD)/XJP2
!c            CPCT=CPCT+(ERS/ERD2)*(ERS/ERD2)/XJP2
37          CONTINUE
!C          CPAT=CPAT/XPOINT
!C          CPBT=CPBT/XPOINT
!C          CPCT=CPCT/XPOINT
              IST=NOBK+1
              IF (IDIAG.EQ.1) THEN
                  WRITE(10,90)XPOINT,K,NCD(K)
   90           FORMAT(/,/,/,10X,'***** DIAGNOSTICS PRIOR TO CALCULATIONS FOR:',&
              /,20X,'NPOINTS=',I6,' SERIES NO.=',I4,' SERIES CODE=',I5,&
              /,10X,'SUM OF DATA',10X,'SUM OF SQUARES')
                DO 91 KK=1,4
                  WRITE(10,89)SUM(KK),SUMSQ(KK)
   89             FORMAT(5X,F15.5,9X,F15.5)
   91           CONTINUE
              WRITE(10,88)CROSS
   88         FORMAT(/,10X,'CROSS PRODUCT SUM (REC*SIM)=',F15.5,/,/)
          ENDIF
          CSS(1)=SUMSQ(1)-2*ERMEAN*SUM(1)+XPOINT*ERMEAN*ERMEAN
          CSS(2)=SUMSQ(2)-2*AEMEAN*SUM(2)+XPOINT*AEMEAN*AEMEAN
          CSS(3)=SUMSQ(3)-2*OBMEAN*SUM(3)+XPOINT*OBMEAN*OBMEAN
          CSS(4)=SUMSQ(4)-2*SIMEAN*SUM(4)+XPOINT*SIMEAN*SIMEAN
          VAR(1)=CSS(1)/XPOINT
          VAR(2)=CSS(2)/XPOINT
          VAR(3)=CSS(3)/XPOINT
          VAR(4)=CSS(4)/XPOINT
          XP1=(XPOINT-1.D0)
          SEM=CSS(1)/(XP1)
          AEM=SUM(2)/XPOINT
!c      RMSE=DSQRT(CSS(1)/XPOINT)
!c----change based on Marlon's comments (07/06/93)----------
            RMSE=DSQRT(SUMSQ(1)/XPOINT)
            ERSTD=DSQRT(CSS(1)/(XP1))
            AESTD=DSQRT(CSS(2)/(XP1))
            OBSTD=DSQRT(CSS(3)/(XP1))
            SISTD=DSQRT(CSS(4)/(XP1))
            SECOR=SECOR/(ERSTD*ERSTD*(XP1))
            SAECOR=SAECOR/(AESTD*AESTD*(XP1))
!c -rmc-06/02---
!c      RPEARM=(CROSS-OBMEAN*SUM(4)-SIMEAN*SUM(3)
!c       ! + XPOINT*OBMEAN*SIMEAN)/(OBSTD*SISTD*XPOINT)
            RPEARM=(XPOINT*CROSS-SUM(4)*SUM(3))/SQRT((XPOINT*SUMSQ(3)-SUM(3)*&
```

```
        SUM(3))*(XPOINT*SUMSQ(4)-SUM(4)*SUM(4)))
          R2PEAR=RPEARM*RPEARM
          W=SISTD/OBSTD
          IF (W.GT.1.D0) THEN
              WGHTRP=RPEARM/W
          ELSE
              WGHTRP=RPEARM*W
          ENDIF
          CPAP=1.D0-SUMSQ(1)/CSS(3)
          SLPNI=CROSS/SUMSQ(3)
          SLPI=(CROSS-SUM(3)*SUM(4)/XPOINT)/(SUMSQ(3)-SUM(3)*SUM(3)/XPOINT)
          YINT=SIMEAN-SLPI*OBMEAN
          CORI=SLPI*OBSTD/SISTD
!C*** EJS --- R-SQUARED TO MATCH SAS
          SSINT=SUM(4)*SUM(4)/XPOINT
          EJDEN1=SUMSQ(3)-SUM(3)*SUM(3)/XPOINT
          EJDEN2=SUMSQ(4)-SUM(4)*SUM(4)/XPOINT
          EJSNUM=(CROSS-SUM(3)*SUM(4)/XPOINT)
          SSB1B0=SLPI*EJSNUM
          RESID=SUMSQ(4)-SSINT-SSB1B0
          EMSRES=RESID/(XPOINT-2.D0)
          STESLP=DSQRT(EMSRES/EJDEN1)
          STEINT=DSQRT(EMSRES*SUMSQ(3)/(XPOINT*EJDEN1))
!C*** COMPUTATIONS FOR NO INT ?
          SSB1=SLPNI*EJSNUM
          RESNI=SUMSQ(4)-SSB1
          EMSRNI=RESNI/(XPOINT-1.D0)
          SESLPN=DSQRT(EMSRNI/EJDEN1)
          CD=SSB1/EJDEN2
          CALL GMEDN(KOUNT,DAERR,DREC,OBMEAN,R29)
          R21TOP=SUMSQ(3)-2.D0*CROSS+SUMSQ(4)
          R21=1.D0 - R21TOP/CSS(3)
          R22TOP=SUMSQ(4)-2.D0*SUM(4)*OBMEAN+ XPOINT*OBMEAN*OBMEAN
          R22=R22TOP/CSS(3)
          R23=CSS(4)/CSS(3)
          R24=1.D0 - CSS(1)/CSS(3)
          R27=1.D0 - R21TOP/SUMSQ(3)
!c    print*,obstd,covaryyc
          R28=SUMSQ(4)/SUMSQ(3)

          WRITE(10,100)NCD(K),XPOINT
  100     FORMAT(/,10X,&
          'SUMMARY STATISTICS FOR COMPARING TWO SERIES OF OBSERVED vs.',&
          ' PREDICTED VALUES',/,10X,'SERIES CODE =',I4,10X,&
          'NUMBER OF SERIES POINTS=',F6.0,/)
          WRITE(10,*)'    VARIABLE      SUM           MEAN         SUMSQ&
              CORR. SS     SAMP.STD.     VARIANCE     COEF. OF VAR.'
          WRITE(10,*)
            VARBLE='ERROR'
            CV=ERSTD/ERMEAN
            WRITE(10,102)VARBLE,SUM(1),ERMEAN,SUMSQ(1),CSS(1),ERSTD,VAR(1),CV
            VARBLE='AERROR'
            CV=AESTD/AEMEAN
            WRITE(10,102)VARBLE,SUM(2),AEMEAN,SUMSQ(2),CSS(2),AESTD,VAR(2),CV
            VARBLE='OBSED'
            CV=OBSTD/OBMEAN
            WRITE(10,102)VARBLE,SUM(3),OBMEAN,SUMSQ(3),CSS(3),OBSTD,VAR(3),CV
```

```
          VARBLE='SIMED'
          CV=SISTD/SIMEAN
          WRITE(10,102)VARBLE,SUM(4),SIMEAN,SUMSQ(4),CSS(4),SISTD,VAR(4),CV
!c  102 FORMAT(5X,A6,5X,E12.3,5X,e11.4,5X,e15.4,5X,e11.4,5X,e10.5,
!c     !    5X,e10.5,5X,e11.4)
  102   FORMAT(5X,A6,E14.4,e14.4,e14.4,e14.4,e14.4,e14.4,e14.4)
          WRITE(10,103)RPEARM,WGHTRP,R2PEAR,R21,R22,R23,R24,R27,R28,R29
        WRITE(10,105)RMSE,AEM,SEM
103     FORMAT(/,/,5X,'***** CORREL. COMPARISONS ******',&
        /,15X,'PEARSON MOMENT    =',F10.5,'  (FIRST TWO CORREL. TYPES)',&
        /,15X,'WGHTED PEAR. MOM. =',F10.5,'  (EQN 11.13)',&
        /,15X,'PEAR. MOM. SQUAR. =',F10.5,'  (KVALSETH R25, R26 MULT. R)',&
        '  (NOTE: FROM HERE DOWN R-SQUARED TYPES)',&
        /,15X,'KVALSETH R21      =',F10.5,'  (0<=R21<=1, GENERALLY)',&
        '   (1 - RATIO OF SUM (OBS-SIM)**2/ CSS-OBS)',&
        /,15X,'KVALSETH R22      =',F10.5,'  (MAY EXCEED 1)',&
        '   ( RATIO OF SUM (SIM-OBMEAN)**2/ CSS-OBS)',&
        /,15X,'KVALSETH R23      =',F10.5,'  (MAY EXCEED 1)',&
        '   ( RATIO OF CSS-SIM/ CSS-OBS)',&
        /,15X,'KVALSETH R24      =',F10.5,'  (0<=R24<=1, GENERALLY)',&
        '   (1 - RATIO OF CSS-ERR/ CSS-OBS)',&
        /,15X,'KVALSETH R27      =',F10.5,'  (RECOMMEND LINEAR NOINT.)',&
        '   (1 - RATIO OF SUM ERR**2/ SUM OBS**2)',&
        /,15X,'KVALSETH R28      =',F10.5,'  (RECOMMEND LIN. NOINT.)',&
        '   ( R28 MAY EXCEED 1, RATIO OF SUM SIM**2/ SUM OBS**2)',&
        /,15X,'KVALSETH R29      =',F10.5,'  (RESISTANT OR ROBUST FIT)')
  105   FORMAT(15X,'ROOT MEAN SQ. ERR.=',E14.5,'  [(OBS-SIM)**2/N)**.5]',&
        /,15X,'MEAN ABS. ERROR   =',E14.5,&
        /,15X,'MEAN SQ. ERROR    =',E14.5,'  (ASS. ONE MODEL PARAMETER)',&
        '   [(OBS-SIM)**2/(N-1)]')
          WRITE(10,104)CPAP,SECOR,SAECOR
  104   FORMAT(15X,'COEF. OF EFF. (NASH AND SUTCLIFF) =',F15.5,&
        '     (RATIO SS-ERR/ CSS-OBS)',/,&
        15X,'SERIAL CORR. (ERROR)     =',F10.5,5X,'LAG 1',&
        /,15X,'SERIAL CORR. (ABS. ERROR)=',F10.5,5X,'LAG 1')


!SJM: Write results for graphing in Surfer
        !@!IF(SURFERVID.EQ.99) THEN !Calculating stats at multiple time to
make a video
            IF(TOTALT.LT.10) THEN

OPEN(1100+TOTALT,FILE='Surfer'//SURFERCASE//'_T'//SURFERSTRING1//'.dat')
            ELSEIF(TOTALT.LT.100) THEN

OPEN(1100+TOTALT,FILE='Surfer'//SURFERCASE//'_T'//SURFERSTRING2//'.dat')
            ELSEIF(TOTALT.GE.100) THEN

OPEN(1100+TOTALT,FILE='Surfer'//SURFERCASE//'_T'//SURFERSTRING3//'.dat')
            ENDIF

            !Print one line of headers
            IF(FILELABELS.EQ.0) THEN
                WRITE(1100+TOTALT,'(2A5,4A12)') "X", "Y", "RMSE", "AEM",
"SEM", "CPAP(N-S)"
                FILELABELS=1
            ENDIF
```

```
            IF(CPAP.NE.CPAP) CPAP=10
            WRITE(1100+TOTALT,'(2I5,4F12.8)') MM,NN,RMSE,AEM,SEM,CPAP
            IF(CPAP.NE.CPAP) CPAP=10
            WRITE(1100,'(2I5,4F10.4)') MM,NN,RMSE,AEM,SEM,CPAP

          WRITE(10,106)CPAT,CPBT
!c    ,CPCT
  106   FORMAT(/,/,5X,'****** RESIDUAL MASS CURVES (ACCUMULATED ERRORS)',&
        '  DIVIDED BY NPOINTS, SIMILAR TO A VARIANCE',&
        /,15X,'CPAT -- EQN 11.31 =',G13.6,&
        /,15X,'CPBT -- EQN 11.32 =',G13.6,/)
!c ! /,15X,'CPCT -- EQN 11.33 =',G13.6,/)
          CORI2=CORI*CORI
          WRITE(10,109)SLPNI,CD,SESLPN,SLPI,YINT,CORI,CORI2,STESLP,STEINT
  109   FORMAT(/,/,5X,'****** REGRESSION ANALYSIS SIM VS OBS *******',&
        /,10X,'NO-INTERCEPT MODEL, SLOPE =',F10.5,'   JPR-RSQ?=',F10.5,&
        '   JPSTD. ERR. SLP.?=',F10.5,&
        /,10X,'INTERCEPT MODEL, SLOPE    =',F10.5,'  INTERCEPT=',F10.5,&
        '    CORRELATION COEF.=',F8.5,'  CORR**2=',F8.5,&
        /,25X,'STD. ERR. SLOPE =',F10.5,'    STD. ERR. INT. =',F10.5)

!c--rmc----04/93---Error over the 1:1 line, observed vs. predicted ---------
          WRITE(10,*)
          WRITE(10,*)
          WRITE(10,*)'     ****** ERROR MEASURE FROM THE 1:1 LINE ********'

!c --rmc and arr 06/02--- R2= 1-RSSmodel/RSSnull model, where RSS=res. sum
sq.
!c -- null model= line y=cte=ymean=obs_mean; model = 1:1 line = y=x ->
pred=obs
!c -- old--  covaryyc=dsqrt(cosse/(xpoint-2.d0))

          covaryyc=dsqrt(cosse/(xpoint-1.d0))
          rsq1to1=(1.d0-(covaryyc*covaryyc)/(obstd*obstd))
          if(rsq1to1.lt.0)rsq1to1=0
          r1to1=dsqrt(rsq1to1)
          if(rsq1to1.gt.0) then
                WRITE(10,113)covaryyc,r1to1,rsq1to1
          else
                WRITE(10,114)covaryyc
          endif
113     format(10x,'1:1 COVARIANCE OBSERVED vs. PREDICTED = ',E14.4,&
        /,10X,'1:1 SAMPLE COEFFICIENT OF DETERMINATION (R1:1) = ',f10.4,&
        /,10x,'1:1 SAMPLE CORRELATION COEFFICIENT   (RSQ1:1)  = ',f10.4)
114     format(10x,'1:1 COVARIANCE OBSERVED vs. PREDICTED = ',E14.4,&
        /,10X,'1:1 SAMPLE COEFFICIENT OF DETERMINATION (R1:1) < 0.01',&
        /,10x,'1:1 SAMPLE CORRELATION COEFFICIENT   (RSQ1:1)  < 0.01')

!C-----------------------------------------------------------------------
!c--rmc----06/98---Paired t-test ---------
          WRITE(10,*)
          WRITE(10,*)
          WRITE(10,*)'     ******  PAIRED t-TEST  ********'
          call tptest(data1,data2,KOUNT,t1,prob1)
          if(prob1.ge..05) then
                WRITE(10,120)NCD(K),KOUNT,t1,prob1
```

```
          else
                WRITE(10,121)NCD(K),KOUNT,t1,prob1
          endif
          t1=0.
          prob1=0.
120       format(10x,'No. Series= ',i4,'; n= ',i4,'; t= ',f10.6,&
              '; Prob= ',f10.4,'  Means not significantly different')
121       format(10x,'No. Series= ',i4,'; n= ',i4,'; t= ',f10.6,&
              '; Prob= ',f10.4,' * Means significantly different')

          WRITE(10,111)
111     FORMAT(/,125('-'))
          WRITE(10,112)
112     FORMAT('1')
25  CONTINUE
    CLOSE(8)
      RETURN
      END

      SUBROUTINE GMEDN(N,ER,REC,RECM,R29)
!C**** COMPUTATION OF MEDIANS FOR R29 FROM KVALSETH
      IMPLICIT REAL*8 (A-H,O-Z)
      DIMENSION ER(*),REC(*),TER(1000),DREC(1000)
      DO 5 I=1,N
            TER(I)=ER(I)
            DREC(I)=DABS(REC(I)-RECM)
5     CONTINUE
      DO 10 I=1,N
          DO 9 J=I+1,N
            IF (TER(J).LT.TER(I)) THEN
                  TEM=TER(I)
                  TER(I)=TER(J)
                  TER(J)=TEM
            ENDIF
            IF (DREC(J).LT.DREC(I)) THEN
                  TEM=DREC(I)
                  DREC(I)=DREC(J)
                  DREC(J)=TEM
            ENDIF
9       CONTINUE
10  CONTINUE
      IMED=N/2
      DRM=DREC(IMED)
      ERM=TER(IMED)
      RAT=ERM/DRM
      R29=1.D0-RAT*RAT
      RETURN
      END

    SUBROUTINE tptest(data1,data2,n,t,prob)
    INTEGER n
    REAL prob,t,data1(n),data2(n)
!CU    USES avevar,betai
    INTEGER j
    REAL ave1,ave2,cov,df,sd,var1,var2,betai
!c--rmc-
!c    write(*,*)n,t,prob
```

```
!c    do 5 i=1,n
!c          WRITE(*,*)data1(i),data2(i)
!c5   continue
!c--rmc-
      call avevar(data1,n,ave1,var1)
      call avevar(data2,n,ave2,var2)
      cov=0.
      do 11 j=1,n
          cov=cov+(data1(j)-ave1)*(data2(j)-ave2)
11    continue
      df=n-1
      cov=cov/df
      sd=sqrt((var1+var2-2.*cov)/n)
      t=(ave1-ave2)/sd
      prob=betai(0.5*df,0.5,df/(df+t**2))
      return
      END
!C    (C) Copr. 1986-92 Numerical Recipes Software iPJ-5.1:#>0K!.
      SUBROUTINE avevar(data,n,ave,var)
      INTEGER n
      REAL ave,var,data(n)
      INTEGER j
      REAL s,ep
      ave=0.0
      do 11 j=1,n
          ave=ave+data(j)
11    continue
      ave=ave/n
      var=0.0
      ep=0.0
      do 12 j=1,n
          s=data(j)-ave
          ep=ep+s
          var=var+s*s
12    continue
      var=(var-ep**2/n)/(n-1)
      return
      END
!C    (C) Copr. 1986-92 Numerical Recipes Software iPJ-5.1:#>0K!.
      FUNCTION betacf(a,b,x)
      INTEGER MAXIT
      REAL betacf,a,b,x,EPS,FPMIN
      PARAMETER (MAXIT=100,EPS=3.e-7,FPMIN=1.e-30)
      INTEGER m,m2
      REAL aa,c,d,del,h,qab,qam,qap
      qab=a+b
      qap=a+1.
      qam=a-1.
      c=1.
      d=1.-qab*x/qap
      if(abs(d).lt.FPMIN)d=FPMIN
      d=1./d
      h=d
      do 11 m=1,MAXIT
          m2=2*m
          aa=m*(b-m)*x/((qam+m2)*(a+m2))
          d=1.+aa*d
```

```
        if(abs(d).lt.FPMIN)d=FPMIN
        c=1.+aa/c
        if(abs(c).lt.FPMIN)c=FPMIN
        d=1./d
        h=h*d*c
        aa=-(a+m)*(qab+m)*x/((a+m2)*(qap+m2))
        d=1.+aa*d
        if(abs(d).lt.FPMIN)d=FPMIN
        c=1.+aa/c
        if(abs(c).lt.FPMIN)c=FPMIN
        d=1./d
        del=d*c
        h=h*del
        if(abs(del-1.).lt.EPS)goto 1
11  continue

1   betacf=h
    return
    END
!C  (C) Copr. 1986-92 Numerical Recipes Software iPJ-5.1:#>0K!.
    FUNCTION betai(a,b,x)
    REAL betai,a,b,x
!CU    USES betacf,gammln
    REAL bt,betacf,gammln
    if(x.lt.0..or.x.gt.1.)pause 'bad argument x in betai'
    if(x.eq.0..or.x.eq.1.)then
        bt=0.
    else
        bt=exp(gammln(a+b)-gammln(a)-gammln(b)+a*log(x)+b*log(1.-x))
    endif
    if(x.lt.(a+1.)/(a+b+2.))then
        betai=bt*betacf(a,b,x)/a
        return
    else
        betai=1.-bt*betacf(b,a,1.-x)/b
        return
    endif
    END
!C  (C) Copr. 1986-92 Numerical Recipes Software iPJ-5.1:#>0K!.
    FUNCTION gammln(xx)
    REAL gammln,xx
    INTEGER j
    DOUBLE PRECISION ser,stp,tmp,x,y,cof(6)
    SAVE cof,stp
    DATA cof,stp/76.18009172947146d0,-86.50532032941677d0,&
    24.01409824083091d0,-1.231739572450155d0,.1208650973866179d-2,&
    -.5395239384953d-5,2.5066282746310005d0/
    x=xx
    y=x
    tmp=x+5.5d0
    tmp=(x+0.5d0)*log(tmp)-tmp
    ser=1.000000000190015d0
    do 11 j=1,6
        y=y+1.d0
        ser=ser+cof(j)/y
11  continue
    gammln=tmp+log(stp*ser/x)
```

```
      return
      END
!C  (C) Copr. 1986-92 Numerical Recipes Software iPJ-5.1:#>0K!.
```

APPENDIX C
WATER-QUALITY APPLICATION CODE AND INPUT FILES

Section C1

Additional Subroutines for Water-Quality Inputs

The following two subroutines were required for input of water-quality boundary conditions. The subroutine EDIT_INPUTFILE is used to edit time-series concentrations at specified head boundaries in the Part 3 of the SWIFT2D input file. The subroutine STRUNCTCONCS reads in discharge source concentrations from the INPUTFLOWCONCS.dat input file (see Section C2).

Subroutine EDIT_INPUTFILE

```
PROGRAM Edit_inputfile

    IMPLICIT NONE
    INTEGER X,COUNT1,COUNT2,i,j,NTCT1,LENGTH,DAY,DAYCHK,P3_READ,DAYMAX
    REAL TITI
    CHARACTER THE_REST*60,TEMP*1050,THE_REST_19*19
    CHARACTER*7 BC1(500),BC2(500),BC3(500),BC4(500)
    DATA X,COUNT1,COUNT2,P3_READ,DAYMAX/0,0,0,0,0/

    OPEN(10,FILE='wetlands_PBC_SICS.inp')   !original .inp
    OPEN(20,FILE='wetlands.inp')            !.inp produced by this code
    OPEN(30,FILE='BC_concs.inp')            !source for BC concs

    j=0
    DO WHILE (X.EQ.0)
        j=j+1
        READ(30,*,END=100) DAYCHK,BC1(j),BC2(j),BC3(j),BC4(j)
        WRITE(40,'(I4,1X,A8,1X,A8,1X,A8,1X,A8,1X)')
DAYCHK,BC1(j),BC2(j),BC3(j),BC4(j)
    ENDDO
!
100 CONTINUE

!*****************************!
! Write PART 1 and PART 2 data !
!*****************************!
    DO i=1,1158 !1133 !Look at the .inp file to see what the row number is up
to Part 3 data
        IF(i.GE.806.AND.i.LE.903) THEN
            READ(10,'(A1050)') TEMP
        ELSE
            READ(10,'(A100)') TEMP
```

```
        ENDIF
        LENGTH=LEN_TRIM(TEMP)
        WRITE(20,'(A<LENGTH>)') TEMP
    ENDDO
    PAUSE
    !READ(10,'(A100)') TEMP
    !PRINT*, TEMP
    !PAUSE

    DO WHILE (X.EQ.0)
        READ(10,'(I1,A39)') NTCT1,THE_REST
        LENGTH=LEN_TRIM(THE_REST)
        IF(NTCT1.EQ.0) P3_READ=P3_READ+1
        DAY=P3_READ/96+1
        IF(DAY.GE.499) DAYMAX=1 !498 days of BC input data - after day 498
completed then just copy and repeat remaining lines.
        IF(DAYMAX.EQ.1) GOTO 110
        IF(NTCT1.EQ.0) THEN
            WRITE(20,'(I1,A<LENGTH>)') NTCT1,THE_REST
        ELSEIF(NTCT1.EQ.1) THEN
            THE_REST_19=THE_REST
            COUNT1=COUNT1+1
            IF(COUNT1.LE.4) THEN
                IF(COUNT1.EQ.1) WRITE(20,'(I1,A19,1X,A7)')
NTCT1,THE_REST_19,BC1(DAY)
                IF(COUNT1.EQ.2) WRITE(20,'(I1,A19,1X,A7)')
NTCT1,THE_REST_19,BC2(DAY)
                IF(COUNT1.EQ.3) WRITE(20,'(I1,A19,1X,A7)')
NTCT1,THE_REST_19,BC3(DAY)
                IF(COUNT1.EQ.4) WRITE(20,'(I1,A19,1X,A7)')
NTCT1,THE_REST_19,BC4(DAY)
            ELSEIF(COUNT1.LE.8) THEN
                WRITE(20,'(I1,A19,A8)') NTCT1,THE_REST,'   0.005'
                IF(COUNT1.EQ.8)COUNT1=0
            ENDIF
        ELSEIF(NTCT1.EQ.2) THEN
            THE_REST_19=THE_REST
            COUNT2=COUNT2+1
            IF(COUNT2.LE.4) THEN
                IF(COUNT2.EQ.1) WRITE(20,'(I1,A19,1X,A7)')
NTCT1,THE_REST_19,BC1(DAY)
                IF(COUNT2.EQ.2) WRITE(20,'(I1,A19,1X,A7)')
NTCT1,THE_REST_19,BC2(DAY)
                IF(COUNT2.EQ.3) WRITE(20,'(I1,A19,1X,A7)')
NTCT1,THE_REST_19,BC3(DAY)
                IF(COUNT2.EQ.4) WRITE(20,'(I1,A19,1X,A7)')
NTCT1,THE_REST_19,BC4(DAY)
            ELSEIF(COUNT2.LE.8) THEN
                WRITE(20,'(I1,A19,A8)') NTCT1,THE_REST,'   0.005'
                IF(COUNT2.EQ.8)COUNT2=0
            ENDIF
        ELSEIF(NTCT1.GT.2) THEN
            WRITE(20,'(I1,A<LENGTH>)') NTCT1,THE_REST
        ENDIF
110     IF(DAYMAX.EQ.1) THEN
            IF(NTCT1.EQ.0) WRITE(20,'(I1,A<LENGTH>)') NTCT1,THE_REST
            IF((NTCT1.EQ.1).OR.(NTCT1.EQ.2)) WRITE(20,'(I1,A<LENGTH>)')
```

```
NTCT1,THE_REST
            IF(NTCT1.GT.2) WRITE(20,'(I1,A<LENGTH>)') NTCT1,THE_REST
          ENDIF
        ENDDO

        END PROGRAM Edit_inputfile
```

Subroutine STRUCTCONCS

```
SUBROUTINE STRUCTCONCS
      USE SWIFTDIM
      USE COUPLING
      REAL*4 DAY !STRCFLOWCONC(40),STRCFLOWCONC2(40) - moved to SWIFTDIM
      REAL*8 DAYCHK
      DATA IFIRST/1/,IUSFLOWCONCS/175/
      IF(IFIRST .EQ. 1)THEN
        OPEN(IUSFLOWCONCS,FILE='..\Input\FLOWS\INPUTFLOWCONCS.DAT',
     1    STATUS='OLD',ACCESS='SEQUENTIAL')
        READ(IUSFLOWCONCS,*) NUMSTRUCS
        NUMSTRUCS=NUMSTRUCS+1
        DO J=2,NUMSTRUCS
          READ(IUSFLOWCONCS,*) NFLWPTS(J),NRANGES(J)
          DO I=1,NFLWPTS(J)+2*NRANGES(J)
            READ(IUSFLOWCONCS,*) MSTRUC(J,I),NSTRUC(J,I),IXYFLOW(J,I)
          ENDDO
          NTOTPTS(J)=NFLWPTS(J)
          IF(NRANGES(J).GT.0) THEN
            DO I=NFLWPTS(J)+1,NFLWPTS(J)+2*NRANGES(J)-1,2
              IP1=I+1
              MSTRUC(J,IP1)=MSTRUC(J,IP1)-MSTRUC(J,I)
              NSTRUC(J,IP1)=NSTRUC(J,IP1)-NSTRUC(J,I)
              IF(ABS(MSTRUC(J,IP1)).GT.ABS(NSTRUC(J,IP1)))NSTRUC(J,IP1)=0
                  IF(ABS(NSTRUC(J,IP1)).GT.ABS(MSTRUC(J,IP1)))MSTRUC(J,IP1)=0
              MAXMN=MAX(ABS(MSTRUC(J,IP1)),ABS(NSTRUC(J,IP1)))+1
              NTOTPTS(J)=NTOTPTS(J)+MAXMN
            ENDDO
          ENDIF
        ENDDO
        !If more than one solute (excl salinity and temp) then need to have
one line in inputfile for each L
        !for each day,
        !e.g. Line1: Day1 Conc(L1,strc1) Conc(L1,strc2) Conc(L1,strc3)
        !     Line2: Day1 Conc(L2,strc1) Conc(L2,strc2) Conc(L2,strc3)
        !     Line3: Day2 Conc(L1,strc1) Conc(L1,strc2) Conc(L1,strc3)
        !     Line4: Day2 Conc(L2,strc1) Conc(L2,strc2) Conc(L2,strc3)
        DO L=1,LMAX
          IF(L.EQ.LSAL)GOTO 115  !Skip salinity and temp so don't have to add
these to input file
          IF(L.EQ.LTEMP)GOTO 115
          READ(IUSFLOWCONCS,*)(STRCFLOWCONC(L,J), J=1,NUMSTRUCS)  !Assumes 1
solute
115       CONTINUE
        ENDDO
        DO L=1,LMAX
          IF(L.EQ.LSAL)GOTO 116  !Skip salinity and temp so don't have to add
```

```
these to input file
          IF(L.EQ.LTEMP)GOTO 116
          READ(IUSFLOWCONCS,*)(STRCFLOWCONC2(L,J), J=1,NUMSTRUCS)   !Assumes
1 solute
116       CONTINUE
        ENDDO
        IFIRST=0
      ENDIF
C * * SECTION EXECUTED EVERY TIMESTEP
C * * Convert time in min to Julian days.
      DAY=(KBND+1)*HALFDT/1440.+1.+DAYOFFSTSWIFT
C SJM: WRITE DAY to screen to monitor sim progression
      !WRITE(*,*)DAY !SJM DELETE!
      DO L=1,LMAX
        IF((L.EQ.LSAL).OR.(L.EQ.LTEMP)) GOTO 1166
        IF(DAY.GT.STRCFLOWCONC(L,1)) DAYCHK=STRCFLOWCONC(L,1)  !Assumes data
for different L's given at same time in input file
1166    CONTINUE
      ENDDO
 !10   IF(DAY .GT. STRCFLOWCONC(1))THEN
 10   IF(DAY .GT. DAYCHK)THEN
        STRCFLOWCONC=STRCFLOWCONC2
        !If more than one solute (excl salinity and temp) then need to have
one line in inputfile for each L
        !for each day,
        !e.g. Line1: Day1 Conc(L1,strc1) Conc(L1,strc2) Conc(L1,strc3)
        !     Line2: Day1 Conc(L2,strc1) Conc(L2,strc2) Conc(L2,strc3)
        !     Line3: Day2 Conc(L1,strc1) Conc(L1,strc2) Conc(L1,strc3)
        !     Line4: Day2 Conc(L2,strc1) Conc(L2,strc2) Conc(L2,strc3)
        DO L=1,LMAX
          IF(L.EQ.LSAL)GOTO 117  !Skip salinity and temp so don't have to add
these to input file
          IF(L.EQ.LTEMP)GOTO 117
          READ(IUSFLOWCONCS,*)(STRCFLOWCONC2(L,J), J=1,NUMSTRUCS)   !Assumes
1 solute
          DAYCHK=STRCFLOWCONC(L,1)
117       CONTINUE
        ENDDO
        GO TO 10
      ENDIF
      RETURN
      END
```

Section C2

Important Input Files for the SICS Water-Quality Simulation

Input files and used in the simulation of SICS surface-water phosphorus are presented. These include the input concentrations at discharge sources (INPUTFLOWCONCS.dat), the atmospheric deposition data for each of the three options tested, the SWIFT2D input file (WETLANDS.inp), and the IWQ input file (IWQINPUT.iwq), which are needed by SWIFT2D. The XML input file (XMLINPUT.xml) was required for aRSE.

Format for INPUTFLOWCONCS.dat

```
3
1       0       TSB
90      90      3
1       0       L-31W
100     88      3
1       0       C-111
120     64      3
1.00            0.0044          0.0062          0.003
2.00            0.0044          0.0062          0.003
3.00            0.0044          0.0062          0.003
4.00            0.0044          0.0062          0.003
5.00            0.0044          0.0062          0.003
6.00            0.0044          0.0062          0.003
7.00            0.0044          0.0062          0.003
8.00            0.0044          0.0062          0.003
9.00            0.0044          0.0062          0.003
10.00           0.0044          0.0062          0.003
11.00           0.0044          0.0062          0.003
12.00           0.0044          0.0062          0.003
13.00           0.0044          0.0062          0.003
14.00           0.0044          0.0062          0.003
15.00           0.0044          0.0062          0.003
16.00           0.0044          0.0062          0.003
17.00           0.0044          0.0062          0.003
18.00           0.0101          0.0031          0.0032
19.00           0.0101          0.0031          0.0032
20.00           0.0101          0.0031          0.0032
21.00           0.0101          0.0031          0.0032
22.00           0.0101          0.0031          0.0032
```

23.00	0.0101	0.0031	0.0032
24.00	0.0101	0.0031	0.0032
25.00	0.0101	0.0031	0.0032
26.00	0.0101	0.0031	0.0032
27.00	0.0101	0.0031	0.0032
28.00	0.0101	0.0031	0.0032
29.00	0.0101	0.0031	0.0032
30.00	0.0101	0.0031	0.0032

*incomplete file

Total Phosphorus Atmospheric Deposition Rates for Model 2

Table C-1 below shows the total phosphorus atmospheric deposition rates applied to Model 2 for each of the three atmospheric deposition options tested.

Table C-1. Atmospheric deposition rates input to Model 2

Day	Date	Variable rate proportionate to rain volume [g TP/m^2/d]	Constant rate per rain day [g TP/m^2/d]	Constant rate per day [g TP/m^2/d]
1	07/15/96	9.93915E-05	9.70874E-05	8.2192E-05
2	07/16/96	0.000686837	9.70874E-05	8.2192E-05
3	07/17/96	3.68857E-05	9.70874E-05	8.2192E-05
4	07/18/96	1.12111E-05	9.70874E-05	8.2192E-05
5	07/19/96	1.38821E-05	9.70874E-05	8.2192E-05
6	07/20/96	0.000110112	9.70874E-05	8.2192E-05
7	07/21/96	1.06841E-06	9.70874E-05	8.2192E-05
8	07/22/96	0	0	8.2192E-05
9	07/23/96	2.1441E-05	9.70874E-05	8.2192E-05
10	07/24/96	4.27002E-06	9.70874E-05	8.2192E-05
11	07/25/96	0	0	8.2192E-05
12	07/26/96	0	0	8.2192E-05
13	07/27/96	2.88908E-05	9.70874E-05	8.2192E-05
14	07/28/96	3.36151E-05	9.70874E-05	8.2192E-05
15	07/29/96	0.000136277	9.70874E-05	8.2192E-05
16	07/30/96	1.92605E-05	9.70874E-05	8.2192E-05
17	07/31/96	2.67103E-06	9.70874E-05	8.2192E-05
18	08/1/96	2.39848E-05	9.70874E-05	8.2192E-05
19	08/2/96	2.1441E-06	9.70874E-05	8.2192E-05
20	08/3/96	0.000190788	9.70874E-05	8.2192E-05
21	08/4/96	1.33552E-05	9.70874E-05	8.2192E-05
22	08/5/96	2.5075E-05	9.70874E-05	8.2192E-05
23	08/6/96	0.000323431	9.70874E-05	8.2192E-05
24	08/7/96	1.06841E-06	9.70874E-05	8.2192E-05

Table C-1. Continued

Day	Date	Variable rate proportionate to rain volume [g TP/m^2/d]	Constant rate per rain day [g TP/m^2/d]	Constant rate per day [g TP/m^2/d]
25	08/8/96	0.000174071	9.70874E-05	8.2192E-05
26	08/9/96	1.06841E-05	9.70874E-05	8.2192E-05
27	08/10/96	6.41411E-06	9.70874E-05	8.2192E-05
28	08/11/96	5.86901E-06	9.70874E-05	8.2192E-05
29	08/12/96	0	0	8.2192E-05
30	08/13/96	2.83457E-05	9.70874E-05	8.2192E-05
31	08/14/96	2.94359E-05	9.70874E-05	8.2192E-05
32	08/15/96	8.64906E-05	9.70874E-05	8.2192E-05
33	08/16/96	4.76062E-05	9.70874E-05	8.2192E-05
34	08/17/96	1.76252E-05	9.70874E-05	8.2192E-05
35	08/18/96	0.000174617	9.70874E-05	8.2192E-05
36	08/19/96	0.000723178	9.70874E-05	8.2192E-05
37	08/20/96	0.000256201	9.70874E-05	8.2192E-05
38	08/21/96	0.000159717	9.70874E-05	8.2192E-05
39	08/22/96	0.00018352	9.70874E-05	8.2192E-05
40	08/23/96	0.000261652	9.70874E-05	8.2192E-05
41	08/24/96	4.59709E-05	9.70874E-05	8.2192E-05
42	08/25/96	5.34207E-07	9.70874E-05	8.2192E-05
43	08/26/96	0.000110657	9.70874E-05	8.2192E-05
44	08/27/96	4.90598E-05	9.70874E-05	8.2192E-05
45	08/28/96	1.12111E-05	9.70874E-05	8.2192E-05
46	08/29/96	2.67103E-06	9.70874E-05	8.2192E-05
47	08/30/96	4.48806E-05	9.70874E-05	8.2192E-05
48	08/31/96	9.61209E-06	9.70874E-05	8.2192E-05
49	09/1/96	6.46863E-05	9.70874E-05	8.2192E-05
50	09/2/96	0.000160807	9.70874E-05	8.2192E-05
51	09/3/96	7.37714E-05	9.70874E-05	8.2192E-05
52	09/4/96	1.38821E-05	9.70874E-05	8.2192E-05
53	09/5/96	0.000120106	9.70874E-05	8.2192E-05
54	09/6/96	9.61209E-06	9.70874E-05	8.2192E-05
55	09/7/96	7.48616E-06	9.70874E-05	8.2192E-05
56	09/8/96	5.92352E-05	9.70874E-05	8.2192E-05
57	09/9/96	0.000437904	9.70874E-05	8.2192E-05
58	09/10/96	0.000688654	9.70874E-05	8.2192E-05
59	09/11/96	2.28946E-05	9.70874E-05	8.2192E-05
60	09/12/96	0.000120651	9.70874E-05	8.2192E-05
61	09/13/96	6.41411E-06	9.70874E-05	8.2192E-05
62	09/14/96	0.000113746	9.70874E-05	8.2192E-05
63	09/15/96	1.01572E-05	9.70874E-05	8.2192E-05

Table C-1. Continued

Day	Date	Variable rate proportionate to rain volume [g TP/m^2/d]	Constant rate per rain day [g TP/m^2/d]	Constant rate per day [g TP/m^2/d]
64	09/16/96	2.56201E-05	9.70874E-05	8.2192E-05
65	09/17/96	0.000174071	9.70874E-05	8.2192E-05
66	09/18/96	8.43102E-05	9.70874E-05	8.2192E-05
67	09/19/96	9.50307E-05	9.70874E-05	8.2192E-05
68	09/20/96	0.000325248	9.70874E-05	8.2192E-05
69	09/21/96	0.000190788	9.70874E-05	8.2192E-05
70	09/22/96	4.76062E-05	9.70874E-05	8.2192E-05
71	09/23/96	0.000170437	9.70874E-05	8.2192E-05
72	09/24/96	6.30509E-05	9.70874E-05	8.2192E-05
73	09/25/96	0	0	8.2192E-05
74	09/26/96	4.27002E-06	9.70874E-05	8.2192E-05
75	09/27/96	0	0	8.2192E-05
76	09/28/96	3.41602E-05	9.70874E-05	8.2192E-05
77	09/29/96	1.54993E-05	9.70874E-05	8.2192E-05
78	09/30/96	0.000368857	9.70874E-05	8.2192E-05
79	10/1/96	6.52314E-05	9.70874E-05	8.2192E-05
80	10/2/96	3.74308E-06	9.70874E-05	8.2192E-05
81	10/3/96	0.000107932	9.70874E-05	8.2192E-05
82	10/4/96	0.000188971	9.70874E-05	8.2192E-05
83	10/5/96	0.000461526	9.70874E-05	8.2192E-05
84	10/6/96	0.000132461	9.70874E-05	8.2192E-05
85	10/7/96	0.000223495	9.70874E-05	8.2192E-05
86	10/8/96	0.000236214	9.70874E-05	8.2192E-05
87	10/9/96	0.000130826	9.70874E-05	8.2192E-05
88	10/10/96	0	0	8.2192E-05
89	10/11/96	0	0	8.2192E-05
90	10/12/96	0.001019354	9.70874E-05	8.2192E-05
91	10/13/96	0.001010269	9.70874E-05	8.2192E-05
92	10/14/96	0.000228946	9.70874E-05	8.2192E-05
93	10/15/96	0.000288908	9.70874E-05	8.2192E-05
94	10/16/96	6.46863E-05	9.70874E-05	8.2192E-05
95	10/17/96	0.000423368	9.70874E-05	8.2192E-05
96	10/18/96	0.000310712	9.70874E-05	8.2192E-05
97	10/19/96	8.70357E-05	9.70874E-05	8.2192E-05
98	10/20/96	3.19797E-06	9.70874E-05	8.2192E-05
99	10/21/96	1.60262E-06	9.70874E-05	8.2192E-05
100	10/22/96	1.60262E-06	9.70874E-05	8.2192E-05
101	10/23/96	0	0	8.2192E-05
102	10/24/96	0	0	8.2192E-05

Table C-1. Continued

Day	Date	Variable rate proportionate to rain volume [g TP/m^2/d]	Constant rate per rain day [g TP/m^2/d]	Constant rate per day [g TP/m^2/d]
103	10/25/96	3.74308E-06	9.70874E-05	8.2192E-05
104	10/26/96	1.06841E-06	9.70874E-05	8.2192E-05
105	10/27/96	8.54004E-06	9.70874E-05	8.2192E-05
106	10/28/96	1.06841E-06	9.70874E-05	8.2192E-05
107	10/29/96	0	0	8.2192E-05
108	10/30/96	1.70982E-05	9.70874E-05	8.2192E-05
109	10/31/96	5.34207E-07	9.70874E-05	8.2192E-05
110	11/1/96	5.34207E-07	9.70874E-05	8.2192E-05
111	11/2/96	3.74308E-06	9.70874E-05	8.2192E-05
112	11/3/96	5.34207E-07	9.70874E-05	8.2192E-05
113	11/4/96	2.1441E-06	9.70874E-05	8.2192E-05
114	11/5/96	1.81703E-05	9.70874E-05	8.2192E-05
115	11/6/96	0	0	8.2192E-05
116	11/7/96	3.74308E-06	9.70874E-05	8.2192E-05
117	11/8/96	1.06841E-06	9.70874E-05	8.2192E-05
118	11/9/96	0	0	8.2192E-05
119	11/10/96	0	0	8.2192E-05
120	11/11/96	0	0	8.2192E-05
121	11/12/96	0	0	8.2192E-05
122	11/13/96	0	0	8.2192E-05
123	11/14/96	5.015E-05	9.70874E-05	8.2192E-05
124	11/15/96	4.59709E-05	9.70874E-05	8.2192E-05
125	11/16/96	1.54993E-05	9.70874E-05	8.2192E-05
126	11/17/96	0	0	8.2192E-05
127	11/18/96	2.1441E-06	9.70874E-05	8.2192E-05
128	11/19/96	1.06841E-06	9.70874E-05	8.2192E-05
129	11/20/96	0	0	8.2192E-05
130	11/21/96	1.06841E-06	9.70874E-05	8.2192E-05
131	11/22/96	2.67103E-06	9.70874E-05	8.2192E-05
132	11/23/96	4.81513E-06	9.70874E-05	8.2192E-05
133	11/24/96	0	0	8.2192E-05
134	11/25/96	0	0	8.2192E-05
135	11/26/96	0	0	8.2192E-05
136	11/27/96	0	0	8.2192E-05
137	11/28/96	7.21361E-05	9.70874E-05	8.2192E-05
138	11/29/96	0	0	8.2192E-05
139	11/30/96	0	0	8.2192E-05
140	12/1/96	0	0	8.2192E-05
141	12/2/96	1.33552E-05	9.70874E-05	8.2192E-05

Table C-1. Continued

Day	Date	Variable rate proportionate to rain volume [g TP/m^2/d]	Constant rate per rain day [g TP/m^2/d]	Constant rate per day [g TP/m^2/d]
142	12/3/96	1.12111E-05	9.70874E-05	8.2192E-05
143	12/4/96	0	0	8.2192E-05
144	12/5/96	7.63152E-05	9.70874E-05	8.2192E-05
145	12/6/96	1.33552E-05	9.70874E-05	8.2192E-05
146	12/7/96	5.34207E-07	9.70874E-05	8.2192E-05
147	12/8/96	4.81513E-06	9.70874E-05	8.2192E-05
148	12/9/96	0	0	8.2192E-05
149	12/10/96	0	0	8.2192E-05
150	12/11/96	0	0	8.2192E-05
151	12/12/96	0	0	8.2192E-05
152	12/13/96	0.000261652	9.70874E-05	8.2192E-05
153	12/14/96	4.27002E-06	9.70874E-05	8.2192E-05
154	12/15/96	1.06841E-06	9.70874E-05	8.2192E-05
155	12/16/96	0	0	8.2192E-05
156	12/17/96	0	0	8.2192E-05
157	12/18/96	8.54004E-06	9.70874E-05	8.2192E-05
158	12/19/96	4.81513E-06	9.70874E-05	8.2192E-05
159	12/20/96	0	0	8.2192E-05
160	12/21/96	5.34207E-07	9.70874E-05	8.2192E-05
161	12/22/96	6.41411E-06	9.70874E-05	8.2192E-05
162	12/23/96	0	0	8.2192E-05
163	12/24/96	0	0	8.2192E-05
164	12/25/96	1.06841E-06	9.70874E-05	8.2192E-05
165	12/26/96	8.54004E-06	9.70874E-05	8.2192E-05
166	12/27/96	4.81513E-06	9.70874E-05	8.2192E-05
167	12/28/96	1.06841E-06	9.70874E-05	8.2192E-05
168	12/29/96	2.67103E-06	9.70874E-05	8.2192E-05
169	12/30/96	4.81513E-06	9.70874E-05	8.2192E-05
170	12/31/96	1.06841E-06	9.70874E-05	8.2192E-05
171	01/1/97	1.06841E-06	9.70874E-05	8.2192E-05
172	01/2/97	1.60262E-06	9.70874E-05	8.2192E-05
173	01/3/97	1.06841E-06	9.70874E-05	8.2192E-05
174	01/4/97	2.1441E-06	9.70874E-05	8.2192E-05
175	01/5/97	5.34207E-07	9.70874E-05	8.2192E-05
176	01/6/97	1.06841E-06	9.70874E-05	8.2192E-05
177	01/7/97	6.41411E-06	9.70874E-05	8.2192E-05
178	01/8/97	4.81513E-06	9.70874E-05	8.2192E-05
179	01/9/97	1.60262E-06	9.70874E-05	8.2192E-05
180	01/10/97	9.72111E-05	9.70874E-05	8.2192E-05

Table C-1. Continued

Day	Date	Variable rate proportionate to rain volume [g TP/m^2/d]	Constant rate per rain day [g TP/m^2/d]	Constant rate per day [g TP/m^2/d]
181	01/11/97	1.60262E-05	9.70874E-05	8.2192E-05
182	01/12/97	0.000359772	9.70874E-05	8.2192E-05
183	01/13/97	0.000370674	9.70874E-05	8.2192E-05
184	01/14/97	0.000168802	9.70874E-05	8.2192E-05
185	01/15/97	0.000185337	9.70874E-05	8.2192E-05
186	01/16/97	0.00020169	9.70874E-05	8.2192E-05
187	01/17/97	0	0	8.2192E-05
188	01/18/97	0	0	8.2192E-05
189	01/19/97	0	0	8.2192E-05
190	01/20/97	0	0	8.2192E-05
191	01/21/97	5.34207E-07	9.70874E-05	8.2192E-05
192	01/22/97	1.06841E-06	9.70874E-05	8.2192E-05
193	01/23/97	5.34207E-07	9.70874E-05	8.2192E-05
194	01/24/97	0	0	8.2192E-05
195	01/25/97	3.74308E-05	9.70874E-05	8.2192E-05
196	01/26/97	3.90661E-05	9.70874E-05	8.2192E-05
197	01/27/97	0	0	8.2192E-05
198	01/28/97	1.44272E-05	9.70874E-05	8.2192E-05
199	01/29/97	0.000134097	9.70874E-05	8.2192E-05
200	01/30/97	8.34017E-05	9.70874E-05	8.2192E-05
201	01/31/97	0	0	8.2192E-05
202	02/1/97	0	0	8.2192E-05
203	02/2/97	2.1441E-06	9.70874E-05	8.2192E-05
204	02/3/97	3.19797E-06	9.70874E-05	8.2192E-05
205	02/4/97	2.39848E-05	9.70874E-05	8.2192E-05
206	02/5/97	4.81513E-06	9.70874E-05	8.2192E-05
207	02/6/97	1.60262E-06	9.70874E-05	8.2192E-05
208	02/7/97	5.34207E-07	9.70874E-05	8.2192E-05
209	02/8/97	2.1441E-06	9.70874E-05	8.2192E-05
210	02/9/97	1.65531E-05	9.70874E-05	8.2192E-05
211	02/10/97	1.06841E-06	9.70874E-05	8.2192E-05
212	02/11/97	0	0	8.2192E-05
213	02/12/97	0	0	8.2192E-05
214	02/13/97	5.34207E-07	9.70874E-05	8.2192E-05
215	02/14/97	6.41411E-06	9.70874E-05	8.2192E-05
216	02/15/97	1.06841E-06	9.70874E-05	8.2192E-05
217	02/16/97	0.000152267	9.70874E-05	8.2192E-05
218	02/17/97	9.61209E-06	9.70874E-05	8.2192E-05
219	02/18/97	0.00020169	9.70874E-05	8.2192E-05

Table C-1. Continued

Day	Date	Variable rate proportionate to rain volume [g TP/m^2/d]	Constant rate per rain day [g TP/m^2/d]	Constant rate per day [g TP/m^2/d]
220	02/19/97	2.39848E-05	9.70874E-05	8.2192E-05
221	02/20/97	3.74308E-06	9.70874E-05	8.2192E-05
222	02/21/97	5.34207E-07	9.70874E-05	8.2192E-05
223	02/22/97	5.34207E-07	9.70874E-05	8.2192E-05
224	02/23/97	2.1441E-06	9.70874E-05	8.2192E-05
225	02/24/97	2.72554E-05	9.70874E-05	8.2192E-05
226	02/25/97	1.60262E-05	9.70874E-05	8.2192E-05
227	02/26/97	0	0	8.2192E-05
228	02/27/97	0	0	8.2192E-05
229	02/28/97	0	0	8.2192E-05
230	03/1/97	0	0	8.2192E-05
231	03/2/97	0	0	8.2192E-05
232	03/3/97	5.34207E-07	9.70874E-05	8.2192E-05
233	03/4/97	5.34207E-07	9.70874E-05	8.2192E-05
234	03/5/97	0	0	8.2192E-05
235	03/6/97	4.27002E-06	9.70874E-05	8.2192E-05
236	03/7/97	1.33552E-05	9.70874E-05	8.2192E-05
237	03/8/97	5.34207E-07	9.70874E-05	8.2192E-05
238	03/9/97	5.34207E-07	9.70874E-05	8.2192E-05
239	03/10/97	5.86901E-06	9.70874E-05	8.2192E-05
240	03/11/97	5.34207E-07	9.70874E-05	8.2192E-05
241	03/12/97	2.1441E-06	9.70874E-05	8.2192E-05
242	03/13/97	5.34207E-07	9.70874E-05	8.2192E-05
243	03/14/97	0.000632326	9.70874E-05	8.2192E-05
244	03/15/97	8.23114E-05	9.70874E-05	8.2192E-05
245	03/16/97	1.06841E-06	9.70874E-05	8.2192E-05
246	03/17/97	5.34207E-07	9.70874E-05	8.2192E-05
247	03/18/97	0	0	8.2192E-05
248	03/19/97	1.06841E-06	9.70874E-05	8.2192E-05
249	03/20/97	5.34207E-07	9.70874E-05	8.2192E-05
250	03/21/97	0.000219861	9.70874E-05	8.2192E-05
251	03/22/97	6.41411E-06	9.70874E-05	8.2192E-05
252	03/23/97	5.34207E-07	9.70874E-05	8.2192E-05
253	03/24/97	0.000106296	9.70874E-05	8.2192E-05
254	03/25/97	1.28282E-05	9.70874E-05	8.2192E-05
255	03/26/97	0	0	8.2192E-05
256	03/27/97	1.81703E-05	9.70874E-05	8.2192E-05
257	03/28/97	2.67103E-06	9.70874E-05	8.2192E-05
258	03/29/97	5.34207E-07	9.70874E-05	8.2192E-05

Table C-1. Continued

Day	Date	Variable rate proportionate to rain volume [g TP/m^2/d]	Constant rate per rain day [g TP/m^2/d]	Constant rate per day [g TP/m^2/d]
259	03/30/97	5.34207E-07	9.70874E-05	8.2192E-05
260	03/31/97	2.08958E-05	9.70874E-05	8.2192E-05
261	04/1/97	2.1441E-06	9.70874E-05	8.2192E-05
262	04/2/97	0	0	8.2192E-05
263	04/3/97	0	0	8.2192E-05
264	04/4/97	0	0	8.2192E-05
265	04/5/97	0	0	8.2192E-05
266	04/6/97	0	0	8.2192E-05
267	04/7/97	0	0	8.2192E-05
268	04/8/97	2.1441E-06	9.70874E-05	8.2192E-05
269	04/9/97	3.14346E-05	9.70874E-05	8.2192E-05
270	04/10/97	1.44272E-05	9.70874E-05	8.2192E-05
271	04/11/97	1.70982E-05	9.70874E-05	8.2192E-05
272	04/12/97	5.39658E-05	9.70874E-05	8.2192E-05
273	04/13/97	7.10459E-05	9.70874E-05	8.2192E-05
274	04/14/97	3.19797E-06	9.70874E-05	8.2192E-05
275	04/15/97	0.000117562	9.70874E-05	8.2192E-05
276	04/16/97	0.000141002	9.70874E-05	8.2192E-05
277	04/17/97	1.01572E-05	9.70874E-05	8.2192E-05
278	04/18/97	0	0	8.2192E-05
279	04/19/97	0	0	8.2192E-05
280	04/20/97	0	0	8.2192E-05
281	04/21/97	1.92605E-05	9.70874E-05	8.2192E-05
282	04/22/97	9.08515E-06	9.70874E-05	8.2192E-05
283	04/23/97	5.86901E-06	9.70874E-05	8.2192E-05
284	04/24/97	4.27002E-06	9.70874E-05	8.2192E-05
285	04/25/97	3.19797E-06	9.70874E-05	8.2192E-05
286	04/26/97	0.000129191	9.70874E-05	8.2192E-05
287	04/27/97	2.67103E-06	9.70874E-05	8.2192E-05
288	04/28/97	0.000134097	9.70874E-05	8.2192E-05
289	04/29/97	1.33552E-05	9.70874E-05	8.2192E-05
290	04/30/97	9.55758E-05	9.70874E-05	8.2192E-05
291	05/1/97	5.86901E-05	9.70874E-05	8.2192E-05
292	05/2/97	6.94105E-06	9.70874E-05	8.2192E-05
293	05/3/97	0	0	8.2192E-05
294	05/4/97	6.30509E-05	9.70874E-05	8.2192E-05
295	05/5/97	1.01572E-05	9.70874E-05	8.2192E-05
296	05/6/97	0	0	8.2192E-05
297	05/7/97	0	0	8.2192E-05

Table C-1. Continued

Day	Date	Variable rate proportionate to rain volume [g TP/m^2/d]	Constant rate per rain day [g TP/m^2/d]	Constant rate per day [g TP/m^2/d]
298	05/8/97	0	0	8.2192E-05
299	05/9/97	0	0	8.2192E-05
300	05/10/97	0	0	8.2192E-05
301	05/11/97	1.06841E-06	9.70874E-05	8.2192E-05
302	05/12/97	0.000466977	9.70874E-05	8.2192E-05
303	05/13/97	0.000145362	9.70874E-05	8.2192E-05
304	05/14/97	0	0	8.2192E-05
305	05/15/97	5.34207E-07	9.70874E-05	8.2192E-05
306	05/16/97	0	0	8.2192E-05
307	05/17/97	2.08958E-05	9.70874E-05	8.2192E-05
308	05/18/97	6.41411E-06	9.70874E-05	8.2192E-05
309	05/19/97	2.1441E-06	9.70874E-05	8.2192E-05
310	05/20/97	5.34207E-06	9.70874E-05	8.2192E-05
311	05/21/97	1.60262E-05	9.70874E-05	8.2192E-05
312	05/22/97	0.000181158	9.70874E-05	8.2192E-05
313	05/23/97	8.81259E-05	9.70874E-05	8.2192E-05
314	05/24/97	0.000179523	9.70874E-05	8.2192E-05
315	05/25/97	0	0	8.2192E-05
316	05/26/97	4.54257E-05	9.70874E-05	8.2192E-05
317	05/27/97	5.34207E-07	9.70874E-05	8.2192E-05
318	05/28/97	0.000259835	9.70874E-05	8.2192E-05
319	05/29/97	0.000100482	9.70874E-05	8.2192E-05
320	05/30/97	7.05008E-05	9.70874E-05	8.2192E-05
321	05/31/97	0.000119197	9.70874E-05	8.2192E-05
322	06/1/97	0.000122831	9.70874E-05	8.2192E-05
323	06/2/97	0.000739531	9.70874E-05	8.2192E-05
324	06/3/97	7.26812E-05	9.70874E-05	8.2192E-05
325	06/4/97	1.70982E-05	9.70874E-05	8.2192E-05
326	06/5/97	4.81513E-06	9.70874E-05	8.2192E-05
327	06/6/97	0	0	8.2192E-05
328	06/7/97	1.17562E-05	9.70874E-05	8.2192E-05
329	06/8/97	0.000741348	9.70874E-05	8.2192E-05
330	06/9/97	0.004197339	9.70874E-05	8.2192E-05
331	06/10/97	0.001475428	9.70874E-05	8.2192E-05
332	06/11/97	0.000292542	9.70874E-05	8.2192E-05
333	06/12/97	1.92605E-05	9.70874E-05	8.2192E-05
334	06/13/97	2.88908E-05	9.70874E-05	8.2192E-05
335	06/14/97	1.38821E-05	9.70874E-05	8.2192E-05
336	06/15/97	0.000432453	9.70874E-05	8.2192E-05

Table C-1. Continued

Day	Date	Variable rate proportionate to rain volume [g TP/m^2/d]	Constant rate per rain day [g TP/m^2/d]	Constant rate per day [g TP/m^2/d]
337	06/16/97	0.000115926	9.70874E-05	8.2192E-05
338	06/17/97	2.1441E-06	9.70874E-05	8.2192E-05
339	06/18/97	3.19797E-06	9.70874E-05	8.2192E-05
340	06/19/97	4.27002E-06	9.70874E-05	8.2192E-05
341	06/20/97	1.54993E-05	9.70874E-05	8.2192E-05
342	06/21/97	7.57701E-05	9.70874E-05	8.2192E-05
343	06/22/97	0.000414283	9.70874E-05	8.2192E-05
344	06/23/97	7.05008E-05	9.70874E-05	8.2192E-05
345	06/24/97	0.000185337	9.70874E-05	8.2192E-05
346	06/25/97	0.000101027	9.70874E-05	8.2192E-05
347	06/26/97	9.08515E-06	9.70874E-05	8.2192E-05
348	06/27/97	1.17562E-05	9.70874E-05	8.2192E-05
349	06/28/97	0	0	8.2192E-05
350	06/29/97	1.60262E-06	9.70874E-05	8.2192E-05
351	06/30/97	5.77815E-05	9.70874E-05	8.2192E-05
352	07/1/97	0.000135732	9.70874E-05	8.2192E-05
353	07/2/97	0.000247116	9.70874E-05	8.2192E-05
354	07/3/97	9.88464E-05	9.70874E-05	8.2192E-05
355	07/4/97	0.000321614	9.70874E-05	8.2192E-05
356	07/5/97	4.27002E-06	9.70874E-05	8.2192E-05
357	07/6/97	3.36151E-05	9.70874E-05	8.2192E-05
358	07/7/97	5.86901E-06	9.70874E-05	8.2192E-05
359	07/8/97	5.86901E-06	9.70874E-05	8.2192E-05
360	07/9/97	4.27002E-06	9.70874E-05	8.2192E-05
361	07/10/97	0.000108477	9.70874E-05	8.2192E-05
362	07/11/97	0.000144272	9.70874E-05	8.2192E-05
363	07/12/97	0.000254384	9.70874E-05	8.2192E-05
364	07/13/97	0.000205324	9.70874E-05	8.2192E-05
365	07/14/97	0.000185337	9.70874E-05	8.2192E-05
366	07/15/97	5.34207E-05	9.70874E-05	8.2192E-05
367	07/16/97	0.000243482	9.70874E-05	8.2192E-05
368	07/17/97	0.000161897	9.70874E-05	8.2192E-05
369	07/18/97	0.000156446	9.70874E-05	8.2192E-05
370	07/19/97	0.000142092	9.70874E-05	8.2192E-05
371	07/20/97	0.000118107	9.70874E-05	8.2192E-05
372	07/21/97	3.47053E-05	9.70874E-05	8.2192E-05
373	07/22/97	0.00020169	9.70874E-05	8.2192E-05
374	07/23/97	0.000120651	9.70874E-05	8.2192E-05
375	07/24/97	1.06841E-05	9.70874E-05	8.2192E-05

Table C-1. Continued

Day	Date	Variable rate proportionate to rain volume [g TP/m^2/d]	Constant rate per rain day [g TP/m^2/d]	Constant rate per day [g TP/m^2/d]
376	07/25/97	9.61209E-06	9.70874E-05	8.2192E-05
377	07/26/97	0.000123376	9.70874E-05	8.2192E-05
378	07/27/97	5.77815E-05	9.70874E-05	8.2192E-05
379	07/28/97	2.1441E-05	9.70874E-05	8.2192E-05
380	07/29/97	5.34207E-07	9.70874E-05	8.2192E-05
381	07/30/97	4.27002E-06	9.70874E-05	8.2192E-05
382	07/31/97	1.81703E-05	9.70874E-05	8.2192E-05
383	08/1/97	0.000160262	9.70874E-05	8.2192E-05
384	08/2/97	0.000107386	9.70874E-05	8.2192E-05
385	08/3/97	0	0	8.2192E-05
386	08/4/97	7.63152E-05	9.70874E-05	8.2192E-05
387	08/5/97	7.48616E-06	9.70874E-05	8.2192E-05
388	08/6/97	0.000110657	9.70874E-05	8.2192E-05
389	08/7/97	4.161E-05	9.70874E-05	8.2192E-05
390	08/8/97	5.45109E-05	9.70874E-05	8.2192E-05
391	08/9/97	0.000354321	9.70874E-05	8.2192E-05
392	08/10/97	0.00021441	9.70874E-05	8.2192E-05
393	08/11/97	3.96112E-05	9.70874E-05	8.2192E-05
394	08/12/97	2.78006E-05	9.70874E-05	8.2192E-05
395	08/13/97	0	0	8.2192E-05
396	08/14/97	5.34207E-07	9.70874E-05	8.2192E-05
397	08/15/97	0.000153357	9.70874E-05	8.2192E-05
398	08/16/97	3.99747E-05	9.70874E-05	8.2192E-05
399	08/17/97	6.41411E-06	9.70874E-05	8.2192E-05
400	08/18/97	1.60262E-05	9.70874E-05	8.2192E-05
401	08/19/97	5.86901E-06	9.70874E-05	8.2192E-05
402	08/20/97	7.37714E-05	9.70874E-05	8.2192E-05
403	08/21/97	0.000252567	9.70874E-05	8.2192E-05
404	08/22/97	2.5075E-05	9.70874E-05	8.2192E-05
405	08/23/97	2.19861E-05	9.70874E-05	8.2192E-05
406	08/24/97	4.70611E-05	9.70874E-05	8.2192E-05
407	08/25/97	0.000199873	9.70874E-05	8.2192E-05
408	08/26/97	0.000121741	9.70874E-05	8.2192E-05
409	08/27/97	0.000128282	9.70874E-05	8.2192E-05
410	08/28/97	4.81513E-05	9.70874E-05	8.2192E-05
411	08/29/97	6.72301E-05	9.70874E-05	8.2192E-05
412	08/30/97	0.000279823	9.70874E-05	8.2192E-05
413	08/31/97	0.000219861	9.70874E-05	8.2192E-05
414	09/1/97	0.000138276	9.70874E-05	8.2192E-05

Table C-1. Continued

Day	Date	Variable rate proportionate to rain volume [g TP/m^2/d]	Constant rate per rain day [g TP/m^2/d]	Constant rate per day [g TP/m^2/d]
415	09/2/97	0.000133552	9.70874E-05	8.2192E-05
416	09/3/97	3.25248E-05	9.70874E-05	8.2192E-05
417	09/4/97	9.83013E-05	9.70874E-05	8.2192E-05
418	09/5/97	0.000321614	9.70874E-05	8.2192E-05
419	09/6/97	0.000305261	9.70874E-05	8.2192E-05
420	09/7/97	4.27002E-06	9.70874E-05	8.2192E-05
421	09/8/97	3.47053E-05	9.70874E-05	8.2192E-05
422	09/9/97	1.06841E-06	9.70874E-05	8.2192E-05
423	09/10/97	5.34207E-07	9.70874E-05	8.2192E-05
424	09/11/97	9.24868E-05	9.70874E-05	8.2192E-05
425	09/12/97	5.72364E-05	9.70874E-05	8.2192E-05
426	09/13/97	4.43355E-05	9.70874E-05	8.2192E-05
427	09/14/97	0.000100482	9.70874E-05	8.2192E-05
428	09/15/97	0.000129191	9.70874E-05	8.2192E-05
429	09/16/97	3.52504E-05	9.70874E-05	8.2192E-05
430	09/17/97	0.000116472	9.70874E-05	8.2192E-05
431	09/18/97	5.86901E-05	9.70874E-05	8.2192E-05
432	09/19/97	0.000198056	9.70874E-05	8.2192E-05
433	09/20/97	3.30699E-05	9.70874E-05	8.2192E-05
434	09/21/97	2.34397E-05	9.70874E-05	8.2192E-05
435	09/22/97	2.1441E-06	9.70874E-05	8.2192E-05
436	09/23/97	3.41602E-05	9.70874E-05	8.2192E-05
437	09/24/97	0.000119742	9.70874E-05	8.2192E-05
438	09/25/97	5.72364E-05	9.70874E-05	8.2192E-05
439	09/26/97	0.000221678	9.70874E-05	8.2192E-05
440	09/27/97	6.03254E-05	9.70874E-05	8.2192E-05
441	09/28/97	0.000207141	9.70874E-05	8.2192E-05
442	09/29/97	0.000223495	9.70874E-05	8.2192E-05
443	09/30/97	0.000332516	9.70874E-05	8.2192E-05
444	10/1/97	0.000288908	9.70874E-05	8.2192E-05
445	10/2/97	0.000187154	9.70874E-05	8.2192E-05
446	10/3/97	4.81513E-06	9.70874E-05	8.2192E-05
447	10/4/97	2.1441E-06	9.70874E-05	8.2192E-05
448	10/5/97	4.81513E-06	9.70874E-05	8.2192E-05
449	10/6/97	9.55758E-05	9.70874E-05	8.2192E-05
450	10/7/97	2.1441E-06	9.70874E-05	8.2192E-05
451	10/8/97	0	0	8.2192E-05
452	10/9/97	4.81513E-06	9.70874E-05	8.2192E-05
453	10/10/97	0.000104116	9.70874E-05	8.2192E-05

Table C-1. Continued

Day	Date	Variable rate proportionate to rain volume [g TP/m^2/d]	Constant rate per rain day [g TP/m^2/d]	Constant rate per day [g TP/m^2/d]
454	10/11/97	6.94105E-06	9.70874E-05	8.2192E-05
455	10/12/97	2.5075E-05	9.70874E-05	8.2192E-05
456	10/13/97	9.61209E-06	9.70874E-05	8.2192E-05
457	10/14/97	7.48616E-06	9.70874E-05	8.2192E-05
458	10/15/97	2.67103E-06	9.70874E-05	8.2192E-05
459	10/16/97	1.28282E-05	9.70874E-05	8.2192E-05
460	10/17/97	9.08515E-06	9.70874E-05	8.2192E-05
461	10/18/97	1.22831E-05	9.70874E-05	8.2192E-05
462	10/19/97	0	0	8.2192E-05
463	10/20/97	1.06841E-05	9.70874E-05	8.2192E-05
464	10/21/97	0	0	8.2192E-05
465	10/22/97	0	0	8.2192E-05
466	10/23/97	5.34207E-07	9.70874E-05	8.2192E-05
467	10/24/97	0	0	8.2192E-05
468	10/25/97	5.34207E-07	9.70874E-05	8.2192E-05
469	10/26/97	5.34207E-07	9.70874E-05	8.2192E-05
470	10/27/97	0	0	8.2192E-05
471	10/28/97	0	0	8.2192E-05
472	10/29/97	1.01572E-05	9.70874E-05	8.2192E-05
473	10/30/97	0.000236214	9.70874E-05	8.2192E-05
474	10/31/97	2.1441E-06	9.70874E-05	8.2192E-05
475	11/1/97	0	0	8.2192E-05
476	11/2/97	9.61209E-06	9.70874E-05	8.2192E-05
477	11/3/97	5.72364E-05	9.70874E-05	8.2192E-05
478	11/4/97	2.1441E-06	9.70874E-05	8.2192E-05
479	11/5/97	1.01572E-05	9.70874E-05	8.2192E-05
480	11/6/97	4.81513E-06	9.70874E-05	8.2192E-05
481	11/7/97	3.74308E-06	9.70874E-05	8.2192E-05
482	11/8/97	0	0	8.2192E-05
483	11/9/97	0	0	8.2192E-05
484	11/10/97	0	0	8.2192E-05
485	11/11/97	1.06841E-06	9.70874E-05	8.2192E-05
486	11/12/97	0	0	8.2192E-05

Section C3

XML Input File for Model 3 (XMLINPUT.xml)

```
<?xml version="1.0" encoding="utf-8"?>
<wq version="0.1">
  <reaction_sets>
    <reaction_set name="rs1" full_name="Reaction Set Number 1">
      <coverage>
        <cell>all</cell>
        <segment>all</segment>
      </coverage>
      <stores>
        <store full_name="Surface-water" distribution="heterogeneous"
              location="element" section="gw" actuator="rsm_wm">
          <name>surface_water</name>
          <components>
            <variables>
              <variable type="mobile">
                <name full_name="Water Column TP">Sal</name>
                <initial_distribution type="constant">
                  10.0
                </initial_distribution>
              </variable>
              <variable type="mobile">
                <name full_name="Water Column TP">TP_sw_conc</name>
                <initial_distribution type="constant">
                  10.0
                </initial_distribution>
              </variable>
              <variable type="stabile">
                <name full_name="Water Column TP">TP_sw_mass1</name>
                <initial_distribution type="constant">
                  10.0
                </initial_distribution>
              </variable>
              <variable type="stabile">
                <name full_name="Water Column TP">TP_sw_mass2</name>
                <initial_distribution type="constant">
                  10.0
                </initial_distribution>
              </variable>
              <variable type="stabile">
                <name full_name="Water Column TP">TP_uptake1</name>
                <initial_distribution type="constant">
                  10.0
                </initial_distribution>
              </variable>
              <variable type="stabile">
                <name full_name="Water Column TP">TP_uptake2</name>
                <initial_distribution type="constant">
                  10.0
                </initial_distribution>
              </variable>
              <variable type="stabile">
```

```
  <name full_name="Water Column TP">TP_soil1</name>
  <initial_distribution type="constant">
    10.0
  </initial_distribution>
</variable>
<variable type="stabile">
  <name full_name="Water Column TP">TP_soil2</name>
  <initial_distribution type="constant">
    10.0
  </initial_distribution>
</variable>
<variable type="stabile">
  <name full_name="Water Column TP">TP_live1</name>
  <initial_distribution type="constant">
    10.0
  </initial_distribution>
</variable>
<variable type="stabile">
  <name full_name="Water Column TP">TP_live2</name>
  <initial_distribution type="constant">
    10.0
  </initial_distribution>
</variable>
<variable type="stabile">
  <name full_name="Water Column TP">TP_dead1</name>
  <initial_distribution type="constant">
    10.0
  </initial_distribution>
</variable>
<variable type="stabile">
  <name full_name="Water Column TP">TP_dead2</name>
  <initial_distribution type="constant">
    10.0
  </initial_distribution>
</variable>
<variable type="stabile">
  <name full_name="Water Column TP">TP_senesc</name>
  <initial_distribution type="constant">
    10.0
  </initial_distribution>
</variable>
<variable type="stabile">
  <name full_name="Water Column TP">TP_decomp</name>
  <initial_distribution type="constant">
    10.0
  </initial_distribution>
</variable>
<variable type="stabile">
  <name full_name="Water Column TP">TP_bury</name>
  <initial_distribution type="constant">
    10.0
  </initial_distribution>
</variable>
<variable type="stabile">
  <name full_name="Water Column TP">K_wet</name>
  <initial_distribution type="constant">
```

```
      10.0
    </initial_distribution>
  </variable>
</variables>
<parameters>
  <parameter units="meter">
    <name>longitudinal_dispersivity</name>
    <initial_distribution type="constant">
      10.0
    </initial_distribution>
  </parameter>
  <parameter units="meter">
    <name>transverse_dispersivity</name>
    <initial_distribution type="constant">
      10.0
    </initial_distribution>
  </parameter>
  <parameter units="meter">
    <name>molecular_diffusion</name>
    <initial_distribution type="constant">
      0.00001
    </initial_distribution>
  </parameter>
  <parameter units="none">
    <name>surface_porosity</name>
    <initial_distribution type="constant">
      1.0
    </initial_distribution>
  </parameter>
  <parameter units="meter">
    <name>subsurface_longitudinal_dispersivity</name>
    <initial_distribution type="constant">
      10.0
    </initial_distribution>
  </parameter>
  <parameter units="meter">
    <name>subsurface_transverse_dispersivity</name>
    <initial_distribution type="constant">
      10.0
    </initial_distribution>
  </parameter>
  <parameter units="meter">
    <name>subsurface_molecular_diffusion</name>
    <initial_distribution type="constant">
      0.00001
    </initial_distribution>
  </parameter>
  <parameter units="none">
    <name>subsurface_porosity</name>
    <initial_distribution type="constant">
      1.0
    </initial_distribution>
  </parameter>
  <parameter units="none">
    <name>k_uptake</name>
    <initial_distribution type="constant">
```

```
          0.084375
        </initial_distribution>
      </parameter>
      <parameter units="none">
        <name>k_senesc</name>
        <initial_distribution type="constant">
          0.25
        </initial_distribution>
      </parameter>
      <parameter units="none">
        <name>k_decomp</name>
        <initial_distribution type="constant">
          0.0001
        </initial_distribution>
      </parameter>
      <parameter units="none">
        <name>k_soil</name>
        <initial_distribution type="constant">
          0.13
        </initial_distribution>
      </parameter>
    </parameters>
  </components>
 </store>
</stores>
<equations>
 <equation type="pre">
  <lhs>TP_sw_mass2</lhs>
  <rhs>(1-k_uptake)*TP_sw_conc*depth</rhs>
 </equation>
 <equation type="pre">
  <lhs>TP_uptake2</lhs>
  <rhs>k_uptake*K_wet*TP_sw_mass1</rhs>
 </equation>
 <equation type="pre">
  <lhs>TP_senesc</lhs>
  <rhs>k_senesc*TP_uptake1</rhs>
 </equation>
 <equation type="pre">
  <lhs>TP_decomp</lhs>
  <rhs>k_decomp*TP_dead2</rhs>
 </equation>
 <equation type="pre">
  <lhs>TP_bury</lhs>
  <rhs>k_soil*TP_uptake1</rhs>
 </equation>
 <equation type="pre">
  <lhs>TP_live1</lhs>
  <rhs>TP_live2</rhs>
 </equation>
 <equation type="pre">
  <lhs>TP_dead1</lhs>
  <rhs>TP_dead2</rhs>
 </equation>
 <equation type="pre">
  <lhs>TP_soil1</lhs>
```

```
        <rhs>TP_soil2</rhs>
       </equation>
       <equation type="post">
        <lhs>TP_uptake1</lhs>
        <rhs>TP_uptake2</rhs>
       </equation>
       <equation type="post">
        <lhs>TP_sw_mass1</lhs>
        <rhs>TP_sw_mass2</rhs>
       </equation>
       <equation type="post">
        <lhs>TP_dead2</lhs>
        <rhs>TP_dead1+TP_senesc-TP_decomp</rhs>
       </equation>
       <equation type="post">
        <lhs>TP_live2</lhs>
        <rhs>TP_live1+TP_uptake2-TP_senesc</rhs>
       </equation>
       <equation type="post">
        <lhs>TP_soil2</lhs>
        <rhs>TP_soil1+TP_bury</rhs>
       </equation>
       <equation type="post">
        <lhs>TP_sw_conc</lhs>
        <rhs>(TP_sw_mass2+TP_decomp)/depth</rhs>
       </equation>
      </equations>
    </reaction_set>
  </reaction_sets>
</wq>
```

IWQ input File for Model 3 (IWQINPUT.iwq)

```
1 2 14 5 1 0
'XMLINPUT.xml' 'XMLOUTPUT.xml' 'rs1'
Sal 5.01 TP_sw_conc 0.005
TP_sw_mass1 0.01 TP_sw_mass2 0.01 TP_uptake1 0.0008 TP_uptake2 0.0008
TP_soil1 0.0001 TP_soil2 0.0001 TP_live1 0.04 TP_live2 0.04 TP_dead1 0.014
TP_dead2 0.014 TP_senesc 0.0002 TP_decomp 0.0001 TP_bury 0 K_wet 1
0 0 0 0 0 0 0 0 0 0 0 0 0 0
k_uptake 0.084375 k_senesc 0.25 k_decomp 0.0001 k_soil 0.0
0
depth 0.52 time_step 3600 area 92903
```

SWIFT2D Input File (WETLANDS.inp) for Model 3

```
SOUTHERN INLAND AND COASTAL SYSTEMS MODEL
END NOTE                                                    END NOTE
    NOSAMV=       1(NUMBER OF DIMENSIONS THAT MUST STAY THE SAME)
    NODIMV=       2(NUMBER OF DIMENSIONS TOTAL)
WETMTZ  /IDP...R07       00       00       00       00       00
RUN NUMBER 1                                                    R2 TITL
WETLANDS       15 JUL '96  98/ 8/2517:23:39 IDPV514                   R3 DATE
Halfdt Titide Tstart Trst   Tstop   Tirst Tihisp Tihist DAYOFFSTSWIFT
  1.50   15.0    0.0  0.0 999999. 999999.  1440.  1440.           0  R4 TIMEA
99999999999999999999999.   45.   30.999999   60.999999999999999999    0.R5 TIMEB
    0    0    2    1    0    5    1    0    0    0    0    0R6 FLAGS
    7    3    4    4    0    4                              R7 INPR1
    1                                                     R8 INPR2
    0  1440  1440  1440    0    0    0    0    0               R9 OTPR1
  1440  1440  1440  1440    0    0    0                         R10OTPR2
545760545880546000546120546240546360546480546600546720546840546960547080R11 PRT1
547200547320547440547560547680547800547920548040548160548280548400548520R12 PRT2
548640548760548880549000549120549240549360549480549600549720549840549960R13 PRT3
550080550200550320550440550560550680                                                    R14 PRT4
   148    98    2   14   33    4   25    3    5    8    0    1R15 DIMA
    94   128                                                R16 DIMB
           0.5     0                         1                R17 CNST
25.000   0.0 304.8  0.20   0.0  0.10   1.  1.00   0.5   1.0   5.0 300.0R18 PHCH
   9.81  0.0012   1.205   998.2  1.0000    14.3  1000.0    0.97  0.0023R19 COFA
FR80      35SPRO          1.0   1.0                         R20 Ploter D
   25     1   0.0  13.0  20.0  14.0K/HR            5                R21 Nctitl D
   4.0 170.0  2.00 121.0 163.0  1.25  74.0  89.0  1.00 122.0 103.0  1.00R22 Hx  USED
   1.0   2.0   2.0   2.0   2.0                              R23 Dxpdy ED
    1     1     2   0.5   1.0 -0.40 -0.40  0.25   1.0   0.0     1    1R24Iplc SED
                                                          R25 Linx SED
   25.0  1.0250   0.698   1.0                               R26 COFB
   1   57   36 CP                                           RS1 WL-Sta
   2  109   78 EVER4                                          RS1 WL-Sta
   3  100   58 EVER5A                                         RS1 WL-Sta
   4   69   45 E146                                         RS1 WL-Sta
   5   98   97 E158                                         RS1 WL-Sta
   6  142   52 EP12R                                          RS1 WL-Sta
   7  139   57 EP1R                                          RS1 WL-Sta
   8  123   55 EPGW                                           RS1 WL-Sta
   9  120   61 EVER6                                          RS1 WL-Sta
  10  110   65 EVER7                                          RS1 WL-Sta
  11   74   73 NP67                                         RS1 WL-Sta
  12   62   56 P37                                          RS1 WL-Sta
  13   89   81 R127                                         RS1 WL-Sta
  14   81   66 TSH                                          RS1 WL-Sta
   1   28   18 Alligat_T                                    RS2 Curr-Sta
   2   28   17 Alligat_C                                    RS2 Curr-Sta
   3   28   16 Alligat_B                                    RS2 Curr-Sta
   4   47   14 McCorm_L                                       RS2 Curr-Sta
   5   48   14 McCorm_C                                       RS2 Curr-Sta
   6   49   14 McCorm_R                                       RS2 Curr-Sta
   7   77   23 Taylor_L                                     RS2 Curr-Sta
   8   78   23 Taylor_C                                     RS2 Curr-Sta
   9   79   23 Taylor_R                                     RS2 Curr-Sta
  10   84   26 East_L                                       RS2 Curr-Sta
  11   85   26 East_C                                       RS2 Curr-Sta
  12   86   26 East_R                                       RS2 Curr-Sta
  13   96   27 Mud_T                                        RS2 Curr-Sta
  14   96   28 Mud_C                                        RS2 Curr-Sta
  15   96   29 Mud_B                                        RS2 Curr-Sta
  16  113   32 Trout_L                                      RS2 Curr-Sta
  17  114   32 Trout_C                                      RS2 Curr-Sta
  18  115   32 Trout_R                                      RS2 Curr-Sta
  19  127   30 Shell_L                                      RS2 Curr-Sta
  20  128   30 Shell_C                                      RS2 Curr-Sta
  21  129   30 Shell_R                                      RS2 Curr-Sta
  22  128   36 Stillw_L                                     RS2 Curr-Sta
```

```
23  129   36 Stillw_C                    RS2 Curr-Sta
24  130   36 Stillw_R                    RS2 Curr-Sta
25  138   40 Oregon_L                     RS2 Curr-Sta
26  139   40 Oregon_C                     RS2 Curr-Sta
27  140   40 Oregon_R                     RS2 Curr-Sta
28  140   41 WestHi_L                     RS2 Curr-Sta
29  141   41 WestHi_C                     RS2 Curr-Sta
30  142   41 WestHi_R                     RS2 Curr-Sta
31  142   42 EastHi_L                    RS2 Curr-Sta
32  143   42 EastHi_C                     RS2 Curr-Sta
33  144   42 EastHi_R                     RS2 Curr-Sta
 1   90   90 TSB                        RS3 Src
 2  100   88 L-31W                       RS3 Src
 3  120   64 C-111                      RS3 Src
 4  148   98 Dummy (ex solar)              RS3 Sol
 1   57   36 CP                         RS4 Con-Sta
 2  109   78 EVER4                        RS4 Con-Sta
 3  100   58 EVER5A                       RS4 Con-Sta
 4   69   45 E146                       RS4 Con-Sta
 5   98   97 E158                       RS4 Con-Sta
 6  142   52 EP12R                        RS4 Con-Sta
 7  139   57 EP1R                       RS4 Con-Sta
 8  123   55 EPGW                         RS4 Con-Sta
 9  120   61 EVER6                        RS4 Con-Sta
10  110   65 EVER7                        RS4 Con-Sta
11   74   73 NP67                       RS4 Con-Sta
12   62   56 P37                        RS4 Con-Sta
13   89   81 R127                       RS4 Con-Sta
14   81   66 TSH                        RS4 Con-Sta
15   28   17 Alligat_c                  RS4 Con-Sta
16   48   14 McCorm_c                      RS4 Con-Sta
17   78   23 Taylor_c                    RS4 Con-Sta
18   85   26 East_c                      RS4 Con-Sta
19   96   28 Mud_c                       RS4 Con-Sta
20  114   32 Trout_c                     RS4 Con-Sta
21  128   30 Shell_c                     RS4 Con-Sta
22  129   36 Stillw_c                    RS4 Con-Sta
23  139   40 Oregon_c                      RS4 Con-Sta
24  141   41 WestHi_c                      RS4 Con-Sta
25  143   42 EastHi_c                     RS4 Con-Sta
 1   93   31   36 Joe Bay 1               RS5 U-tran-Sta
 2   98   36   40 Joe Bay 2               RS5 U-tran-Sta
 3  116   34   39 Joe Bay 3                RS5 U-tran-Sta
 1   36   93   98 Joe Bay 4               RS6 V-tran-Sta
 2   40   98  101 Joe Bay 5                RS6 V-tran-Sta
 3   41  102  107 Joe Bay 6                 RS6 V-tran-Sta
 4   40  108  110 Joe Bay 7                 RS6 V-tran-Sta
 5   39  111  116 Joe Bay 8                 RS6 V-tran-Sta
                                      RS7 Dam
                                      RS8 Wind/Temp
                                         RS9 Bar/Sluice
 1    1   13   17
 1    2   15   16
 1    3   17   15
 1    4   18   14
 1    5   19   17
 1    6   19   18
 1    7   20   15
 1    8   20   16
 1    9   20   19
 1   10   21   20
 1   11   23   21
 1   12   26   19
 1   13   27   18
 1   14   27   15
 1   15   28   17                        Alligator
 1   16   28   16
 1   17   28   14
 1   18   30   14
 1   19   31   13
 1   20   32   15
```

1	21	33	13	
1	22	35	12	
1	23	36	13	
1	24	38	13	
1	25	40	12	
1	26	41	11	
1	27	42	12	
1	28	42	13	
1	29	43	14	
1	30	44	13	
1	31	46	13	
1	32	46	18	
1	33	47	14	
1	34	49	14	
1	35	50	16	
1	36	50	17	
1	37	51	12	
1	38	52	11	
1	39	54	10	
1	40	56	9	
1	41	57	10	
1	42	58	11	
1	43	58	12	
1	44	59	13	
1	45	60	14	
1	46	61	15	
1	47	63	16	
1	48	64	17	
1	49	66	17	
1	50	68	17	
1	51	69	16	
1	52	69	15	
1	53	70	14	
1	54	70	18	
1	55	70	19	
1	56	71	15	
1	57	71	16	
1	58	71	17	
1	59	71	20	
1	60	73	21	
1	61	74	22	
1	62	74	23	
1	63	76	23	
1	64	78	23	
1	65	80	24	
1	66	81	25	
1	67	83	25	
1	68	84	26	
1	69	86	26	
1	70	89	27	
1	71	91	27	
1	72	92	26	
1	73	94	26	
1	74	96	27	
1	75	96	28	Mud Creek
1	76	96	29	
1	77	98	30	
1	78	100	30	
1	79	102	30	
1	80	104	30	
1	81	105	31	
1	82	107	31	
1	83	109	30	
1	84	111	31	
1	85	113	31	
1	86	114	32	
1	87	115	33	
1	88	116	34	
1	89	118	34	
1	90	119	33	

1	91	120	32
1	92	121	31
1	93	122	30
1	94	123	29
2	1	4	18
2	2	5	18
2	3	6	18
2	4	7	18
2	5	8	18
2	6	9	18
2	7	10	18
2	8	11	17
2	9	12	17
2	10	13	17
2	11	14	16
2	12	15	16
2	13	16	15
2	14	17	15
2	15	18	14
2	16	19	15
2	17	20	19
2	18	21	20
2	19	22	21
2	20	23	21
2	21	24	20
2	22	25	20
2	23	25	25
2	24	26	19
2	25	27	15
2	26	27	18
2	27	28	14
2	28	29	14
2	29	29	25
2	30	30	14
2	31	31	13
2	32	32	13
2	33	33	13
2	34	34	12
2	35	34	20
2	36	35	12
2	37	36	13
2	38	37	13
2	39	38	13
2	40	39	12
2	41	40	12
2	42	41	11
2	43	43	14
2	44	44	13
2	45	45	13
2	46	46	13
2	47	48	14
2	48	49	14
2	49	50	16
2	50	51	12
2	51	52	11
2	52	53	10
2	53	54	10
2	54	55	9
2	55	56	9
2	56	57	10
2	57	59	13
2	58	60	14
2	59	61	15
2	60	62	16
2	61	63	16
2	62	64	17
2	63	65	17
2	64	66	17
2	65	67	17
2	66	68	17

McCormick Creek

2 67 70 14
2 68 71 20
2 69 72 21
2 70 73 21
2 71 75 23
2 72 76 23
2 73 77 23
2 74 78 23 Taylor Creek
2 75 79 23
2 76 80 24
2 77 81 25
2 78 82 25
2 79 83 25
2 80 84 26
2 81 85 26 East Creek
2 82 86 26
2 83 87 26
2 84 88 27
2 85 89 27
2 86 90 27
2 87 91 27
2 88 92 26
2 89 93 26
2 90 94 26
2 91 95 26
2 92 97 30
2 93 98 30
2 94 99 30
2 95 100 30
2 96 101 30
2 97 102 30
2 98 103 30
2 99 104 30
2 100 105 31
2 101 106 31
2 102 107 31
2 103 108 31
2 104 109 30
2 105 110 30
2 106 111 31
2 107 112 31
2 108 113 31
2 109 114 32 Trout Creek
2 110 115 33
2 111 116 34
2 112 117 34
2 113 118 34
2 114 119 33
2 115 120 32
2 116 121 31
2 117 122 30
2 118 123 29
2 119 127 29
2 120 128 30 Shell Creek
2 121 129 36 Stillwater Creek
2 122 130 36
2 123 138 40
2 124 139 40 Oregon Creek
2 125 140 41
2 126 141 41 West Highway
2 127 142 42
2 128 143 42 East Highway
1 1269.9778269.9778269.9778269.9778269.9778269.9778
1 2269.9778269.9778269.9778269.9778269.9778269.9778
1 3269.9778269.9778269.9778269.9778269.9778269.9778
1 4269.9778269.9778269.9778269.9778269.9778269.9778
1 5269.9778269.9778269.9778269.9778269.9778269.9778
1 6269.9778269.9778269.9778269.9778269.9778269.9778
1 7269.9778269.9778269.9778269.9778269.9778269.9778
1 8 43.1964 43.1964 43.1964 43.1964 43.1964 43.1964

1 9269.9778269.9778269.9778269.9778269.9778269.9778
1 10269.9778269.9778269.9778269.9778269.9778269.9778
1 11269.9778269.9778269.9778269.9778269.9778269.9778
1 12269.9778269.9778269.9778269.9778269.9778269.9778
1 13269.9778269.9778269.9778269.9778269.9778269.9778
1 14269.9778269.9778269.9778269.9778269.9778269.9778
1 15 26.9978 26.9978 26.9978 26.9978 26.9978 26.9978 Alligator
1 16269.9778269.9778269.9778269.9778269.9778269.9778
1 17269.9778269.9778269.9778269.9778269.9778269.9778
1 18269.9778269.9778269.9778269.9778269.9778269.9778
1 19269.9778269.9778269.9778269.9778269.9778269.9778
1 20 53.9956 53.9956 53.9956 53.9956 53.9956 53.9956
1 21269.9778269.9778269.9778269.9778269.9778269.9778
1 22269.9778269.9778269.9778269.9778269.9778269.9778
1 23269.9778269.9778269.9778269.9778269.9778269.9778
1 24269.9778269.9778269.9778269.9778269.9778269.9778
1 25269.9778269.9778269.9778269.9778269.9778269.9778
1 26269.9778269.9778269.9778269.9778269.9778269.9778
1 27269.9778269.9778269.9778269.9778269.9778269.9778
1 28269.9778269.9778269.9778269.9778269.9778269.9778
1 29269.9778269.9778269.9778269.9778269.9778269.9778
1 30269.9778269.9778269.9778269.9778269.9778269.9778
1 31269.9778269.9778269.9778269.9778269.9778269.9778
1 32 32.3973 32.3973 32.3973 32.3973 32.3973 32.3973
1 33269.9778269.9778269.9778269.9778269.9778269.9778
1 34269.9778269.9778269.9778269.9778269.9778269.9778
1 35 21.5982 21.5982 21.5982 21.5982 21.5982 21.5982
1 36269.9778269.9778269.9778269.9778269.9778269.9778
1 37269.9778269.9778269.9778269.9778269.9778269.9778
1 38269.9778269.9778269.9778269.9778269.9778269.9778
1 39269.9778269.9778269.9778269.9778269.9778269.9778
1 40269.9778269.9778269.9778269.9778269.9778269.9778
1 41269.9778269.9778269.9778269.9778269.9778269.9778
1 42269.9778269.9778269.9778269.9778269.9778269.9778
1 43269.9778269.9778269.9778269.9778269.9778269.9778
1 44269.9778269.9778269.9778269.9778269.9778269.9778
1 45269.9778269.9778269.9778269.9778269.9778269.9778
1 46269.9778269.9778269.9778269.9778269.9778269.9778
1 47269.9778269.9778269.9778269.9778269.9778269.9778
1 48 32.3973 32.3973 32.3973 32.3973 32.3973 32.3973
1 49269.9778269.9778269.9778269.9778269.9778269.9778
1 50269.9778269.9778269.9778269.9778269.9778269.9778
1 51269.9778269.9778269.9778269.9778269.9778269.9778
1 52269.9778269.9778269.9778269.9778269.9778269.9778
1 53269.9778269.9778269.9778269.9778269.9778269.9778
1 54269.9778269.9778269.9778269.9778269.9778269.9778
1 55269.9778269.9778269.9778269.9778269.9778269.9778
1 56269.9778269.9778269.9778269.9778269.9778269.9778
1 57269.9778269.9778269.9778269.9778269.9778269.9778
1 58269.9778269.9778269.9778269.9778269.9778269.9778
1 59269.9778269.9778269.9778269.9778269.9778269.9778
1 60269.9778269.9778269.9778269.9778269.9778269.9778
1 61269.9778269.9778269.9778269.9778269.9778269.9778
1 62269.9778269.9778269.9778269.9778269.9778269.9778
1 63269.9778269.9778269.9778269.9778269.9778269.9778
1 64269.9778269.9778269.9778269.9778269.9778269.9778
1 65269.9778269.9778269.9778269.9778269.9778269.9778
1 66269.9778269.9778269.9778269.9778269.9778269.9778
1 67269.9778269.9778269.9778269.9778269.9778269.9778
1 68269.9778269.9778269.9778269.9778269.9778269.9778
1 69269.9778269.9778269.9778269.9778269.9778269.9778
1 70269.9778269.9778269.9778269.9778269.9778269.9778
1 71269.9778269.9778269.9778269.9778269.9778269.9778
1 72269.9778269.9778269.9778269.9778269.9778269.9778
1 73269.9778269.9778269.9778269.9778269.9778269.9778
1 74269.9778269.9778269.9778269.9778269.9778269.9778
1 75 18.8984 18.8984 18.8984 18.8984 18.8984 18.8984 Mud Creek
1 76269.9778269.9778269.9778269.9778269.9778269.9778
1 77269.9778269.9778269.9778269.9778269.9778269.9778
1 78269.9778269.9778269.9778269.9778269.9778269.9778

1 79269.9778269.9778269.9778269.9778269.9778269.9778
1 80269.9778269.9778269.9778269.9778269.9778269.9778
1 81269.9778269.9778269.9778269.9778269.9778269.9778
1 82269.9778269.9778269.9778269.9778269.9778269.9778
1 83269.9778269.9778269.9778269.9778269.9778269.9778
1 84269.9778269.9778269.9778269.9778269.9778269.9778
1 85269.9778269.9778269.9778269.9778269.9778269.9778
1 86269.9778269.9778269.9778269.9778269.9778269.9778
1 87269.9778269.9778269.9778269.9778269.9778269.9778
1 88269.9778269.9778269.9778269.9778269.9778269.9778
1 89269.9778269.9778269.9778269.9778269.9778269.9778
1 90269.9778269.9778269.9778269.9778269.9778269.9778
1 91269.9778269.9778269.9778269.9778269.9778269.9778
1 92269.9778269.9778269.9778269.9778269.9778269.9778
1 93269.9778269.9778269.9778269.9778269.9778269.9778
1 94269.9778269.9778269.9778269.9778269.9778269.9778
2 1269.9778269.9778269.9778269.9778269.9778269.9778
2 2269.9778269.9778269.9778269.9778269.9778269.9778
2 3269.9778269.9778269.9778269.9778269.9778269.9778
2 4269.9778269.9778269.9778269.9778269.9778269.9778
2 5269.9778269.9778269.9778269.9778269.9778269.9778
2 6269.9778269.9778269.9778269.9778269.9778269.9778
2 7269.9778269.9778269.9778269.9778269.9778269.9778
2 8269.9778269.9778269.9778269.9778269.9778269.9778
2 9269.9778269.9778269.9778269.9778269.9778269.9778
2 10269.9778269.9778269.9778269.9778269.9778269.9778
2 11269.9778269.9778269.9778269.9778269.9778269.9778
2 12269.9778269.9778269.9778269.9778269.9778269.9778
2 13269.9778269.9778269.9778269.9778269.9778269.9778
2 14269.9778269.9778269.9778269.9778269.9778269.9778
2 15269.9778269.9778269.9778269.9778269.9778269.9778
2 16269.9778269.9778269.9778269.9778269.9778269.9778
2 17269.9778269.9778269.9778269.9778269.9778269.9778
2 18269.9778269.9778269.9778269.9778269.9778269.9778
2 19269.9778269.9778269.9778269.9778269.9778269.9778
2 20269.9778269.9778269.9778269.9778269.9778269.9778
2 21269.9778269.9778269.9778269.9778269.9778269.9778
2 22269.9778269.9778269.9778269.9778269.9778269.9778
2 23 43.1964 43.1964 43.1964 43.1964 43.1964 43.1964
2 24269.9778269.9778269.9778269.9778269.9778269.9778
2 25269.9778269.9778269.9778269.9778269.9778269.9778
2 26269.9778269.9778269.9778269.9778269.9778269.9778
2 27269.9778269.9778269.9778269.9778269.9778269.9778
2 28269.9778269.9778269.9778269.9778269.9778269.9778
2 29 43.1964 43.1964 43.1964 43.1964 43.1964 43.1964
2 30269.9778269.9778269.9778269.9778269.9778269.9778
2 31269.9778269.9778269.9778269.9778269.9778269.9778
2 32269.9778269.9778269.9778269.9778269.9778269.9778
2 33269.9778269.9778269.9778269.9778269.9778269.9778
2 34269.9778269.9778269.9778269.9778269.9778269.9778
2 35 43.1964 43.1964 43.1964 43.1964 43.1964 43.1964
2 36269.9778269.9778269.9778269.9778269.9778269.9778
2 37269.9778269.9778269.9778269.9778269.9778269.9778
2 38269.9778269.9778269.9778269.9778269.9778269.9778
2 39269.9778269.9778269.9778269.9778269.9778269.9778
2 40269.9778269.9778269.9778269.9778269.9778269.9778
2 41269.9778269.9778269.9778269.9778269.9778269.9778
2 42269.9778269.9778269.9778269.9778269.9778269.9778
2 43269.9778269.9778269.9778269.9778269.9778269.9778
2 44269.9778269.9778269.9778269.9778269.9778269.9778
2 45269.9778269.9778269.9778269.9778269.9778269.9778
2 46269.9778269.9778269.9778269.9778269.9778269.9778
2 47 37.1219 37.1219 37.1219 37.1219 37.1219 37.1219 McCormick Creek
2 48269.9778269.9778269.9778269.9778269.9778269.9778
2 49269.9778269.9778269.9778269.9778269.9778269.9778
2 50269.9778269.9778269.9778269.9778269.9778269.9778
2 51269.9778269.9778269.9778269.9778269.9778269.9778
2 52 18.8984 18.8984 18.8984 18.8984 18.8984 18.8984
2 53269.9778269.9778269.9778269.9778269.9778269.9778
2 54269.9778269.9778269.9778269.9778269.9778269.9778

2 55269.9778269.9778269.9778269.9778269.9778269.9778
2 56269.9778269.9778269.9778269.9778269.9778269.9778
2 57269.9778269.9778269.9778269.9778269.9778269.9778
2 58269.9778269.9778269.9778269.9778269.9778269.9778
2 59269.9778269.9778269.9778269.9778269.9778269.9778
2 60269.9778269.9778269.9778269.9778269.9778269.9778
2 61269.9778269.9778269.9778269.9778269.9778269.9778
2 62269.9778269.9778269.9778269.9778269.9778269.9778
2 63269.9778269.9778269.9778269.9778269.9778269.9778
2 64269.9778269.9778269.9778269.9778269.9778269.9778
2 65269.9778269.9778269.9778269.9778269.9778269.9778
2 66269.9778269.9778269.9778269.9778269.9778269.9778
2 67809.9334809.9334809.9334809.9334809.9334809.9334
2 68269.9778269.9778269.9778269.9778269.9778269.9778
2 69269.9778269.9778269.9778269.9778269.9778269.9778
2 70269.9778269.9778269.9778269.9778269.9778269.9778
2 71269.9778269.9778269.9778269.9778269.9778269.9778
2 72269.9778269.9778269.9778269.9778269.9778269.9778
2 73269.9778269.9778269.9778269.9778269.9778269.9778
2 74 11.8790 11.8790 11.8790 11.8790 11.8790 11.8790 Taylor River
2 75269.9778269.9778269.9778269.9778269.9778269.9778
2 76269.9778269.9778269.9778269.9778269.9778269.9778
2 77269.9778269.9778269.9778269.9778269.9778269.9778
2 78269.9778269.9778269.9778269.9778269.9778269.9778
2 79269.9778269.9778269.9778269.9778269.9778269.9778
2 80269.9778269.9778269.9778269.9778269.9778269.9778
2 81 26.9978 26.9978 26.9978 26.9978 26.9978 26.9978 East Creek
2 82269.9778269.9778269.9778269.9778269.9778269.9778
2 83269.9778269.9778269.9778269.9778269.9778269.9778
2 84269.9778269.9778269.9778269.9778269.9778269.9778
2 85269.9778269.9778269.9778269.9778269.9778269.9778
2 86269.9778269.9778269.9778269.9778269.9778269.9778
2 87269.9778269.9778269.9778269.9778269.9778269.9778
2 88269.9778269.9778269.9778269.9778269.9778269.9778
2 89269.9778269.9778269.9778269.9778269.9778269.9778
2 90269.9778269.9778269.9778269.9778269.9778269.9778
2 91269.9778269.9778269.9778269.9778269.9778269.9778
2 92269.9778269.9778269.9778269.9778269.9778269.9778
2 93269.9778269.9778269.9778269.9778269.9778269.9778
2 94269.9778269.9778269.9778269.9778269.9778269.9778
2 95269.9778269.9778269.9778269.9778269.9778269.9778
2 96269.9778269.9778269.9778269.9778269.9778269.9778
2 97269.9778269.9778269.9778269.9778269.9778269.9778
2 98269.9778269.9778269.9778269.9778269.9778269.9778
2 99269.9778269.9778269.9778269.9778269.9778269.9778
2 100269.9778269.9778269.9778269.9778269.9778269.9778
2 101269.9778269.9778269.9778269.9778269.9778269.9778
2 102269.9778269.9778269.9778269.9778269.9778269.9778
2 103269.9778269.9778269.9778269.9778269.9778269.9778
2 104269.9778269.9778269.9778269.9778269.9778269.9778
2 105269.9778269.9778269.9778269.9778269.9778269.9778
2 106269.9778269.9778269.9778269.9778269.9778269.9778
2 107269.9778269.9778269.9778269.9778269.9778269.9778
2 108269.9778269.9778269.9778269.9778269.9778269.9778
2 109 40.4967 40.4967 40.4967 40.4967 40.4967 40.4967 Trout Creek
2 110269.9778269.9778269.9778269.9778269.9778269.9778
2 111269.9778269.9778269.9778269.9778269.9778269.9778
2 112269.9778269.9778269.9778269.9778269.9778269.9778
2 113269.9778269.9778269.9778269.9778269.9778269.9778
2 114269.9778269.9778269.9778269.9778269.9778269.9778
2 115269.9778269.9778269.9778269.9778269.9778269.9778
2 116269.9778269.9778269.9778269.9778269.9778269.9778
2 117269.9778269.9778269.9778269.9778269.9778269.9778
2 118269.9778269.9778269.9778269.9778269.9778269.9778
2 119269.9778269.9778269.9778269.9778269.9778269.9778
2 120 10.7991 10.7991 10.7991 10.7991 10.7991 10.7991 Shell Creek
2 121 16.1987 16.1987 16.1987 16.1987 16.1987 16.1987 Stllwater Creek
2 122269.9778269.9778269.9778269.9778269.9778269.9778
2 123269.9778269.9778269.9778269.9778269.9778269.9778
2 124 8.0993 8.0993 8.0993 8.0993 8.0993 8.0993 Orgeon Creek

```
2  125269.9778269.9778269.9778269.9778269.9778269.9778
2  126 56.6953 56.6953 56.6953 56.6953 56.6953 56.6953          West Highway Creek
2  127269.9778269.9778269.9778269.9778269.9778269.9778
2  128 26.9978 26.9978 26.9978 26.9978 26.9978 26.9978          East Highway Creek
1   1   -0.12     10.    1.0                          RS11 Bar Init
1   2    0.03     10.    1.0
1   3   -0.12     10.    1.0
1   4    0.03     10.    1.0
1   5   -0.12     10.    1.0
1   6    0.03     10.    1.0
1   7   -0.12     10.    1.0
1   8    1.52     10.   0.08
1   9   -0.12     10.    1.0
1  10    0.03     10.    1.0
1  11   -0.12     10.    1.0
1  12   -0.12     10.    1.0
1  13    0.03     10.    1.0
1  14   -0.12     10.    1.0
1  15    1.52     10.   0.05                                                    Alligator Creek
1  16    0.03     10.    1.0
1  17   -0.12     10.    1.0
1  18    0.03     10.    1.0
1  19   -0.12     10.    1.0
1  20    1.52     10.   0.080
1  21    0.03     10.    1.0
1  22   -0.12     10.    1.0
1  23    0.03     10.    1.0
1  24   -0.12     10.    1.0
1  25    0.03     10.    1.0
1  26   -0.12     10.    1.0
1  27    0.03     10.    1.0
1  28   -0.12     10.    1.0
1  29    0.03     10.    1.0
1  30   -0.12     10.    1.0
1  31    0.03     10.    1.0
1  32    1.52     10.   0.080
1  33   -0.12     10.    1.0
1  34    0.03     10.    1.0
1  35    1.52     10.   0.080
1  36    0.03     10.    1.0
1  37   -0.12     10.    1.0
1  38    0.03     10.    1.0
1  39   -0.12     10.    1.0
1  40    0.03     10.    1.0
1  41   -0.12     10.    1.0
1  42    0.03     10.    1.0
1  43   -0.12     10.    1.0
1  44    0.03     10.    1.0
1  45   -0.01     10.    1.0
1  46   -0.15     10.    1.0
1  47   -0.30     10.    1.0
1  48    1.52     10.   0.080
1  49   -0.15     10.    1.0
1  50   -0.30     10.    1.0
1  51   -0.15     10.    1.0
1  52   -0.30     10.    1.0
1  53   -0.15     10.    1.0
1  54   -0.30     10.    1.0
1  55   -0.30     10.    1.0
1  56   -0.30     10.    1.0
1  57   -0.30     10.    1.0
1  58   -0.30     10.    1.0
1  59   -0.30     10.    1.0
1  60   -0.30     10.    1.0
1  61   -0.30     10.    1.0
1  62   -0.30     10.    1.0
1  63   -0.30     10.    1.0
1  64   -0.30     10.    1.0
1  65   -0.30     10.    1.0
1  66   -0.30     10.    1.0
```

1	67	-0.30	10.	1.0
1	68	-0.30	10.	1.0
1	69	-0.30	10.	1.0
1	70	-0.30	10.	1.0
1	71	-0.30	10.	1.0
1	72	-0.30	10.	1.0
1	73	-0.30	10.	1.0
1	74	-0.30	10.	1.0
1	75	1.52	10.	0.040
1	76	-0.30	10.	1.0
1	77	-0.30	10.	1.0
1	78	-0.30	10.	1.0
1	79	-0.30	10.	1.0
1	80	-0.30	10.	1.0
1	81	-0.30	10.	1.0
1	82	-0.15	10.	1.0
1	83	-0.30	10.	1.0
1	84	-0.15	10.	1.0
1	85	-0.30	10.	1.0
1	86	-0.15	10.	1.0
1	87	-0.30	10.	1.0
1	88	-0.15	10.	1.0
1	89	-0.30	10.	1.0
1	90	-0.15	10.	1.0
1	91	-0.30	10.	1.0
1	92	-0.15	10.	1.0
1	93	-0.30	10.	1.0
1	94	-0.15	10.	1.0
2	1	1.22	10.	1.0
2	2	1.22	10.	1.0
2	3	1.22	10.	1.0
2	4	1.22	10.	1.0
2	5	1.22	10.	1.0
2	6	1.0	10.	1.0
2	7	0.30	10.	1.0
2	8	0.03	10.	1.0
2	9	-0.12	10.	1.0
2	10	0.03	10.	1.0
2	11	-0.12	10.	1.0
2	12	0.03	10.	1.0
2	13	-0.12	10.	1.0
2	14	0.03	10.	1.0
2	15	-0.12	10.	1.0
2	16	0.03	10.	1.0
2	17	-0.12	10.	1.0
2	18	0.03	10.	1.0
2	19	-0.12	10.	1.0
2	20	0.03	10.	1.0
2	21	-0.12	10.	1.0
2	22	0.03	10.	1.0
2	23	1.52	10.	0.080
2	24	-0.12	10.	1.0
2	25	0.03	10.	1.0
2	26	-0.12	10.	1.0
2	27	0.03	10.	1.0
2	28	-0.12	10.	1.0
2	29	1.52	10.	0.080
2	30	0.03	10.	1.0
2	31	-0.12	10.	1.0
2	32	0.03	10.	1.0
2	33	-0.12	10.	1.0
2	34	0.03	10.	1.0
2	35	1.52	10.	0.080
2	36	-0.12	10.	1.0
2	37	0.03	10.	1.0
2	38	-0.12	10.	1.0
2	39	0.03	10.	1.0
2	40	-0.12	10.	1.0
2	41	0.03	10.	1.0
2	42	-0.12	10.	1.0

Mud Creek

2	43	0.03	10.	1.0	
2	44	-0.12	10.	1.0	
2	45	0.03	10.	1.0	
2	46	-0.12	10.	1.0	
2	47	1.52	10.	0.055	McCormick
2	48	0.03	10.	1.0	
2	49	-0.12	10.	1.0	
2	50	0.03	10.	1.0	
2	51	-0.12	10.	1.0	
2	52	1.52	10.	0.020	
2	53	-0.12	10.	1.0	
2	54	0.03	10.	1.0	
2	55	-0.12	10.	1.0	
2	56	0.03	10.	1.0	
2	57	-0.12	10.	1.0	
2	58	0.03	10.	1.0	
2	59	-0.3	10.	1.0	
2	60	-0.15	10.	1.0	
2	61	-0.30	10.	1.0	
2	62	-0.15	10.	1.0	
2	63	-0.30	10.	1.0	
2	64	-0.15	10.	1.0	
2	65	-0.30	10.	1.0	
2	66	-0.15	10.	1.0	
2	67	-0.30	10.	1.0	
2	68	-0.30	10.	1.0	
2	69	-0.30	10.	1.0	
2	70	-0.30	10.	1.0	
2	71	-0.30	10.	1.0	
2	72	-0.30	10.	1.0	
2	73	-0.30	10.	1.0	
2	74	1.52	10.	0.022	Taylor
2	75	-0.30	10.	1.0	
2	76	-0.30	10.	1.0	
2	77	-0.30	10.	1.0	
2	78	-0.30	10.	1.0	
2	79	-0.30	10.	1.0	
2	80	-0.30	10.	1.0	
2	81	1.52	10.	0.040	East
2	82	-0.30	10.	1.0	
2	83	-0.30	10.	1.0	
2	84	-0.30	10.	1.0	
2	85	-0.30	10.	1.0	
2	86	-0.30	10.	1.0	
2	87	-0.30	10.	1.0	
2	88	-0.30	10.	1.0	
2	89	-0.30	10.	1.0	
2	90	-0.30	10.	1.0	
2	91	-0.30	10.	1.0	
2	92	-0.30	10.	1.0	
2	93	-0.30	10.	1.0	
2	94	-0.30	10.	1.0	
2	95	-0.30	10.	1.0	
2	96	-0.15	10.	1.0	
2	97	-0.30	10.	1.0	
2	98	-0.15	10.	1.0	
2	99	-0.30	10.	1.0	
2	100	-0.15	10.	1.0	
2	101	-0.30	10.	1.0	
2	102	-0.15	10.	1.0	
2	103	-0.30	10.	1.0	
2	104	-0.15	10.	1.0	
2	105	-0.30	10.	1.0	
2	106	-0.15	10.	1.0	
2	107	-0.30	10.	1.0	
2	108	-0.15	10.	1.0	
2	109	1.52	10.	0.120	Trout Creek
2	110	-0.30	10.	1.0	
2	111	-0.15	10.	1.0	
2	112	-0.30	10.	1.0	

```
   2  113    -0.15      10.      1.0
   2  114    -0.30      10.      1.0
   2  115    -0.15      10.      1.0
   2  116    -0.30      10.      1.0
   2  117    -0.15      10.      1.0
   2  118    -0.30      10.      1.0
   2  119     -0.1      10.      1.0
   2  120     1.52      10.    0.020                                                    Shell Creek
   2  121     1.52      10.    0.030                                                    Stillwater Creek
   2  122     -0.1      10.      1.0
   2  123     -0.1      10.      1.0
   2  124     1.52      10.    0.015                                                    Oregon Creek
   2  125     -0.1      10.      1.0
   2  126     1.52      10.    0.070                                                    West Highway
Creek
   2  127     -0.1      10.      1.0
   2  128     1.52      10.    0.050                                                    East Highway
Creek
 1 5  1 15  1  2 0    60.0SOUTHWEST SHORE     SOUTHWEST CORNER         RS12_1
 2 8  2  1 78  1 0    60.0SOUTHWEST CORNER    SOUTH OF TAYLOR          RS12_2
 3 8 79  1137  1 0    60.0SOUTH OF TAYLOR     SOUTHEAST CORNER         RS12_3
 4 7144 40144 38 0     60.0CULVERTS AT US 1                          RS12_4
 5 7118 69118 85 0     60.0GW INTERACTION WITH C-111                 RS12_5
 6 5 25 44 25 69 0     60.0CULVERTS ON WEST SIDE                     RS12_6
 7 6 30 72 47 72 0     60.0FROM P46 TO CY3                           RS12_7
 8 6 48 72 68 72 0     60.0FROM CY3 TO P67                           RS12_8
 1   0.200  15.0    40.0  0.0182                                     RS13_1
 2   0.200  15.0    40.0  0.0143                                     RS13_2
 3   0.200  15.0    40.0  0.0048                                     RS13_3
 4   0.200  15.0     3.6  0.0064                                     RS13_4
 5   0.200  15.0     0.0  0.0053                                     RS13_5
 6   0.200  15.0     0.0   0.004                                     RS13_6
 7   0.200  15.0     0.0   0.004                                     RS13_7
 8   0.200  15.0     0.0   0.004                                     RS13_8
 1   0.200  15.0    40.0  0.0182                                     RS14_1
 2   0.200  15.0    40.0  0.0143                                     RS14_2
 3   0.200  15.0    40.0  0.0048                                     RS14_3
 4   0.200  15.0     3.6  0.0064                                     RS14_4
 5   0.200  15.0     0.0  0.0053                                     RS14_5
 6   0.200  15.0     0.0   0.004                                     RS14_6
 7   0.200  15.0     0.0   0.004                                     RS14_7
 8   0.200  15.0     0.0   0.004                                     RS14_8
 1    5.01   salinity                                                RS20_1
 2   0.005   TP:TSB water     mg/L=g/m3=ppm                          RS20_2
 1                                                                   RS21_1
 2                                                                   RS21_2
 1    0.01    0.10    0.20     0.5     1.0     2.0   5.0             RS22_1
 2    0.01    0.10    0.20     0.5     1.0     2.0   5.0             RS22_2
     0.01    0.10    0.20     0.5     1.0     2.0   5.0             RS23
      1.0     2.0     5.      10.     50.    100.    200.    500. 1000.  RS24
     -0.5    -0.2    -0.1    -0.05   0.001    0.1     0.2     0.5   1.0  RS25
   0.6   0.6   0.6   0.6   0.7   0.7   0.7   0.7   0.8   0.8   0.8   0.8   0.9   0.9   0.9   0.9   0.9   1.0   1.0   1.1   1.2   1.2   1.3
1.2   1.1   1.0   0.9   0.8   0.7   0.6   0.7   0.9   1.0   1.2   1.2   1.2   1.2   1.3   1.3   1.3   1.4   1.5   1.2   1.0   0.8   0.6
0.8   1.0   1.2   1.5   1.4   1.4   1.3   1.2   1.2   1.2   1.2   0.9   0.8   0.7   0.7   0.7   0.7   0.7   0.6   0.6   0.6   0.6   0.6
0.6   0.7   0.9   1.0   1.1   1.2   1.4   1.5   1.7   1.8   2.0   2.0   2.0   2.0   2.0   2.0   2.0   2.0   2.0   2.0   2.0   2.0   2.0
2.0   2.0   2.0   2.0   2.0   2.0   2.0   2.0   2.0   2.0   2.0   2.0   2.0   2.0   2.0   2.0   2.0   2.0   2.0   2.0   2.0   2.0   2.0
2.0   2.0   2.0   2.0   2.0   2.0   2.0   2.0   2.0   2.0   2.0   2.0   2.0   2.0   2.0   2.0   2.0   2.0   2.0   2.0   2.0   2.0 -99.9 -
99.9 -99.9 -99.9 -99.9 -99.9 -99.9 -99.9 -99.9 -99.9 -99.9 -99.9
   0.6   0.6   0.6   0.6   0.6   0.7   0.7   0.7   0.7   0.8   0.8   0.8   0.8   0.9   0.9   0.9   0.9   0.9   1.0   1.0   1.1   1.2   1.3
1.2   1.0   0.9   0.8   0.7   0.6   0.5   0.7   0.9   0.9   1.0   1.1   1.1   1.2   1.2   1.2   1.2   1.3   1.4   1.2   0.9   0.7   0.6
1.3   1.3   1.5   1.5   1.4   1.4   1.3   1.2   1.2   1.2   1.0   0.9   0.8   0.8   0.7   0.7   0.7   0.6   0.6   0.6   0.6   0.6   0.6
0.6   0.7   0.8   0.9   1.1   1.2   1.3   1.4   1.6   1.7   1.8   1.8   1.8   1.8   1.8   1.8   1.8   1.8   1.8   1.9   1.9   1.8   1.9
1.9   1.9   1.9   1.9   1.9   1.9   1.9   1.9   1.9   1.9   1.9   1.9   1.9   1.9   1.9   1.9   1.9   1.9   1.9   1.9   1.9   1.9   1.9
1.9   1.9   1.9   1.9   1.9   1.9   0.1   1.9   1.9   1.9   1.9   1.9   1.9   1.9   1.9   1.9   1.9   1.9   1.9   1.9   1.9   1.9 -99.9 -
99.9 -99.9 -99.9 -99.9 -99.9 -99.9 -99.9 -99.9 -99.9 -99.9 -99.9
   0.6   0.6   0.6   0.6   0.6   0.7   0.7   0.7   0.7   0.8   0.8   0.8   0.8   0.9   0.9   0.9   0.9   0.9   0.9   1.0   1.0   1.1   1.2
1.1   1.0   0.9   0.8   0.7   0.6   0.5   0.7   0.8   0.8   0.7   1.0   1.1   1.1   1.1   1.1   1.2   1.4   1.3   1.3   1.0   0.7   0.6
1.0   1.0   1.0   1.0   1.1   1.0   0.9   0.8   0.7   1.0   1.0   0.9   0.8   0.8   0.8   0.7   0.7   0.7   0.6   0.6   0.6   0.6   0.6
0.6   0.7   0.8   0.9   1.0   1.1   1.2   1.3   1.4   1.6   1.7   1.7   1.7   1.7   1.7   1.7   1.7   1.7   1.7   1.8   1.8   1.7   1.8
1.8   1.8   1.8   1.8   1.8   1.8   1.8   1.8   1.8   1.8   1.8   1.8   1.8   1.8   1.9   1.9   1.9   1.9   1.9   1.9   1.9   1.9   1.9
```

1.9 1.8 1.8 1.8 1.8 0.1 0.1 1.8 1.8 1.8 1.8 1.8 1.8 1.8 1.8 1.8 1.8 1.8 1.8 1.8 1.8 1.8 0.2 -99.9 -99.9 -99.9 -99.9 -99.9 -99.9 -99.9 -99.9 -99.9 -99.9 -99.9
0.6 0.6 0.6 0.6 0.6 0.7 0.7 0.7 0.7 0.8 0.8 0.8 0.8 0.8 0.9 0.9 0.9 0.9 0.9 0.9 1.0 1.1 1.2 1.1 0.9 0.8 0.7 0.7 0.6 0.5 0.6 0.8 0.7 -0.1 0.9 1.0 1.0 1.1 1.1 1.1 1.2 1.2 1.0 1.0 0.6 0.6
1.0 1.0 1.0 1.0 1.1 1.2 1.2 0.1 0.7 0.8 0.9 0.8 0.8 0.9 0.9 0.9 0.9 1.0 1.0 1.0 0.1 0.4 0.5
0.6 0.7 0.8 0.9 1.0 1.1 1.2 1.3 1.4 1.5 1.6 1.6 1.7 1.7 1.7 1.7 1.7 1.7 1.7 1.7 1.7 1.6 1.8
1.8 1.8 1.8 1.8 1.8 1.8 1.8 1.8 1.8 1.8 1.8 1.8 0.2 1.8 1.8 1.8 1.8 1.8 1.8 1.8 1.8 1.8 1.8
1.8 1.8 1.8 1.8 1.8 1.8 1.8 1.8 1.8 1.8 1.8 1.8 1.7 1.7 1.7 1.7 1.7 1.7 1.7 1.7 1.7 1.7 0.2 -99.9 -99.9 -99.9 -99.9 -99.9 -99.9 -99.9 -99.9 -99.9 -99.9 -99.9
0.6 0.6 0.6 0.6 0.6 0.6 0.7 0.7 0.7 0.7 0.7 0.8 0.8 0.8 0.8 0.8 0.9 0.9 0.9 0.9 0.9 1.0 1.1 1.1 0.9 0.7 0.7 0.6 0.5 0.5 0.6 0.8 0.6 0.1 0.2 0.9 1.0 1.0 1.0 1.0 1.1 1.1 1.0 0.5 0.6 0.6
0.6 0.7 1.0 0.9 1.0 1.1 1.0 0.9 1.0 0.7 0.7 0.8 0.8 0.9 0.9 0.9 0.9 0.9 0.9 0.9 0.9 0.1 0.2
0.1 -0.2 0.6 0.6 1.0 1.2 1.3 1.5 1.6 1.6 1.6 1.6 1.6 1.6 1.6 1.6 1.7 1.7 1.7 1.7 1.7 1.6 1.7
1.7 1.7 1.7 1.7 1.7 1.7 1.7 1.7 1.7 1.7 1.7 0.1 1.7 1.7 1.8 1.8 1.8 1.8 1.8 1.8 1.8 1.8 1.8
1.8 1.7 1.7 1.7 1.7 1.7 1.7 1.7 1.7 1.7 1.7 1.7 1.6 1.6 1.6 1.6 1.6 1.6 1.6 1.6 1.6 1.6 0.2 -99.9 -99.9 -99.9 -99.9 -99.9 -99.9 -99.9 -99.9 -99.9 -99.9 -99.9
0.6 0.6 0.6 0.6 0.6 0.6 0.7 0.7 0.7 0.8 0.8 0.8 0.8 0.8 0.8 0.9 0.9 0.9 0.9 1.0 1.1 1.0 -0.2 0.7 0.6 0.6 0.5 0.5 0.6 0.7 0.6 0.6 0.1 0.9 0.9 0.9 0.9 0.9 1.1 1.0 0.4 0.1 0.1 0.1
0.1 0.1 0.1 0.7 1.0 1.0 1.0 0.7 1.0 0.1 1.0 1.0 0.9 0.9 0.9 0.9 1.0 1.0 1.1 1.2 1.0 1.0 0.7 0.6
0.1 0.0 0.4 0.4 0.8 1.2 1.2 1.4 1.5 1.6 1.6 1.6 1.6 1.6 1.6 1.6 1.6 1.6 1.6 1.7 1.7 1.7 1.7
1.7 1.7 1.7 1.7 1.7 1.7 1.7 1.7 1.7 1.7 1.7 0.1 1.7 1.7 1.7 1.7 1.7 1.7 1.7 1.7 1.7 1.7 1.7
1.7 1.7 1.7 1.7 1.7 1.7 1.7 1.7 1.6 1.6 1.6 1.6 1.6 1.6 1.6 1.6 1.6 1.6 1.6 1.6 1.6 1.6 0.2 -99.9 -99.9 -99.9 -99.9 -99.9 -99.9 -99.9 -99.9 -99.9 -99.9 -99.9
0.6 0.6 0.6 0.6 0.6 0.6 0.7 0.7 0.7 0.7 0.7 0.8 0.8 0.8 0.8 0.8 0.8 0.8 0.8 0.9 0.9 0.9 1.0 1.0 -0.2 0.6 0.6 0.5 0.5 0.5 0.6 0.7 0.5 0.6 -0.1 0.8 0.8 0.9 0.8 0.8 1.0 0.4 0.1 0.1 0.1 0.1
0.1 0.1 0.1 0.7 0.8 0.9 0.9 1.0 0.1 0.1 1.0 1.0 1.0 1.0 1.1 1.2 1.2 1.2 1.2 1.1 1.0 1.0 0.4
0.4 0.1 0.1 0.1 0.4 1.1 1.2 1.4 1.6 1.6 1.6 1.6 1.6 1.6 1.6 1.6 1.6 1.6 1.6 1.6 1.6 1.6 1.6
1.6 1.6 1.6 1.6 1.6 1.6 1.7 1.7 1.7 1.7 0.1 1.7 1.7 1.7 1.7 1.7 1.7 1.7 1.7 1.7 1.7 1.7 1.7
1.7 1.7 1.7 1.7 1.7 0.1 1.6 1.6 1.6 1.6 1.6 1.6 1.6 1.6 1.6 1.6 1.5 1.5 1.5 1.5 1.5 0.1 0.2 -99.9 -99.9 -99.9 -99.9 -99.9 -99.9 -99.9 -99.9 -99.9 -99.9 -99.9
0.6 0.6 0.6 0.6 0.6 0.6 0.7 0.7 0.7 0.7 0.7 0.8 0.8 0.8 0.8 0.8 0.8 0.8 0.8 0.8 0.8 0.8 0.9 0.9 0.9 -0.1 0.5 0.5 0.5 0.5 0.5 0.5 0.7 0.5 -0.4 -0.2 0.8 0.8 0.8 0.7 0.7 0.2 0.1 0.1 0.1 0.2 0.5
0.7 0.7 0.7 0.8 0.7 1.5 1.5 0.1 0.1 0.1 0.9 0.9 1.0 1.0 1.1 1.2 1.2 1.2 1.2 1.2 1.2 1.1 1.0
0.4 0.4 0.0 0.4 1.0 1.1 1.2 1.4 1.5 1.6 1.6 1.6 1.6 1.6 1.6 1.6 1.6 1.6 1.6 1.6 1.6 1.6 1.6
1.6 1.6 1.6 1.6 1.6 1.6 1.6 1.6 1.6 1.7 1.7 1.7 1.7 1.7 1.7 1.7 1.7 1.7 1.7 1.7 1.7 1.7 1.7
1.7 1.7 1.7 1.7 1.6 1.6 1.6 1.6 1.6 1.6 1.6 1.6 1.6 1.5 1.5 1.5 1.5 1.5 1.4 1.4 1.4 0.1 -99.9 -99.9 -99.9 -99.9 -99.9 -99.9 -99.9 -99.9 -99.9 -99.9 -99.9 -99.9
0.6 0.6 0.6 0.6 0.6 0.6 0.7 0.7 0.7 0.7 0.7 0.7 0.8 0.8 0.8 0.8 0.8 0.8 0.8 0.8 0.8 0.8 0.9 0.9 0.1 0.5 0.5 0.5 0.5 0.5 0.5 0.6 0.4 0.1 0.6 0.7 0.7 0.7 0.6 0.1 0.1 0.2 0.1 0.7 0.7 0.7
0.7 0.8 0.7 0.1 0.0 1.5 1.5 0.4 0.2 0.1 0.1 0.1 1.0 1.0 1.1 1.1 1.2 1.2 1.2 1.2 1.2 1.2 1.1
1.0 0.5 0.5 -0.1 1.0 1.1 1.2 1.3 1.5 1.5 1.5 1.5 1.5 1.5 1.5 1.5 1.6 1.6 1.6 1.6 1.6 1.6 1.6
1.6 1.6 1.6 1.6 1.6 1.6 1.6 1.6 1.6 1.6 1.6 1.6 1.6 1.6 1.7 1.7 1.7 1.7 1.7 1.7 1.7 1.7 1.7
1.7 1.7 1.6 1.6 1.6 1.6 1.6 1.6 1.6 1.6 1.6 1.6 1.6 1.5 1.5 1.5 1.4 1.4 1.4 1.4 1.3 1.3 0.1 -99.9 -99.9 -99.9 -99.9 -99.9 -99.9 -99.9 -99.9 -99.9 -99.9 -99.9
0.6 0.6 0.6 0.6 0.6 0.6 0.7 0.7 0.7 0.7 0.7 0.7 0.8 0.7 0.7 0.7 0.7 0.7 0.7 0.8 0.7 0.8 0.8 0.8 -0.2 0.4 0.5 0.4 0.4 0.4 0.5 0.6 0.3 0.0 0.6 0.6 0.6 0.6 0.6 0.0 0.1 0.1 0.1 0.7 0.7 0.7
0.7 0.8 0.7 0.1 0.2 1.5 1.5 0.2 0.1 0.1 0.1 0.1 0.1 1.1 1.2 1.2 1.2 1.2 1.2 1.2 1.2 1.2 1.1
1.1 1.0 1.0 -0.1 -0.1 1.1 1.4 1.4 1.5 1.5 1.5 1.5 1.5 1.5 1.5 1.5 1.5 1.5 1.5 1.6 1.6 1.6 1.6
1.6 1.6 1.6 1.6 1.6 1.6 0.0 1.6 1.6 1.6 1.6 1.6 1.6 1.6 1.7 1.7 1.7 1.7 1.7 1.7 1.7 1.7 1.7
1.7 1.7 1.6 1.6 1.6 1.6 1.6 1.6 1.6 1.6 1.6 1.5 1.5 1.5 1.4 1.4 1.4 1.4 1.3 1.3 0.1 -99.9 -99.9 -99.9 -99.9 -99.9 -99.9 -99.9 -99.9 -99.9 -99.9 -99.9
0.6 0.6 0.6 0.6 0.6 0.6 0.7 0.7 0.7 0.7 0.7 0.7 0.8 0.7 0.7 0.7 0.7 0.7 0.7 0.7 0.7 0.7 0.8 0.8 -0.2 0.0 0.4 0.4 0.4 0.4 0.5 0.6 0.3 0.0 0.6 0.6 0.6 0.6 0.1 0.1 0.1 0.1 0.6 0.7 0.6 0.6
0.4 0.8 0.7 0.6 0.2 1.5 1.5 0.4 0.1 0.1 0.1 0.1 0.1 1.1 1.1 1.2 1.2 1.2 1.2 1.2 1.2 1.2 1.2
1.1 1.1 1.1 1.0 -0.1 1.2 1.4 1.4 1.4 1.4 1.5 1.5 1.5 1.5 1.5 1.5 1.5 1.5 1.5 1.5 1.5 1.5 1.4
1.3 1.3 0.9 1.5 1.5 1.5 -0.1 1.5 1.5 1.6 1.6 1.6 1.6 1.6 0.2 1.6 1.6 1.6 1.6 1.6 1.6 1.6 1.6
1.6 1.6 1.6 1.6 1.6 1.6 1.6 1.6 1.6 1.5 1.5 1.5 1.5 1.5 1.5 1.4 1.4 1.4 1.4 1.3 1.3 0.1 -99.9 -99.9 -99.9 -99.9 -99.9 -99.9 -99.9 -99.9 -99.9 -99.9 -99.9 -99.9
0.6 0.6 0.6 0.6 0.6 0.6 0.6 0.6 0.7 0.7 0.7 0.7 0.7 0.7 0.7 -0.2 0.4 0.4 0.6 0.6 0.6 0.7 0.7 0.7 0.6 0.1 0.4 0.4 0.4 0.4 0.5 0.6 -0.1 0.0 0.0 0.0 0.0 0.0 0.1 0.1 0.1 0.1 0.6 0.7 0.7 0.1
1.5 1.5 0.7 0.4 0.1 0.2 0.4 0.2 0.1 0.0 0.1 0.1 0.1 1.2 1.1 1.1 1.1 1.2 1.1 1.0 1.0 1.0 1.5
1.5 1.0 1.0 1.0 0.0 1.2 1.4 1.4 1.4 1.4 1.4 1.4 1.5 1.5 1.5 1.5 1.5 1.5 1.5 1.5 1.5 1.3 1.2
1.1 1.0 -0.1 0.9 1.5 1.5 1.5 1.5 1.5 1.5 1.6 1.6 1.6 1.6 0.2 1.6 1.6 1.6 1.6 1.6 1.6 1.6 1.6
1.6 1.6 1.6 1.6 1.6 1.6 1.6 1.6 1.5 1.5 1.5 1.5 1.5 1.4 1.4 1.4 1.4 1.4 1.4 1.3 1.3 1.3 -99.9 -99.9 -99.9 -99.9 -99.9 -99.9 -99.9 -99.9 -99.9 -99.9 -99.9 -99.9
0.6 0.6 0.6 0.6 0.6 0.6 0.6 0.6 0.7 0.7 0.7 0.7 0.7 0.7 -0.1 0.1 0.0 -0.1 0.4 0.6 0.6 0.7 0.7 0.5 -0.1 0.0 0.1 0.1 -0.2 -0.2 -0.1 0.0 0.0 -0.1 0.1 0.1 0.1 0.2 0.2 0.1 0.0 0.1 0.4 0.1 0.1
1.5 1.5 0.7 0.0 -0.1 -0.1 0.1 0.1 -0.1 0.3 0.2 0.2 -0.1 0.0 1.0 1.1 1.1 1.1 0.9 0.1 1.0 1.0 1.5
1.5 1.0 1.0 1.0 0.1 1.2 1.4 1.4 1.4 1.4 1.4 1.4 1.4 1.4 1.4 1.4 1.4 1.4 1.4 1.5 1.5 1.2 0.0
0.0 0.0 0.0 0.9 1.4 1.5 1.5 1.5 1.5 1.6 1.6 1.6 1.6 1.6 1.6 1.7 1.6 1.6 1.6 1.6 1.6 1.6 1.6

1.6 1.6 1.6 1.6 1.6 1.6 1.6 1.6 1.6 1.5 1.5 1.5 1.5 1.5 1.4 1.4 1.4 1.4 1.4 1.3 1.3 1.3 -99.9 -
99.9 -99.9 -99.9 -99.9 -99.9 -99.9 -99.9 -99.9 -99.9 -99.9 -99.9
0.6 0.6 0.6 0.6 0.6 0.6 0.6 0.6 0.7 0.7 0.7 0.7 0.7 0.7 -0.1 0.0 0.9 0.1 0.1 0.3 0.1 0.6 0.6
0.6 0.5 -0.3 0.0 0.1 0.9 1.5 1.5 1.5 1.5 1.5 0.3 0.4 0.4 0.3 0.2 0.1 0.1 0.1 0.1 0.7 0.8 0.8
1.5 1.5 0.1 0.0 0.0 0.1 0.1 0.2 0.3 0.3 0.3 0.2 0.0 -0.1 -0.1 1.0 1.0 1.1 1.1 0.1 0.1 0.9 1.5
1.5 0.7 1.0 0.1 0.1 1.2 1.4 1.4 1.4 1.4 1.4 1.4 1.4 1.4 1.4 1.4 1.4 1.4 1.4 1.4 1.4 0.0 0.0
0.0 -0.1 -0.1 1.0 1.4 1.4 1.4 1.5 1.5 1.5 1.5 1.5 1.5 1.6 1.6 1.6 1.6 1.6 1.6 1.6 1.6 1.6 1.6
1.6 1.6 1.6 1.5 1.5 1.5 1.5 1.5 1.5 1.5 1.5 1.5 1.5 1.4 1.4 1.4 1.4 1.4 1.4 1.3 1.3 1.3 1.3 -
99.9 -99.9 -99.9 -99.9 -99.9 -99.9 -99.9 -99.9 -99.9 -99.9 -99.9
0.6 0.6 0.6 0.6 0.6 0.6 0.6 0.6 0.7 0.7 0.7 0.7 0.7 -0.2 -0.1 0.1 0.1 1.5 1.5 1.5 1.5 0.1 0.6
0.6 0.4 0.4 0.0 0.1 0.9 1.5 1.5 1.5 1.5 1.5 0.9 0.9 0.9 0.9 0.1 0.1 0.1 0.1 0.1 0.4 1.5 1.5
1.5 1.5 0.6 0.0 0.0 0.1 0.1 0.2 0.2 0.3 0.2 0.2 0.2 0.1 0.1 0.1 0.0 1.0 1.1 0.0 0.1 0.9 1.5
1.5 0.0 0.0 0.1 0.1 1.3 1.3 1.4 1.4 1.4 1.4 1.4 1.4 1.4 1.4 1.4 1.4 1.4 1.4 1.4 1.4 -0.1 -0.1 -
0.1 0.0 0.0 1.0 1.3 1.4 1.4 1.4 1.4 1.4 1.4 1.4 1.4 1.5 1.5 1.5 1.5 1.5 1.5 1.5 1.5 1.5 1.5
1.5 1.5 1.5 1.5 1.5 1.5 1.5 1.5 1.4 1.4 1.4 1.4 1.4 1.4 1.4 1.3 1.3 1.3 1.2 1.2 1.2 1.2 1.2 -
99.9 -99.9 -99.9 -99.9 -99.9 -99.9 -99.9 -99.9 -99.9 -99.9 -99.9
0.4 0.4 0.4 0.4 0.5 0.5 0.5 0.5 0.5 0.5 0.6 -0.1 -0.1 0.1 0.1 0.0 1.5 1.5 1.5 1.5 0.6 0.6
0.6 0.6 1.5 1.5 1.5 1.5 1.5 1.5 0.1 1.5 1.5 0.9 0.6 0.9 0.6 0.1 0.1 0.1 0.1 0.4 0.5 1.5 1.5
0.1 1.5 1.5 1.5 1.5 0.3 0.1 0.2 0.2 0.3 0.2 0.2 0.3 0.2 0.2 0.2 0.1 0.1 1.0 0.0 0.1 0.0 0.1
0.1 0.1 0.1 0.1 0.1 0.1 1.3 1.3 1.3 1.3 1.3 1.3 1.3 1.3 1.3 1.3 1.3 1.3 1.3 1.4 -0.1 0.0 1.0
1.0 1.1 1.2 1.3 1.3 1.3 1.3 1.3 1.3 1.3 1.3 1.3 1.4 1.4 1.4 1.4 1.4 1.4 1.4 1.4 1.4 1.4 1.4
1.4 1.4 1.4 1.4 1.4 1.4 1.4 1.4 1.4 1.4 1.4 1.4 1.4 1.4 1.4 1.3 1.3 1.3 1.2 1.2 1.2 1.2 1.2 -
99.9 -99.9 -99.9 -99.9 -99.9 -99.9 -99.9 -99.9 -99.9 -99.9
-0.2 -0.1 0.0 0.1 -0.1 -0.1 -0.1 -0.1 0.0 -0.1 -0.2 -0.2 -0.2 0.1 0.1 0.1 0.1 0.2 0.3 0.3 0.3 0.6 0.6
0.6 0.6 1.5 1.5 1.5 1.5 1.5 1.5 0.1 1.5 1.5 0.1 0.1 0.1 0.1 0.1 0.1 0.1 0.7 0.8 1.5 1.5 1.5
1.5 1.5 1.5 1.5 1.5 0.9 0.0 0.2 0.5 0.2 0.4 0.4 0.5 0.3 0.4 0.4 0.3 0.1 0.2 0.2 0.2 0.2 0.1
0.1 0.9 0.1 0.1 0.1 0.1 0.0 -0.1 -0.1 0.0 1.3 1.3 1.3 1.3 1.3 1.3 1.3 1.3 1.3 1.3 1.3 1.3 1.3
1.3 1.3 1.2 1.2 1.2 1.3 1.3 1.3 1.3 1.3 1.3 1.3 1.3 1.3 1.3 1.3 1.3 1.3 1.3 1.3 1.3 1.3 1.3
1.3 1.3 1.4 1.4 1.4 1.4 1.4 1.4 1.4 1.4 1.4 1.4 1.4 1.4 1.4 1.3 1.3 1.3 1.3 1.2 1.2 1.2 1.2 1.2
1.2 -99.9 -99.9 -99.9 -99.9 -99.9 -99.9 -99.9 -99.9 -99.9 -99.9
-0.2 -0.2 -0.2 -0.2 -0.1 -0.2 -0.2 -0.3 -0.3 -0.2 -0.1 -0.1 0.0 0.0 0.1 0.1 0.2 0.1 0.0 0.0 0.3 0.6 0.6
0.6 0.6 0.6 0.6 -0.1 0.3 0.4 0.1 0.0 1.5 1.5 0.1 0.0 0.0 0.1 0.1 0.9 0.9 0.9 0.9 1.5 1.5 1.5
1.5 0.9 0.9 1.5 1.2 0.9 0.1 0.0 0.5 0.6 0.5 0.5 0.4 0.4 0.4 0.5 0.7 0.5 0.5 0.4 0.4 0.2 0.1
0.1 1.0 1.0 1.1 1.1 1.1 1.1 1.2 1.2 1.2 1.2 1.2 1.2 1.3 1.2 -0.1 -0.1 -0.1 -0.1 1.2 1.2 1.2 1.2
1.2 1.1 1.1 1.1 1.2 1.2 1.2 1.3 1.2 1.2 1.2 1.2 1.2 1.2 1.2 1.2 1.2 1.2 1.3 1.3 1.3 1.3 1.3 1.3
1.3 1.3 1.3 1.3 1.3 1.3 1.3 1.3 1.3 1.4 1.4 1.4 1.4 1.4 1.3 1.3 1.3 1.3 1.2 1.2 1.2 1.2 1.2
1.2 -99.9 -99.9 -99.9 -99.9 -99.9 -99.9 -99.9 -99.9 -99.9 -99.9
-0.2 -0.1 -0.1 -0.1 -0.1 -0.1 -0.2 -0.2 -0.1 -0.1 0.0 0.0 0.0 0.0 0.1 0.1 0.1 0.1 0.1 0.1 -0.1 -0.1 0.9
-0.4 -0.3 -0.2 -0.1 -0.1 -0.1 0.0 0.0 0.0 1.5 1.5 0.0 0.0 0.0 0.0 0.1 0.1 0.1 0.9 0.9 0.8 0.7 0.1
0.9 0.9 0.1 0.0 0.9 0.9 0.9 0.1 0.3 0.5 0.4 0.3 0.3 0.4 0.4 0.4 0.4 0.4 0.5 0.4 0.3 0.2 0.2
0.1 -0.1 1.0 1.1 1.2 1.2 1.3 1.3 1.3 1.3 1.3 1.3 1.0 -0.1 -0.1 -0.1 -0.1 0.0 0.0 1.0 1.1 1.1 1.1
1.2 1.2 1.2 1.2 1.2 1.2 1.2 1.2 1.1 1.1 1.1 1.2 1.2 1.2 1.2 1.2 1.2 1.2 1.2 1.2 1.2 1.2 1.2
1.2 1.2 1.2 1.2 1.2 1.3 1.3 1.3 1.3 1.3 1.3 1.3 1.4 1.3 1.3 1.3 1.3 1.3 1.2 1.2 1.2 1.2 1.2
1.2 1.2 -99.9 -99.9 -99.9 -99.9 -99.9 -99.9 -99.9 -99.9
-0.2 -0.1 -0.1 -0.1 -0.1 -0.1 -0.1 -0.2 -0.1 0.0 0.0 0.0 0.0 0.0 0.1 0.1 0.1 0.1 0.1 0.1 -0.1 -0.1 -0.4
-0.4 -0.3 -0.2 -0.1 -0.1 -0.1 -0.1 0.0 0.0 1.5 1.5 -0.1 0.0 0.0 0.0 0.0 0.0 0.6 0.1 0.2 0.1 0.1 0.1
0.1 0.1 0.1 0.7 0.9 0.9 0.9 0.9 0.2 0.4 0.3 0.2 0.3 0.4 0.4 0.3 0.2 0.2 0.4 0.4 0.2 0.2 0.2
0.1 0.0 0.1 0.1 1.0 1.1 1.2 1.2 1.3 1.3 1.4 1.4 1.3 1.2 1.2 1.1 1.1 1.0 0.0 0.1 1.0 1.0 1.0
1.1 1.1 1.1 1.1 1.1 1.2 1.2 1.2 1.0 1.0 1.0 1.1 1.2 1.2 1.2 1.2 1.2 0.5 0.4 0.4 1.2 1.2 1.2
1.2 1.2 1.2 1.2 1.2 1.2 1.3 1.3 1.3 1.3 1.4 1.4 1.4 1.4 1.4 1.3 1.3 1.2 1.2 1.2 1.2 1.2
1.2 1.2 -99.9 -99.9 -99.9 -99.9 -99.9 -99.9 -99.9 -99.9
-0.2 -0.1 -0.1 -0.1 0.1 0.0 -0.1 -0.1 0.1 0.1 0.1 0.1 0.1 0.1 0.1 0.1 0.2 0.2 0.1 0.0 -0.1 -0.2 -0.2
1.5 1.5 1.5 1.5 1.5 1.5 1.5 1.5 1.5 1.5 1.5 -0.1 -0.1 -0.1 -0.1 -0.1 -0.1 -0.1 0.0 0.0 0.1 0.1 0.1
0.9 0.1 0.1 1.0 1.0 0.9 0.9 0.2 0.1 0.3 0.3 0.3 0.4 0.5 0.2 0.2 0.1 0.1 0.4 0.3 0.1 0.0 0.0
0.2 0.4 0.2 0.1 1.2 1.2 1.2 1.5 1.5 1.2 1.3 1.3 1.3 1.3 1.3 1.3 1.3 1.3 1.2 0.2 0.2 1.0 1.1
1.0 1.0 1.0 1.0 1.1 1.1 1.1 1.1 1.0 1.0 1.0 1.0 1.1 1.1 1.1 1.1 1.1 1.1 1.1 1.1 0.3 0.3 1.2
1.2 1.2 1.2 1.2 1.2 1.2 1.2 1.2 1.2 1.2 1.3 1.3 1.3 1.3 1.3 1.3 1.3 1.3 1.2 1.2 1.2 1.2 1.1
1.1 1.1 1.0 -99.9 -99.9 -99.9 -99.9 -99.9 -99.9 -99.9
0.1 0.1 0.1 0.0 -0.1 -0.1 -0.1 -0.1 0.1 0.0 0.0 0.0 -0.1 -0.1 -0.1 -0.1 -0.1 0.0 0.0 -0.1 -0.3 -0.2 -0.1
1.5 1.5 1.5 1.5 1.5 1.5 1.5 1.5 1.5 1.5 1.5 0.0 -0.1 -0.1 -0.1 -0.2 -0.2 -0.1 0.0 -0.1 0.1 0.1 0.0
0.1 0.1 1.0 1.0 0.9 0.9 0.9 0.2 0.3 0.2 0.5 0.5 0.3 0.3 0.2 0.2 0.3 0.5 0.7 0.5 0.3 0.0 0.2
0.2 0.2 0.2 0.1 0.1 0.9 0.0 1.5 1.5 1.1 1.2 1.3 1.3 1.4 1.4 1.3 1.3 1.2 1.2 1.1 0.4 0.4 0.3
1.0 1.0 1.0 1.0 1.0 1.0 1.0 1.1 1.0 1.0 1.0 1.0 1.1 1.1 1.1 1.1 1.1 1.1 1.1 1.1 0.4 1.2 1.2
1.2 1.2 1.2 1.2 1.2 1.2 1.2 1.2 1.2 1.2 1.2 1.3 1.3 1.2 1.2 1.2 1.2 1.2 1.3 1.3 1.3 1.2 1.2
1.1 1.1 1.0 -99.9 -99.9 -99.9 -99.9 -99.9 -99.9 -99.9
0.0 0.0 0.0 -0.1 -0.1 -0.1 -0.1 -0.1 0.0 0.0 -0.1 -0.1 -0.1 -0.2 -0.2 -0.2 -0.1 -0.1 -0.1 -0.1 -0.1 0.0 0.0
1.5 1.5 0.1 0.0 1.5 1.5 0.9 0.7 -0.1 -0.1 -0.1 -0.1 -0.1 -0.1 0.9 0.9 -0.1 -0.1 -0.1 0.0 0.1 0.9 0.9
0.9 0.9 0.9 0.9 0.9 0.2 0.2 0.2 0.2 0.3 0.4 0.4 0.2 0.4 0.2 0.2 0.2 0.4 0.5 0.5 0.5 0.4 0.2
0.3 0.4 0.2 0.2 0.2 0.2 0.2 1.5 1.5 0.1 -0.1 1.1 1.1 1.1 1.2 1.2 1.2 1.2 1.1 1.1 0.2 0.9 0.9
0.0 1.0 1.0 1.0 1.0 1.0 1.0 1.0 1.0 0.7 1.0 1.0 1.0 1.0 1.0 1.1 1.0 1.0 1.0 0.4 1.0 1.1 1.1

1.1 1.1 1.1 1.2 1.2 1.2 1.2 1.2 1.2 1.2 1.2 1.2 1.2 1.2 1.2 1.2 1.1 1.1 1.0 1.0 1.0 1.0 1.0
1.0 1.0 1.0 0.2 -99.9 -99.9 -99.9 -99.9 -99.9 -99.9
0.0 0.0 -0.1 -0.1 -0.1 -0.1 -0.1 -0.1 0.0 0.0 -0.1 -0.1 -0.1 -0.2 -0.2 -0.2 -0.2 -0.2 -0.1 -0.1 -0.1 0.1 0.0
1.5 1.5 0.9 0.9 1.5 1.5 -0.1 -0.1 -0.1 -0.2 -0.2 -0.1 -0.1 0.0 0.9 0.9 0.9 0.0 0.4 0.9 0.9 0.9 0.9
0.9 0.9 0.9 0.9 0.1 0.2 0.2 0.2 0.1 0.3 0.4 0.5 0.4 0.4 0.3 0.2 0.2 0.5 0.5 0.5 0.5 0.4 0.3
0.3 0.5 0.2 0.2 0.3 0.4 0.3 1.5 1.5 0.1 -0.1 0.1 1.0 0.2 1.5 1.5 1.1 1.1 1.1 1.1 0.3 0.9 0.9
0.0 1.0 1.0 1.0 1.0 1.0 0.9 0.0 0.1 0.0 0.7 1.0 1.0 1.0 1.0 1.0 1.0 1.0 1.0 1.0 1.0 1.1 1.1
1.1 1.1 1.1 1.2 1.1 1.1 1.1 1.1 1.1 1.1 1.2 1.2 1.2 1.2 1.2 1.2 1.1 1.1 1.1 1.0 1.0 1.0 1.0
1.0 1.0 0.2 0.2 -99.9 -99.9 -99.9 -99.9 -99.9 -99.9
0.1 -0.1 -0.1 -0.1 -0.1 -0.1 -0.1 0.0 0.1 0.0 -0.1 -0.1 -0.1 -0.1 -0.1 -0.2 -0.2 -0.2 -0.1 0.0 0.1 0.3 0.0
1.5 1.5 0.0 0.9 1.5 1.5 1.5 -0.1 -0.2 -0.2 -0.4 -0.1 0.4 0.9 0.0 0.0 0.9 0.2 0.1 0.9 0.9 0.9 1.0
0.9 0.9 0.9 0.1 0.1 0.2 0.2 0.3 0.1 0.3 0.4 0.5 0.9 0.5 0.4 0.4 0.5 0.9 0.3 0.3 0.3 0.1 0.2
0.2 0.2 0.1 0.2 0.5 0.7 0.3 0.3 0.9 0.3 0.1 0.1 0.2 0.2 1.5 1.5 1.0 1.0 1.0 1.0 0.4 0.3 0.9
0.2 0.2 1.0 1.0 1.0 1.0 0.1 0.0 0.1 0.0 0.1 0.7 1.0 1.0 1.0 1.0 1.0 1.0 1.0 1.0 1.0 1.1 1.1
1.1 1.1 1.1 1.1 1.2 1.1 1.1 1.1 1.1 1.1 1.1 1.2 1.1 1.1 1.1 1.1 1.1 1.0 1.0 1.0 1.0 1.0 1.0
1.0 1.0 0.2 0.2 0.2 1.0 -99.9 -99.9 -99.9 -99.9
-99.9 -0.2 -0.1 -0.1 0.0 0.0 -0.1 -0.1 0.0 -0.1 -0.1 -0.1 -0.1 0.9 0.9 0.9 0.9 0.9 0.9 0.9 0.9 0.4 0.3
1.5 1.5 0.9 -0.1 1.5 1.5 1.5 0.9 0.9 0.6 0.6 0.7 0.7 0.5 0.2 0.1 0.2 0.2 0.0 0.2 0.9 0.9 0.9
0.9 0.9 0.9 -0.1 0.1 0.2 0.3 0.4 0.5 0.2 0.2 0.3 0.4 0.5 0.4 0.4 0.5 -0.1 0.5 0.5 0.4 0.2 0.2
0.2 0.2 0.2 0.4 0.4 0.3 0.4 0.4 0.3 0.4 0.4 0.3 0.3 0.4 1.5 1.5 0.4 0.4 0.4 1.0 0.4 0.3 0.6
0.3 0.2 0.0 0.0 1.0 1.0 0.0 1.0 1.0 0.0 0.1 0.2 1.0 1.0 1.0 1.0 1.0 1.0 1.0 0.4 1.0 1.1 1.1
1.1 1.1 1.1 1.1 1.2 1.1 1.1 1.1 1.0 0.1 1.1 1.1 1.1 1.1 1.1 1.0 1.0 1.0 1.0 1.0 1.0 1.0 1.0
1.0 0.2 1.0 1.0 1.0 1.0 1.0 -99.9 -99.9 -99.9
-99.9 -99.9 0.0 0.0 0.0 0.0 0.0 -0.1 0.9 0.9 0.9 0.6 0.9 0.9 0.9 1.0 1.0 1.0 1.0 0.9 0.9 0.9 0.9
0.9 0.9 0.9 -0.1 -0.1 0.9 0.9 0.9 0.9 0.9 0.9 1.0 1.0 0.7 0.4 0.2 0.4 0.4 0.2 0.1 0.7 0.9 0.9
0.9 0.0 -0.1 0.0 0.2 0.1 0.3 0.4 0.4 0.4 0.4 0.4 0.3 0.5 0.5 0.5 0.4 0.3 0.4 0.3 0.2 0.1 0.4
0.4 0.4 0.4 0.4 0.5 0.6 0.3 0.9 0.4 0.3 0.3 0.6 0.3 0.4 1.5 1.5 0.4 0.4 0.4 0.5 0.4 0.9 0.9
0.9 1.5 1.5 1.5 1.5 1.0 1.0 1.0 1.0 0.1 0.1 0.2 1.0 1.0 1.0 1.0 1.0 1.0 0.5 1.0 1.0 1.1 1.1
1.1 1.1 1.1 1.1 1.2 1.0 1.0 1.0 0.1 0.1 1.0 1.1 1.0 1.0 1.0 1.0 1.0 1.0 1.0 1.0 1.0 1.0 1.0
0.1 0.2 1.1 1.1 1.1 1.1 1.1 1.1 1.1 -99.9
-99.9 -99.9 -99.9 0.1 0.0 0.0 0.0 0.9 0.9 0.9 0.9 0.9 0.9 1.0 1.1 1.1 1.2 1.1 1.1 1.1 1.0 1.0
0.9 0.9 0.9 0.9 -0.1 -0.1 0.9 0.9 0.9 1.0 1.0 1.0 0.9 0.9 0.9 0.3 0.3 0.4 0.4 0.4 0.2 0.1 0.1
0.9 0.9 0.1 0.0 0.0 0.3 0.2 0.3 0.3 0.3 0.5 0.5 0.5 0.5 0.6 0.7 0.6 0.5 0.5 0.5 0.4 0.3 0.3
0.5 0.5 0.5 0.6 0.5 0.7 0.8 1.1 0.6 0.5 0.4 0.4 0.6 0.4 0.9 0.9 0.9 0.5 0.4 0.3 0.4 0.4 0.9
0.9 0.9 1.5 1.5 1.5 1.5 1.0 1.0 1.0 1.0 1.0 0.1 0.1 1.0 1.0 1.0 1.0 0.3 0.3 0.5 1.0 1.0 1.1
1.1 1.1 1.1 1.1 1.1 1.1 1.0 0.2 0.1 0.1 0.1 0.9 1.5 1.5 1.0 1.0 1.0 1.0 1.0 1.0 1.0 1.0 1.0
0.1 0.1 1.1 1.1 1.1 1.1 1.2 1.2 1.1 1.1 1.1
-99.9 -99.9 -99.9 -99.9 -99.9 0.0 0.0 0.9 0.9 0.9 0.9 0.9 0.9 1.0 1.0 1.0 1.0 1.0 1.0 0.9 0.9 0.9
0.9 0.9 0.1 0.1 -0.1 -0.1 -0.1 0.0 0.9 0.3 0.4 0.4 0.5 0.7 0.9 0.1 0.5 0.4 0.4 0.5 0.2 0.2 0.1
0.0 0.2 0.2 0.1 0.9 0.3 0.3 0.3 0.3 0.4 0.5 0.5 0.6 0.8 0.8 0.8 0.8 0.8 0.7 0.5 0.5 0.6 0.4
0.8 0.7 0.6 0.8 0.6 0.9 1.1 1.2 1.0 0.5 0.4 0.3 0.3 0.9 0.9 0.9 0.9 0.4 0.3 0.3 0.5 0.9 0.9
0.9 0.9 0.9 0.0 0.7 0.7 1.0 1.0 1.0 1.0 1.0 0.1 0.7 1.0 1.0 1.0 1.0 0.4 0.4 0.3 1.0 1.0 1.1
0.6 1.1 1.1 1.1 1.1 1.1 1.0 0.2 0.1 0.9 0.9 0.6 1.5 1.5 1.0 1.0 1.0 1.0 1.0 1.0 1.0 0.1 0.0
0.1 1.1 1.1 1.1 1.2 1.2 1.2 1.1 1.1 1.1 -99.9
-99.9 -99.9 -99.9 -99.9 -99.9 -99.9 0.1 0.1 0.0 0.9 0.9 0.9 0.9 0.9 0.9 0.9 0.9 0.9 0.9 0.9 0.9 0.9
0.9 0.1 0.1 0.1 0.3 0.2 0.1 0.9 0.9 0.9 0.9 0.9 0.9 0.9 0.9 0.3 0.5 0.3 0.3 0.3 0.2 0.1 0.1
0.0 0.5 0.4 0.2 0.2 0.4 0.4 0.3 0.2 0.8 0.5 0.5 0.5 0.5 0.5 0.4 0.4 0.4 0.2 0.1 0.3 0.4 0.8
0.5 0.5 0.6 0.6 0.6 0.6 0.4 0.4 0.5 0.4 0.3 0.2 0.6 0.9 0.9 0.9 0.2 0.2 0.4 0.9 0.7 0.9 0.3
0.9 0.2 0.1 0.9 1.1 0.0 0.0 0.0 0.1 0.1 0.1 0.1 0.2 0.2 1.0 1.0 0.3 0.4 0.3 1.0 1.0 1.5 1.5
1.0 1.0 1.0 1.0 1.1 1.1 0.1 0.2 0.1 0.1 0.1 0.1 1.5 1.5 0.1 0.4 1.0 0.1 0.1 0.1 0.1 0.1 0.0
1.0 1.1 1.2 1.2 1.3 1.3 1.2 1.2 1.1 1.1 -99.9
-99.9 -99.9 -99.9 -99.9 -99.9 -99.9 -99.9 -99.9 0.1 0.0 0.0 0.0 0.0 0.1 -0.1 0.0 0.9 0.2 0.3 0.3 0.2 0.9
0.2 0.3 0.3 0.2 0.2 0.2 0.1 0.1 0.1 0.7 0.0 0.1 0.1 0.1 0.2 0.4 0.4 0.4 0.3 0.1 0.3 0.2 0.2
0.2 0.4 0.3 0.2 0.2 0.2 0.4 0.4 0.3 0.5 0.2 0.4 0.4 0.2 0.4 0.4 0.4 0.3 -0.1 0.2 0.3 0.3 0.4
0.5 0.4 0.3 0.4 0.4 0.6 0.6 0.6 0.4 0.4 0.3 0.0 0.1 0.2 0.2 0.2 0.2 0.3 0.4 0.5 0.9 0.9 0.3
0.2 0.1 0.1 1.2 1.3 1.2 1.2 1.2 1.2 1.2 1.1 0.5 0.1 0.2 0.2 0.4 0.3 0.4 0.4 0.4 0.7 1.5 1.5
1.0 1.0 1.0 1.0 1.1 1.0 0.2 0.4 0.1 0.1 0.2 0.4 1.5 1.5 0.9 0.1 0.1 0.1 0.1 0.0 0.1 0.0 1.0
1.1 1.2 1.3 1.4 1.4 1.4 1.3 1.2 1.1 1.1 -99.9
-99.9 -99.9 -99.9 -99.9 -99.9 -99.9 -99.9 -99.9 -99.9 0.1 0.1 0.1 0.0 0.0 0.0 0.1 0.3 0.3 0.3 0.3 0.3 0.3
0.3 0.3 0.3 0.2 0.2 0.2 0.2 0.3 0.3 0.2 0.2 0.3 0.3 0.3 0.4 0.5 0.5 0.4 0.3 0.1 0.2 0.2 0.2
0.3 0.3 0.2 0.2 0.3 0.3 0.4 0.4 0.4 0.4 0.3 0.4 0.4 0.2 0.3 0.4 0.4 0.4 0.1 0.2 0.3 0.3 0.4
0.4 0.3 0.2 0.3 0.4 0.6 0.6 0.4 0.3 0.4 0.3 0.2 0.2 0.3 0.3 0.3 0.3 0.3 0.9 0.5 0.9 0.5 0.3
0.2 0.1 0.1 1.4 1.4 1.4 1.4 1.4 1.3 1.2 1.2 1.0 0.2 0.2 0.3 1.0 1.0 0.9 0.9 1.1 0.9 1.5 1.5
0.2 1.0 1.0 1.0 1.0 0.3 0.6 0.6 0.4 0.2 0.1 0.1 1.0 1.0 1.0 1.0 0.5 0.6 0.7 0.5 0.5 0.1 1.0
1.1 1.2 1.4 1.4 1.4 1.4 1.4 1.2 1.2 1.1 -99.9
-99.9 -99.9 -99.9 -99.9 -99.9 -99.9 -99.9 -99.9 -99.9 -99.9 -99.9 0.1 0.9 0.9 0.1 0.1 0.4 0.4 0.3 0.3 0.5
0.5 0.4 0.3 0.2 0.4 0.3 0.2 0.2 0.5 0.5 0.5 0.5 0.5 0.5 0.5 0.5 0.6 0.7 0.5 0.4 -0.1 0.2 0.2
0.2 0.3 0.3 0.2 0.3 0.4 0.4 0.5 0.5 0.5 0.4 0.5 0.5 0.5 0.2 0.2 0.3 0.4 0.5 0.3 0.2 0.3 0.4
0.4 0.4 0.3 0.3 0.3 0.6 0.5 0.5 0.2 0.4 0.3 0.3 0.5 0.5 0.4 0.3 0.3 0.3 0.3 0.4 0.5 0.5 0.5
0.3 0.1 0.1 1.4 1.5 1.5 1.4 1.4 1.2 1.3 1.6 1.2 1.2 0.2 0.2 0.2 1.1 1.1 1.0 1.1 1.4 1.0 1.5

1.5 1.1 0.2 1.0 1.0 0.2 0.6 1.0 0.9 0.5 0.9 0.1 0.1 1.0 1.0 1.0 1.0 1.0 1.1 1.3 1.2 1.0 0.5
0.1 0.4 1.2 1.2 1.4 1.4 1.4 1.4 1.2 1.1 -99.9 -99.9
-99.9 -99.9 -99.9 -99.9 -99.9 -99.9 -99.9 -99.9 -99.9 -99.9 -99.9 -99.9 -99.9 0.2 0.1 0.1 0.2 0.2 0.3 0.3 0.8
0.7 0.4 0.3 0.1 0.1 0.1 0.2 0.2 -0.1 0.6 0.5 0.5 0.7 0.6 0.6 0.6 0.5 0.5 0.3 0.2 0.4 0.2 0.1
0.1 0.1 0.3 0.5 0.5 0.5 0.4 0.4 0.5 0.5 0.4 0.5 0.4 0.2 -0.1 0.2 0.0 0.1 0.3 0.4 0.4 0.3 0.3
0.4 0.3 0.3 0.4 0.5 0.7 0.5 0.4 0.7 0.4 0.1 0.1 0.3 0.3 0.4 0.4 0.3 0.3 0.2 0.4 0.3 0.5 0.8
0.9 0.1 1.1 1.4 1.3 1.3 1.4 1.4 1.4 1.3 1.2 1.2 1.2 1.2 0.9 0.9 1.0 1.3 1.0 1.2 1.2 1.4 1.3
1.4 0.7 0.2 0.2 0.2 0.2 0.4 0.9 0.9 0.9 0.1 0.1 1.0 1.0 1.0 1.0 1.0 1.0 1.0 1.0 1.3 1.3 1.2
1.1 1.1 1.2 1.2 1.3 1.3 1.2 1.2 1.1 1.0 -99.9 -99.9
-99.9 -99.9 -99.9 -99.9 -99.9 -99.9 -99.9 -99.9 -99.9 -99.9 -99.9 -99.9 -99.9 -99.9 -99.9 0.2 0.2 0.2 0.3 0.4 0.5 0.6
0.5 0.3 0.3 0.4 0.8 0.3 0.2 0.2 0.5 0.6 0.7 0.7 0.3 0.6 0.4 0.4 0.6 0.7 0.5 0.3 -0.1 0.1 0.2
0.2 0.1 0.4 0.3 0.4 0.4 0.4 0.4 0.5 0.5 0.5 0.5 0.4 0.3 0.2 0.3 0.2 0.2 0.4 0.3 0.3 0.3 0.3
0.4 0.3 0.3 0.3 0.2 0.4 0.3 0.3 0.4 0.3 0.3 0.3 0.3 0.3 0.3 0.2 0.3 0.4 0.5 0.4 0.4 0.7 0.4
0.3 0.2 1.2 1.2 1.1 1.1 1.2 1.4 1.4 1.3 1.4 1.5 1.3 1.3 1.2 1.4 1.2 1.4 1.4 1.2 1.3 1.5 1.5
1.3 0.9 0.3 0.2 0.3 0.2 0.3 0.9 0.9 0.9 0.2 0.2 0.1 1.0 1.0 1.0 0.0 1.0 1.0 1.1 1.2 1.2 1.3
1.3 1.3 1.2 1.2 0.1 0.1 0.1 0.2 0.2 0.2 -99.9 -99.9
-99.9 -99.9 -99.9 -99.9 -99.9 -99.9 -99.9 -99.9 -99.9 -99.9 -99.9 -99.9 -99.9 -99.9 -99.9 -99.9 -99.9 0.2 0.2 0.3 0.4 0.5
0.4 0.3 0.3 0.4 0.5 0.3 0.3 0.3 0.3 0.6 0.7 0.7 0.5 0.5 0.4 0.4 0.5 0.5 0.5 0.3 0.1 0.1 0.2
0.3 0.3 0.4 0.4 0.4 0.4 0.4 0.4 0.4 0.5 0.4 0.5 0.4 0.4 0.3 0.3 0.2 0.3 0.4 0.3 0.3 0.3 0.3
0.3 0.3 0.3 0.3 0.3 0.3 0.2 0.2 0.3 0.3 0.3 0.3 0.3 0.3 0.3 0.2 0.3 0.3 0.4 0.4 0.4 0.5 0.4
0.3 0.2 0.5 0.5 0.2 0.1 1.1 1.0 1.2 1.4 1.4 1.3 1.3 1.3 1.3 1.5 1.4 1.5 1.5 1.4 1.5 1.1 1.5
1.2 1.0 0.9 0.2 0.2 0.3 0.9 0.9 0.4 0.9 0.3 0.2 0.1 0.2 0.1 0.1 0.1 0.1 1.0 1.0 1.0 1.0 1.1
1.1 1.1 1.3 1.3 1.2 1.1 1.0 0.2 0.2 -99.9 -99.9 -99.9
-99.9 -99.9 -99.9 -99.9 -99.9 -99.9 -99.9 -99.9 -99.9 -99.9 -99.9 -99.9 -99.9 -99.9 -99.9 -99.9 -99.9 -99.9 0.2 0.2 0.3 0.5
0.3 0.4 0.3 0.2 0.4 0.4 0.4 0.3 0.2 0.6 0.7 0.7 0.7 0.4 0.5 0.5 0.5 0.3 0.4 0.3 0.2 0.1 0.3
0.4 0.4 0.4 0.4 0.4 0.4 0.3 0.3 0.4 0.4 0.4 0.4 0.4 0.4 0.4 0.3 0.3 0.3 0.4 0.4 0.4 0.3 0.3
0.3 0.3 0.3 0.3 0.3 0.3 0.2 0.2 0.3 0.3 0.3 0.3 0.3 0.3 0.3 0.2 0.2 0.3 0.4 0.3 0.3 0.3 0.4
0.4 0.2 0.3 0.3 0.2 0.1 0.1 0.2 1.2 1.2 1.3 1.4 1.2 1.2 1.2 1.4 1.5 1.5 0.9 1.1 1.2 0.8 1.2
1.0 1.2 0.9 0.2 0.3 0.3 0.9 0.9 0.5 0.4 0.3 0.9 0.2 0.2 0.2 0.2 0.2 0.9 0.1 0.1 0.1 1.0 1.1
1.1 1.2 1.2 1.3 1.3 1.2 1.1 1.0 0.2 -99.9 -99.9 -99.9
-99.9 -99.9 -99.9 -99.9 -99.9 -99.9 -99.9 -99.9 -99.9 -99.9 -99.9 -99.9 -99.9 -99.9 -99.9 -99.9 -99.9 -99.9 -99.9 0.3 0.3
0.1 0.9 0.5 0.4 0.3 0.1 0.6 0.4 0.2 0.3 0.4 0.5 0.6 0.6 0.2 0.5 0.5 0.5 0.4 0.2 0.2 0.0 0.5
0.5 0.4 0.3 0.4 0.4 0.4 0.3 -0.1 0.4 0.4 0.4 0.3 0.4 0.4 0.4 0.4 0.5 0.5 0.4 0.4 0.4 0.4 0.3
0.2 0.3 0.3 0.3 0.3 0.3 0.3 0.3 0.3 0.3 0.2 0.3 0.3 0.5 0.2 0.2 0.2 0.2 0.2 0.2 0.2 0.3 0.3
0.5 0.4 0.3 0.3 0.5 0.3 0.2 0.1 0.1 1.1 1.2 1.2 1.3 0.6 1.1 1.1 1.4 1.4 1.4 1.1 0.1 0.5 0.5
0.9 0.9 0.3 0.3 0.3 0.4 0.5 0.3 0.1 0.3 0.2 0.4 0.4 0.5 0.2 0.9 0.9 0.2 0.9 0.2 0.2 0.1 0.2
1.0 1.1 1.2 1.2 1.3 1.3 1.2 1.2 1.1 1.0 -99.9 -99.9 -99.9
-99.9 -99.9
0.1 0.2 0.6 0.6 0.8 0.5 0.5 0.5 0.7 0.7 0.1 0.3 0.2 0.6 0.6 0.5 0.4 0.2 0.1 0.2 0.2 0.2 0.5
0.3 0.4 0.5 0.4 0.5 0.4 0.4 0.4 0.4 0.4 0.3 0.3 0.3 0.3 0.3 0.3 0.4 0.3 0.3 0.5 0.4 0.4 0.3
0.2 0.2 0.3 0.3 0.3 0.3 0.2 0.2 0.2 0.2 0.3 0.3 0.3 0.3 0.3 0.2 0.2 0.1 0.1 0.1 0.1 0.2 0.3
0.3 0.2 0.3 0.3 0.3 0.3 0.5 0.3 0.2 0.9 1.1 1.1 1.0 0.3 1.0 1.2 1.4 1.2 1.2 0.1 0.1 0.9 0.9
0.9 0.2 0.4 0.3 0.4 0.9 0.3 0.2 0.5 0.2 0.2 0.9 0.3 0.5 0.4 0.2 0.2 0.4 0.2 0.2 0.1 0.2 0.3
0.1 0.2 0.2 1.5 1.5 1.3 1.2 1.2 1.1 1.0 -99.9 -99.9 -99.9
-99.9 -
99.9 0.2 0.4 0.5 0.4 0.4 0.4 0.5 0.6 0.4 0.4 0.4 0.4 0.4 0.5 0.4 0.3 0.3 0.3 0.3 0.3 0.4 0.4
0.4 0.4 0.5 0.4 0.4 0.4 0.4 0.4 0.4 0.3 0.3 0.3 0.3 0.3 0.3 0.3 0.3 0.3 0.3 0.4 0.3 0.3 0.3
0.2 0.2 0.2 0.3 0.3 0.3 0.2 0.2 0.2 0.2 0.3 0.2 0.2 0.3 0.2 0.2 0.2 0.1 0.1 0.1 0.1 0.2 0.2
0.2 0.2 0.3 0.3 0.3 0.3 0.2 0.2 0.2 0.2 0.2 1.0 0.2 0.4 1.0 1.1 1.1 0.3 0.3 0.3 0.2 0.1 0.1
0.2 0.2 0.3 0.4 0.4 0.3 0.3 0.2 0.2 0.2 0.2 0.3 0.4 0.3 0.3 0.3 0.3 0.3 0.3 0.3 0.4 0.5
0.9 0.9 0.2 1.5 1.5 1.1 1.0 1.0 1.0 -99.9 -99.9 -99.9 -99.9
-99.9 -
99.9 -99.9 -99.9 0.3 0.3 0.2 0.2 0.3 0.4 0.2 0.5 0.5 0.5 0.2 0.4 0.4 0.3 0.3 0.5 0.3 0.3 0.5 0.4
0.3 0.3 0.4 0.5 0.4 0.4 0.4 0.4 0.3 0.3 0.3 0.3 0.3 0.3 0.3 0.3 0.3 0.2 0.3 0.4 0.3 0.3 0.2
0.2 0.2 0.2 0.2 0.2 0.2 0.2 0.2 0.2 0.2 0.2 0.2 0.2 0.2 0.2 0.2 0.1 0.1 0.2 0.1 0.1 0.1 0.2
0.2 0.2 0.3 0.3 0.3 0.3 0.2 0.2 0.2 0.3 0.2 0.2 0.2 0.2 0.2 1.0 1.0 0.4 0.4 0.4 0.2 0.2 0.2
0.2 0.2 0.3 0.3 0.3 0.3 0.2 0.2 0.1 0.1 0.2 0.2 0.3 0.3 0.3 0.4 0.3 0.3 0.4 0.3 0.3 0.4 0.5
0.4 0.2 0.9 1.5 1.5 0.2 0.2 1.0 1.0 -99.9 -99.9 -99.9 -99.9
-99.9 -
99.9 -99.9 -99.9 -99.9 0.2 0.1 0.0 0.1 0.2 0.1 0.6 0.5 0.6 0.6 0.3 0.2 0.2 0.2 0.0 0.4 0.4 0.3 0.4
0.3 0.3 0.3 0.4 0.5 0.4 0.3 0.4 0.2 0.2 0.2 0.2 0.3 0.3 0.3 0.2 0.2 0.1 0.2 0.4 0.4 0.3 0.3
0.3 0.3 0.3 0.2 0.2 0.2 0.2 0.2 0.2 0.2 0.2 0.2 0.2 0.1 0.2 0.2 -0.1 0.2 0.5 0.2 0.2 0.2 0.2
0.3 0.3 0.3 0.5 0.4 0.3 0.3 0.3 0.2 0.4 0.4 0.6 0.6 0.0 0.2 0.3 0.2 0.2 0.3 0.4 0.5 0.2 0.2
0.2 0.1 0.1 0.2 0.2 0.2 0.1 0.0 0.0 -0.1 0.1 0.2 0.2 0.3 0.4 0.2 0.2 0.2 0.4 0.2 0.3 0.4 0.9
0.3 0.2 0.1 1.5 1.5 0.9 0.2 0.4 0.4 -99.9 -99.9 -99.9 -99.9
-99.9 -
99.9 -99.9 -99.9 -99.9 0.9 0.9 0.2 0.2 0.3 0.5 0.2 0.4 0.5 0.9 0.5 0.2 0.2 0.5 0.4 0.4 0.3 0.2 0.3
0.4 0.4 0.4 0.6 0.3 0.3 0.2 0.3 0.3 0.3 0.3 0.2 0.3 0.4 0.1 0.2 0.2 0.1 0.2 0.3 0.4 0.3 0.2
0.2 0.2 0.2 0.2 0.2 0.2 0.2 0.2 0.2 0.2 0.1 0.2 0.2 0.2 0.2 0.2 0.2 0.2 0.2 0.2 0.3 0.2 0.2
0.3 0.2 0.4 0.3 0.2 0.2 0.3 0.3 0.3 0.4 0.5 0.4 0.3 0.2 0.3 0.5 0.5 0.5 0.4 0.5 0.4 0.3 0.2

0.2 0.2 0.2 0.2 0.2 0.2 0.2 0.1 0.1 0.1 0.1 0.2 0.2 0.2 0.2 0.3 0.2 0.2 0.2 0.2 0.2 0.2 0.2
0.2 0.3 0.2 0.4 0.6 0.3 0.9 0.9 0.2 -99.9 -99.9 -99.9 -99.9
-99.9 -
99.9 -99.9 -99.9 -99.9 0.9 0.9 0.5 0.4 0.4 0.2 0.4 0.5 0.5 0.5 0.5 0.3 0.2 0.4 0.4 0.4 0.3 0.3 0.4
0.4 0.4 0.4 0.4 0.3 0.3 0.3 0.3 0.3 0.3 0.3 0.2 0.2 0.3 0.2 0.2 0.2 0.2 0.3 0.3 0.3 0.3 0.2
0.2 0.2 0.2 0.2 0.2 0.2 0.2 0.2 0.2 0.2 0.2 0.2 0.2 0.2 0.2 0.2 0.2 0.2 0.3 0.3 0.3 0.3
0.3 0.3 0.3 0.3 0.3 0.3 0.3 0.3 0.3 0.4 0.4 0.5 0.4 0.3 0.3 0.4 0.5 0.4 0.4 0.4 0.4 0.3 0.3
0.2 0.2 0.2 0.2 0.2 0.2 0.2 0.2 0.1 0.1 0.2 0.2 0.2 0.2 0.2 0.2 0.2 0.2 0.2 0.2 0.2 0.2 0.2
0.3 0.4 0.5 0.6 0.4 0.4 0.3 0.2 -99.9 -99.9 -99.9 -99.9 -99.9
-99.9 -
99.9 -99.9 -99.9 -99.9 0.9 0.9 0.7 0.5 0.4 0.2 0.4 0.5 0.5 0.4 0.5 0.3 0.3 0.4 0.4 0.4 0.3 0.3 0.4
0.4 0.4 0.3 0.3 0.3 0.3 0.3 0.3 0.3 0.3 0.3 0.2 0.3 0.3 0.3 0.3 0.3 0.3 0.3 0.3 0.3 0.3 0.2
0.2 0.2 0.2 0.2 0.2 0.2 0.2 0.2 0.2 0.2 0.2 0.2 0.2 0.3 0.2 0.2 0.2 0.2 0.2 0.3 0.3 0.2 0.3
0.3 0.3 0.3 0.3 0.3 0.3 0.3 0.3 0.3 0.3 0.4 0.5 0.4 0.4 0.3 0.4 0.4 0.4 0.4 0.4 0.3 0.3 0.3
0.3 0.3 0.2 0.2 0.2 0.3 0.3 0.3 0.2 0.2 0.2 0.2 0.2 0.2 0.2 0.2 0.2 0.2 0.2 0.1 0.2 0.2 0.2 0.1
0.2 0.3 0.3 0.4 0.9 0.3 0.4 0.9 -99.9 -99.9 -99.9 -99.9 -99.9
-99.9 -
99.9 -99.9 -99.9 -99.9 0.9 0.9 0.5 0.5 0.4 -0.1 0.1 0.4 0.5 0.6 0.5 0.4 0.4 0.5 0.4 0.3 0.3 0.3 0.4
0.4 0.3 0.3 0.5 0.3 0.3 0.3 0.3 0.4 0.3 0.3 0.2 0.3 0.3 0.3 0.3 0.3 0.4 0.3 0.2 0.3 0.3 0.2
0.2 0.2 0.2 0.2 0.2 0.2 0.2 0.2 0.2 0.1 0.2 0.2 0.2 0.3 0.2 0.2 0.2 0.2 0.2 0.2 0.2 0.2 0.3
0.3 0.3 0.3 0.2 0.2 0.2 0.4 0.4 0.4 0.4 0.4 0.4 0.4 0.3 0.3 0.4 0.3 0.4 0.3 0.3 0.3 0.3 0.3
0.3 0.4 0.2 0.2 0.3 0.4 0.4 0.3 0.3 0.2 0.2 0.2 0.2 0.2 0.2 0.2 0.1 0.1 0.1 0.1 0.2 0.2 0.2
0.2 0.2 0.2 0.3 0.4 0.5 0.5 0.5 -99.9 -99.9 -99.9 -99.9 -99.9
-99.9 -
99.9 -99.9 -99.9 -99.9 0.9 0.9 0.4 0.4 0.4 0.2 0.4 0.4 0.5 0.5 0.5 0.4 0.3 0.1 0.4 0.3 0.3 0.3 0.3
0.2 0.2 0.2 0.3 0.3 0.2 0.2 0.2 0.2 0.3 0.3 0.2 0.2 0.2 0.3 0.3 0.3 0.3 0.3 0.4 0.3 0.2 0.2
0.2 0.1 0.2 0.2 0.2 0.2 0.1 0.1 0.1 0.1 0.1 0.1 0.1 0.1 0.1 0.2 0.2 0.2 0.2 0.2 0.2 0.2 0.2
0.2 0.3 0.3 0.3 0.3 0.3 0.3 0.2 0.3 0.3 0.3 0.3 0.2 0.2 0.3 0.3 0.3 0.2 0.2 0.3 0.2 0.3 0.3
0.2 0.2 0.2 0.2 0.2 0.2 0.2 0.2 0.2 0.2 0.2 0.2 0.2 0.2 0.2 0.2 0.2 0.1 0.2 0.2 0.2 0.2 0.2 0.2
0.2 0.2 0.2 0.2 0.5 0.4 0.3 0.2 -99.9 -99.9 -99.9 -99.9 -99.9
-99.9 -
99.9 -99.9 -99.9 -99.9 0.9 0.9 0.3 0.3 0.4 0.4 0.3 0.3 0.4 0.3 0.4 0.3 0.3 0.2 0.1 0.2 0.2 0.3 0.3
0.3 0.3 0.2 0.2 0.2 0.2 0.2 0.2 0.2 0.3 0.3 0.2 0.2 0.3 0.3 0.3 0.3 0.3 0.3 0.2 0.2 0.2
0.2 0.1 0.1 0.1 0.1 0.1 0.1 0.1 0.1 0.2 0.2 0.2 0.2 0.2 0.2 0.2 0.2 0.2 0.2 0.2 0.2 0.2
0.2 0.3 0.3 0.3 0.3 0.3 0.3 0.3 0.3 0.3 0.3 0.3 0.2 0.2 0.2 0.2 0.2 0.2 0.2 0.2 0.2 0.2
0.2 0.2 0.2 0.2 0.3 0.2 0.2 0.2 0.2 0.2 0.2 0.2 0.2 0.2 0.1 0.1 0.1 0.1 0.2 0.2 0.2 0.2 0.1 0.2
0.2 0.2 0.2 0.2 0.3 0.3 0.1 -0.6 -99.9 -99.9 -99.9 -99.9 -99.9
-99.9 -
99.9 -99.9 -99.9 -99.9 0.9 0.9 0.2 0.2 0.3 0.4 0.3 0.3 0.3 0.3 0.3 0.3 0.3 0.2 0.1 0.2 0.2 0.2 0.2
0.3 0.2 0.2 0.2 0.2 0.2 0.2 0.2 0.2 0.2 0.2 0.2 0.2 0.2 0.3 0.3 0.3 0.3 0.3 0.2 0.2 0.2 0.2
0.2 0.1 0.1 0.1 0.1 0.2 0.1 0.1 0.1 0.1 0.2 0.2 0.2 0.2 0.1 0.2 0.2 0.2 0.2 0.2 0.2 0.2 0.2
0.2 0.3 0.3 0.2 0.2 0.2 0.3 0.3 0.3 0.2 0.3 0.2 0.2 0.2 0.2 0.2 0.2 0.2 0.2 0.2 0.2 0.2 0.2
0.2 0.2 0.2 0.2 0.3 0.2 0.2 0.2 0.2 0.2 0.1 0.1 0.2 0.2 0.2 0.2 0.2 0.2 0.2 0.2 0.2 0.1 0.2
0.2 0.2 0.2 0.2 0.2 0.2 0.1 -0.4 -99.9 -99.9 -99.9 -99.9 -99.9
-99.9 -
99.9 -99.9 -99.9 -99.9 0.9 0.9 0.1 0.1 0.1 0.5 0.1 0.4 0.3 0.2 0.2 0.3 0.3 0.2 0.2 0.2 0.2 0.2 0.2
0.2 0.2 0.2 0.3 0.2 0.2 0.2 0.2 0.2 0.2 0.2 0.1 0.2 0.2 0.2 0.3 0.2 0.3 0.3 0.2 0.3 0.2 0.2
0.1 0.1 0.1 0.1 0.2 0.2 0.1 0.1 0.1 0.1 0.1 0.1 0.2 0.2 0.2 0.2 0.2 0.3 0.2 0.2 0.2 0.2 0.2
0.2 0.2 0.2 0.2 0.2 0.2 0.2 0.3 0.3 0.2 0.3 0.2 0.2 0.2 0.2 0.2 0.2 0.2 0.2 0.2 0.2 0.2 0.3
0.3 0.2 0.2 0.2 0.2 0.2 0.2 0.2 0.2 0.1 0.2 0.2 0.2 0.2 0.2 0.2 0.2 0.2 0.2 0.2 0.2 0.2 0.3
0.2 0.2 0.2 0.2 0.2 0.2 0.2 0.1 -99.9 -99.9 -99.9 -99.9 -99.9
-99.9 -
99.9 -99.9 -99.9 -99.9 0.9 0.9 -0.2 0.2 0.3 0.3 0.4 0.3 0.3 0.3 0.2 0.2 0.2 0.2 0.2 0.3 0.2 0.2 0.2
0.1 0.2 0.2 0.2 0.2 0.2 0.2 0.3 0.2 0.2 0.2 0.2 0.2 0.2 0.2 0.2 0.4 0.2 0.2 0.3 0.4 0.3 0.2
0.2 0.2 0.1 0.1 0.1 0.1 0.1 0.1 0.1 0.1 0.1 0.1 0.1 0.1 0.0 0.1 0.3 0.2 0.2 0.2 0.2 0.2 0.2
0.3 0.3 0.2 0.2 0.2 0.2 0.2 0.2 0.2 0.2 0.2 0.2 0.2 0.2 0.1 0.1 0.1 0.1 0.2 0.2 0.2 0.2 0.2
0.2 0.2 0.2 0.2 0.2 0.2 0.1 0.1 0.2 0.1 0.1 0.3 0.1 0.0 0.1 0.2 0.2 0.1 0.1 0.1 0.1 0.1 0.1
0.1 0.2 0.2 0.2 0.2 0.2 0.1 0.0 -99.9 -99.9 -99.9 -99.9 -99.9
-99.9 -
99.9 -99.9 -99.9 -99.9 0.9 0.9 0.1 0.2 0.2 0.3 0.3 0.3 0.3 0.2 0.2 0.2 0.2 0.2 0.2 0.2 0.2 0.1 0.1
0.1 0.1 0.1 0.1 0.1 0.1 0.2 0.2 0.2 0.1 0.1 0.1 0.1 0.1 0.1 0.1 0.1 0.1 0.2 0.2 0.2 0.2 0.1
0.1 0.2 0.1 0.1 0.2 0.1 0.0 0.1 0.1 0.0 0.1 0.1 0.1 0.0 0.0 0.1 0.1 0.1 0.2 0.2 0.2 0.2 0.2
0.2 0.2 0.2 0.2 0.3 0.3 0.3 0.3 0.3 0.3 0.4 0.3 0.2 0.2 0.2 0.2 0.2 0.2 0.2 0.2 0.2 0.3 0.2
0.2 0.1 0.2 0.2 0.1 0.2 0.2 0.1 0.1 0.1 0.1 0.2 0.2 0.2 0.2 0.2 0.2 0.2 0.2 0.2 0.2 0.1 0.1 0.1
0.1 0.1 0.1 0.2 0.2 0.2 0.2 -99.9 -99.9 -99.9 -99.9 -99.9 -99.9
-99.9 -
99.9 -99.9 -99.9 -99.9 0.9 0.9 0.2 0.2 0.2 0.2 0.2 0.2 0.2 0.2 0.2 0.2 0.2 0.2 0.2 0.2 0.2 0.1 0.1
0.1 0.1 0.1 0.1 0.1 0.1 0.1 0.1 0.1 0.1 0.1 0.2 0.1 0.1 0.1 0.1 0.1 0.2 0.2 0.2 0.2 0.1 0.1
0.2 0.2 0.1 0.1 0.1 0.1 0.0 0.1 0.1 0.1 0.1 0.1 0.1 0.0 0.0 0.1 0.1 0.1 0.1 0.2 0.2 0.2 0.2
0.2 0.2 0.2 0.2 0.3 0.2 0.2 0.2 0.3 0.2 0.3 0.3 0.2 0.2 0.2 0.2 0.2 0.2 0.2 0.2 0.2 0.2 0.2

0.1 0.1 0.1 0.1 0.1 0.2 0.2 0.2 0.1 0.1 0.2 0.1 0.1 0.1 0.2 0.2 0.2 0.2 0.2 0.2 0.1 0.1 0.1
0.1 0.1 0.1 0.1 0.2 0.2 0.2 -99.9 -99.9 -99.9 -99.9 -99.9 -99.9
-99.9 -
99.9 -99.9 -99.9 -99.9 0.9 0.9 0.2 0.2 0.2 0.2 0.2 0.2 0.2 0.2 0.2 0.2 0.2 0.1 0.1 0.1 0.1 0.1 0.1
0.1 0.1 0.2 0.1 0.0 0.0 0.0 0.1 0.1 0.0 0.0 0.2 0.1 0.1 0.1 0.1 0.2 0.2 0.2 0.2 0.2 0.1 0.2
0.2 0.2 0.1 0.1 0.2 0.0 0.0 0.1 0.1 0.1 0.1 0.1 0.1 0.0 -0.1 0.0 0.1 0.1 0.1 0.2 0.2 0.2 0.2
0.2 0.2 0.2 0.2 0.2 0.2 0.2 0.1 0.1 0.1 0.1 0.2 0.2 0.2 0.2 0.2 0.2 0.2 0.2 0.2 0.2 0.2 0.2
0.1 0.1 0.1 0.1 0.1 0.1 0.2 0.2 0.2 0.1 0.2 0.1 0.1 0.1 0.1 0.2 0.1 0.2 0.2 0.2 0.2 0.1 0.1
0.1 0.1 0.1 0.1 0.1 0.0 0.1 -99.9 -99.9 -99.9 -99.9 -99.9 -99.9
-99.9 -
99.9 -99.9 -99.9 -99.9 0.9 0.9 0.3 0.2 0.2 0.2 0.2 0.2 0.2 0.2 0.2 0.2 0.1 0.2 0.1 0.1 0.1 0.2 0.1
0.1 0.1 0.2 0.1 0.1 0.1 0.0 0.1 0.1 0.0 0.1 0.1 0.1 0.1 0.1 0.2 0.1 0.1 0.1 0.2 0.3 0.2 0.2
0.1 0.2 0.0 0.1 0.1 0.2 0.2 0.2 0.2 0.2 0.1 0.1 0.1 -0.1 -0.1 -0.1 0.0 0.1 0.0 0.1 0.1 0.1 0.2
0.1 0.2 0.2 0.2 0.1 0.2 0.1 0.2 0.2 0.1 0.1 0.1 0.1 0.3 0.2 0.2 0.2 0.2 0.2 0.2 0.2 0.2 0.1
0.1 0.1 0.1 0.1 0.1 0.2 0.1 0.1 0.1 0.1 0.1 0.2 0.2 0.2 0.2 0.2 0.2 0.2 0.2 0.2 0.2 0.2 0.2
0.2 0.1 0.1 0.1 0.1 0.1 0.2 -99.9 -99.9 -99.9 -99.9 -99.9 -99.9
-99.9 -
99.9 -99.9 -99.9 -99.9 0.9 0.9 0.2 0.2 0.2 0.2 0.2 0.2 0.2 0.2 0.1 0.2 0.2 0.2 0.1 0.1 0.1 0.1 0.1
0.1 0.1 0.1 0.0 0.1 0.0 0.0 -0.1 0.0 0.0 0.0 0.0 0.0 0.0 0.0 0.1 0.2 0.1 0.1 0.1 0.1 0.1 0.1
0.1 0.2 0.2 0.1 0.1 0.1 0.2 0.2 0.2 0.1 0.1 0.1 0.1 0.1 -0.1 -0.1 -0.1 -0.1 0.0 0.0 0.1 0.1 0.1
0.1 0.1 0.1 0.1 0.1 0.1 0.1 0.1 0.1 0.1 0.1 0.1 0.2 0.2 0.2 0.2 0.1 0.1 0.1 0.1 0.1 0.1 0.1
0.1 0.1 0.2 0.1 0.1 0.1 0.1 0.1 0.1 0.1 0.1 0.1 0.0 0.1 0.1 0.0 0.1 0.2 0.1 0.1 0.3 0.2 0.1
0.2 0.2 0.9 0.9 0.9 0.9 0.6 -99.9 -99.9 -99.9 -99.9 -99.9 -99.9
-99.9 -
99.9 -99.9 -99.9 -99.9 0.9 0.9 0.2 0.2 0.2 0.2 0.2 0.2 0.2 0.2 0.2 0.2 0.2 0.2 0.1 0.1 0.1 0.1 0.0 0.1
0.1 0.1 0.1 0.1 0.1 0.0 0.0 0.0 -0.1 0.0 0.0 0.0 0.0 0.0 0.0 0.0 0.1 0.1 0.1 0.1 0.1 0.1 0.1
0.2 0.2 0.2 0.1 0.1 0.1 0.2 0.2 0.1 0.1 0.1 0.1 0.1 0.1 -0.1 -0.1 -0.1 -0.1 0.0 0.0 0.0 0.0 0.1
0.1 0.1 0.1 0.1 0.1 0.1 0.1 0.1 0.1 0.1 0.1 0.1 0.1 0.1 0.1 0.1 0.1 0.1 0.1 0.1 0.1 0.1 0.1
0.1 0.1 0.1 0.2 0.1 0.1 0.1 0.1 0.1 0.1 0.1 0.1 0.1 0.1 0.2 0.1 0.2 0.2 0.1 0.1 0.2 0.2 0.9
0.9 0.9 0.9 0.9 0.9 0.9 0.6 -99.9 -99.9 -99.9 -99.9 -99.9 -99.9
-99.9 -
99.9 -99.9 -99.9 -99.9 0.9 0.9 0.2 0.2 0.2 0.2 0.2 0.2 0.2 0.2 0.1 0.1 0.1 0.1 0.1 0.1 0.1 0.0 0.1
0.1 0.1 0.1 0.1 0.0 0.0 -0.1 0.0 -0.1 -0.1 -0.1 -0.1 -0.1 0.0 0.0 0.0 0.1 0.1 0.1 0.1 0.1 0.1 0.1
0.1 0.2 0.2 0.1 0.1 0.1 0.2 0.1 0.1 0.1 0.1 0.1 0.1 0.1 0.1 0.0 -0.1 -0.1 0.0 0.0 -0.1 0.0 0.1
0.1 0.1 0.1 0.1 0.1 0.1 0.1 0.0 0.0 0.0 0.1 0.1 0.1 0.1 0.1 0.1 0.1 0.1 0.1 0.1 0.1 0.1 0.1
0.1 0.1 0.1 0.1 0.1 0.1 0.0 0.0 0.1 0.1 0.1 0.1 0.1 0.1 0.1 0.1 0.2 0.2 0.1 0.1 0.9 0.9 0.9
0.9 0.9 0.9 0.9 -99.9 -99.9 -99.9 -99.9 -99.9 -99.9 -99.9 -99.9 -99.9
-99.9 -
99.9 -99.9 -99.9 -99.9 0.9 0.9 0.2 0.2 0.2 0.2 0.2 0.2 0.1 0.2 0.1 0.1 0.1 0.1 0.0 0.1 0.1 0.0 0.1
0.1 0.1 0.1 0.0 0.0 -0.1 -0.1 0.1 -0.1 -0.1 -0.1 -0.1 -0.1 -0.1 -0.1 -0.1 0.1 0.1 0.1 0.1 -0.1 0.1 0.1
0.1 0.1 0.2 0.2 0.1 0.1 0.1 0.1 0.2 0.1 -0.1 0.1 0.1 0.2 -0.1 0.0 0.0 -0.1 -0.1 0.0 -0.1 0.0 0.0
0.0 0.1 0.0 0.0 0.0 0.1 0.0 0.0 0.1 0.1 0.0 0.0 0.0 0.1 0.1 0.1 0.1 0.1 0.1 0.1 0.1 0.1 0.1
0.1 0.0 0.1 0.1 0.1 0.1 0.0 0.0 0.0 0.1 0.1 0.1 0.1 0.1 0.1 0.1 0.1 0.1 0.9 0.9 0.9 0.9 0.9 0.9
0.9 0.9 -99.9 -99.9 -99.9 -99.9 -99.9 -99.9 -99.9 -99.9 -99.9 -99.9 -99.9 -99.9 -99.9
-99.9 -
99.9 -99.9 -99.9 -99.9 0.9 0.9 0.1 0.1 0.1 0.1 0.1 0.1 0.1 0.1 0.1 0.0 0.0 0.1 0.0 0.0 0.0 0.0 0.1
0.1 0.1 0.1 0.0 -0.1 -0.1 -0.1 -0.2 -0.1 -0.1 -0.1 -0.1 -0.1 -0.1 -0.1 -0.1 -0.1 0.0 0.0 0.0 -0.1 0.0 0.0
0.0 0.0 0.1 0.1 0.1 0.1 0.0 0.1 0.1 0.1 0.1 0.1 0.1 0.1 -0.1 -0.1 -0.1 -0.1 -0.1 -0.1 -0.1 -0.1 0.0
0.0 0.0 0.0 0.0 0.0 0.0 0.0 0.0 0.0 0.0 0.0 0.1 0.1 0.1 0.1 0.1 0.1 0.1 0.1 0.1 0.1 0.1 0.0
0.1 0.1 0.1 0.1 0.1 0.1 0.1 0.1 0.1 0.1 0.1 0.1 0.1 0.1 0.9 0.9 0.9 0.9 0.9 0.9 0.9 -99.9 -
99.9 -99.9 -99.9 -99.9 -99.9 -99.9 -99.9 -99.9 -99.9 -99.9 -99.9 -99.9 -99.9
-99.9 -
99.9 -99.9 -99.9 -99.9 0.9 0.9 0.1 0.1 0.1 0.1 0.0 0.0 0.0 0.1 0.0 0.0 0.0 0.0 -0.1 -0.1 -0.1 -0.1 -0.1
-0.1 0.0 0.0 0.0 -0.1 -0.1 -0.1 -0.2 -0.2 -0.1 -0.1 -0.1 -0.1 -0.1 -0.1 -0.1 -0.1 -0.1 -0.1 -0.1 -0.1 0.0 -0.1 -0.1
0.0 0.1 0.1 0.1 0.1 0.0 0.1 0.1 0.1 0.1 0.1 0.1 0.1 0.1 0.0 -0.1 -0.1 -0.1 -0.1 -0.1 -0.1 -0.1 -0.1 -
0.1 -0.1 -0.1 -0.1 0.0 -0.1 -0.1 -0.1 -0.1 -0.1 0.0 0.0 0.0 0.1 0.1 0.1 0.1 0.1 0.1 0.0 0.0 0.0 0.0
0.1 0.1 0.1 0.1 0.1 0.1 0.1 0.1 0.1 0.1 0.1 0.1 0.9 0.9 0.9 0.9 0.9 0.9 0.9 0.9 -99.9 -99.9 -99.9 -
99.9 -99.9 -99.9 -99.9 -99.9 -99.9 -99.9 -99.9 -99.9 -99.9 -99.9 -99.9 -99.9 -99.9 -99.9 -99.9 -99.9
-99.9 -
99.9 -99.9 -99.9 -99.9 0.9 0.9 0.1 0.1 0.1 0.1 0.0 0.0 0.0 0.0 0.0 -0.1 -0.1 -0.1 -0.1 -0.1 -0.1 -0.1 -0.1
-0.1 -0.1 0.0 -0.1 -0.1 -0.1 -0.1 -0.2 -0.2 -0.1 -0.1 -0.2 -0.1 -0.1 -0.1 -0.1 -0.1 -0.1 -0.1 -0.1 -0.1 0.0 -0.1 -0.1
0.0 0.1 0.1 0.1 0.1 -0.1 0.1 0.1 0.1 0.1 0.1 0.1 0.1 0.0 0.0 -0.1 -0.1 -0.1 -0.1 -0.1 -0.2 -0.2 -0.1 -
0.1 -0.1 -0.1 -0.1 -0.1 -0.1 -0.1 -0.1 -0.1 -0.1 -0.1 0.0 0.0 0.0 0.0 0.0 0.0 0.0 0.0 0.0 -0.1 0.0 0.0
0.0 0.1 0.1 0.1 0.1 0.1 0.0 0.1 0.1 0.9 0.9 0.9 0.9 0.9 0.9 0.9 0.9 -99.9 -99.9 -99.9 -99.9 -99.9 -99.9
-99.9 -99.9 -99.9 -99.9 -99.9 -99.9 -99.9 -99.9 -99.9 -99.9 -99.9 -99.9 -99.9
-99.9 -
99.9 -99.9 -99.9 -99.9 0.9 0.9 0.0 0.0 0.0 0.0 -0.1 -0.1 -0.1 -0.1 -0.1 -0.1 -0.1 -0.1 -0.1 -0.1 -0.1 -0.1 -
0.1 -0.1 -0.1 -0.1 -0.1 -0.2 -0.1 -0.1 -0.2 -0.1 -0.1 -0.1 -0.1 -0.1 -0.1 -0.1 -0.1 -0.2 0.0 -0.1 -0.1 -0.1 0.0 -0.1
-0.1 0.0 0.1 0.2 0.2 0.2 0.2 0.0 0.1 0.1 0.2 0.1 0.1 0.1 -0.2 -0.2 -0.1 -0.1 -0.2 -0.2 -0.2 -0.2 -0.2 -
0.2 -0.2 -0.2 -0.2 -0.2 -0.2 -0.2 -0.2 -0.2 -0.1 -0.1 -0.1 -0.1 -0.1 -0.1 -0.1 -0.1 0.0 0.0 -0.1 -0.1 0.0 -0.1 0.0

0.0 0.0 0.1 0.1 -0.1 -0.1 -0.1 -0.1 0.9 0.9 0.9 0.9 0.9 0.9 0.9 0.9 -99.9 -99.9 -99.9 -99.9 -99.9 -99.9 -
99.9 -99.9 -99.9 -99.9 -99.9 -99.9 -99.9 -99.9 -99.9 -99.9 -99.9 -99.9 -99.9 -99.9 -99.9
-99.9 -
99.9 -99.9 -99.9 -99.9 0.9 0.9 0.0 0.0 0.0 -0.1 -0.1 -0.1 -0.1 -0.1 -0.1 -0.1 -0.1 -0.1 -0.1 -0.2 -0.2 -0.1 -
0.2 -0.2 -0.1 -0.1 -0.2 -0.1 -0.1 -0.2 -0.2 -0.2 -0.1 -0.1 -0.2 -0.2 -0.2 -0.2 -0.1 -0.1 -0.1 -0.1 -0.1 0.1 -0.1
-0.1 -0.1 -0.1 0.1 0.1 0.1 0.2 0.2 0.2 0.2 0.3 0.2 0.1 0.1 0.0 -0.1 -0.1 -0.1 -0.2 -0.2 -0.2 -0.2 -0.2 -
0.2 -0.2 -0.2 -0.2 -0.2 -0.2 -0.2 -0.2 -0.2 -0.2 -0.2 -0.1 -0.1 -0.1 -0.1 -0.1 -0.1 -0.1 -0.1 -0.1 -0.1 0.0 0.0
0.0 0.0 0.0 0.1 0.0 -0.1 0.9 0.9 0.9 0.9 0.9 0.9 0.9 -99.9 -99.9 -99.9 -99.9 -99.9 -99.9 -99.9 -99.9 -99.9 -
99.9 -99.9 -99.9 -99.9 -99.9 -99.9 -99.9 -99.9 -99.9 -99.9 -99.9 -99.9 -99.9 -99.9 -99.9
-99.9 -
99.9 -99.9 -99.9 -99.9 0.9 0.9 0.0 0.0 -0.1 -0.1 -0.1 -0.1 -0.1 -0.1 -0.1 -0.1 -0.1 -0.1 -0.2 -0.2 -0.2 -0.2 -
0.2 -0.2 -0.2 -0.2 -0.2 -0.2 -0.2 -0.2 -0.3 -0.1 -0.1 -0.1 0.0 0.0 -0.1 -0.1 0.0 0.0 0.0 0.0 -0.1 0.0 0.1
0.0 0.0 0.1 0.2 0.2 0.2 0.2 0.2 0.2 0.2 0.2 0.2 0.1 0.1 0.0 -0.1 -0.1 -0.2 -0.2 -0.2 -0.2 -0.2 -0.2 -
0.2 -0.2 -0.2 -0.2 -0.2 -0.2 -0.2 -0.2 -0.3 -0.2 -0.2 -0.2 -0.1 -0.1 -0.1 -0.1 -0.1 -0.1 -0.1 0.0 0.0 0.0 0.0
0.0 0.0 0.0 0.0 0.9 0.9 0.9 0.9 0.9 0.9 -99.9 -99.9 -99.9 -99.9 -99.9 -99.9 -99.9 -99.9 -99.9 -99.9 -99.9 -99.9
-99.9 -99.9 -99.9 -99.9 -99.9 -99.9 -99.9 -99.9 -99.9 -99.9 -99.9 -99.9 -99.9 -99.9 -99.9
-99.9 -
99.9 -99.9 -99.9 -99.9 0.9 0.9 0.0 -0.1 -0.1 -0.1 -0.1 -0.1 -0.1 -0.1 -0.1 -0.1 -0.1 -0.2 -0.2 -0.2 -0.2 -0.2 -
0.2 -0.2 -0.2 -0.2 -0.2 -0.2 -0.2 -0.3 -0.3 -0.1 -0.1 -0.1 0.0 -0.1 -0.1 -0.1 -0.1 -0.1 -0.1 -0.1 -0.1 -0.1 0.0
0.0 0.0 0.1 0.2 0.2 0.2 0.2 0.2 0.2 0.2 0.2 0.2 0.1 0.1 0.0 -0.1 -0.1 -0.2 -0.2 -0.2 -0.2 -0.2 -0.2 -
0.2 -0.2 -0.2 -0.2 -0.2 -0.2 -0.2 -0.2 -0.3 -0.2 -0.2 -0.2 -0.2 -0.1 -0.1 -0.1 -0.1 -0.1 -0.1 0.0 0.0 0.0 0.0
0.0 0.0 0.0 0.0 0.9 0.9 0.9 0.9 -99.9 -99.9 -99.9 -99.9 -99.9 -99.9 -99.9 -99.9 -99.9 -99.9 -99.9 -99.9 -99.9 -
99.9 -99.9 -99.9 -99.9 -99.9 -99.9 -99.9 -99.9 -99.9 -99.9 -99.9 -99.9 -99.9 -99.9 -99.9 -99.9
-99.9 -
99.9 -99.9 -99.9 -99.9 0.9 0.9 -0.1 -0.1 -0.1 -0.1 -0.2 -0.1 -0.1 -0.2 -0.2 -0.2 -0.2 -0.2 -0.2 -0.2 -0.2 -0.2 -
0.2 -0.3 -0.3 -0.2 -0.3 -0.3 -0.3 -0.3 -0.3 -0.3 -0.3 -0.3 -0.3 -0.2 -0.2 -0.2 -0.2 -0.2 -0.2 -0.2 -0.1 -0.2 -0.1
-0.1 -0.1 -0.2 0.0 0.0 0.0 0.1 0.1 0.1 0.1 0.1 0.1 0.1 0.1 -0.1 -0.1 -0.2 -0.2 -0.2 -0.2 -0.3 -0.2 -0.3
-0.2 -0.3 -0.2 -0.1 -0.2 -0.3 -0.3 -0.3 -0.3 -0.2 -0.2 -0.2 -0.2 -0.1 0.0 -0.1 -0.1 -0.1 -0.1 0.1 -0.1 -0.1 -0.1
0.0 0.0 0.1 0.1 0.9 0.9 -99.9 -99.9 -99.9 -99.9 -99.9 -99.9 -99.9 -99.9 -99.9 -99.9 -99.9 -99.9 -99.9 -99.9 -99.9 -
99.9 -99.9 -99.9 -99.9 -99.9 -99.9 -99.9 -99.9 -99.9 -99.9 -99.9 -99.9 -99.9 -99.9 -99.9 -99.9
-99.9 -
99.9 -99.9 -99.9 -99.9 0.9 0.9 -0.1 -0.1 -0.1 -0.1 -0.1 -0.1 -0.1 -0.2 -0.1 -0.2 -0.2 -0.2 -0.1 -0.2 -0.2 -0.2 -
0.1 -0.2 -0.2 -0.3 -0.2 -0.3 -0.3 -0.3 -0.3 -0.2 -0.3 -0.3 -0.4 -0.3 -0.3 -0.3 -0.3 -0.3 -0.2 -0.2 -0.2 -0.3 -0.2
-0.2 -0.2 -0.2 -0.2 -0.1 -0.1 -0.2 -0.1 0.0 0.0 -0.1 -0.1 -0.1 -0.1 -0.1 -0.1 -0.1 -0.1 -0.1 -0.3 -0.2 -0.3 -0.3
-0.2 -0.2 -0.1 0.0 -0.1 -0.2 -0.2 -0.2 -0.2 -0.2 -0.2 -0.2 -0.1 -0.1 -0.1 -0.1 0.0 -0.1 -0.1 -0.1 0.0 -0.1 -0.1
0.0 0.1 0.1 0.1 -99.9 -99.9 -99.9 -99.9 -99.9 -99.9 -99.9 -99.9 -99.9 -99.9 -99.9 -99.9 -99.9 -99.9 -99.9 -99.9 -99.9 -
99.9 -99.9 -99.9 -99.9 -99.9 -99.9 -99.9 -99.9 -99.9 -99.9 -99.9 -99.9 -99.9 -99.9 -99.9 -99.9
-99.9 -
99.9 -99.9 -99.9 -99.9 0.9 0.9 -0.1 -0.1 -0.1 0.0 -0.1 -0.1 -0.1 -0.1 -0.1 -0.2 -0.2 -0.2 -0.2 -0.2 -0.2 -0.2 -
0.2 -0.2 -0.3 -0.2 -0.3 -0.3 -0.3 -0.3 -0.3 -0.3 -0.3 -0.3 -0.3 -0.4 -0.4 -0.4 -0.4 -0.3 -0.3 -0.3 -0.3 -0.2 -0.2
-0.2 -0.2 -0.3 -0.2 -0.2 -0.2 -0.2 0.0 0.0 0.0 0.1 -0.1 -0.1 -0.1 -0.1 -0.1 -0.1 -0.1 -0.2 -0.2 -0.2 -0.2 -0.2
-0.2 -0.2 -0.2 -0.2 -0.2 -0.2 -0.2 -0.3 -0.3 -0.3 -0.2 -0.2 -0.2 0.6 0.6 -1.0 -0.5 -0.2 -0.2 -0.1 -0.1 -0.1 -0.1
-0.1 0.0 -0.1 -0.1 0.9 0.9 -99.9 -99.9 -99.9 -99.9 -99.9 -99.9 -99.9 -99.9 -99.9 -99.9 -99.9 -99.9 -99.9 -99.9 -99.9 -
99.9 -99.9 -99.9 -99.9 -99.9 -99.9 -99.9 -99.9 -99.9 -99.9 -99.9 -99.9 -99.9 -99.9 -99.9 -99.9
-99.9 -
99.9 -99.9 -99.9 -99.9 -99.9 -99.9 -0.1 -0.1 0.9 0.9 0.9 0.9 0.9 0.9 0.9 0.9 0.9 0.9 0.9 0.9 0.9 0.9
0.9 0.9 0.9 0.9 0.9 0.9 0.9 0.9 0.9 0.9 0.9 0.9 0.9 0.9 0.9 0.9 0.9 0.9 0.9 0.9 0.9 0.9 0.9
0.9 0.9 0.9 -0.3 -0.2 -0.2 -0.2 -0.1 -0.1 -0.1 0.0 -0.1 -0.1 -0.1 -0.1 -0.1 -0.1 -0.1 -0.1 -0.1 -0.1 -0.2 -0.2
-0.2 -0.2 -0.2 -0.2 -0.2 -0.2 -0.3 -0.3 -0.3 -0.3 -0.3 -0.2 -0.2 0.6 0.6 -1.2 -0.6 -0.2 -0.2 -0.1 -0.1 -0.1 -0.1
-0.1 -0.1 -0.1 -0.1 0.9 0.9 -99.9 -99.9 -99.9 -99.9 -99.9 -99.9 -99.9 -99.9 -99.9 -99.9 -99.9 -99.9 -99.9 -99.9 -99.9 -
99.9 -99.9 -99.9 -99.9 -99.9 -99.9 -99.9 -99.9 -99.9 -99.9 -99.9 -99.9 -99.9 -99.9 -99.9 -99.9
-99.9 -
99.9 -99.9 -99.9 -99.9 -99.9 -99.9 -99.9 -0.1 0.9 0.9 0.9 0.9 0.9 0.9 0.9 0.9 0.9 0.9 0.9 0.9 0.9 0.9
0.9 0.9 0.9 0.9 0.9 0.9 0.9 0.9 0.9 0.9 0.9 0.9 0.9 0.9 0.9 0.9 0.9 0.9 0.9 0.9 0.9 0.9 0.9
0.9 0.9 0.9 -0.3 -0.3 -0.2 -0.2 -0.1 -0.1 -0.1 -0.1 -0.1 -0.1 -0.1 0.1 -0.1 0.0 0.0 -0.1 -0.1 -0.1 -0.2 -0.2
-0.2 -0.2 -0.2 -0.2 -0.2 -0.2 -0.3 -0.3 -0.2 -0.2 -0.3 -0.2 -0.2 0.6 0.6 -0.3 -0.2 -0.2 -0.2 -0.2 -0.2 -0.2 -0.1
-0.1 -0.1 -0.1 -0.1 0.9 0.9 -99.9 -99.9 -99.9 -99.9 -99.9 -99.9 -99.9 -99.9 -99.9 -99.9 -99.9 -99.9 -99.9 -99.9 -99.9 -
99.9 -99.9 -99.9 -99.9 -99.9 -99.9 -99.9 -99.9 -99.9 -99.9 -99.9 -99.9 -99.9 -99.9 -99.9 -99.9
-99.9 -
99.9 -99.9 -99.9 -99.9 -99.9 -99.9 -99.9 -99.9 0.9 0.9 0.9 0.9 0.9 0.9 0.9 0.9 0.9 0.9 0.9 0.9 0.9 0.9
0.9 0.9 0.9 0.9 0.9 0.9 0.9 0.9 0.9 0.9 0.9 0.9 0.9 0.9 0.9 0.9 0.9 0.9 0.9 0.9 0.9 0.9 0.9
0.9 0.9 0.9 -0.3 -0.3 -0.3 -0.2 -0.2 -0.2 -0.2 -0.1 0.1 -0.1 -0.1 0.0 0.0 0.0 0.0 0.0 -0.1 -0.1 -0.1 -0.1 -
0.2 -0.2 -0.2 -0.2 -0.3 -0.2 -0.2 -0.3 -0.3 -0.3 -0.3 -0.3 -0.3 0.5 0.5 -0.3 -0.3 -0.2 -0.3 -0.2 -0.2 -0.2 -0.2
-0.2 -0.2 -0.2 -0.2 0.9 0.9 -99.9 -99.9 -99.9 -99.9 -99.9 -99.9 -99.9 -99.9 -99.9 -99.9 -99.9 -99.9 -99.9 -99.9 -99.9 -
99.9 -99.9 -99.9 -99.9 -99.9 -99.9 -99.9 -99.9 -99.9 -99.9 -99.9 -99.9 -99.9 -99.9 -99.9 -99.9
-99.9 -
99.9 -
99.9 -
99.9 -99.9 -99.9 -99.9 -99.9 -99.9 -99.9 -99.9 -0.3 -0.3 -0.2 -0.2 -0.1 -0.1 -0.1 -0.1 -0.1 -0.1 -0.1 0.1 0.1 0.1
-0.1 0.0 0.0 -0.1 -0.1 -0.1 -0.2 -0.2 -0.2 -0.2 -0.2 -0.2 -0.2 -0.3 -0.3 -0.2 -0.2 -0.2 -0.3 0.5 0.5 -0.2 -0.2

-0.2 -0.2 -0.2 -0.2 -0.2 -0.2 -0.2 -0.2 -0.2 -0.2 0.9 0.9 -99.9 -99.9 -99.9 -99.9 -99.9 -99.9 -99.9 -99.9 -99.9 -99.9
-99.9 -
99.9
-99.9 -
99.9 -
99.9 -
99.9 -99.9 -99.9 -99.9 -99.9 -99.9 -99.9 -99.9 -99.9 -99.9 -99.9 -99.9 -99.9 -99.9 -99.9 -0.1 -0.2 -0.1 -0.1 0.0 0.1
0.1 0.1 0.1 0.0 -0.1 0.0 -0.1 -0.1 -0.1 -0.2 -0.2 -0.2 -0.2 -0.2 -0.2 -0.2 -0.2 -0.2 -0.3 -0.3 0.5 0.5 -0.2 -
0.2 -0.2 -0.2 -0.2 -0.2 -0.2 -0.2 -0.2 -0.2 -0.2 -0.2 0.9 0.9 -99.9 -99.9 -99.9 -99.9 -99.9 -99.9 -99.9 -99.9 -99.9 -
99.9 -
99.9 -99.9
-99.9 -
99.9 -
99.9 -
99.9 -99.9 -99.9 -99.9 -99.9 -99.9 -99.9 -99.9 -99.9 -99.9 -99.9 -99.9 -99.9 -99.9 -99.9 -0.2 -0.2 -0.2 -0.1 -0.1 0.1
0.1 0.2 0.1 0.1 -0.1 0.1 0.0 -0.1 -0.1 -0.2 -0.2 -0.2 -0.2 -0.2 -0.2 -0.2 -0.1 -0.3 -0.3 -0.3 0.5 0.5 -0.3 -
0.2 -0.2 -0.1 -0.2 -0.2 -0.2 -0.2 -0.2 -0.2 -0.2 -0.2 0.9 0.9 -99.9 -99.9 -99.9 -99.9 -99.9 -99.9 -99.9 -99.9 -99.9 -
99.9 -
99.9 -99.9
-99.9 -
99.9 -
99.9 -
99.9 -99.9 -99.9 -99.9 -99.9 -99.9 -99.9 -99.9 -99.9 -99.9 -99.9 -99.9 -99.9 -99.9 -99.9 -99.9 -0.1 -0.1 -0.1 0.0 0.2
0.1 0.1 0.2 0.1 0.1 0.1 0.1 0.2 -0.1 -0.1 -0.2 -0.2 -0.1 -0.2 -0.3 -0.4 -0.2 -0.2 -0.3 -0.3 0.5 0.5 -0.3 -
0.3 -0.2 -0.2 -0.2 -0.2 -0.2 -0.2 -0.2 -0.1 -0.2 -0.2 0.9 0.9 -99.9 -99.9 -99.9 -99.9 -99.9 -99.9 -99.9 -99.9 -99.9 -
99.9 -
99.9 -99.9
-99.9 -
99.9 -
99.9 -
99.9 -99.9 -99.9 -99.9 -99.9 -99.9 -99.9 -99.9 -99.9 -99.9 -99.9 -99.9 -99.9 -99.9 -99.9 -99.9 -0.2 -0.2 -0.2 -0.3 -0.1
0.0 0.1 0.1 0.1 0.1 0.0 0.0 0.0 0.0 -0.1 -0.1 -0.1 -0.1 -0.1 -0.2 -0.2 -0.2 -0.2 -0.2 -0.2 0.5 0.5 -0.2 -
0.2 -0.2 -0.2 -0.2 -0.2 -0.3 -0.3 -0.3 -0.2 -0.2 -0.2 0.9 0.9 -99.9 -99.9 -99.9 -99.9 -99.9 -99.9 -99.9 -99.9 -99.9 -
99.9 -
99.9 -99.9
-99.9 -
99.9 -
99.9 -
99.9 -99.9 -99.9 -99.9 -99.9 -99.9 -99.9 -99.9 -99.9 -99.9 -99.9 -99.9 -99.9 -99.9 -99.9 -99.9 -99.9 -0.2 -0.2 -0.2 -0.2
-0.1 0.0 0.1 0.0 0.1 0.1 0.1 0.0 0.0 -0.1 0.0 0.0 0.0 0.0 0.0 -0.1 -0.1 -0.2 -0.2 -0.2 0.5 0.5 -0.2 -
0.2 -0.2 -0.2 -0.2 -0.2 -0.2 -0.2 -0.2 -0.2 -0.2 -0.2 0.9 0.9 -99.9 -99.9 -99.9 -99.9 -99.9 -99.9 -99.9 -99.9 -99.9 -
99.9 -
99.9 -99.9
-99.9 -
99.9 -
99.9 -
99.9 -99.9 -99.9 -99.9 -99.9 -99.9 -99.9 -99.9 -99.9 -99.9 -99.9 -99.9 -99.9 -99.9 -99.9 -99.9 -99.9 -0.3 -0.3 -0.2 -0.2
-0.1 -0.1 -0.1 0.0 0.0 0.1 0.1 0.0 -0.1 -0.1 -0.1 0.0 0.1 0.1 0.1 0.0 0.0 -0.1 -0.2 -0.2 0.5 0.5 -0.2 -
0.2 -0.2 -0.2 -0.2 -0.2 -0.2 -0.2 -0.2 -0.2 -0.2 -0.2 0.9 0.9 -99.9 -99.9 -99.9 -99.9 -99.9 -99.9 -99.9 -99.9 -99.9 -
99.9 -
99.9 -99.9
-99.9 -
99.9 -
99.9 -
99.9 -99.9 -99.9 -99.9 -99.9 -99.9 -99.9 -99.9 -99.9 -99.9 -99.9 -99.9 -99.9 -99.9 -99.9 -99.9 -99.9 -99.9 -0.3 -0.3 -0.3
-0.3 -0.2 -0.1 0.0 0.1 0.1 -0.1 -0.1 -0.1 -0.1 -0.1 -0.1 0.0 0.0 0.0 0.0 -0.1 -0.1 -0.2 -0.2 0.5 0.5 -0.2
-0.3 -0.2 -0.2 -0.1 -0.2 -0.2 -0.3 -0.3 -0.3 -0.2 -0.2 0.9 0.9 -99.9 -99.9 -99.9 -99.9 -99.9 -99.9 -99.9 -99.9 -99.9
-99.9 -
99.9 -99.9
-99.9 -
99.9 -
99.9 -
99.9 -99.9 -99.9 -99.9 -99.9 -99.9 -99.9 -99.9 -99.9 -99.9 -99.9 -99.9 -99.9 -99.9 -99.9 -99.9 -99.9 -99.9 -0.3 -0.3 -0.2
-0.2 -0.2 -0.2 -0.1 -0.1 -0.1 -0.1 0.0 -0.1 -0.1 -0.1 -0.1 -0.1 -0.1 0.0 0.0 -0.1 0.1 -0.1 -0.2 0.5 0.5 -0.3
-0.2 -0.3 -0.2 -0.2 -0.2 -0.2 -0.2 -0.2 -0.2 -0.2 -0.2 0.9 0.9 -99.9 -99.9 -99.9 -99.9 -99.9 -99.9 -99.9 -99.9 -99.9
-99.9 -
99.9 -99.9
-99.9 -
99.9 -
99.9 -

99.9 -99.9 -99.9 -99.9 -99.9 -99.9 -99.9 -99.9 -99.9 -99.9 -99.9 -99.9 -99.9 -99.9 -99.9 -99.9 -99.9 -99.9 -99.9 -0.3 -0.3
-0.2 -0.2 -0.2 -0.2 -0.1 -0.1 -0.1 -0.1 -0.1 -0.1 -0.1 -0.1 -0.1 -0.1 -0.1 -0.1 -0.1 0.4 0.4 0.4 0.4 0.5 0.4
0.4 0.4 0.4 0.4 0.4 -0.2 -0.2 -0.2 -0.2 -0.2 -0.2 0.9 0.9 -99.9 -99.9 -99.9 -99.9 -99.9 -99.9 -99.9 -99.9 -99.9 -
99.9 -
99.9 -99.9
-99.9 -
99.9 -
99.9 -
99.9 -99.9 -99.9 -99.9 -99.9 -99.9 -99.9 -99.9 -99.9 -99.9 -99.9 -99.9 -99.9 -99.9 -99.9 -99.9 -99.9 -99.9 -99.9 -0.3 -0.3
-0.2 -0.2 -0.2 -0.2 -0.2 -0.1 -0.1 -0.1 -0.1 -0.1 -0.1 -0.1 -0.1 -0.1 -0.1 -0.1 -0.2 0.4 0.4 0.4 0.4 0.4 0.4
0.4 0.4 0.4 0.4 0.4 -0.2 -0.3 -0.2 -0.2 -0.2 -0.2 0.9 0.9 -99.9 -99.9 -99.9 -99.9 -99.9 -99.9 -99.9 -99.9 -99.9 -
99.9 -
99.9 -99.9
-99.9 -
99.9 -
99.9 -
99.9 -0.1
-0.2 -0.2 -0.2 -0.1 -0.1 -0.2 -0.1 -0.1 -0.2 -0.1 -0.1 -0.2 -0.2 -0.2 -0.2 -0.2 -0.2 0.4 0.4 -0.1 -0.1 -0.2 -0.2
-0.4 -0.3 -0.3 -0.2 -0.3 -0.3 -0.3 -0.2 -0.2 -0.2 0.9 0.9 0.9 -99.9 -99.9 -99.9 -99.9 -99.9 -99.9 -99.9 -99.9 -99.9
-99.9 -
99.9 -99.9
-99.9 -
99.9 -
99.9 -
99.9 -
99.9 -0.4 -0.2 -0.1 -0.1 -0.2 -0.1 -0.1 -0.1 -0.1 -0.2 -0.2 -0.2 -0.2 -0.1 -0.2 -0.2 -0.2 0.4 0.4 -0.2 -0.2 -0.2
-0.1 -0.3 -0.3 -0.4 -0.2 -0.3 -0.3 -0.3 -0.2 -0.2 0.9 0.9 0.9 0.9 -99.9 -99.9 -99.9 -99.9 -99.9 -99.9 -99.9 -99.9 -
99.9 -
99.9 -99.9 -99.9
-99.9 -
99.9 -
99.9 -
99.9 -
99.9 -99.9 -0.3 -0.2 -0.2 -0.2 -0.2 -0.2 -0.1 -0.1 -0.2 -0.2 -0.2 -0.1 -0.2 -0.2 -0.3 -0.2 0.4 0.4 -0.2 -0.2 -0.2
-0.2 -0.3 -0.3 -0.3 -0.3 -0.3 -0.3 -0.2 -0.2 0.9 0.9 0.9 -99.9 -99.9 -99.9 -99.9 -99.9 -99.9 -99.9 -99.9 -99.9 -99.9
-99.9 -
99.9 -99.9 -99.9
-99.9 -
99.9 -
99.9 -
99.9 -
99.9 -99.9 -0.3 -0.3 -0.3 -0.2 -0.2 -0.2 -0.2 -0.1 -0.2 -0.2 -0.2 -0.2 -0.2 -0.2 -0.3 -0.3 0.4 0.4 -0.2 -0.2 -0.2
-0.2 -0.2 -0.3 -0.3 -0.2 -0.3 -0.2 0.9 0.9 0.9 0.9 -99.9 -99.9 -99.9 -99.9 -99.9 -99.9 -99.9 -99.9 -99.9 -99.9 -99.9
-99.9 -
99.9 -99.9 -99.9
-99.9 -
99.9 -
99.9 -
99.9 -
99.9 -99.9 -99.9 -0.2 -0.2 -0.3 -0.2 -0.3 -0.2 -0.1 -0.2 -0.2 -0.3 -0.2 -0.1 -0.2 -0.3 -0.3 0.9 0.9 -0.2 -0.1 -
0.2 -0.2 -0.2 -0.3 -0.2 -0.2 -0.3 0.9 0.9 0.9 0.9 -99.9 -99.9 -99.9 -99.9 -99.9 -99.9 -99.9 -99.9 -99.9 -99.9 -99.9
-99.9 -
99.9 -99.9 -99.9 -99.9
-99.9 -
99.9 -
99.9 -
99.9 -
99.9 -99.9 -99.9 -0.2 -0.3 -0.4 -0.5 -0.4 0.6 0.6 -0.2 -0.2 -0.2 -0.2 -0.1 -0.3 -0.3 -0.3 0.4 0.9 -0.1 -0.1 -
0.1 -0.1 -0.1 -0.2 -0.3 -0.4 0.9 0.9 0.9 0.9 -99.9 -99.9 -99.9 -99.9 -99.9 -99.9 -99.9 -99.9 -99.9 -99.9 -99.9 -99.9
-99.9 -
99.9 -99.9 -99.9 -99.9
-99.9 -
99.9 -
99.9 -
99.9 -
99.9 -99.9 -99.9 -99.9 -0.3 -0.4 -0.4 0.6 0.6 0.6 0.6 0.6 -0.2 -0.2 -0.2 -0.2 -0.3 -0.3 0.4 0.4 -0.2 -0.1 -
0.1 -0.1 -0.2 -0.2 -0.3 0.9 0.9 0.9 -99.9 -99.9 -99.9 -99.9 -99.9 -99.9 -99.9 -99.9 -99.9 -99.9 -99.9 -99.9 -99.9 -
99.9 -
99.9 -99.9 -99.9 -99.9 -99.9

-99.9 -
99.9 -
99.9 -
99.9 -
99.9 -99.9 -99.9 -99.9 -0.3 -0.4 -0.3 -0.3 0.6 0.6 0.6 -0.2 -0.2 -0.2 -0.2 -0.2 -0.3 -0.3 0.4 0.4 -0.2 -0.1 -
0.1 -0.1 -0.1 -0.2 0.9 0.9 0.9 -99.9 -99.9 -99.9 -99.9 -99.9 -99.9 -99.9 -99.9 -99.9 -99.9 -99.9 -99.9 -99.9 -99.9 -
99.9 -
99.9 -99.9 -99.9 -99.9 -99.9
-99.9 -
99.9 -
99.9 -
99.9 -
99.9 -99.9 -99.9 -99.9 -99.9 -99.9 -99.9 -99.9 -99.9 -99.9 -0.1 -0.2 -0.2 -0.2 -0.2 -0.2 -0.3 -0.3 0.4 0.4 -0.2 -0.1
-0.1 -0.1 -0.2 0.9 0.9 0.9 -99.9 -99.9 -99.9 -99.9 -99.9 -99.9 -99.9 -99.9 -99.9 -99.9 -99.9 -99.9 -99.9 -99.9 -99.9 -
99.9 -
99.9 -99.9 -99.9 -99.9 -99.9
-99.9 -
99.9 -
99.9 -
99.9 -
99.9 -99.9 -99.9 -99.9 -99.9 -99.9 -99.9 -99.9 -99.9 -99.9 -99.9 -99.9 -99.9 -0.2 -0.2 -0.2 -0.3 -0.3 0.4 0.4 -0.2 -
0.1 -0.1 -0.1 -99.9 -99.9 -99.9 -99.9 -99.9 -99.9 -99.9 -99.9 -99.9 -99.9 -99.9 -99.9 -99.9 -99.9 -99.9 -99.9 -99.9 -99.9 -
99.9 -
99.9 -99.9 -99.9 -99.9 -99.9 -99.9
-99.9 -
99.9 -
99.9 -
99.9 -
99.9 -99.9 -99.9 -99.9 -99.9 -99.9 -99.9 -99.9 -99.9 -99.9 -99.9 -99.9 -99.9 -99.9 -0.2 -0.2 -0.2 -0.3 0.4 0.4 -0.2 -
0.2 -0.1 -0.1 -99.9 -99.9 -99.9 -99.9 -99.9 -99.9 -99.9 -99.9 -99.9 -99.9 -99.9 -99.9 -99.9 -99.9 -99.9 -99.9 -99.9 -99.9 -
99.9 -
99.9 -99.9 -99.9 -99.9 -99.9 -99.9
-99.9 -
99.9 -
99.9 -
99.9 -
99.9 -99.9 -99.9 -99.9 -99.9 -99.9 -99.9 -99.9 -99.9 -99.9 -99.9 -99.9 -99.9 -99.9 -99.9 -99.9 -0.2 -0.3 0.4 0.4 -0.2 -
0.1 -0.1 -0.1 -99.9 -99.9 -99.9 -99.9 -99.9 -99.9 -99.9 -99.9 -99.9 -99.9 -99.9 -99.9 -99.9 -99.9 -99.9 -99.9 -99.9 -99.9 -
99.9 -
99.9 -99.9 -99.9 -99.9 -99.9 -99.9
-99.9 -
99.9 -
99.9 -
99.9 -
99.9 -99.9 -99.9 -99.9 -99.9 -99.9 -99.9 -99.9 -99.9 -99.9 -99.9 -99.9 -99.9 -99.9 -99.9 -99.9 -99.9 -0.3 0.4 0.4 -0.2
-0.1 -0.1 -0.1 -99.9 -99.9 -99.9 -99.9 -99.9 -99.9 -99.9 -99.9 -99.9 -99.9 -99.9 -99.9 -99.9 -99.9 -99.9 -99.9 -99.9 -99.9
-99.9 -
99.9 -99.9 -99.9 -99.9 -99.9 -99.9
-99.9 -
99.9 -
99.9 -
99.9 -
99.9 -0.2
-0.1 -0.1 -0.1 -99.9 -99.9 -99.9 -99.9 -99.9 -99.9 -99.9 -99.9 -99.9 -99.9 -99.9 -99.9 -99.9 -99.9 -99.9 -99.9 -99.9 -99.9
-99.9 -
99.9 -99.9 -99.9 -99.9 -99.9 -99.9
-99.9 -
99.9 -
99.9 -
99.9 -
99.9 -
99.9 -99.9 0.0 0.0 -99.9 -99.9 -99.9 -99.9 -99.9 -99.9 -99.9 -99.9 -99.9 -99.9 -99.9 -99.9 -99.9 -99.9 -99.9 -99.9 -99.9
-99.9 -
99.9 -99.9 -99.9 -99.9 -99.9 -99.9 -99.9
0.005 RS28 VIS COEF
RS29 END VISC
0. 1 RS30 DIF COEF
RS31 END DIFF
0.400 RS32 MAN COEF
1 RS33 Flag VEGMANNING

RS33 END MANN

0. RS34 BEN VALU

RS35 END BENV

RS36 END CONC

RS37 END TITL

RS39A COMP ROWS

2	2	137	2	1
3	2	137	2	1
4	2	137	2	1
5	2	137	2	1
6	2	137	2	1
7	2	137	2	1
8	2	137	2	1
9	2	137	2	1
10	2	137	2	1
11	2	137	2	1
12	2	137	2	1
13	2	137	2	1
14	2	137	2	1
15	2	138	2	1
16	2	138	1	1
17	2	138	1	1
18	2	139	1	1
19	2	139	1	1
20	2	140	1	1
21	2	140	1	1
22	2	141	1	1
23	2	141	1	1
24	2	142	1	1
25	2	142	1	1
26	3	144	1	1
27	4	145	1	1
28	6	147	1	1
29	7	146	1	1
30	8	146	1	1
31	10	146	1	1
32	11	146	1	1
33	13	145	1	1
34	15	145	1	1
35	16	145	1	1
36	18	145	1	1
37	19	143	1	1
38	20	143	1	2
39	22	143	1	2
40	23	143	1	2
41	25	143	1	1
42	26	143	1	1
43	26	143	1	1
44	26	143	2	1
45	26	143	2	1
46	26	143	2	1
47	26	143	2	1
48	26	143	2	1
49	26	143	2	1
50	26	143	2	1
51	26	143	2	1
52	26	142	2	1
53	26	142	2	1
54	26	142	2	1
55	26	142	2	1
56	26	142	2	1
57	26	140	2	1
58	26	138	2	1
59	26	136	2	1
60	26	133	2	1
61	26	130	2	1
62	26	127	2	1
63	26	125	2	1
64	26	122	2	1
65	26	119	2	1
66	26	117	2	1

67	26	115	2	1
68	26	115	2	1
69	26	117	2	2
70	28	117	1	2
71	29	117	1	2
72	69	117	1	2
73	69	117	1	2
74	77	117	1	2
75	77	117	1	2
76	78	117	1	2
77	78	117	1	2
78	79	117	1	2
79	79	117	1	2
80	80	117	1	2
81	80	117	1	2
82	81	117	1	2
83	81	117	1	2
84	82	117	1	2
85	83	117	1	2
86	84	115	1	1
87	84	114	1	1
88	85	113	1	1
89	85	112	1	1
90	86	110	1	1
91	91	109	1	1
92	93	108	1	1
93	95	104	1	1
94	96	104	1	1
95	98	104	1	1
96	99	104	1	1
97	102	104	1	1

END RS39A

RS40A COMP COLS

2	2	25	2	1
3	2	26	2	1
4	2	27	2	1
5	2	27	2	1
6	2	28	2	1
7	2	29	2	1
8	2	30	2	1
9	2	31	2	1
10	2	32	2	1
11	2	32	2	1
12	2	33	2	1
13	2	34	2	1
14	2	35	2	1
15	2	35	2	1
16	2	36	2	1
17	2	36	2	1
18	2	37	2	1
19	2	38	2	1
20	2	38	2	1
21	2	39	2	1
22	2	39	2	1
23	2	40	2	1
24	2	41	2	1
25	2	41	2	1
26	2	69	2	1
27	2	70	2	1
28	2	71	2	1
29	2	71	2	1
30	2	71	2	2
31	2	71	2	2
32	2	71	2	2
33	2	71	2	2
34	2	71	2	2
35	2	71	2	2
36	2	71	2	2
37	2	71	2	2
38	2	71	2	2
39	2	71	2	2

40	2	71	2	2
41	2	71	2	2
42	2	71	2	2
43	2	71	2	2
44	2	71	2	2
45	2	71	2	2
46	2	71	2	2
47	2	71	2	2
48	2	71	2	2
49	2	71	2	2
50	2	71	2	2
51	2	71	2	2
52	2	71	2	2
53	2	71	2	2
54	2	71	2	2
55	2	71	2	2
56	2	71	2	2
57	2	71	2	2
58	2	71	2	2
59	2	71	2	2
60	2	71	2	2
61	2	71	2	2
62	2	71	2	2
63	2	71	2	2
64	2	71	2	2
65	2	71	2	2
66	2	71	2	2
67	2	71	2	2
68	2	72	2	2
69	2	73	2	1
70	2	73	2	1
71	2	73	2	1
72	2	73	2	1
73	2	73	2	1
74	2	73	2	1
75	2	73	2	1
76	2	74	2	1
77	2	75	2	1
78	2	77	2	1
79	2	79	2	1
80	2	81	2	1
81	2	83	2	1
82	2	85	2	1
83	2	86	2	1
84	2	89	2	1
85	2	90	2	1
86	2	90	2	1
87	2	90	2	1
88	2	91	2	1
89	2	91	2	1
90	2	91	2	1
91	2	91	2	1
92	2	92	2	1
93	2	92	2	1
94	2	93	2	1
95	2	93	2	1
96	2	94	2	1
97	2	95	2	1
98	2	95	2	1
99	2	96	2	1
100	2	96	2	1
101	2	96	2	1
102	2	97	2	1
103	2	97	2	2
104	2	97	2	2
105	2	92	2	1
106	2	92	2	1
107	2	92	2	1
108	2	92	2	1
109	2	91	2	1

```
 110   2  90   2   1
 111   2  89   2   1
 112   2  89   2   1
 113   2  88   2   1
 114   2  87   2   1
 115   2  86   2   1
 116   2  85   2   1
 117   2  85   2   1
 118   2  66   2   1
 119   2  66   2   1
 120   2  65   2   1
 121   2  65   2   1
 122   2  64   2   1
 123   2  64   2   1
 124   2  63   2   1
 125   2  63   2   1
 126   2  62   2   1
 127   2  62   2   1
 128   2  61   2   1
 129   2  61   2   1
 130   2  61   2   1
 131   2  61   2   1
 132   2  60   2   1
 133   2  60   2   1
 134   2  60   2   1
 135   2  60   2   1
 136   2  59   2   1
 137   2  59   2   1
 138  11  58   1   1
 139  15  58   1   1
 140  17  57   1   1
 141  19  57   1   1
 142  21  57   1   1
 143  23  52   1   1
 144  24  36   1   1
 145  25  36   1   1
 146  26  33   1   1
 147  26  30   1   1
                                                    END RS40A
0   15.000    4         0.00 140.000
1   0.200     22.820 0.01722
1   0.200     22.820 0.01232
1   0.200     22.820 0.00475
1   0.200      7.310 0.00683
1   0.200      0.000  0.005
1  -0.070      0.000  0.005
1   0.089      0.000  0.005
1   0.269      0.000  0.005
2   0.200     22.820 0.01722
2   0.200     22.820 0.01232
2   0.200     16.660 0.00475
2   0.200      7.310 0.00683
2   0.200      0.000  0.005
2   0.089      0.000  0.005
2   0.269      0.000  0.005
2   0.314      0.000  0.005
5  1   -1.00    0.00
5  2    0.00    0.00
5  3   -6.94    0.00
5  4   -0.20
0   30.000    1         0.01 136.000
1   0.199     22.785 0.01722
1   0.199     22.785 0.01232
1   0.199     22.785 0.00475
1   0.199      7.295 0.00683
1   0.200      0.000  0.005
1  -0.070      0.000  0.005
1   0.089      0.000  0.005
1   0.269      0.000  0.005
2   0.199     22.785 0.01722
```

```
2   0.199     22.785 0.01232
2   0.199     16.710 0.00475
2   0.199      7.295 0.00683
2   0.200      0.000   0.005
2   0.089      0.000   0.005
2   0.269      0.000   0.005
2   0.314      0.000   0.005
5  4   -0.10
0    45.000     1          0.01 112.000
1   0.199     22.750 0.01722
1   0.199     22.750 0.01232
1   0.199     22.750 0.00475
1   0.199      7.280 0.00683
1   0.200      0.000   0.005
1  -0.070      0.000   0.005
1   0.089      0.000   0.005
1   0.269      0.000   0.005
2   0.199     22.750 0.01722
2   0.199     22.750 0.01232
2   0.199     16.760 0.00475
2   0.199      7.280 0.00683
2   0.200      0.000   0.005
2   0.089      0.000   0.005
2   0.269      0.000   0.005
2   0.314      0.000   0.005
5  4   -0.10
0    60.000     1          0.01 127.000
1   0.199     22.715 0.01722
1   0.199     22.715 0.01232
1   0.199     22.715 0.00475
1   0.199      7.265 0.00683
1   0.200      0.000   0.005
1  -0.070      0.000   0.005
1   0.089      0.000   0.005
1   0.269      0.000   0.005
2   0.199     22.715 0.01722
2   0.199     22.715 0.01232
2   0.199     16.810 0.00475
2   0.199      7.265 0.00683
2   0.200      0.000   0.005
2   0.089      0.000   0.005
2   0.269      0.000   0.005
2   0.314      0.000   0.005
```

*incomplete file

LIST OF REFERENCES

Ahn, H., 1999. Statistical modeling of total phosphorus concentrations measured in south Florida rainfall. Ecological Modelling 116:33–44.

Aitken, A.P. 1973. Assessing systematic errors in rainfall-runoff models. Journal of Hydrology 20:121-136.

Arhonditsis, G.B., Brett M.T., 2004. Evaluation of the current state of mechanistic aquatic biogeochemical modeling. Marine Ecology Progress Series 271:13-26.

Armentano, T.V., Sah, J.P., Ross, M.S., Jones, D.T., Cooley, H.C., Smith, C.S., 2006. Rapid responses of vegetation to hydrological changes in Taylor Slough, Everglades National Park, Florida, USA. Hydrobiologia 569:293-309.

Arnholm, C.A., 1997. Mixed language programming using C++ and FORTRAN 77. Available at: http://arnholm.org/software/cppf77/cppf77.htm. Accessed 10/10, 2009.

Arthur, W.B., 1999. Complexity and the economy. Science 284(5411):107-109.

Ascough, J.C., Maier, H.R., Ravalico, J.K., Strudley, M.W., 2008. Future research challenges for incorporation of uncertainty in environmental and ecological decision-making. Ecological Modelling 219:383-399.

Bales, J.D., Robbins, J.C., 1995. Simulation of hydrodynamics and solute transport in the Pamlico River Estuary, North Carolina. U.S. Geological Survey Open-File Report 94-454, 85pp.

Basmadjian, D., 1999. The Art of Modeling in Science and Engineering. Boca Raton, Florida, USA: Chapman and Hall/CRC Press.

Bays, J.S., Knight, R.L., Wenkert, L., Clark, R., Gong, S., 2001. Progress in the research and demonstration of Everglades periphyton-based stormwater treatment areas. Water Science and Technology 44:123-130.

Beccue, S., 1999. Endangered species: Everglades National Park. Available at: http://www.nps.gov/ever/eco/danger.htm. Accessed 08/20, 2003.

Beck, M.B., 1987. Water-quality modeling: a review of the analysis of uncertainty. Water Resources Research 23(8):1393-1442.

Beisner, B.E., Haydon, D.T., Cuddington, K., 2003. Alternative stable states in ecology. Frontiers in Ecology and the Environment 1(7):376-382.

Benque, J.P., Cunge, J.A., Feuillet, J., Hauguel, A., Holly, F.M., 1982. New method for tidal current computation. Journal of the Waterway, Port, Coastal, and Ocean Division, ASCE 108(3):396-417.

Beven, K., 2006a. A manifesto for the equifinality thesis. Journal of Hydrology 320:18-36.

Beven, K., 2006b. On undermining the science? Hydrological Process 20(14):3141-3146.

Beven, K., 1993. Prophecy, reality and uncertainty in distributed hydrological modeling. Advances in Water Resources 16(1):41-51.

Beven, K., Binley, A., 1992. The future of distributed models: model calibration and uncertainty prediction. Hydrological Processes 6:279-298.

Boyer, J.N., Fourqurean, J.W., Jones, R.D., 1999. Seasonal and long-term trends in the water-quality of Florida Bay (1989-1997). Estuaries 22(2B):417-430.

Brion, L.M., Senarath, S., Lal, W., 2000. Concepts and algorithms for an integrated surface-water/ground-water model for natural areas, in Proceedings of the Greater Everglades Ecosystem Restoration (GEER) Science Conference; Naples, florida, December 11-15, 2000, p280.

Brun, R., Reichert, P., Künsch, H.R., 2001. Practical identifiably analysis of large environmental simulation models. Water Resources Research 37:115-130.

Cacuci, D.G., 2003. Sensitivity and Uncertainty Analysis Volume 1: Theory. Boca Raton, Florida, USA: Chapman and Hall/CRC Press.

Campolongo, F., Cariboni, J., Saltelli, A., 2007. An effective screening design for sensitivity analysis of large models. Environmental Modelling and Software 22:1509-1518.

Campolongo, F., Saltelli, A., 1997. Sensitivity analysis of an environmental model: an application of different analysis methods. Reliability Engineering and System Safety 57(1):49-69.

Cariboni, J., Gatelli, D., Liska, R., Saltelli, A., 2007. The role of sensitivity analysis in ecological modeling. Ecological Modelling 203:167-182.

Cary, J.R., Shasharina, S.G., Cummings, J.C., Reynders, J.V.W., Hinker, P.J., 1998. Comparison of C++ and Fortran 90 for object-oriented scientific programming. Computer Physics Communications 105(1):20-36.

Chen, R.H., Twilley, R.R., 1999. Patterns of mangrove forest structure and soil nutrient dynamics along the Shark River estuary, Florida. Estuaries 22(4):955-970.

Childers, D.L., 2006. A synthesis of long-term research by the Florida Coastal Everglades LTER Program. Hydrobiologia 569:531-544.

Chwif, L., Barretto, M., Paul, R., 2000. On simulation model complexity. Proceedings of the 32nd Conference on Winter Simulation, 449-455.

Cichra, M.F., Badylak, S., Henderson, N., Rueter, B.H., Phlips, E.G., 1995. phytoplankton community structure in the open water zone of a shallow subtropical lake (Lake Okeechobee, Florida, USA). Advances in Limnology 45:157-175.

Cleckner, L.B., Gilmour, C.C., Hurley, J.P., Krabbenhoft, D.P., 1999. Mercury methylation in periphyton of the Florida Everglades. Limnology and Oceanography 44(7):1815-1825

Costanza, R., Sklar, F.H., White, M.L., 1990. Modeling coastal landscape dynamics. Bioscience 40:91-107.

Cox, G.M., Gibbons, J.M., Wood, A.T.A., Craigon, J., Ramsden, S.J., Crout, N.M.J., 2006. Towards the systematic simplification of models. Ecological Modelling 198:240-246.

Cressie, N., Calder, C.A., Clark, J.S., Ver Hoef, J.M., Wikle, C.K., 2009. Accounting for uncertainty in ecological analysis: the strengths and limitations of hierarchical statistical modeling. Ecological Applications 19(3):553-570.

CRGEE, NRC, 2002. Florida Bay Research Programs and their Relation to the Comprehensive Everglades Restoration Plan. Committee on Restoration of the Greater Everglades Ecosystem: National Research Council.

Davis SM. 1994. Phosphorous inputs and vegetation sensitivity in the Everglades. In: Davis SM, Ogden JC, editors. Everglades: the ecosystem and its restoration. Delray Beach, Florida: St. Lucie Press, p 357–78.

DeBusk, W. F., and K. R. Reddy (1998), Turnover of detrital organic carbon in a nutrient-impacted Everglades marsh, Soil Science Society Of America Journal, 62, 1460-1468.

de Kanal, J., Morse, J.W., 1978. The chemistry of orthophosphate uptake from seawater onto calcite and aragonite. Geochimica et Cosmochimica Acta 42:1335-1340.

Desmond, G., 2000. Topography of the Florida Everglades, in Proceedings of the Greater Everglades Ecosystem Restoration (GEER) Conference; December 11-15, 2000: U.S. Geological Survey Open-File Report 00-449.

Doerr, H.M., 1996. Stella ten years later: a review of the literature. International Journal of Computers for Mathematical Learning 1(2):201-224.

Draper, D., 1995. Assessment and propagation of model uncertainty. Journal of the Royal Statistical Society Series B-Methodological 57(1):45-97.

Dronkers, J., van Os, A.G., Leendertse, J.J., 1981. Predictive salinity modeling of the Oosterschelde with hydraulic and mathematical models: Transport models for inland and coastal waters. Proceedings of the Symposium on Predictive Abilities, New York, N.Y.: Academic Press, p. 451-482.

Eagleson, P.S., 1970. Dynamic Hydrology. New York, NY: McGraw-Hill Book Company.

Ebel, B.A., Loague, K., 2006. Physics-based hydrologic-response simulation: Seeing through the fog of equifinality. Hydrological Processes 20(13):2887-2900.

Elder, J.W., 1959. The dispersion of marked fluid in turbulent shear flow. Journal of Fluid Mechanics 5(4):544-560.

Fennema, R.J., Neidrauer, C.J., Johnson, R.A., MacVicar, T.K., Persons, W.A., 1994. A computer model to simulate natural Everglades hydrology. In: Davis, S.M., Ogden, J.C. (Eds.), Everglades: The Ecosystem and its Restoration: St. Lucie Press.

Fischer, H.B., List, J.E., Koh, R.C.Y. et al., 1979. Mixing in inland and coastal waters. New York, N.Y.: Academic Press, p. 126-127.

Fisher, B.E.A., Ireland, M.P., Boyland, D.T., Critten, S.P., 2002. Why use one model? An approach for encompassing model uncertainty and improving best practice. Environmental Modeling and Assessment 7(4):291-299.

Fitz, H.C., Sklar, F.H., 1999. Ecosystem analysis of phosphorus impacts and altered hydrology in the Everglades: a landscape modeling approach. In: Reddy KR, O'Connor GA, Schelske CL, editors. Phosphorous biogeochemistry in subtropical ecosystems. Boca Raton (FL): Lewis Publishers, p 585–620.

Fourqurean, J.W., Robblee, M.B., 1999. Florida Bay: A history of recent ecological changes. Estuaries 22(2B):345-357.

Fourqurean, J.W., Zieman, J.C., Powell, G.V.N., 1992. Phosphorus limitation of primary production in Florida Bay - Evidence from C-N-P ratios of the dominant seagrass Thalassia-Testudinum. Limnology and Oceanography 37(1):162-171.

Gaiser, E.E., Scinto, L.J., Richards, J.H., Jayachandaran, K., Childers, D.L., Trexler, J.D., Jones, R.D., 2004. Phosphorus in periphyton mats provides best metric for detecting low-level nutrient enrichment in an oligotrophic wetland. Water Resources 38:507-516.

Gaiser, E.E., Trexler, J.C., Richards, Childers, Lee, D., Edwards, A.L., Scinto, L.J., , Jayachandaran, K., Noe, G.B., Jones, R.D., 2005. Cascading ecological effects of low-level phosphorus enrichment in the Florida Everglades. Journal of Environmental Quality 34:717-723.

Gaiser, E.E., Childers, D.L., Jones, R.D., Richards, J.H., Scinto, L.J., Trexler, J.C., 2006. Periphyton responses to eutrophication in the Florida Everglades: Cross-system patterns of structural and compositional change. Limnology and Oceanography 51(1):617-630.

German, E.R., 2000. Regional evaluation of evapotranspiration in the Everglades. U.S. Geological Survey Water-Resources Investigations Report 00–4217, 48pp.

Getz, W.M., 1998. An introspection on the art of modeling in population ecology. Bioscience 48(7):540-552.

Goodwin, C.R., 1987. Tidal-flow, circulation, and flushing changes caused by dredge and fill in Tampa Bay, Florida. U.S. Geological Survey Water-Supply Paper 2282, 88p.

Goodwin, C.R., 1991. Tidal-flow, circulation, and flushing changes caused by dredge and fill in Hillsborough Bay, Florida. U.S. Geological Survey Water-Supply Paper 2376, 49 p.

Graham, W.F., Duce, R.A., 1982. The atmospheric transport of phosphorus to the western North Atlantic. Atmospheric Environment 16:1089-1097.

Guo, Weixing, and Langevin, C.D., 2002, User's guide to SEAWAT: A computer program for simulation of three-dimensional variable-density ground-water flow: U.S. Geological Survey Techniques of Water-Resources Investigations, book 6, chap. A7, 77 p.

Haan, C.T., 1989. Parametric uncertainty in hydrologic modeling. Transactions of the ASAE 32(1):137-146.

Haan, C.T., Allred, B., Storm, D.E., Sabbagh, G.J., Prabhu, S., 1995. Statistical procedure for evaluating hydrologic water-quality models. Transactions of the ASAE 38(3):725-733.

Haan, C.T., Storm, D.E., Al-Issa, T., Prabhu, S., Sabbagh, G.J., Edwards, D.R., 1998. Effect of parameter distributions on uncertainty analysis of hydrologic models. Transactions of the ASAE 41(1):65-70.

Hamrick, J.M., Moustafa, M.Z., 2003. Florida Bay hydrodynamic and salinity model analysis, in Proceedings of the Greater Everglades and Florida Bay Ecosystem Conference, Palm Harbor, Florida, April 13-18, 2003.

Hanna, S.R., 1988. Air-quality model evaluation and uncertainty. International Journal of Air Pollution Control and Hazardous Waste Management 38(4):406-412.

Harleman D.R.F., 1966. Diffusion Processes in Stratified Flow—Estuary and Coastline Hydrodynamics. New York, NY: McGraw-Hill Book Company.

Heisenberg W., 1958. Physics and Philosophy: The Revolution in Modern Science. New York, NY: Harper.

Hittle, C.D., 2000. Quantity, timing, and distribution of freshwater flows into northeastern Florida Bay: U.S. Geological Survey Program on the South Florida Ecosystem, in Proceedings of the Greater Everglades Ecosystem Restoration (GEER) Conference; December 11-15, 2000: U.S. Geological Survey Open-File Report 00-449, pp27-28.

James, A.I., Jawitz, J.W., Muñoz-Carpena, R., 2009. Development and implementation of a transport method for the Transport and Reaction Simulation Engine (TaRSE) based on the Godunov-Mixed Finite Element Method. U.S. Geological Survey Scientific Investigations Report 2009-5034, 40pp.

Jawitz, J.W., Muñoz-Carpena, R., Muller, S.J., Grace, K.A., James, A.I., 2008. Development, testing and sensitivity and uncertainty analyses of a Transport and Reaction Simulation Engine (TaRSE) for spatially-distributed modeling of phosphorus in south Florida peat marsh wetlands. U.S. Geological Survey Scientific Investigations Report 2008-5029, 109pp.

Jenter, H., 1999. Laboratory experiments for evaluating the effects of wind forcing on shallow waters with emergent vegetation, in Coastal Ocean Processes Symposium: A Tribute to William T. Grant: Woods Hole Oceanographic Institution Technical Report, 15pp.

Jury, W.A., Gardner, W.R., Gardner, W.H., 1991. Soil Physics. New York, NY: Wiley and Sons.

Kadlec, R.H., 1997. An autobiotic wetland phosphorus model. Ecological Engineering 8:145-172.

Kadlec, R.H., Knight, R.L., 1996. Treatment Wetlands: Boca Raton, Florida: Lewis Publishers, 893 p.

Konikow, L.F., Bredehoeft, J.D., 1992. Ground-water models cannot be validated. Advances in Water Resources 15(1):75-83.

Kotz, S., van Dorp, J.R., 2004. Beyond Beta. Singapore: World Scientific Publishing Co. Pty. Ltd.

Lal, A.M.W., van Zee, R., Belnap, M., 2005. Case study: Model to simulate regional flow in South Florida. Journal of Hydraulic Engineering-ASCE 131(4):247-258.

Landing W (1997) Measurements of aerosol phosphorus in South Florida. In: Redfield G & Urban N (Eds) Atmospheric Deposition into South Florida: Measuring Net Atmospheric Inputs of Nutrients.: SFWMD Conference on Atmospheric Deposition into South Florida. West Palm Beach, Florida. October 1997

Langevin, C.D., 2001. Simulation of ground-water discharge to Biscayne Bay, southeastern Florida. U.S. Geological Survey Water-Resources Investigations Report 00-4251, 137pp.

Langevin, C.D., Swain, E., Wolfert, M., 2005. Simulation of integrated surface-water/ground-water flow and salinity for a coastal wetland and adjacent estuary. Journal of Hydrology 314(1-4):212-34.

Langevin, C.D., Guo, W., 2006. MODFLOW/MT3DMS–based simulation of variable-density ground water flow and transport. Ground Water 44(3):339-351.

Lawrie, J., Hearne, J., 2007. Reducing model complexity via output sensitivity. Ecological Modelling 207(2-4):137-44.

Leamer, E.E., 1990. Let's Take the Con Out of Econometrics. In: Granger, C.W.J., (Ed.), Modelling Economic Series, Oxford, UK: Clarendon Press.

Leendertse, J.J., 1970, A water-quality simulation model for well-mixed estuaries and coastal seas: Volume I, Principles of Computation: Santa Monica, Calif., The Rand Corporation, Report RM-6230-RC, 71 p.

Leendertse, J.J., 1972, A water-quality simulation model for well-mixed estuaries and coastal seas: Volume IV, Jamaica Bay Tidal Flows: New York, The New York City Rand Institute, Report R-1009-NYC, 48 p.

Leendertse, J.J., 1987, Aspects of SIMSYS2D, a system for two-dimensional flow computation: Santa Monica, Calif., The Rand Corporation, Report R-3572-USGS, 80 p.

Leendertse, J.J., 1988, A summary of experiments with a model of the Eastern Scheldt: Santa Monica, Calif., The Rand Corporation, Report R-3611-NETH, 41 p.

Leendertse, J.J., and Gritton, E.C., 1971, A water-quality simulation model for well-mixed estuaries and coastal seas: Volume II, Computation Procedures: New York, The New York City Rand Institute, Report R-708-NYC, 48 p.

Leendertse, J.J., Langerak, A., and de Ras, M.A.M., 1981, Two-dimensional tidal models for the Delta Works: Transport models for inland and coastal waters: Proceedings of the Symposium on Predictive Abilities: New York, N.Y., Academic Press, p. 408-450.

Leij, F.J., Bradford S.A., 1994. 3DADE: A computer program for evaluating three-dimensional equilibrium solute transport in porous media. U.S. Department of Agriculture- Salinity Laboratory, 134pp.

Leonard, L., Croft, A., Childers, D., Mitchell-Bruker, S., Solo-Gabriele, H., Ross, M,. 2006. Characteristics of surface-water flows in the ridge and slough landscape of Everglades National Park: Implications for particulate transport. Hydrobiologia 569:5-22.

Limpert, E., Stahel, W.A., Abbot, M., 2001. Log-normal distributions across the sciences: Keys and clues. Bioscience 51(5):341-352.

Lin, H.C., Talbot, C.A., Richards, D.R., Jones, N.L., 2000. Development of a multidimensional modeling system for simulating canal, overland, and ground-water flow in south Florida. Waterways Experiment Station, Vicksburg, Mississippi, U.S. Army Corps of Engineers report.

Lindenschmidt, K.-E., 2006. The effect of complexity on parameter sensitivity and model uncertainty in river water-quality modelling. Ecological Modelling 190(1-2):72-86.

Lindenschmidt, K.-E., Wodrich, R., Hesse, C., 2006. The effects of scaling and model complexity in simulating the transport of inorganic micropollutants in a lowland river reach. Water-quality Research Journal of Canada 41(1):24-36.

Lindenschmidt, K.-E., Fleischbein, K., Baborowski, M., 2007. Structural uncertainty in a river water quality modeling system. Ecological Modelling 204:289-300.

Loaiciga, H.A., Yeh, W.W.-G., Ortega-Guerrero, M.A., 2007. Probability density functions in the analysis of hydraulic conductivity data. Journal of Hydrologic Engineering. 11(5):442-450.

Luo, Y., Weng, E., Wu, X., Gao, C., Zhou, X., Zhang, L., 2009. Parameter identifiability, constraint, and equifinality in data assimilation with ecosystem models. Ecological Applications 19(3):571-574.

MacVicar, T.K., van Lent, T., Castro, A., 1984. South Florida Water Management Model documentation report. South Florida Water Management District Technical Publication 84-3, 123pp.

Manson, S.M., 2008. Does scale exist? An epistemological scale continuum for complex human-environment systems. Geoforum 39(2):776-788.

Manson, S.M., 2007. Challenges in evaluating models of geographic complexity. Environment and Planning B-Planning and Design 34(2):245-260.

McCormick, P.V., Rawlik, P.S., Lurding, K., Smith, E.P., Sklar, F.H., 1996. Periphyton-water relationships along a nutrient gradient in the northern Florida Everglades. Journal of the North American Benthological Society 15(4):433-449.

McCuen, R.H., Knight, Z., Cutter, A.G., 2006. Evaluation of the Nash-Sutcliffe efficiency index. Journal of Hydrologic Engineering 11(6):597-602.

McDonald, M.G., and Harbaugh, A.W., 1988, A modular three-dimensional finite-difference ground-water flow model: U.S. Geological Survey Techniques of Water-Resources Investigations Report, book 6, chap. A1.

McPherson, B.F., Torres, A.E., 2006. Freshwater and nutrient fluxes to coastal waters of Everglades National Park- A synthesis. U.S. Geological Survey Fact Sheet 2006-3076.

Messina, J.P., Evans, T.P., Manson, S.M., Shortridge, A.M., Deadman, P.J., Verburg, P.H., 2008. Complex systems models and the management of error and uncertainty. Journal of Land Use Science 3(1):11-25.

Meyers, T.P., Lindberg, S.E., 1997. An assessment of the relative contribution of dry deposition to the total atmospheric input of phosphorus. In: Redfield G & Urban N (Eds) Atmospheric Deposition into South Florida: Measuring Net Atmospheric Inputs of Nutrients.: SFWMD Conference on Atmospheric Deposition into South Florida. West Palm Beach, Florida.

Min, J.-H., Paudel, R., Jawitz, J.W., 2010. Spatially distributed modeling of surface water flow dynamics in the Everglades ridge and slough landscape. Journal of Hydrology, in press.

Mitsch, W.J., Cronk, J.K., Wu, X.Y., Nairn, R.W., Hey, D.L., 1995. Phosphorus retention in constructed fresh-water riparian marshes. Ecological Applications 5:830-845.

Mitsch, W.J., Gosselink, J.G., 2000. Wetlands. New York, N.Y.: John Wiley and Sons, Inc., 920p.

Morris, M.D., 1991. Factorial sampling plans for preliminary computational experiments. Technometrics 33(2):161-174.

Moustafa, M.Z., Chimney, M.J., Fontaine, T.D., Shih, G., Davis, S., 1996. The response of a freshwater wetland to long-term “low level” nutrient loads—marsh efficiency. Ecol Eng 7:15–33.

Muller, S.J., Muñoz-Carpena, R., 2005. Design of a phosphorus model for south Florida based on a simplified approach. ASAE Paper No. 052252, St. Joseph, MI.

Muñoz-Carpena, R., Zajac, Z., Kuo, Y.M., 2007. Global sensitivity and uncertainty analyses of the water-quality model VFSMOD-W. Transactions of the ASABE 50(5):1719-1732.

Munson, R.K., Roy, S.B., Gherini, S.A., MacNeil, A.L., Hudson, R.J.M., Blette, V.L., 2002. Model prediction of the effects of changing phosphorus loads on the Everglades Protection Area. Water Air and Soil Pollution 134(1-4):255-273.

Nash, J.E., Sutcliffe, J.V., 1970. River flow forecasting through conceptual models part I — A discussion of principles. Journal of Hydrology 10(3):282-290

Naylor, T.H., Finger, J.M., 1967. Verification of computer simulation models. Management Science 14(2):B92-B101.

Newman, S., and K. Pietro, 2001. Phosphorus storage and release in response to flooding: implications for Everglades stormwater treatment areas, Ecological Engineering, 18, 23-38.

Nihoul, J.C.J., 1994. Do not use a simple model when a complex one will do. Journal of Marine Systems 5(6):401-6.

Noe, G.B., Childers, D.L., 2007. Phosphorus budgets in Everglades wetland ecosystems: The effects of hydrology and nutrient enrichment. Wetlands Ecology and Management 15:189-205.

Noe, G.B., Childers, D.L., Jones, R.D., 2001. Phosphorus biogeochemistry and the impact of phosphorus enrichment: Why is the everglades so unique? Ecosystems 4(7):603-24.

Noe, G.B., Scinto, L.J., Taylor, J., Childers, D.L., Jones, R.D., 2003. Phosphorus cycling and partitioning in an oligotrophic Everglades wetland ecosystem: A radioisotope tracing study. Freshwater Biology 48(11):1993-2008.

Oliphant, T.E., 2007. Python for scientific computing. Computing in Science and Engineering 9(3):10-20.

Omlin, M., Brun, R., Reichert, P., 2001. Biogeochemical model of Lake Zurich: Sensitivity, identifiability and uncertainty analysis. Ecological Modelling 141(1-3):105-123.

Oreskes, N., Shraderfrechette, K., Belitz, K., 1994. Verification, validation, and confirmation of numerical models in the earth-sciences. Science 263(5147):641-646.

Paerl H.W., 1995. Coastal eutrophication in relation to atmospheric nitrogen deposition: current perspectives. Ophelia 41: 237-259.

Perry, W.B., 2008. Everglades restoration and water-quality challenges in south Florida. Ecotoxicology 17(7):569-578.

Pimm, S.L., Lockwood, J.L., Jenkins, C.N., Curnutt, J.L., Nott, M.P., Powell, R.D., Bass Jr., O.L., 2002. Sparrow in the grass: A report on the first ten years of research on the Cape Sable Seaside Sparrow (*Ammodramus maritimus mirabilis*). Homestead, Florida: South Florida Natural Resources Center, 204pp.

Pohl, C., van Genderen, J.L., 1998. Multisensor image fusion in remote sensing: Concepts, methods and applications. International Journal of Remote Sensing 19(5):823-854.

Polman, C., Gill, G., Landing, W., Guentzel, J., Bare, D., Porella, D., Zillioux, E., Atkeson, T., 1995. Overview of the Florida Atmospheric Deposition Study (FAMS). Water, Soil, and Air Pollution 80:285-290.

Price, R.M., Swart, P.K., Fourqurean, J.W., 2006. Coastal ground-water discharge - An additional source of phosphorus for the oligotrophic wetlands of the Everglades. Hydrobiologia 569:23-36.

Reddy, K.R., Kadlec, R.H., Flaig, E., Gale, P.M., 1999. Phosphorus retention in streams and wetlands: A review: Critical Reviews in Environmental Science and Technology 29:83-146.

Redfield, G., 1998. Quantifying atmospheric deposition of phosphorus: A conceptual model and literature review for environmental management. South Florida Water Management District.

Regan, H.M., Colyvan, M., Burgman, M.A., 2002. A taxonomy and treatment of uncertainty for ecology and conservation biology. Ecological Applications. 12(2):618-628.

Richardson, C.J., Marshall, P.E., 1986. Processes controlling movement, storage, and export of phosphorus in a fen peatland. Ecological Monographs 56:279-302.

Ridderinkhof, H., Zimmerman, J.T.F., 1992. Chaotic stirring in a tidal system. Science 258:1107-1111.

Robbins, J.C., Bales, J.D., 1995. Simulation of hydrodynamics and solute transport in the Neuse River Estuary, North Carolina. U.S. Geological Survey Open-File Report 94-511, 85 p.

Roache, P.J., 1982. Computational Fluid Dynamics. Albuquerque, NM, USA: Hermosa Publishers.

Rudnick, D.T., Chen, Z., Childers, D.L., Boyer, J.N., Fontaine III, T.D., 1999. Phosphorus and nitrogen inputs to Florida Bay: The importance of the Everglades watershed. Estuaries 22(2B):398-416.

De Saint-Venant, A.J.C., 1871. Theorie du mouvement non-permanent des eaux, avec application aux crues des rivieres et a l'introduction des marees dans leur lit. C. R. Acad. Sc. Paris, 73:147 154.

Saltelli, A., 1999. Sensitivity analysis: Could better methods be used?. Journal of Geophysical Research 104(D3):3789-3793.

Saltelli, A., Tarantola, S., Campolongo, F., 2000. Sensitivity analysis as an ingredient of modeling. Statistical Science 15(4):377-395.

Saltelli, A., Tarantola, S., Campolongo, F., Ratto, M., 2004. Sensitivity Analysis in Practice: A Guide to Assessing Scientific Models. Chinchester, UK: John Wiley and Sons.

Saltelli, A., Ratto, M., Tarantola, S., Campolongo, F., 2005. Sensitivity analysis for chemical models. Chemical Reviews 105(7):2811-2827.

Saltelli A., Ratto, M., Andres, T., Campolongo, F., Cariboni, J., Gatelli, D., et al., 2008. Global Sensitivity Analysis: The Primer. Chinchester, UK: Wiley-Interscience.

Schaffranek, R.W., 1986. Hydrodynamic simulation of the upper Potomac Estuary. Proceedings of the Water Forum 86: World Water Issues in Evolution, ASCE, New York, N.Y. 2:1572-1581.

Schaffranek, R.W., 2004. Simulation of surface-water integrated flow and transport in two dimensions: SWIFT2D user's manual. U.S. Geological Survey Techniques and Methods Book 6, Chapter B-1, 115pp.

Schaller, P.R., 1997. Moore's Law: Past, present and future. IEEE Spectrum 34(6):52-58.

Scheffer, M., 2009. Critical Transitions in Nature and Society. Princeton, NY: Princeton University Press.

Scheffer, M., 1990. Multiplicity of stable states in fresh-water systems. Hydrobiologia 200:475-86.

Scheffer, M., Hosper, S.H., Meijer, M.L., Moss, B., Jeppesen, E., 1993. Alternative equilibria in shallow lakes. Trends in Ecology and Evolution 8(8):275-279.

Scott, E.M., 1996. Uncertainty and sensitivity studies of models of environmental systems. In: Charnes, J.M., Morrice, D.J., Brunner, D.T., Swain, J.J., (Eds.), Proceedings of the 1996 Winter Simulation Conference, Coronado, California, USA.

SFWMD, 2005. Documentation of the South Florida Water Management Model, Version 5.5. South Florida Water Management District, West Palm Beach, Florida.

SFWMD, FDEP, 2004. Comprehensive Everglades Restoration Plan: 2003 Annual Report. South Florida Water Management District, West Palm Beach, Florida.

Sheikh, P.A., Carter, N.T., 2005. Everglades restoration: the Federal role in funding. Congressional Research Service Report for Congress.

Shirmohammadi, A., Chaubey, I., Harmel, R.D., Bosch, D.D., Muñoz-Carpena, R., Dharmasri, C., et al,, 2006. Uncertainty in TMDL models. Transactions of the ASABE 49(4):1033-1049.

Simunek, J.M., van Genuchten, T.H., Sejna, M., Toride, N., Leij, F.J., 1999. The STANMOD computer software for evaluating solute transport in porous media using analytical solutions of convection-dispersion equation. Versions 1.0 and 2.0. IGWMC - TPS - 71. International Ground-water Modeling Center, Colorado School of Mines, Golden, Colorado, 32pp.

Smith III, T.J., 1998. Imperiled wetlands: Review of mangroves and salt marshes. Nature 395:131-132.

Snowling, S.D., Kramer, J.R., 2001. Evaluating modelling uncertainty for model selection. Ecological Modelling 138(1-3):17-30.

Sutula, M., Day, J.W., Cable, J., Rudnick, D., 2001. Hydrological and nutrient budgets of freshwater and estuarine wetlands of Taylor Slough in southern Everglades, Florida (USA). Biogeochemistry 56:287-310.

Swain, E.D., 2005. A model for simulation of surface-water integrated flow and transport in two dimensions: User's guide for application to coastal wetlands. U.S. Geological Survey Open-File Report 2005-1033, 88pp.

Swain, E.D., Wolfert, M.A., Bales, J.D., Goodwin, C.R., 2004. Two-dimensional hydrodynamic simulation of surface-water flow and transport to Florida Bay through the Southern Inland and Coastal Systems (SICS). U.S. Geological Survey Water-Resources Investigations Report 03-4287, 56pp.

Valle, D., Staudhammer, C.L., Cropper, Jr., W.P., van Gardingen, P.R., 2009. The importance of multimodel projections to assess uncertainty in projections from simulation models. Ecological Applications 19(7):1680-1692.

van Lent, T.J., Snow, R.W., Fred, J., 1998. An examination of the Modified Water Deliveries Project, the C-111 Project and the Experimental Water Deliveries Project: Hydrologic analyses and effects on endangered species. Everglades National Park Technical Report, 232pp.

Walker, W.W., 1995. Design basis for Everglades Stormwater Treatment Areas. Water Resources Bulletin 31:671-685.

Walker, W.W., 1998. Estimation of inputs to Florida Bay. U.S. Army Corps of Engineers & U.S. Department of the Interior. http://wwwalker.net/flabay.

Wang, N.M., Mitsch, W.J., 2000. A detailed ecosystem model of phosphorus dynamics in created riparian wetlands. Ecological Modelling 126:101-130.

Wang, Y., Reddy, R., Gomez, R., Lim, J., Sanielevici, S., Ray, J., et al., 2005. A general approach to creating FORTRAN interface for C++ application libraries. In: Zhang, W., Tong, W., Chen, Z., Glowinski, R. (Eds.), Current Trends in High Performance Computing and its Applications, Berlin, Heidelberg: Springer.

Wang, J.D., Swain, E.D., Wolfert, M.A., Langevin, C.D., James, D.E., Telis, P.A., 2007. Application of FTLOADDS to simulate flow, salinity, and surface-water stage in the southern Everglades, Florida. U.S. Geological Survey Scientific Investigations Report 2007–5010, 90pp.

Weare, T.J., 1979. Errors arising from irregular boundaries in ADI solutions of the shallow-water equations. International Journal of Numerical Methods in Engineering 14(6):921-31.

Wesseling, C.G., van Deursen, W.P.A., Burrough, P.A., 1996. A spatial modelling language that unifies dynamic environmental models and GIS, in Proceedings of the Third International Conference/Workshop on Integrating GIS and Environmental Modeling, Santa Fe, New Mexico, USA, January 21-26.

Wyss, G.D., Jørgensen, K.H., 1998. A user guide to LHS: Sandia's Latin hypercube sampling software. Sandia National Laboratories Technical Report SAND98-0210:1-140.

Zadeh, L.A., 1973. Outline of a new approach to the analysis of complex systems and decision processes. IEEE Transactions on Systems, Man and Cybernetics 3:28-44.

Zimmermann, T., Dubois-Pèlerin, Y., Bomme, P., 1992. Object-oriented finite element programming: I. Governing principles. Computer Methods in Applied Mechanics Engineering 98(2):291-303.

BIOGRAPHICAL SKETCH

Stuart John Muller hails from South Africa, where he received an excellent education at Hillcrest High School in KwaZulu-Natal. He matriculated as Head Boy and *proxime accessit dux*, before subsequently acquiring a Bachelor of Science degree in agricultural engineering from the University of Natal (the university and degree have since been renamed to Bioresources Engineering and the University of KwaZulu-Natal, respectively). There followed 18 months of global travel to Kenya, Tanzania, Zambia, Botswana, United Kingdom (where he taught high-school students mathematics and science), Nepal (where he trekked to Base Camp at Mount Everest), Thailand, Cambodia, Australia, and New Zealand. In 2003, he moved to Florida to pursue a Master of Science in Engineering degree in agricultural and biological engineering at the University of Florida . Before he was able to complete his master's, he was seduced by an opportunity to embark on a Ph.D. in the same department . That was in 2004. He would go on to claim the Guinness World Record for the World's Longest Eyelash in 2007, and to eventually become a Doctor of Philosophy in 2010.